



UNIwersytet Medyczny
IM. PIASTÓW ŚLĄSKICH WE WROCLAWIU

mgr farm. Maciej Spiegel

Badania *in silico*
aktywności antyoksydacyjnej
związków fitochemicznych

In silico studies of
the antioxidant activity of
the phytochemical compounds

Rozprawa doktorska w oparciu o monotematyczny cykl publikacji
w dziedzinie nauk medycznych i nauk o zdrowiu
w dyscyplinie nauki farmaceutyczne

Promotor:

prof. dr hab. Zbigniew Sroka
Katedra i Zakład Farmakognozji i Leku Roślinnego

Wrocław 2023

SPIS TREŚCI

STRESZCZENIE	4
SUMMARY	4
WYKAZ PRAC NAUKOWYCH WŁĄCZONYCH DO CYKLU PUBLIKACJI	5
1. Wprowadzenie.....	6
2. Założenia i cel pracy	8
2.1. Cele szczegółowe poszczególnych prac	8
3. Materiały i metody.....	8
3.1. Oprogramowanie	8
3.2. Metody mechaniki molekularnej oraz kwantowej.....	9
3.2.1. <i>Informacje ogólne</i>	9
3.2.2. <i>Stale dysocjacji oraz procentowe stężenie molowe</i>	9
3.2.3. <i>Indeksy reaktywności</i>	9
3.2.4. <i>Pierwszorzędowa aktywność antyoksydacyjna</i>	11
3.2.5. <i>Drugorzędowa aktywność antyoksydacyjna</i>	12
4. Wyniki, dyskusja i wnioski	13
4.1. Publikacja [A].....	13
4.2. Publikacja [B].....	13
4.3. Publikacja [C].....	14
4.4. Publikacja [D].....	15
5. Piśmiennictwo	16
ZAŁĄCZNIKI	18
I. Publikacja [A].....	18
i. <i>Materiały dodatkowe</i>	40
ii. <i>Oświadczenia współautorów</i>	47
II. Publikacja [B].....	50
i. <i>Oświadczenia współautorów</i>	65
III. Publikacja [C].....	72
i. <i>Oświadczenia współautorów</i>	82
IV. Publikacja [D].....	84
V. Wykaz publikacji potwierdzony przez Bibliotekę UMW	105
VI. Osiągnięcia naukowo-badawcze	108
i. <i>Analiza bibliometryczna całkowitego dorobku naukowego</i>	108
ii. <i>Konferencje naukowe</i>	108
iii. <i>Projekty krajowe</i>	108
iv. <i>Wyróżnienia i nagrody</i>	108
v. <i>Aktywność recenzencka</i>	108
vi. <i>Warsztaty, kursy, seminaria</i>	108
vii. <i>Staża zagraniczne</i>	109
viii. <i>Pozostałe aktywności</i>	109

STRESZCZENIE

Zmiany oksydacyjne w obrębie biocząsteczek organizmu stanowią istotny czynnik indukujący zaburzenia homeostazy organizmu mogący objawiać się w obrazie klinicznym pacjenta rozwojem szeregu poważnych chorób, takich jak miażdżycy, cukrzyca, Alzheimer, Parkinson czy nowotwory. Fizjologiczne systemy redoks przeciwdziałają temu zjawisku, jednak utrzymanie równowagi między pro- i anty-oksydantami jest w obecnych czasach utrudnione biorąc pod uwagę stale rosnącą ekspozycję na utleniacze. Istotnym wydaje się suplementacja organizmu w składniki zdolne zmiatać wolne rodniki, chelatować jony metali oraz oddziaływać z odpowiednimi enzymami, aby przeciwdziałać narastającemu stresowi oksydacyjnemu.

Większość warzyw, owoców oraz produktów pochodzenia roślinnego zawiera w składzie substancje fenolowe. Liczne badania *in vitro* oraz *in vivo* wykazały prozdrowotny efekt tej klasy związków fitochemicznych wynikający z ich potencjału antyoksydacyjnego. Aktywność, jaką przeciwutleniacz wykazuje w organizmie jest jednak wypadkową wielu czynników które modulują reaktywność czy właściwości fizykochemiczne, spośród których największe znaczenie ma struktura chemiczna.

Metody chemii obliczeniowej stanowią aktualnie nieoceniony sposób badań, jeśli chodzi o analizę zjawisk niekoniecznie mierzalnych eksperymentalnie. W ramach doktoratu skupiono się na zastosowaniu mechaniki kwantowej do badań nad wybranymi związkami z grup fenolokwasów oraz flawonoidów. Dokonano analizy wpływu struktury na aktywność antyoksydacyjną wskazując na istotę zjawiska rezonansu, wiązań wodorowych oraz topologii grup hydroksylowych. Ustalono też indeksy reaktywności dające wstępny wgląd w spodziewaną aktywnością związków. Na przykładzie apigeniny z powodzeniem zastosowano protokół badań umożliwiający projekcję wyników teoretycznych na wymierne wartości, tzn. kinetykę reakcji zmiatania wolnych rodników oraz kompleksowania jonów metali. Dokonano także głębokiego przeglądu literaturowego dotyczącego aktualnie stosowanych technik w badaniach obliczeniowych nad antyoksydantami.

SUMMARY

Oxidative changes within the biomolecules are well-recognized inducers of homeostasis' disorders that can manifest in the patient's clinical profile with the development of several serious diseases such as atherosclerosis, diabetes, Alzheimer's, Parkinson's and cancer. Physiological redox systems counteract this phenomenon but maintaining a balance between pro- and anti-oxidants is difficult these days, given the ever-increasing exposure to oxidants. Hence, supplementing the body with ingredients capable of scavenging free radicals, chelating metal ions and interacting with appropriate enzymes to counteract the present oxidative stress seems vital.

Most vegetables, fruits and products of plant origin contain phenolic substances. Numerous *in vitro* and *in vivo* studies have demonstrated the health-promoting effect of this class of phytochemicals stemming from their antioxidant potential. However, the activity that an antioxidant exhibits in the body is the outcome of many factors that modulate reactivity or physicochemical properties, among which chemical structure is the most important.

Computational chemistry methods are currently an invaluable when it comes to analyzing phenomena that are not necessarily measurable experimentally. This doctoral thesis focused on the application of quantum mechanics to the study of selected compounds from the phenolic acid and flavonoid groups. The effect of structure on the antioxidant activity was analyzed, pointing out the essence of the resonance, the hydrogen bonds, and the topology of hydroxyl groups. Reactivity indices were also determined, giving a preliminary view of the expected activity of the substances investigated. Using apigenin as an example, a research protocol was successfully applied to project theoretical results into quantifiable values, i.e., the kinetics of free radical scavenging and metal ion complexation reactions. An in-depth literature review of currently used techniques in computational studies of antioxidants was also conducted.

WYKAZ PRAC NAUKOWYCH WŁĄCZONYCH DO CYKLU PUBLIKACJI

- [A] **Spiegel, M.***, Andruniów, T., & Sroka, Z. (2020). Flavones' and Flavonols' Antiradical Structure–Activity Relationship–A Quantum Chemical Study. *Antioxidants (Basel, Switzerland)*, 9(6), 461. <https://doi.org/10.3390/antiox9060461>

IF = 6.313
MEiN = 100

- [B] **Spiegel, M.**, Kapusta, K.*, Kołodziejczyk, W., Saloni, J., Żbikowska, B., Hill, G. A., & Sroka, Z. (2020). Antioxidant Activity of Selected Phenolic Acids–Ferric Reducing Antioxidant Power Assay and QSAR Analysis of the Structural Features. *Molecules (Basel, Switzerland)*, 25(13), 3088. <https://doi.org/10.3390/molecules25133088>

IF = 4.412
MEiN = 140

- [C] **Spiegel, M.***, & Sroka, Z. (2023). Quantum–mechanical characteristics of apigenin: Antiradical, metal chelation and inhibitory properties in physiologically relevant media. *Fitoterapia*, 164(October 2022), 105352. <https://doi.org/10.1016/j.fitote.2022.105352>

IF = 3.204
MEiN = 100

- [D] **Spiegel M.*** (2022). Current Trends in Computational Quantum Chemistry Studies on Antioxidant Radical Scavenging Activity. *Journal of Chemical Information and Modeling*, 62(11), 2639–2658. <https://doi.org/10.1021/acs.jcim.2c00104>

IF = 6.162
MEiN = 100

1. Wprowadzenie

Oddychanie tlenowe jest procesem zarówno efektywniejszym, jak również bardziej skomplikowanym niż jego beztlenowy odpowiednik. Chociaż glikoliza stanowi wspólny początek na drodze pozyskiwania energii w postaci adenozyno-5'-trifosforanu (ATP), to zwiększony zysk energetyczny u organizmów aerobowych oparty jest przede wszystkim na etapach następujących po niej. Zbiorczo określone jako cykl Krebsa, generują one zredukowany dinukleotyd nikotynoamidoadeninowy (NADH) i zredukowany dinukleotyd flawinoadeninowy (FADH₂), które w dalszej kolejności ulegają utlenieniu przez enzymy mitochondrialnego łańcucha oddechowego. Utworzony w ten sposób gradient elektrochemiczny, zależny od różnicy stężeń jonów wodorowych między przestrzenią międzybłonową a macierzą, jest wykorzystywany przez syntazę ATP podczas fosforylacji oksydacyjnej. Transport elektronów, zachodzący z udziałem kompleksów I, III i IV oraz ubichinonu, nie jest jednak całkowicie wydajny. W wyniku niekontrolowanego przepływu pewna ich ilość wchodzi w nieenzymatyczne reakcje jednoelektronowe z pobliskimi cząstkami, prowadząc do powstania produktów ubocznych metabolizmu oksydacyjnego, wśród których najczęściej wymienia się rodniki.^[1-3]

Termin rodnik po raz pierwszy został użyty ponad 300 lat temu przez de Morveau w jego pracy z 1782 roku zatytułowanej „*Sur les dénominations chimiques, la nécessité d'en perfectionner le système et les règles pour y parvenir, suivi d'un tableau d'une nomenclature chimique*”. Oryginalne znaczenie różniło się natomiast od dzisiejszej definicji sformułowanej przez IUPAC jako „[...] *indywiduum chemiczne [...] posiadające niesparowany elektron*.”.^[4] Ewolucja koncepcji i rozwój teorii rodnikowej bazował na pracach takich naukowców jak Lavoisiera, Guy-Lussaca, Wöhlera, von Liebiga czy Dumasa; Gomberga oraz Schlenka w obrębie rodników organicznych; a także Michaelisa nad rodnikami generowanymi w procesach biochemicznych. Obecnie uznaje się, że rodniki to liczna klasa indywidualów chemicznych o otwartopowłokowej konfiguracji z jednym, dwoma, trzema^[5] lub nawet czterema^[6] niesparowanymi elektronami. W rezultacie rodniki są zazwyczaj (ale nie zawsze^[7]) bardzo aktywne i spontanicznie reagują z sąsiednimi molekułami w celu stabilizacji swojej struktury elektronowej, co w konsekwencji często skutkuje w zmienionych właściwościach chemicznych oraz fizycznych atakowanej cząstki.

Należy podkreślić, że grupa istotnych biologicznie czynników utleniających obejmuje nie tylko rodniki, ale oprócz tego struktury nierodnikowe, takie jak reaktywne formy tlenu (RFT, *ang. reactive oxygen species, ROS*), azotu (RFA, *ang. reactive nitrogen species, RNS*), siarki (RFS, *ang. reactive sulphur species, RSS*), karbonylu (RFK, *ang. reactive carbonyl species, RCS*) i inne.^[8-10] Ich klasyfikacja opiera się na lokalizacji gęstości spinowej, a każda zdolna jest uszkadzać struktury komórkowe.

Łańcuch oddechowy jest głównym źródłem małych rodników tlenowych, a anionorodnik ponadtlenkowy (O₂⁻) powstaje na skutek niekontrolowanej ucieczki elektronu na tlen atmosferyczny.^[1,11,12] Chociaż O₂⁻, ze względu na ujemny ładunek oraz strukturę elektronową niechętnie przyjmuje dodatkowe elektrony, a tym samym wykazuje minimalną aktywność oksydacyjną wobec biomolekuł^[13,14], to reaguje on z innymi rodnikami i może ulec dysmutacji do nadtlenu wodoru (H₂O₂) w obecności dysmutazy ponadtlenkowej^[15] — H₂O₂ poza tym, że sam jest silnym utleniaczem, jest w stanie także reagować z jonami metali przejściowych, takimi jak żelazo, miedź oraz cynk, w przebiegu reakcji Fentona co prowadzi do jego redukcji do rodnika hydroksylowego (•OH). Ponadto O₂⁻ potrafi również łączyć się z cząsteczkami tlenku azotu (NO[•]), tworząc peroksynitryty, które powodują nitrowanie składników organicznych^[9]

Pomimo że mitochondria produkują reaktywne formy tlenu w sposób nieprzerwany, nie są one jedynym generatorem endogennych oksydantów. Powszechnie wiadomo, że mikrosomy wątroby posiadają enzymatyczny układ oksydazy NADPH, który katalizując utlenianie NADPH przez tlen wytwarza nadtlenek wodoru.^[9] Do innych „fabryk” RFT można zaliczyć peroksyosomy, cechujące się wysokim potencjałem oksydacyjnym powiązanim z występowaniem oksydazy zdolnej do redukcji tlenu do nadtlenu wodoru, jak też enzymy cytozolowe — przykładowo oksydaza ksantynowa wskutek konwersji hipoksantyny do ksantyny i kwasu moczowego z użyciem NADP⁺ lub O₂ jako akceptorów elektronów.^[16] Ostatecznie biologiczne tiole^[17], hydrochinony, katecholaminy^[18] i flawiny^[19] w podobny sposób mogą ulegać reakcjom redoks, przyczyniając się do akumulacji wewnątrzkomórkowych utleniaczy. Warto

wspomnieć, że produkcja rodników ma miejsce w przebiegu większości szlaków metabolicznych, aczkolwiek nie w każdym przypadku jest to zjawisko niepożądane.

Kiedy rozpoczęto badania biomedyczne w dziedzinie fizjologii procesów redoks, początkowo uważano, że utleniacze wywołują wyłącznie efekty toksyczne i są bez wyjątku związane ze zmianami patologicznymi.^[20] Jednak komórki wytwarzają oraz uwalniają $\cdot\text{OH}$, $\text{NO}\cdot$ i $\text{O}_2\cdot^-$ w trakcie normalnych czynności ustroju, a natura tych struktur jest dwójaka. Część z nich odgrywa niezbędną rolę w utrzymaniu homeostazy, partycypując w szeregu istotnych oraz fundamentalnych procesów fizjologicznych. *Ad exemplum*, fagocytarna oksydaza NADPH była pierwszym poznanym systemem, który generuje RFT nie w charakterze produktu ubocznego, ale podstawowej funkcji swojego działania.^[21] $\text{NO}\cdot$ został jednoznacznie zidentyfikowany jako endogenny czynnik sygnalizujący regulujący relaksację śródbłonna naczyń.^[22] RFT są też znaczące w podtrzymywaniu stanu zapalnego podczas odpowiedzi immunologicznej, ze szczególnym uwzględnieniem wybuchu tlenowego będącego metodą walki komórek układu odpornościowego z patogenami.^[23] Z tego powodu przypuszcza się, że niewystarczające stężenie utleniaczy może wręcz osłabić organizm, zapobiegając tzw. pozytywnemu stresowi oksydacyjnemu.^[24,25]

Przyczynę wzmożonej produkcji oksydantów *in vivo* trzeba odnajdywać nie tylko we wpływie już przedstawionych wcześniej czynników wewnętrznych, lecz i zewnętrznych.^[25] Do tych należą m.in. wysokotłuszczowa i wysokocukrowa dieta, nadużywanie leków, palenie tytoniu, spożywanie alkoholu oraz ekspozycja na substancje chemiczne, których metabolizm wiąże się z podwyższoną aktywnością enzymów. Stymulujący efekt ma ponadto zanieczyszczenie powietrza oraz promieniowanie UV, które, choć nie powiązane bezpośrednio, wpływają także na siebie wzajemnie. Modelowo, $\cdot\text{OH}$, $\text{NO}\cdot$ i $\text{Cl}\cdot$, pochodzące głównie z odpadów, uczestniczą w reakcjach łańcuchowych niszczenia warstwy ozonowej, zwiększając ilość docierającego do Ziemi ultrafioletu.^[26]

Tym niemniej, niezależnie od źródła, niekontrolowane wytwarzanie oksydantów nie jest korzystne, a ich nagromadzenie w ilościach znacznie przekraczających wartości fizjologiczne jest uznanym inicjatorem uszkodzeń wewnątrzkomórkowych. Energia, którą dysponują z racji niesparowanego elektronu na powłoce walencyjnej lub zajmowanego stanu wzbudzonego, jest przekazywana na białka, lipidy, cukry, DNA, białka i aminokwasy, przekształcając ich struktury na skutek peroksydacji, chociażby w efekcie rozerwania szkieletów węglowych.^[10,27] Utlenianie lipidów zaburza ciągłość błony komórkowej i zmieniając ciśnienie osmotyczne w komórce inicjuje proces apoptozy; przemiany składników lipidowych oraz białkowych wchodzących w skład lipoprotein o niskiej gęstości powodują magazynowanie się cholesterolu^[28]; z kolei alteracje DNA, w których najbardziej rozpoznawalną jest transformacja guaniny w 8-okso-7,8-dihydro-guaninę, pociąga za sobą podniesione ryzyko aktywacji onkogenów i wystąpienia zmian nowotworowych, ze względu na spotęgowaną sposobność transwersji G do T.^[29] Wszystko to może skutkować w nieodwracalnych modyfikacjach strukturalnych, a często też innym profilem działania atakowanej cząstki, prowadzących do patologii w funkcjonowaniu komórek jak również tkanek. Niedostatecznie szybko zahamowane, przedłożone wyżej uszkodzenia ulegają nawarstwieniu i z czasem manifestują swoją obecność w obrazie klinicznym pacjenta.

Przy nieustannym narażeniu na oksydanty i stopniowym wyczerpywaniu się biologicznych reduktorów, mechanizmy obronne organizmu przestają być wystarczające. Długotrwałe stężenie utleniaczy, wykraczające poza ramy fizjologiczne, w skrajnych przypadkach daje początek zaburzeniom homeostazy oraz stresu oksydacyjnego, który ma negatywny wpływ na zdrowie, a jego pojawieniu się towarzyszy rozwój poważnych chorób cywilizacyjnych. Prowadzi on do sukcesywnej degeneracji komórek i narządów.^[30] Badania wykazały, że utrzymujący się wysoki poziom wolnych rodników wiąże się z rozwojem przewlekłego stanu zapalnego, który jest związany z ostrymi oraz chronicznymi przypadłościami, takimi jak choroby stawów^[31], dróg żółciowych^[32], cukrzyca^[33], choroby autoimmunologiczne (np. toczeń^[34], stwardnienie rozsiane^[35], choroba Hashimoto^[36]), czy nowotwory^[37]. Mózg jest wyjątkowo wrażliwy, ponieważ jego komórki potrzebują stałego dopływu tlenu do produkcji neuroprzekazników, które wpływają na neuroplastyczność. Nadmiar oksydantów uszkadza neurony dopaminergiczne i sprzyja rozwojowi choroby Parkinsona^[38], a także daje o sobie znać w postaci odkładania blaszek amyloidowych — kluczowych markerów choroby Alzheimera.^[39] Dodatkowo utleniacze odgrywają rolę w patofizjologii miażdżycy^[40]. Finalnie stres oksydacyjny może uruchamiać błędne koło, w którym odpowiedź zapalna amplifikuje generowanie rodników i zaostrza istniejący już stan zapalny.^[41]

Organizm, aby utrzymać docelowy poziom oksydantów, wyposażony jest w zintegrowany system obronny, który potrafi regulować ich stężenie. Przynależą do niego nieenzymatyczne przeciwutleniacze — wśród nich wskazać wypada, między innymi, glutation, kwas moczowy oraz kwas liponowy; nadto, jest on wspierany przez egzogenne reduktory, przykładowo karotenoidy (witamina A), kwas askorbinowy (witamina C) i tokoferole (witamina E).^[42] Współdziałają one ze antyoksydantami enzymatycznymi^[43], w szczególności dysmutazą ponadtlenkową, katalazą i peroksydazą glutationową, wspólnie hamując akumulację rodników lub przerywając łańcuch procesów oksydacyjnych, który już się rozpoczął. Ponieważ te antyoksydanty mają odmienne właściwości fizykochemiczne i odpowiednio charakter hydrofilowy, są one rozmieszczone w różnych kompartmentach organizmu zapewniając wszechstronną ochronę. Jednakże w obecnych czasach wydaje się, że bazowanie wyłącznie na zdolnościach ustroju w tym zakresie nie jest wystarczające.

2. Założenia i cel pracy

Świadomość wpływowej roli stresu oksydacyjnego w etiologii chorób oraz procesu starzenia się nadała priorytet badaniom nad skutecznymi i nietoksycznymi związkami o aktywności antyoksydacyjnej mogących mieć zastosowanie farmakologiczne. Interesujące w tym względzie są substancje fitochemiczne. Za prowadzeniem prac nad nimi przemawia ponad tysiącletnia tradycja chińskiej medycyny, oparta w znacznej mierze na surowcach pochodzenia roślinnego, a wciąż będąca źródłem nowych substancji leczniczych co potwierdziła nagroda Nobla z 2015 roku dla profesor Youyou Tu za odkrycie artemizyny jako lekarstwa na malarię.^[44]

Podstawowym celem badań, na których bazuje cykl publikacji niniejszej pracy doktorskiej była ocena, za pomocą chemii obliczeniowej, aktywności antyoksydacyjnej wyselekcjonowanych związków fitochemicznych, jak i potwierdzenie założenie, że metody *in silico* stanowią aktualnie nieocenione narzędzie, jakie można stawiać na równi z eksperymentami. Tym samym istotnym i zamierzonym elementem było zastosowanie różnych technik oraz sposobów interpretacji wyników, w celu podkreślenia wachlarza możliwości jakie metody obliczeniowe niosą za sobą.

2.1. Cele szczegółowe poszczególnych prac

- [A] Analiza jakościowa wpływu elementów strukturalnych na aktywność przeciwrodnikową oraz estymacja specyficznych indeksów reaktywności dla wybranych flawonoli i flawonów.
- [B] Analiza jakościowa oraz ilościowa wpływu elementów strukturalnych fenolokwasów na ich aktywność przeciwutleniającą wobec układu redoks $\text{Fe}^{3+}/\text{Fe}^{2+}$
- [C] Kompletna analiza termochemiczna i kinetyczna aktywności przeciw- OOH oraz zdolności kompleksowania jonów Cu^{2+} i Fe^{3+} , hamowania oksydazy ksantynowej, a także estymacja specyficznych indeksów reaktywności apigeniny w modelowych warunkach fizjologicznych
- [D] Przegląd piśmiennictwa podsumowujący aktualne trendy w modelowaniu aktywności przeciwrodnikowej antyoksydantów

3. Materiały i metody

3.1. Oprogramowanie

Niskoenergetyczne konformery studiowanych cząsteczek były generowane przy użyciu programu Gabedit^[45], w którym zaimplementowana jest procedura symulowanego wyżarzania z dynamiką molekularną opartą na potencjałach mechaniki molekularnej pola siłowego Amber99^[46] oraz wartościach półempirycznych. Badania kwantowo-mechaniczne przeprowadzono z zastosowaniem pakietu obliczeniowego Gaussian16^[47], a do wizualizacji struktur 3D posłużono się oprogramowaniem Avogadro^[48] lub GaussView^[49].

W pracy [B] analizę topologii wykonano w programie Multiwfn (wersja 3.7)^[50], a program PaDEL-Descriptor^[51] został spożytkowany na potrzeby obliczenia deskryptorów oraz wybranych „chemicznych odcisków palca” (*ang. fingerprints*) dostępnych w bazie PubChem^[52]. Modele QSAR (*ang. quantitative structure-activity relationship*) zbudowano wykorzystując oprogramowanie QSARINS (wersja 2.2.4).^[53]

Wyniki dokowania enzymatycznego przedstawione w publikacji [C] otrzymano z użyciem programu AutoDock VINA^[54].

Rysunki oraz grafiki opracowano korzystając z programów MarvinSketch, GIMP, UCSF Chimera^[55] oraz LigPlot+^[56].

Dostęp do programów, zasobów komputerowych oraz przestrzeni dyskowej, a tym samym możliwość realizacji badań, uzyskano z tytułu grantów obliczeniowych we Wrocławskim Centrum Sieciowo-Superkomputerowym (WCSS), grant nr 527; Poznańskim Centrum Superkomputerowo Sieciowym (PCSS), grant nr 467; Centrum Informatycznym Trójmiejskiej Akademickiej Sieci Komputerowej (CI-TASK); oraz Cyfronecie, wchodzącym w skład Infrastruktury PLGrid, grant *plgantioxidants*.

3.2. Metody mechaniki molekularnej oraz kwantowej

3.2.1. Informacje ogólne

Na etapie wyszukiwania lokalnego minimum wdrożono protokół próbkowania konformacyjnego o czasie nagrzewania 1.0 ps, po którym następowala 1.0 ps równowazenia układu. Resztę parametrów pozostawiono domyślnie.

Badania kwantowo-mechaniczne bazowały na teorii funkcjonałów gęstości i jako najwyższe poziomy wykorzystano: B3LYP^[57,58]/6-31+G(d,p)^[59-62]/IEF-PCM^[63] [A], B3LYP/cc-pVDZ^[64]/CPCM^[65] [B], M05-2X^[66]/6-311+G(d,p)^[59,67]/SMD^[68] [C]. W przypadku pracy [C], część obejmującą eksplikację zdolności chelatowania jonów Fe³⁺ oraz Cu²⁺ oparta była na funkcjonale M05^[69], ponieważ w przeciwieństwie do M05-2X, został on sparametryzowany także na układach z metalami.^[70] W celu zmniejszenia zużycia zasobów obliczeniowych i ominięcia konieczności uwzględnienia efektów relatywistycznych dla elektronów rdzenia, chmurę elektronową jonów metali opisano przy użyciu pseudopotencjałów Stuttgart-Dresden^[71] i opowiadającej im bazy funkcyjnej^[72].

Jakkolwiek nie wspomniano *explicitie*, tak w każdym obliczeniu zastosowano bardzo wąskie odcięcie optymalizacji geometrii (*Opt=VeryTight*) oraz ultradrobnią siatkę całkującą (*Int=Ultrafine*). Cząstki otwartopowłokowe — rodniki i jony — były traktowane metodami nierestrykcyjnymi, odpowiednio UB3LYP oraz UM05-2X(UM05). Ponadto, mimo że Gaussian dokonuje anihilacji spinu podczas procedury samouzgodnienia pola, niekiedy jest ona zawodna, zaś zanieczyszczone spinem funkcje falowe nie są wiarygodne i prowadzą do błędów w geometrii, energiach i analizie populacji. Dla takich systemów sprawdzano wartości zanieczyszczenia spinowego, zgodnie z założeniem, że $\langle S^2 \rangle = s(s + 1)$, gdzie s to połowa liczby niesparowanych elektronów, a $\langle S^2 \rangle$ to wartość spodziewana.^[73]

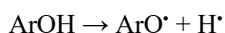
3.2.2. Stałe dysocjacji oraz procentowe stężenie molowe

Oszacowanie wartości stałych dysocjacji dla kwasowych protonów oraz ustalenie preferowanych ścieżek deprotonacji w roztworze wodnym wykonano w myśl sposobu zaproponowanego przez Galano *et al.*^[74] Ucieka się on do dopasowania różnicy energii Gibbsa między sprzężoną zasadą, a jej odpowiadającym kwasem, obliczonymi na tożsamym poziomie teorii, do stworzonego w oparciu o dane eksperymentalne modelu regresji liniowej przy wykorzystaniu wartości współczynnika kierunkowego i wyrazu wolnego właściwych użytemu funkcjonałowi oraz bazy funkcyjnej. Na podstawie uzyskanych stałych dysocjacji wykreślone zostaje procentowe stężenie molowe danej formy antyoksydanta w całym zakresie pH.

3.2.3. Indeksy reaktywności

Studiowane indeksy reaktywności skupiały się na mechanizmach powszechnie referowanych w pracach teoretycznych^[75,76], a do jakich zaliczyć można:

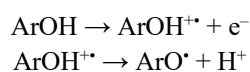
- a) formalny transferu atomu wodoru (*ang. formal hydrogen atom transfer, f-HAT[‡]*), będący najczęściej wymienianą ścieżką reakcji, której antyoksydant ulega w procesie zmiatania rodników. Opiera się on na homolitycznym rozpadzie wiązania pomiędzy wodorem a atomem tlenu aromatycznej grupie hydroksylowej, według schematu:



Energetyczną wypadkową procesu jest energia dysocjacji wiązania (*ang. bond dissociation energy, BDE*) sformułowana równaniem:

$$\text{BDE} = E(\text{ArO}^\bullet) + E(\text{H}^\bullet) - E(\text{ArOH}^\bullet)$$

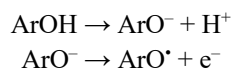
- b) Transferu elektronu—transferu protonu (*ang. electron transfer–proton transfer, ETPT*), czyli dwuetapowej sekwencji uwalniania elektronu z cząsteczki i dalszej dysocjacji protonu z utworzonego kationorodnika:



Pierwszy etap definiowany jest przez adiabatyczny potencjał jonizacji (*ang. adiabatic ionization potential, aIP*), a drugi przez energię dysocjacji protonu (*ang. proton dissociation energy, PDE*):

$$\begin{aligned} \text{IP} &= E(\text{ArOH}^{+\bullet}) + E(e^-) - E(\text{ArOH}) \\ \text{PDE} &= E(\text{ArO}^\bullet) + E(\text{H}^+) - E(\text{ArOH}^{+\bullet}) \end{aligned}$$

- c) Sekwencyjnej utraty protonu—transferu elektronu (*ang. sequential proton loss–electron transfer, SPLET*), w trakcie której dochodzi do dysocjacji protonu z badanego związku, a następnie emisji swobodnego elektronu:



Energetyczny zysk procesu stanowi powinowactwo do protonu (*ang. proton affinity, PA*) i energia transferu elektronu (*ang. electron transfer energy, ETE*) określone przez:

$$\begin{aligned} \text{PA} &= E(\text{ArO}^-) + E(\text{H}^+) - E(\text{ArOH}) \\ \text{ET} &= E(\text{ArO}^\bullet) + E(e^-) - E(\text{ArO}^-) \end{aligned}$$

Wartości referencyjne dla atomu protonu i elektronu zaczerpnięto z odpowiednich prac wskazanych w manuskryptach.

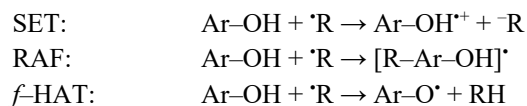
[‡]Określenie *formalny* ma szczególne znaczenie. Zasadniczo reakcja może być oparta na dwóch różnych mechanizmach: 1) bezpośrednim przeniesieniu atomu wodoru (*ang. hydrogen atom transfer, HAT*), dominującym w rozpuszczalnikach niepolarnych i niejonowych roztworach wodnych, albo 2) transferze elektronu sprzężonym z protonem (*ang. proton–coupled electron transfer, PCET*), preferowanym w reakcjach, w których uczestniczą silnie elektronegatywne reagenty. W przypadku HAT atom wodoru przenoszony jest jako jedna całość w oparciu o trójelektronową delokalizację gęstości elektronowej wzdłuż ścieżki reakcji, z kolei w PCET proton i elektron przekazywane są niezależnie od siebie, a tym samym mogą pochodzić z innych orbitali. Co więcej, PCET obejmuje delokalizację czteroelektronową.^[91]

3.2.4. Pierwszorzędowa aktywność antyoksydacyjna

Ocena aktywności przeciwrodnikowej, określanej w literaturze jako pierwszorzędowa, projektowana na typowe warunki fizjologiczne bazowała na zaproponowanym protokole QM-ORSA^[75-77] (*ang. Quantum Mechanics-Based Test for Overall Free Radical Scavenging Activity*). Składający się z trzech etapów zakłada badania w modelu lipidowym oraz wodzie o pH=7.4 jako środowiskach biologicznie najważniejszych.

Za rekomendowany rodnik, $\cdot R$, uważa się $\cdot OOH$ ze względu na wyraźnie niższą reaktywność, w porównaniu do $\cdot OH$. Doświadczalnie zmierzone stałe kinetyczne reakcji $\cdot OH$ z Troloxem C ($k \approx 6.9 \times 10^9 \text{ M}^{-1} \text{ s}^{-1}$)^[78] czy anionem kwasu linolowego ($k \approx 8.0 \times 10^9 \text{ M}^{-1} \text{ s}^{-1}$)^[79] dowodzą, że $\cdot OH$ reaguje błyskawicznie z biomolekułami w swoim najbliższym otoczeniu, ponad granicę dyfuzji ($>10^9 \text{ M}^{-1} \text{ s}^{-1}$ dla warunków standardowych^[80]). Z drugiej strony, wartości eksperymentalne dla $\cdot OOH$ są mniejsze, odpowiednio $< 10^3 \text{ M}^{-1} \text{ s}^{-1}$ ^[81] oraz $(1.18 \pm 0.20) \times 10^3 \text{ M}^{-1} \text{ s}^{-1}$ ^[82], wskazując że antyoksydant ma możliwość przechwycenia go. Co więcej, trzeba podkreślić, że wprawdzie równowaga układu $\cdot OOH \rightleftharpoons O_2^{\cdot -}$ w pH=7.4 jest przesunięta na korzyść ponadtlenku ($pK_a=4.8$; stosowne procenty molowe wynoszą wtedy 0.25% i 99.75%)^[81], to $O_2^{\cdot -}$ jest dobrym nukleofilem, jak również umiarkowanym reduktorem.^[13,14] Z racji tego, akceptuje się, że uszkodzenia oksydacyjne pochodzą przede wszystkim od formy protonowanej.

Dla form przeciwutleniaczy o istotnych stężeniach ($>0.1 \text{ mol}\%$) wykonywane są obliczenia termochemiczne wiodące do otrzymania zmian energii swobodnych, ΔG° , mechanizmów transferu elektronu (*ang. single electron transfer, SET*), utworzenia adduktu (*ang. radical adduct formation, RAF*) oraz, już wspomnianego, formalnego transferu atomu wodoru.



Ścieżki uznane za wykonywalne podlegają dalszym badaniom, tzn. odszukaniu stanów przejściowych łączących relatywne minima (reagenty—produkty) na ścieżce minimum energetycznego reakcji. Jakkolwiek protokół QM-ORSA takie przyjmuje wyłącznie te o negatywnej lub zerowej ΔG° , tak wzięcie pod uwagę dodatkowo tych umiarkowanie endoergicznich ($< 10.0 \text{ kcal/mol}$) jest uzasadnione. Mimo że pozytywna zmiana energii swobodnej implikuje odwracalność danego procesu, może on być wciąż ważny, jeśli tylko powstałe cząstki reagują szybko dalej, w toku wystarczająco egzoergicznym procesów zapewniających siłę napędową pod postacią przesunięcia równowagi, oraz gdy energie aktywacji są dostatecznie niskie. Zważając na złożoność systemów biologicznych, jest to szczególnie prawdopodobne.

Należy jednak nadmienić, że powyższy warunek nie dotyczy transferu elektronu z tytułu całkowicie odmiennego charakteru zjawiska i wskazana jest analiza każdego wyniku. Do oszacowania bariery takiej reakcji, ΔG_{ET}^\ddagger , stosuje się teorię Marcusa^[83]:

$$\Delta G_{ET}^\ddagger = \frac{\lambda}{4} \left(1 + \frac{\Delta G_{ET}^0}{\lambda} \right)^2$$

$$\lambda = \Delta E_{ET} - \Delta G_{ET}^0$$

gdzie λ to energia reorganizacji wyliczona z wertykalnej (ΔE_{ET}) i adiabatycznej (ΔG_{ET}^0) energii reakcji, opisująca relaksację orbitali.

Ostatnim etapem jest estymacja kinetyki reakcji opierająca się na konwencjonalnej teorii stanów przejściowych (*ang. conventional transition state theory, TST*) z uwzględnieniem poprawki Eckarta dla tunelowania, w ramach IM roztworu standardowego, za pomocą równania:

$$k^{TST} = \sigma \kappa(T) \frac{k_B}{h} e^{-\Delta G^\ddagger / RT}$$

gdzie k_B i h to, odpowiednio, stała Boltzmanna i Plancka, ΔG^\ddagger to energia aktywacji, R oraz T oznaczają stałą gazową i temperaturę reakcji, zaś σ opisuje stopień degeneracji ścieżki reakcji, a $\kappa(T)$ to współczynnik transmisji. Poprzez $\kappa(T)$ brana jest pod uwagę średnia Boltzmanna dla klasycznego prawdopodobieństwa zajścia reakcji oraz jej odpowiednika w świecie kwantowym, i jest przeto sugerowany dla reakcji, których reagenty mogą przejść przez barierę potencjału o wysokości większej niż ich energia — do nich zalicza się chociażby mechanizm f -HAT, w którym występuje ruch „lekkiej” cząstki H, a także niektóre ścieżki RAF.

Ponadto, do oceny stałych szybkości w pobliżu granicy dyfuzji, tak częstych dla reakcji rodnikowych, wykorzystuje się teorię Collinsa–Kimballa^[84] oraz równania Smoluchowskiego^[85] i Stokesa–Einsteina^[86]:

$$k^{app} = \frac{k^D k^{TST}}{k^D + k^{TST}}$$

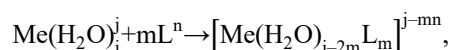
$$k^D = 4\pi R D_{AB} N_A$$

$$D = \frac{k_B T}{6\pi\eta r_A}$$

gdzie R to dystans między reagentami, D_{AB} oznacza ich wzajemny współczynnik dyfuzji ($D_{AB} = D_A + D_B$), N_A to liczba Avogadro, η stanowi lepkość rozpuszczalnika, zaś r to promień substancji, uzyskany obliczeniowo dla objętości wewnątrz konturu o gęstości 0.001elektronów/Bohr³ w ramach modelu polaryzowalnego ośrodka zaproponowanego przez Onsagera.^[87]

3.2.5. Drugorzędowa aktywność antyoksydacyjna

Poza bezpośrednią zdolnością zmiatania wolnych rodników większość antyoksydantów polifenolowych jest w stanie chelatować jony metali przejściowych. Doświadczalnie udowodniono, że Fe^{3+} i Cu^{2+} w formie kompleksu nie uczestniczą tak aktywnie w reakcji Fentona jak niezwiązane, w konsekwencji czego ilość wygenerowanych na drodze katalizowanej redukcji nadtlenu wodoru $\cdot OH$ oraz $\cdot OOH$ maleje.^[88] Badania teoretyczne biorą za cel przetestowaniu możliwości utworzenia takich układów i ich trwałości na podstawie stałych kinetycznych procesu zachodzącego według ogólnego równania:



gdzie j to ładunek akwakompleksu jonu metalu, a i to liczba cząsteczek wody koordynowanych w jego pierwszej warstwie solwatacyjnej. Zmienne m i n to, kolejno, liczba ligandów budujących kompleks ($m=1$ dla kompleksów monodentnych, $m=2$ dla kompleksów bidentnych, *etc.*...) oraz ładunek liganda.

W oparciu o otrzymaną energię swobodną chelatowania w otoczeniu f (ΔG_f°) ustala się stałe równowagi K_f , K_i^{II} oraz K_i^{app} określone równaniami:

$$K_f = e^{-\frac{\Delta G_f^\circ}{RT}}$$

$$K_i^{II} = \sum K_f \times {}^m f_i$$

$$K_i^{app} = \sum K_i^{II}$$

a opisujące, odpowiednio, stałą równowagi kompleksowania w otoczeniu f , stałą równowagi poszczególniej formy antyoksydanta biorąc pod uwagę jego ułamek molowy w badanych warunkach oraz pozorną stałą chelatowania studiowanej substancji. Przez *otoczenie* należy rozumieć daną topologię grup hydroksylowych uczestniczących w tworzeniu centrum koordynacyjnego. Warto wspomnieć, że metodyka została rozwinięta o ocenę potencjału pro- i antyoksydacyjnego powstałych kompleksów z uwzględnieniem askorbinianu oraz jonu ponadtlenkowego jako fizjologicznych reduktorów, lecz właściwa publikacja^[89] nie wchodzi w zakres rozprawy doktorskiej.

4. Wyniki, dyskusja i wnioski

4.1. Publikacja [A]

W rezultacie wykonanych badań udało się opisać elementy strukturalne odpowiadające za reaktywność wybranych flawonów i flawonoli, a także wstępnie oszacować ich pierwszorzędową aktywność przeciwnodnikową bazując na termochemii dostępnych mechanizmów działania. W wyborze związków decydujące było zgromadzenie takich o jak największych różnicach w budowie, co pozwoliło uwiarygodnić obserwacje.

Aby scharakteryzować chmurę elektronową, w początkowej fazie prac zastosowano analizę NBO (*ang. Natural Bond Orbital*)^[90] polegająca na transformacji funkcji falowej do postaci zlokalizowanej — graficznie tożsamej strukturze Lewisa — otrzymując bardziej zrozumiały opis interakcji. Nieobsadzone orbitale p_y w następstwie koniugacji i idącej za nią delokalizacji zmniejszają energię systemu. Wzajemna planarność pierścieni układu AC wobec B stanowi bezpośrednią determinantę efektu. Flawonoidy posiadające podstawnik w pozycji C_3 , takie jak na przykład moryna, tworzą zawadę przestrzenną, uniemożliwiając osiągnięcie zerowego kąta dwuściennego. Z drugiej strony, czyni to wskazane ugrupowanie nadzwyczaj podatnym na usunięcie atomu wodoru, gdyż prowadzi to do spontanicznej rotacji pierścienia B, aż do uzyskania relatywnie płaskiej struktury. Rezonans jest również modulowany obecnością wiązania podwójnego $C_2=C_3$, a jego nasycenie drastycznie osłabia siłę redukcyjną polifenolu. Trzeba nadmienić, że istota procesu jest zamknięta niemal całkowicie w obrębie dwóch, niezależnych od siebie układów elektronowych AC oraz BC, istniejących na skutek koniugacji krzyżowej z powodu obecności grupy karbonylowej przy C_4 . Swoboda ruchu elektronów w granicach danego układu szczególnie istotnie wpływa na aktywność, o ile gęstość spinowa powstaje na atomie, z którego zdolna jest ulec jak największej delokalizacji. Dla pierścienia B takie zjawisko dotyczy przede wszystkim grupy hydroksylowej C_4' , bowiem gęstość spinowa może wtedy sięgać aż do ugrupowania karbonylowego, zaś sam pierścień, wraz z mostkiem łączącym go z układem C, tworzy trwały układ *o*-chinonu.

Powyższe spostrzeżenia znalazły odzwierciedlenie w obliczonych indeksach reaktywności. Rzeczywiście w badaniach nad mechanizmem *f*-HAT najkorzystniejszym miejscem abstrakcji wodoru okazało się ugrupowanie hydroksylowe przy C_4' , ze względu na delokalizację chmury elektronowej na większość układu flawonoidu, lub C_3 , gdy stanowi to warunek *sine qua non* osiągnięcia zerowego kąta dwuściennego między pierścieniami, a więc samą możliwość rozszerzenia rezonansu. Nie jest to jednak reguła — wewnątrzcząsteczkowe wiązania wodorowe pochodzące z sąsiadujących grup hydroksylowych niekiedy prowadzą do stabilizacji tak dużej, że jest ona energetycznie korzystniejsza niż podane wcześniej. Można to zaobserwować w przypadku kwercetyny czy mirycetyny. Dla obu, oraz luteoliny i fisetyny, dokonano analizy zjawiska, wskazując zasadnicze różnice we wspomnianym efekcie, uwarunkowane liczbą partycypujących grup hydroksylowych. Tożsamo ciekawą obserwacją jest stwierdzenie, że spośród dwóch potencjalnie współistniejących konformerów, tzn., gdzie grupa hydroksylowa przy C_2' formuje wiązania wodorowe albo z atomem tlenu pierścienia piranu albo z grupą hydroksylową przy C_3 , właśnie to drugie — pomimo większego kąta torsyjnego między A i B — jest energetycznie faworyzowane.

W teźże pracy udało się oprócz tego wskazać SPLET jako mechanizm preferowany w środowisku wodnym, zaś — powtarzając raz jeszcze — grupę hydroksylową przy C_4' jako najbardziej reaktywną nie tylko w przytoczonym procesie, ale też w jednostkowym wyznaczniku, jakim jest BDE. Również wykazano, że flawonole są aktywniejsze od flawonów. Na niewątpliwą uwagę zasługuje także ugrupowanie katecholowe (C_3-C_4'), w którym po oderwaniu atomu wodoru z $C_4'-OH$, atom wodoru z C_3-OH jest niejako zawieszony pomiędzy oboma tymi elementami strukturalnymi faworyzując kolejne abstrakcję atomu wodoru i skutkującą nią uformowanie znacznie stabilniejszego układu katecholu.

4.2. Publikacja [B]

Tematyka pracy też skupiała się na analizie strukturalnej, z tym że fenolokwasów i w kontekście ich siły redukcji jonów żelaza Fe^{3+} . Zastosowano w niej modele ilościowe QSAR, skonstruowane na łączonych wynikach eksperymentalnych i teoretycznych. W ramach prac przebadano trzy cechy determinujące mierzalne właściwości — wzajemną pozycję grup hydroksylowych, wpływ metylacji, oraz odległość między grupami fenolowymi a karboksylową.

Zauważono, że substancje o największej aktywności w teście FRAP miały dwie lub więcej grup hydroksylowych położonych w pozycjach *orto* lub *para* względem siebie. Dla kontrastu, najniższą reprezentowały związki z wyłącznie jedną grupą hydroksylową, dwoma w pozycji *meta*, a także metylowe pochodne kwasu benzoowego. Analogicznie jak w przypadku flawonoidów efekt rezonansu ma ogromne znaczenie. Widać to szczególnie dla układów *para* oraz *orto*, bowiem w rezultacie powstania gęstości spinowej na jednej z grup hydroksylowych tworzących go dochodzi do aktywacji drugiej grupy. Jest to fenomen bliźniaczy z zaobserwowanym wcześniej dla flawonoidów utworzeniem, odpowiednio, chinonu i katecholu.

Do osłabienia potencjału redukcyjnego przykładają się metylacja, powodująca zmniejszenie ilości grup mogących brać udział w procesie. Na dodatek, zaistniała zawada steryczna utrudnia chelatowanie jonów żelaza, zachodzące tuż przed właściwym etapem przekazania elektronu.

W toku prac wyodrębniono dwa czynniki modulujące aktywność poprzez stabilizację rodnika: rezonans oraz wewnątrzcząsteczkowe wiązanie wodorowe. Dzięki delokalizacji, *orto*–*meta* i *para*–*meta* hydroksylowane kwasy fenolowe wykazują większą aktywność niż kwasy monohydroksylowe i te, które mają dwie grupy hydroksylowe w pozycji *meta* względem siebie. Oprócz stabilizacji rezonansowej, utworzony w przebiegu reakcji redoks rodnik może być stabilizowany przez międzycząsteczkowe wiązania wodorowe pomiędzy grupami funkcyjnymi a polarnymi rozpuszczalnikami protonowymi, a także wewnątrzcząsteczkowe wiązania wodorowe. Dla badanych związków wyodrębniono dwa rodzaje: (1) obejmujące tylko tleny hydroksylowe; (2) pomiędzy grupami karboksylowymi i hydroksylowymi. Zgodnie z przedstawionymi wynikami uzyskanymi z metody QTAİM, tlen grupy hydroksylowej jest mniej wydajnym akceptorem wiązań wodorowych w porównaniu z podwójnie związanym tlenem grupy karboksylowej. Stabilizacja wiązań wodorowych wyjaśniła przyczynę podwyższonej aktywności pochodnych kwasu benzoowego z podstawioną pozycją *orto*.

W celu przedstawienia otrzymanych danych jakościowych w bardziej praktyczny sposób utworzono model wielorakiej regresji liniowej. Eksperymentalnie zmierzone jednostki aktywności TAU zostały opisane przez odpowiednie deskryptory topologiczne. Wybierając je, zwrócono uwagę na to, że: (1) dwie lub więcej grup hydroksylowych w pozycji *orto* względem siebie pozytywnie wpływa na aktywność antyoksydacyjną ze względu na delokalizację ładunku i wewnątrzcząsteczkowe wiązanie wodorowe OH–OH; (2) pochodne kwasu fenylooctowego są wydajniejsze od innych ze względu na obecność jakichkolwiek podstawników *orto*–*meta* lub *para*–*meta*; (3) obecność *orto*–*meta*–podstawionych pochodnych kwasu benzoowego, o silnych wewnątrzcząsteczkowych wiązaniach wodorowych pomiędzy *orto*–hydroksylowymi i karboksylowymi grupami powodujących znaczny wzrost wydajności; (4) metylacja pochodnych kwasu cynamonowego nie zmniejsza krytycznie aktywności tych związków. Przy zadowalających parametrach statystycznych i chemicznie uzasadnionych deskryptorach ($p=0$), opracowano model, który przypuszczalnie, może dobrze odzwierciedlać przebieg reakcji i być potencjalnie wykorzystany do przewidywania wydajności kwasów fenolowych o nieznaną aktywność.

4.3. Publikacja [C]

Całkowicie inna ścieżka badań została podjęta w pracy [C], gdzie na przykładzie apigeniny zademonstrowano jak, podążając protokołem ściśle dedykowanym ocenie zdolności antyoksydacyjnych za pomocą metod obliczeniowych, da się uzyskać wyniki mające bezpośrednie przełożenie na wymierne aktywności, tj. kinetykę reakcji. Ponieważ apigenina wchodziła w zakres analiz przedstawionych w publikacji [A] to charakter tych stanowi uzupełnienie, a także weryfikację wcześniejszych obserwacji otrzymanych na innym poziomie teorii.

Dla zrozumienia zachowania substancji w roztworze wodnym fundamentalna jest znajomość względnych równowag kwasowo–zasadowych. Różnice między aktywnościami możliwych struktur mogą być diametralne i poważnie wpłynąć na ich potencjał redoks. W badanym przypadku uwidoczniono kolejność dysocjacji apigeniny: C_7 ($pK_{a1}=7.40$) \rightleftharpoons C_4 ($pK_{a2}=8.41$) \rightleftharpoons C_5 ($pK_{a3}=11.61$). Tym samym ustalono, że formy neutralne oraz mono–aniony dominują w roztworze wodnym (procenty molowe obu wynoszą 48.7%), aczkolwiek di–anion również występuje w ilościach istotnych dla właściwego oszacowania aktywności przy użyciu metod teoretycznych.

Podobnie jak w publikacji [A] określono indeksy reaktywności, aby mieć wstępny wgląd w mechanizmy aktywności. Energia rozpadu homolitycznego wiązania O–H grupy hydroksylowej przy C₄ okazała się najniższa sugerując tą pozycję jako preferowaną w mechanizmie przekazania atomu wodoru. Jakkolwiek wartości potencjału jonizacji pozostawały wysokie, tak zaobserwowano, że przejście ze środowiska lipidowego do wodnego, oraz dysocjacja, zmniejszają wymagania energetyczne procesu, ułatwiając ewentualny transfer elektronu na rodnik. Porównując wyniki otrzymane w tej pracy dla neutralnej cząsteczki w wodzie z tymi z poprzedniej, ale na poziomie teorii B3LYP/6–31+G(d,p)/IEF–PCM, widać, że pomimo rozdzźwięku w wartościach absolutnych, trendy są tożsame. Wyjątkiem jest wyłącznie energetyka etapu transferu elektronu następującego po oddysocjowaniu wodoru z C₄ oraz C₅; powodem są marginalne różnice między obiema grupami, obecne dla każdego z zastosowanych poziomów teorii. W związku z tym, można uznać, że indeksy reaktywności z pracy [A], uzyskane z użyciem znacznie prostszego poziomu teorii, wiarygodnie — przynajmniej w ramach kryterium jakościowego — odzwierciedlają te obliczone dla M05–2X/6–311+G(d,p)/SMD.

Badania termochemiczne oparte na analizie energetycznej mechanizmów HAT, SET oraz RAF wobec rodnika [•]OOH wskazały, że mechanizm tworzenia adduktu nie jest faworyzowany. Identyczny wniosek da się wysnuć odnośnie mechanizmu SET dla neutralnej form w roztworze wodny — nadmienić należy, że ominięcie oceny jego ergiczności w środowisku lipidowym tłumaczy się charakterem procesu, któremu nie sprzyja apolarny rozpuszczalnik, niezdolny dostatecznie solwatować elektron. W analogiczny sposób, na jaki zwrócono uwagę we wcześniejszym akapicie, transfer ze środowiska lipidowego do wodnego oraz procesy deprotonacji obniżają barierę aktywacji zachodzących reakcji.

Wyznaczenie stałych kinetycznych stanowiło końcowy punkt badań pozwalający rzutować wyniki na dane eksperymentalne. W środowisku lipidowym szybkość zmiatania [•]OOH przez apigeninę jest stosunkowo niska (całkowita stała kinetyczna, *k_{overall}*, wynosi $5.79 \times 10^{-1} \text{ [M}^{-1} \text{ s}^{-1}]$) i zauważalnie mniejsza niż Trolox czy witaminy C. Mimo że w fazie wodnej stałe kinetyczne są większe i narastają z każdą kolejną deprotonacją, apigenina swoją aktywność przeciwrodnikową nadal nie przewyższa wspomnianych substancji, często uznawanych za referencyjne.

W niniejszej pracy przeprowadzono także preliminarne badania nad zdolnością apigeniny do hamowania generowania rodników hydroksylowych wskutek chelatowania jonów Cu²⁺ i Fe³⁺ oraz inhibicji oksydazy ksantynowej. Otrzymana stała kompleksowania, *K_{app}*, jonu żelaza przez apigeninę ($1.09 \times 10^{12} \text{ [M}^{-1} \text{ s}^{-1}]$) jest większa o niemal dziewięć rzędów wielkości niż ta uzyskana dla jonu miedzi ($6.74 \times 10^3 \text{ [M}^{-1} \text{ s}^{-1}]$). Takie chelaty wykazują znacząco mniejszą aktywność w procesach redoks, niż ma to miejsce w przypadku ich akwakompleksów. W oparciu o referencyjną strukturę krystaliczną kwercetyny związanej z centrum aktywnym oksydazy ksantynowej wykonano dokowanie apigeniny. Rezultaty dowodzą, że niezależnie od formy jonowej, każda podobnie wiąże się z aminokwasami tego białka. Można więc spodziewać się, iż wygenerowane przez enzym rodniki mogą być błyskawicznie zmiotane przez związany z nim flawonoid.

4.4. Publikacja [D]

W niniejszej pracy przeglądowej dokonano wnikliwej analizy bibliograficznej nad aktualnymi trendami oraz standardami w badaniach nad pierwszorzędową aktywnością antyoksydacyjną. Zwrócono szczególną uwagę na wybór poziomu teorii, zarówno w odniesieniu do jakości uzyskanych wyników, jak i możliwości porównania z innymi. Przedstawiono szereg wskaźników służących analizie struktury elektronowej, takich jak m.in. teoria orbitali granicznych, mapowanie potencjału elektro– oraz wodorodonorowego czy indeksy Fukui, oraz sposobów ich interpretacji w obrębie tematyki antyoksydantów, a także używane aparaty matematyczne. Kwerenda bibliograficzna zgromadziła wiedzę z ponad 250 publikacji, przedstawiła ją w zorganizowany sposób oraz podkreśliła istniejące braki, jak również zasugerowała nowe drogi, jakimi warto zainteresować się przy tego typu badaniach.

5. Piśmiennictwo

- [1] R. Zhao, S. Jiang, L. Zhang, Z. Yu, *Int. J. Mol. Med.* **2019**, DOI 10.3892/ijmm.2019.4188.
- [2] J. F. Turrens, *Biosci. Rep.* **1997**, *17*, 3–8.
- [3] P. R. Rich, A. Maréchal, *Essays Biochem.* **2010**, *47*, 1–23.
- [4] V. Gold, Ed., *The IUPAC Compendium of Chemical Terminology*, International Union Of Pure And Applied Chemistry (IUPAC), Research Triangle Park, NC, **2019**.
- [5] A. Pichon, *Nat. Chem.* **2010**, DOI 10.1038/nchem.864.
- [6] J. Carilla, L. Julia, J. Riera, E. Brillas, J. A. Garrido, A. Labarta, R. Alcalá, *J. Am. Chem. Soc.* **1991**, *113*, 8281–8284.
- [7] Z. X. Chen, Y. Li, F. Huang, *Chem* **2021**, *7*, 288–332.
- [8] G. I. Giles, C. Jacob, *Biol. Chem.* **2002**, *383*, 375–388.
- [9] A. Weidinger, A. Kozlov, *Biomolecules* **2015**, *5*, 472–484.
- [10] H. Sies, C. Berndt, D. P. Jones, *Annu. Rev. Biochem.* **2017**, *86*, 715–748.
- [11] S. Dröse, U. Brandt, **2012**, pp. 145–169.
- [12] H. Sies, C. Berndt, D. P. Jones, *Annu. Rev. Biochem.* **2017**, *86*, 715–748.
- [13] I. Fridovich, *Annu. Rev. Pharmacol. Toxicol.* **1983**, *23*, 239–257.
- [14] I. Fridovich, *Annu. Rev. Biochem.* **1995**, *64*, 97–112.
- [15] G. R. Buettner, *Anticancer. Agents Med. Chem.* **2012**, *11*, 341–346.
- [16] M. Schrader, H. D. Fahimi, *Biochim. Biophys. Acta - Mol. Cell Res.* **2006**, *1763*, 1755–1766.
- [17] M. Trujillo, B. Alvarez, R. Radi, *Free Radic. Res.* **2016**, *50*, 150–171.
- [18] J. Smythies, *Antioxid. Redox Signal.* **2000**, *2*, 575–583.
- [19] F. Müller, *Free Radic. Biol. Med.* **1987**, *3*, 215–230.
- [20] S. Di Meo, P. Venditti, *Oxid. Med. Cell. Longev.* **2020**, *2020*, 1–32.
- [21] J. Bylund, K. L. Brown, C. Movitz, C. Dahlgren, A. Karlsson, *Free Radic. Biol. Med.* **2010**, *49*, 1834–1845.
- [22] L. J. Ignarro, G. M. Buga, K. S. Wood, R. E. Byrns, G. Chaudhuri, *Proc. Natl. Acad. Sci.* **1987**, *84*, 9265–9269.
- [23] J. A. Knight, *Ann. Clin. Lab. Sci.* **2000**, *30*, 145–158.
- [24] L.-J. Yan, *Redox Biol.* **2014**, *2*, 165–169.
- [25] A. Rahal, A. Kumar, V. Singh, B. Yadav, R. Tiwari, S. Chakraborty, K. Dhama, *Biomed Res. Int.* **2014**, *2014*, DOI 10.1155/2014/761264.
- [26] J. B. Burkholder, R. A. Cox, A. R. Ravishankara, *Chem. Rev.* **2015**, *115*, 3704–3759.
- [27] H. Sies, *Angew. Chemie Int. Ed. English* **1986**, *25*, 1058–1071.
- [28] X. Yang, Y. Li, Y. Li, X. Ren, X. Zhang, D. Hu, Y. Gao, Y. Xing, H. Shang, *Front. Physiol.* **2017**, *8*, 1–16.
- [29] J. L. Barnes, M. Zubair, K. John, M. C. Poirier, F. L. Martin, *Biochem. Soc. Trans.* **2018**, *46*, 1213–1224.
- [30] A. SPECTOR, *J. Ocul. Pharmacol. Ther.* **2000**, *16*, 193–201.
- [31] C. M. Quiñonez-Flores, S. A. González-Chávez, D. Del Río Nájera, C. Pacheco-Tena, *Biomed Res. Int.* **2016**, *2016*, 1–14.
- [32] B. Copples, H. Jaeschke, C. Klaassen, *Semin. Liver Dis.* **2010**, *30*, 195–204.
- [33] A. Ceriello, *Metabolism* **2000**, *49*, 27–29.
- [34] A. Perl, *Nat. Rev. Rheumatol.* **2013**, *9*, 674–686.
- [35] D. Offen, Y. Gilgun-Sherki, E. Melamed, *J. Neurol.* **2004**, *251*, 261–268.
- [36] R. Colucci, F. Dragoni, S. Moretti, *Oxid. Med. Cell. Longev.* **2015**, *2015*, 1–7.
- [37] V. Sosa, T. Moliné, R. Somoza, R. Paciucci, H. Kondoh, M. E. LLeonart, *Ageing Res. Rev.* **2013**, *12*, 376–390.
- [38] P. Jenner, *Ann. Neurol.* **2003**, *53*, S26–S38.
- [39] Y. Christen, *Am. J. Clin. Nutr.* **2000**, *71*, 621–629.
- [40] A. J. Kattoor, N. V. K. Pothineni, D. Palagiri, J. L. Mehta, *Curr. Atheroscler. Rep.* **2017**, *19*, 42.
- [41] M. Hulsmans, P. Holvoet, *J. Cell. Mol. Med.* **2010**, *14*, 70–78.
- [42] I. Mirończuk-Chodakowska, A. M. Witkowska, M. E. Zujko, *Adv. Med. Sci.* **2018**, *63*, 68–78.
- [43] O. M. Ighodaro, O. A. Akinloye, *Alexandria J. Med.* **2018**, *54*, 287–293.
- [44] X.-Z. Su, L. H. Miller, *Sci. China Life Sci.* **2015**, *58*, 1175–1179.
- [45] A. Allouche, *J. Comput. Chem.* **2012**, *32*, 174–182.
- [46] J. Wang, P. Cieplak, P. A. Kollman, *J. Comput. Chem.* **2000**, *21*, 1049–1074.
- [47] M. J. Frisch, G. W. Trucks, H. B. Schlegel, G. E. Scuseria, M. A. Robb, J. R. Cheeseman, G. Scalmani, V. Barone, G. A. Petersson, H. Nakatsuji, X. Li, M. Caricato, A. V. Marenich, J. Bloino, B. G. Janesko, R. Gomperts, B. Mennucci, H. P. Hratchian, J. V. Ortiz, A. F. Izmaylov, J. L. Sonnenberg, Williams, F. Ding, F. Lipparini, F. Egidi, J. Goings, B. Peng, A. Petrone, T. Henderson, D. Ranasinghe, V. G. Zakrzewski, J. Gao, N. Rega, G. Zheng, W. Liang, M. Hada, M. Ehara, K. Toyota, R. Fukuda, J. Hasegawa, M. Ishida, T. Nakajima, Y. Honda, O. Kitao, H. Nakai, T. Vreven, K.

- Throssell, J. A. Montgomery Jr, J. E. Peralta, F. Ogliaro, M. J. Bearpark, J. J. Heyd, E. N. Brothers, K. N. Kudin, V. N. Staroverov, T. A. Keith, R. Kobayashi, J. Normand, K. Raghavachari, A. P. Rendell, J. C. Burant, S. S. Iyengar, J. Tomasi, M. Cossi, J. M. Millam, M. Klene, C. Adamo, R. Cammi, J. W. Ochterski, R. L. Martin, K. Morokuma, O. Farkas, J. B. Foresman, D. J. Fox, **2016**.
- [48] M. D. Hanwell, D. E. Curtis, D. C. Lonie, T. Vandermeersch, E. Zurek, G. R. Hutchison, *J. Cheminform.* **2012**, *4*, DOI 10.1186/1758-2946-4-17.
- [49] R. Dennington, T. A. Keith, J. M. Millam, **2016**.
- [50] T. Lu, F. Chen, *J. Comput. Chem.* **2012**, *33*, 580–592.
- [51] C. W. Yap, *J. Comput. Chem.* **2011**, *32*, 1466–1474.
- [52] S. Kim, P. A. Thiessen, E. E. Bolton, J. Chen, G. Fu, A. Gindulyte, L. Han, J. He, S. He, B. A. Shoemaker, J. Wang, B. Yu, J. Zhang, S. H. Bryant, *Nucleic Acids Res.* **2016**, *44*, D1202–D1213.
- [53] P. Gramatica, N. Chirico, E. Papa, S. Cassani, S. Kovarich, *J. Comput. Chem.* **2013**, *34*, 2121–2132.
- [54] O. Trott, A. J. Olson, *J. Comput. Chem.* **2009**, NA-NA.
- [55] E. F. Pettersen, T. D. Goddard, C. C. Huang, G. S. Couch, D. M. Greenblatt, E. C. Meng, T. E. Ferrin, *J. Comput. Chem.* **2004**, *25*, 1605–1612.
- [56] R. A. Laskowski, M. B. Swindells, *J. Chem. Inf. Model.* **2011**, *51*, 2778–2786.
- [57] A. D. Becke, *J. Chem. Phys.* **1993**, *98*, 5648–5652.
- [58] P. J. Stephens, F. J. Devlin, C. F. Chabalowski, M. J. Frisch, *J. Phys. Chem.* **1994**, *98*, 11623–11627.
- [59] T. Clark, J. Chandrasekhar, G. W. Spitznagel, P. V. R. Schleyer, *J. Comput. Chem.* **1983**, *4*, 294–301.
- [60] R. Ditchfield, W. J. Hehre, J. A. Pople, *J. Chem. Phys.* **1971**, *54*, 724–728.
- [61] P. C. Hariharan, J. A. Pople, *Theor. Chim. Acta* **1973**, *28*, 213–222.
- [62] W. J. Hehre, K. Ditchfield, J. A. Pople, *J. Chem. Phys.* **1972**, *56*, 2257–2261.
- [63] J. Tomasi, B. Mennucci, R. Cammi, *Chem. Rev.* **2005**, *105*, 2999–3094.
- [64] T. H. Dunning, *J. Chem. Phys.* **1989**, *90*, 1007–1023.
- [65] V. Barone, M. Cossi, *J. Phys. Chem. A* **1998**, *102*, 1995–2001.
- [66] Y. Zhao, D. G. Truhlar, *Theor. Chem. Acc.* **2008**, *120*, 215–241.
- [67] R. Krishnan, J. S. Binkley, R. Seeger, J. A. Pople, *J. Chem. Phys.* **1980**, *72*, 650–654.
- [68] A. V. Marenich, C. J. Cramer, D. G. Truhlar, *J. Phys. Chem. B* **2009**, *113*, 6378–6396.
- [69] Y. Zhao, N. E. Schultz, D. G. Truhlar, *J. Chem. Phys.* **2005**, *123*, 161103.
- [70] Y. Zhao, N. E. Schultz, D. G. Truhlar, *J. Chem. Theory Comput.* **2006**, *2*, 364–382.
- [71] M. Dolg, U. Wedig, H. Stoll, H. Preuss, *J. Chem. Phys.* **1987**, *86*, 866–872.
- [72] J. M. L. Martin, A. Sundermann, *J. Chem. Phys.* **2001**, *114*, 3408–3420.
- [73] J. Wang, A. D. Becke, V. H. Smith, *J. Chem. Phys.* **1995**, *102*, 3477–3480.
- [74] A. Galano, A. Pérez-González, R. Castañeda-Arriaga, L. Muñoz-Rugeles, G. Mendoza-Sarmiento, A. Romero-Silva, A. Ibarra-Escutia, A. M. Rebollar-Zepeda, J. R. León-Carmona, M. A. Hernández-Olivares, J. R. Alvarez-Idaboy, *J. Chem. Inf. Model.* **2016**, *56*, 1714–1724.
- [75] A. Galano, J. Raúl Alvarez-Idaboy, *Int. J. Quantum Chem.* **2019**, *119*, e25665.
- [76] A. Galano, G. Mazzone, R. Alvarez-Diduk, T. Marino, J. R. Alvarez-Idaboy, N. Russo, *Annu. Rev. Food Sci. Technol.* **2016**, *7*, 335–352.
- [77] A. Galano, J. R. Alvarez-Idaboy, *J. Comput. Chem.* **2013**, *34*, 2430–2445.
- [78] M. Davies, L. Forni, R. Willson, *Biochem. J.* **1988**, *255*, 513–522.
- [79] L. K. Patterson, K. Hasegawa, *Berichte der Bunsengesellschaft für Phys. Chemie* **1978**, *82*, 951–956.
- [80] G. V. Buxton, C. L. Greenstock, W. P. Helman, A. B. Ross, *J. Phys. Chem. Ref. Data* **1988**, *17*, 513–886.
- [81] B. H. J. Bielski, D. E. Cabelli, R. L. Arudi, A. B. Ross, *J. Phys. Chem. Ref. Data* **1985**, *14*, 1041–1100.
- [82] B. H. Bielski, R. L. Arudi, M. W. Sutherland, *J. Biol. Chem.* **1983**, *258*, 4759–4761.
- [83] R. A. Marcus, N. Sutin, *Biochim. Biophys. Acta - Rev. Bioenerg.* **1985**, *811*, 265–322.
- [84] F. C. Collins, G. E. Kimball, *J. Colloid Sci.* **1949**, *4*, 425–437.
- [85] M. v. Smoluchowski, *Zeitschrift für Phys. Chemie* **1918**, *92U*, 129–168.
- [86] A. Einstein, *Ann. Phys.* **1905**, *322*, 549–560.
- [87] L. Onsager, *J. Am. Chem. Soc.* **1936**, *58*, 1486–1493.
- [88] Y. Pan, R. Qin, M. Hou, J. Xue, M. Zhou, L. Xu, Y. Zhang, *Sep. Purif. Technol.* **2022**, *300*, 121831.
- [89] M. Spiegel, G. Ciardullo, T. Marino, N. Russo, *Front. Chem.* **2023**, *11*, 1–13.
- [90] J. P. Foster, F. Weinhold, *J. Am. Chem. Soc.* **1980**, *102*, 7211–7218.
- [91] W. Lai, C. Li, H. Chen, S. Shaik, *Angew. Chemie - Int. Ed.* **2012**, *51*, 5556–5578.

ZAŁĄCZNIKI

I. Publikacja [A]



Article

Flavones' and Flavonols' Antiradical Structure–Activity Relationship—A Quantum Chemical Study

Maciej Spiegel ^{1,*}, Tadeusz Andruniów ² and Zbigniew Sroka ¹

¹ Department of Pharmacognosy and Herbal Medicine, Wrocław Medical University, Borowska 211A, 50-556 Wrocław, Poland; zbigniew.sroka@umed.wroc.pl

² Advanced Materials Engineering and Modelling Group, Department of Chemistry, Wrocław University of Science and Technology, M. Smoluchowskiego 23, 50-372 Wrocław, Poland; tadeusz.andruniow@pwr.edu.pl

* Correspondence: maciej.spiegel@student.umed.wroc.pl

Received: 28 April 2020; Accepted: 26 May 2020; Published: 27 May 2020



Abstract: Flavonoids are known for their antiradical capacity, and this ability is strongly structure-dependent. In this research, the activity of flavones and flavonols in a water solvent was studied with the density functional theory methods. These included examination of flavonoids' molecular and radical structures with natural bonding orbitals analysis, spin density analysis and frontier molecular orbitals theory. Calculations of determinants were performed: specific, for the three possible mechanisms of action—hydrogen atom transfer (HAT), electron transfer–proton transfer (ETPT) and sequential proton loss electron transfer (SPLET); and the unspecific—reorganization enthalpy (RE) and hydrogen abstraction enthalpy (HAE). Intramolecular hydrogen bonding, catechol moiety activity and the probability of electron density swap between rings were all established. Hydrogen bonding seems to be much more important than the conjugation effect, because some structures tend to form more intramolecular hydrogen bonds instead of being completely planar. The very first hydrogen abstraction mechanism in a water solvent is SPLET, and the most privileged abstraction site, indicated by HAE, can be associated with the C3 hydroxyl group of flavonols and C4' hydroxyl group of flavones. For the catechol moiety, an intramolecular reorganization to an o-benzoquinone-like structure occurs, and the ETPT is favored as the second abstraction mechanism.

Keywords: flavonoids; polyphenols; antioxidants; quantum chemistry; density functional theory (DFT); structure–activity relationship

1. Introduction

The twofold nature of reactive oxygen and nitrogen species (ROS, RNS) in the organism is broadly reported [1–3]. They not only participate in signal transduction [3,4], but also may lead to the breaking of DNA chains [5], lipid peroxidation [6] and protein decomposition [7]. During oxidative stress, the free radical concentration overwhelms natural antioxidants' capacity, damaging cells and initiating severe diseases such as atherosclerosis [8], neoplasms [9] and Parkinson's [10] or Alzheimer's [11] disease.

Flavonols and flavones belong to a large group of polyphenolic compounds of flavonoids, known for their beneficial activity, deriving from the antiradical potential [12]. With a capacity to scavenge free radicals and a wide distribution in vegetables [13], they play a crucial role as an external source of antioxidants. Therefore, it is important to maintain their recommended intake.

Their antioxidative ability was found to depend greatly on the molecular structure and substitution pattern: availability of hydroxyl groups—their absolute and relative position, as well as their number [14–17]; the stabilizing effect of hydrogen bonds—intramolecular and originating from

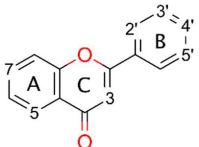
the solvent [18,19]; the electron delocalization across a molecule, which considerably relies on the degree of conjugation [16,20] and hyperconjugation effect [21]; and the substituents effect, especially of methoxy groups [22].

It is believed that A-ring substituents are not directly involved into the scavenging mechanism [17,23]. Therefore, the type of the B-ring substitution is considered as a determinant of flavonoids' antiradical potency—even one hydroxyl group located there guarantees noticeable scavenging potential, especially if it is in position C4'. Similar observations were noted for phenolic acids [16,24,25]. Furthermore, highly active flavonoids usually also possess a catechol moiety the activity of which, found in other classes of polyphenolic compounds, was demonstrated recently [15,26,27]. The C2–C3 double bond extends π -conjugation onto the carbonyl group in the C-ring, so the unsaturated flavonoids' radical scavenging ability is greater than in saturated structures, e.g., flavanones [28–30]. Herein, the catechol moiety is a subject of the investigation in this manuscript as, according to several reports [17,31,32], it can play a significant role in scavenging potential.

Appropriate assessment of flavonoids' activity requires in-depth studies on all possible modes of action: hydrogen atom transfer (HAT), electron transfer–proton transfer (ETPT), and sequential proton loss–electron transfer (SPLET) [33,34]; as well as their defining characteristics, and the mathematical values related to them: bond dissociation enthalpy (BDE)—for HAT; ionization potential (IP) and proton dissociation enthalpy (PDE)—for ETPT; proton affinity (PA) and electron transfer enthalpy (ETE)—for SPLET. Mechanism-independent determinants, reorganization enthalpy (RE) and hydrogen abstraction enthalpy (HAE) were calculated as well, but for more general, kinetic-independent purpose [35].

This study was focused on describing the structure–activity relationship (SAR) and determinants of the flavones' and flavonols' activity, with robust, computational chemistry methods. The investigations include 13 flavonoids differing in a substitution pattern (Table 1). An intramolecular swap reaction was discovered and examined for the catechol moiety in a thermodynamic aspect, and the relevance of the hydrogen bonding in the B-ring was evaluated and the electronic structure deeply explored, involving the spin density distribution, chemical hardness, as well as HOMOs and LUMOs analysis. The obtained results provide the basis for understanding flavonols' and flavones' antioxidative potential and explain the differences between them.

Table 1. Flavonoid structures investigated in this paper.



	Flavonoid	C2'	C3'	C4'	C5'	C3	C5	C7
Flavones	Acacetin			-OCH ₃			-OH	-OH
	Apigenin			-OH			-OH	-OH
	Chrysin						-OH	-OH
	Chrysoeriol		-OCH ₃	-OH			-OH	-OH
	Diosmetin		-OH	-OCH ₃			-OH	-OH
	Genkwanin			-OH			-OH	-OCH ₃
	Luteolin		-OH	-OH			-OH	-OH
Flavonols	Fisetin		-OH	-OH		-OH	-OH	-OH
	Galangin					-OH	-OH	-OH
	Kaempferol			-OH		-OH	-OH	-OH
	Morin	-OH		-OH		-OH	-OH	-OH
	Myricetin		-OH	-OH	-OH	-OH	-OH	-OH
	Quercetin		-OH	-OH		-OH	-OH	-OH

2. Materials and Methods

All energies noted as kcal/mol were converted from atomic units (a.u.) according to the conversion factor, where 1 a.u. equals 627.5 kcal/mol.

2.1. Conformer Geometry Generation

Molecules of the studied flavonoids were generated in Avogadro [36] from their simplified molecular-input line-entry system (SMILES) [37]. The obtained structures were used in the Gabeldit10 [38] Amber Molecular Dynamics Conformational Search procedure to obtain the lowest energy conformers. 1.0 ps of heating followed by 1.0 ps of equilibration molecular dynamic protocols were employed. After completion, obtained conformational isomers of each flavonoid were used for quantum chemistry studies.

Each structure was first optimized in a vacuum with Gaussian16 [39] using the HF/3-21G(d) model chemistry method and then with density functional theory (DFT) B3LYP/6-31G(d,p) [40]. Very tight geometry optimization cutoff and an ultrafine integration grid were used for vibrational frequency calculations. All flavones exhibited exactly one imaginary frequency, indicating that a planar conformation is a first-order saddle point on the potential energy surface. For this reason, the C2–C1' bond of each conformer was successively rotated by 60 degrees and saved for further elaboration, until reaching total 300 degrees of rotation from the origin. Obtained geometries were recalculated at the same computational chemistry level of theory as earlier and all real frequency values were confirmed. The lowest energy conformers were selected as the representatives and optimized once more, but in a polarizable continuum model (PCM) of water solvent, using B3LYP/6-31G + G(d,p) method [41,42]. Calculated enthalpies of the lowest energetical flavonoid isomers are shown in Table S1.

It is interesting to point out that based on our results the gas phase equilibrium structures of flavonols are flat, with the notable exception of morin, while flavones reveal strained geometries, in accord with other studies [43]. The planarity of flavonols is lost in water environment contradictory to Todorova et al.'s [44] findings. In fact, according to our B3LYP/6-31+G(d,p) calculations (this trend was also noticed in a larger basis set, such as 6-31+G(d,p) or aug-cc-pVDZ), all flavonols but morin possess a very flat potential energy surface (PES) for dihedral angles, describing the distortion from planarity, spanning a region of PES ranging from 0 degrees to its equilibrium structure value seen in Table 2. The energy difference between the flat and strained compounds is tiny, up to 0.10 kcal/mol, however, the strained structure always has the lower energy and all real vibrational frequencies, in contrast to the one imaginary frequency found for planar structures of galangin, fisetin and myricetin. It is worth noting that these conclusions hold true for re-optimized equilibrium geometries with an unpruned grid (Grid = 199974) and very tight optimization criteria, as well as re-calculated vibrational frequencies for such high-quality geometries.

2.2. Radical Geometry Generation

The representative geometries from the previous step served as an input for radical calculations. This step includes removing a single hydrogen atom from each hydroxyl group and running computations at UB3LYP/6-31+G(d,p), retaining an implicit water solvent in two ways: with and without geometry optimization. Spin contamination values of open shell DFT results were checked, as they may interfere with the outcome [45,46]. All were in a range of <0.7500, 0.7511> after spin annihilation. Cation-radical, anion-radical and triplet diradical calculations used later in this study were elaborated the same way. The outcomes obtained for the first two forms were in the same range as for radicals, whilst for the latter one they were found in a range of <2.0001, 2.0030>. The ideal values, calculated according to the formula $s(s + 1)$ where s is a half of a number of unpaired electrons, are 0.75 for a radical and 2.0 for a triplet diradical. Since DFT results are in the acceptable range, they could be used for the elaboration. Calculated enthalpies are presented in Table S2. Structural parameters of

flavonoids, such as dihedral angles around the C2–C1' bond (θ) and corresponding values for relaxed radicals (θ^\bullet), are shown in Table 2.

Table 2. C2–C1' dihedral angles of molecules, their corresponding radicals and the difference between them (Δ).

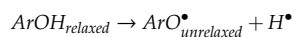
Flavonoid	θ C2–C1'	θ^\bullet C2–C1'						
		C2'	C3'	C4'	C5'	C3	C5	C7
Flavones	Acacetin	-13.7					12.9 ($\Delta = -2.2$)	7.9 ($\Delta = -7.2$)
	Apigenin	-15.5			-5.7 ($\Delta = +9.8$)		-12.5 ($\Delta = +3.0$)	-8.6 ($\Delta = -6.9$)
	Chrysin	20.6					18.7 ($\Delta = -1.9$)	16.3 ($\Delta = -4.3$)
	Chrysoeriol	-16.9			-3.7 ($\Delta = +13.2$)		-18.3 ($\Delta = -1.4$)	-4.9 ($\Delta = +12.0$)
	Diosmetin	16.7		12.1 ($\Delta = -4.6$)			17.6 ($\Delta = +0.9$)	9.9 ($\Delta = -6.8$)
	Genkwanin	-16.0			-4.5 ($\Delta = +11.5$)		-14.7 ($\Delta = +1.3$)	
	Luteolin	15.9		23.5 ($\Delta = +7.6$)	12.2 ($\Delta = -3.7$)		19.2 ($\Delta = +3.3$)	8.3 ($\Delta = -7.6$)
Flavonols	Fisetin	8.8		3.3 ($\Delta = -5.5$)	0.0 ($\Delta = -8.8$)		0.3 ($\Delta = -8.5$)	6.2 ($\Delta = -2.6$)
	Galangin	-15.0				0.0 ($\Delta = +15.0$)	-3.6 ($\Delta = +11.4$)	-14.2 ($\Delta = +0.8$)
	Kaempferol	-3.5			0.0 ($\Delta = +3.5$)		0.0 ($\Delta = +3.5$)	0.1 ($\Delta = +3.6$)
	Morin	35.7	44.7 ($\Delta = +9.0$)		32.6 ($\Delta = -3.1$)		0.0 ($\Delta = -35.7$)	34.4 ($\Delta = -1.3$)
	Myricetin	-9.1		-10.1 ($\Delta = -1.0$)	-2.5 ($\Delta = +6.6$)	-5.3 ($\Delta = +3.8$)	0.0 ($\Delta = +9.1$)	-6.3 ($\Delta = +2.8$)
	Quercetin	-8.5		-10.5 ($\Delta = -2.0$)	0.0 ($\Delta = +8.5$)		0.0 ($\Delta = +8.5$)	-5.7 ($\Delta = +2.6$)

2.3. Quantitative Determinants of Antioxidant Potential

The enthalpy values, $H(x)$, used in this section refer to the unrelaxed forms, include thermal correction and were obtained following Hessian calculations by employing Gaussian16 software [39]. Reorganization enthalpy is the only one that makes use of relaxed radicals' results. The values of enthalpy for H^+ , H^\bullet and e^- in a water solvent were taken from another study [47].

2.3.1. Hydrogen Atom Transfer Mechanism

The hydrogen atom transfer is the simplest reaction path an antioxidant can undergo and is based on a homolytic bond dissociation between the hydrogen and the oxygen atom in the hydroxyl residue:



A quantitative descriptor of this process can be assigned to the bond dissociation enthalpy [BDE; Equation (1)], defined as the change of the enthalpy after the hydrogen abstraction [Equation (2); see results in Table 3]:

$$BDE = H(ArO_{unrelaxed}^\bullet) + H(H^\bullet) - H(ArOH_{relaxed}) \quad (1)$$

$$HAT = BDE \quad (2)$$

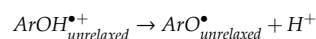
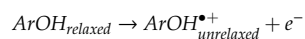
Table 3. Values of bond dissociation enthalpies [kcal/mol].

Flavonoid	Bond Dissociation Enthalpy						
	C2'	C3'	C4'	C5'	C3	C5	C7
Flavones	Acacetin					102.1	91.1
	Apigenin			89.3		100.5	91.7
	Chrysin					102.1	92.8
	Chrysoeriol			87.0		106.7	91.6
	Diosmetin		87.8			106.8	92.0
	Genkwanin			88.8		102.2	
	Luteolin		88.2	84.4		106.1	91.8
Flavonols	Fisetin		83.4	85.1		86.7	90.3
	Galangin					86.9	98.5
	Kaempferol			86.7		85.5	98.3
	Morin	93.4		88.8		84.6	99.1
	Myricetin		87.5	80.7	84.4	86.1	98.3
	Quercetin		87.4	81.4		85.5	98.0

The numbers in bold typeface indicate the lowest value for a given compound.

2.3.2. Electron Transfer–Proton Transfer Mechanism

Another recently proposed mechanism is a two-step sequence of electron release from the molecule, followed by a proton dissociation from the formed cation-radical:



The enthalpy of this process is the sum of the adiabatic ionization potential [IP; Equation (3)] and the proton dissociation enthalpy [PDE; Equation (4)], which can be calculated as follows [Equation (5); see results in Table 4]:

$$IP = H(ArOH_{unrelaxed}^{\bullet+}) + H(e^{-}) - H(ArOH_{relaxed}) \quad (3)$$

$$PDE = H(ArO_{unrelaxed}^{\bullet}) + H(H^{+}) - H(ArOH_{unrelaxed}^{\bullet+}) \quad (4)$$

$$ETPT = IP + PDE \quad (5)$$

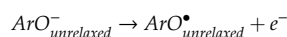
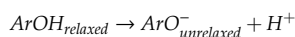
Table 4. Values of ionization potentials and proton dissociation enthalpies [kcal/mol].

Flavonoid	Ionization Potential	Proton Dissociation Enthalpy						
		C2'	C3'	C4'	C5'	C3	C5	C7
Flavones	Acacetin	115.9					16.1	5.0
	Apigenin	117.0			2.2		13.4	4.6
	Chrysin	120.5					11.4	2.1
	Chrysoeriol	113.4			3.5		23.2	8.1
	Diosmetin	113.8		3.9			22.9	8.1
	Genkwanin	117.2			1.4		14.8	
	Luteolin	115.0		3.1	−0.7		20.9	6.6
Flavonols	Fisetin	108.9		4.4	6.0		7.6	11.3
	Galangin	114.3				2.4	14.0	7.2
	Kaempferol	110.2			6.4		5.2	18.0
	Morin	113.3		10.0	5.4		1.3	15.7
	Myricetin	109.0		8.4	1.5	5.3	6.9	19.2
	Quercetin	108.9		8.4	2.4		6.5	19.0

The numbers in bold typeface indicate the lowest value for a given compound.

2.3.3. Sequential Proton Loss–Electron Transfer Mechanism

This path consists of a proton dissociation from the investigated compound and an emission of the free electron afterwards:



The whole reaction is the proton affinity [PA; Equation (6)] enthalpy plus the electron transfer enthalpy [ETE; Equation (7)] [Equation (8); results are presented in Table 5]:

$$PA = H(ArO_{unrelaxed}^-) + H(H^+) - H(ArOH_{relaxed}) \quad (6)$$

$$ETE = H(ArO_{unrelaxed}^\bullet) + H(e^-) - H(ArO_{unrelaxed}^-) \quad (7)$$

$$SPLET = PA + ETE \quad (8)$$

Table 5. Values of proton affinity enthalpies and electron transfer enthalpies [kcal/mol].

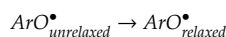
Flavonoid	Proton Affinity Enthalpy							Electron Transfer Enthalpy						
	C2'	C3'	C4'	C5'	C3	C5	C7	C2'	C3'	C4'	C5'	C3	C5	C7
Flavones	Acacetin					45.0	30.8						87.0	90.2
	Apigenin			31.8		43.3	31.4			87.4			87.1	90.1
	Chrysin					44.3	31.0						87.7	91.7
	Chrysoeriol			33.3		45.0	30.7			83.5			91.6	90.8
	Diosmetin		36.7			45.3	30.7		81.0				91.4	91.1
	Genkwanin			31.1		46.0				87.5			86.0	
	Luteolin		35.8	27.4		43.8	31.3		82.3	86.8			92.1	90.3
Flavonols	Fisetin	30.7	34.1		38.5		30.0		82.6	80.8		78.1		90.2
	Galangin				35.2	40.8	30.3					81.6	87.6	91.3
	Kaempferol			32.0		35.5	42.0	30.1		84.6		79.8	86.2	90.1
	Morin	39.2		32.1		28.3	40.6	29.5	84.0			86.6	86.2	88.3
	Myricetin		36.0	29.1	30.1	34.9	41.2	29.9		81.3	81.5	84.2	81.0	87.0
	Quercetin		36.7	27.2		35.5	41.5	30.0		80.6	84.0		79.8	86.4

The numbers in bold typeface indicate the lowest value for a given compound.

2.3.4. Mechanism-Independent Determinants

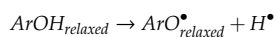
The non-specific indices—the reorganization enthalpy [RE; Equation (9)] and the hydrogen abstraction enthalpy [HAE; Equation (10)]—were also used for a quantitative analysis of the flavonols' and flavones' antioxidative potential.

The reorganization enthalpy describes the energy change upon shift from the unrelaxed to the relaxed form, hence geometry optimization. Thus, it may be an interesting predictor of conformational changes resulting from the hydrogen abstraction:



$$RE = H(ArO_{relaxed}^\bullet) - H(ArO_{unrelaxed}^\bullet) \quad (9)$$

The hydrogen abstraction enthalpy is independent of the scavenging mechanism and its kinetics. It serves as a general determinant of the flavonoid activity that includes reorganization enthalpy correction [35]:



$$HAE = H(ArO_{relaxed}^\bullet) + H(H^\bullet) - H(ArOH_{relaxed}) \quad (10)$$

The obtained RE and HAE values are presented in Table 6.

Table 6. Values of reorganization enthalpies and hydrogen abstraction enthalpies [kcal/mol].

Flavonoid	Reorganization Enthalpies							Hydrogen Abstraction Enthalpies						
	C2'	C3'	C4'	C5'	C3	C5	C7	C2'	C3'	C4'	C5'	C3	C5	C7
Flavones	Acacetin					-8.7	-5.1						93.5	86.0
	Apigenin					-7.1	-5.0			82.6			93.5	86.7
	Chrysin			-6.7		-8.6	-5.6						93.5	87.2
	Chrysoeriol			-7.7		-2.4	-5.2			79.3			104.3	86.5
	Diosmetin		-7.2			-2.4	-5.4		80.6				104.4	86.6
	Genkwanin			-6.3		-8.5					82.4			93.7
	Luteolin	-7.0	-8.6			-1.7	-5.0		81.2	75.9				104.4
Flavonols	Fisetin	-7.5	-7.8		-9.1		-5.9		75.9	77.3		77.6		84.4
	Galangin				-8.6	-8.4	-5.8					78.3	90.1	85.9
	Kaempferol			-6.9	-8.7	-8.5	-5.5			79.8		76.8	89.8	84.8
	Morin	-8.4		-6.2	-12.6	-9.1	-5.3	85.0				72.1	90.0	86.1
	Myricetin		-6.8	-8.3	-7.2	-9.4	-8.5	-6.0	80.7	72.4	77.1	76.7	89.8	85.0
	Quercetin		-7.0	-8.0		-8.8	-8.7	-5.6	80.4	73.4		76.7	89.3	84.9

The numbers in bold typeface indicate the lowest value for a given compound.

3. Results and Discussion

3.1. Molecule and Radical Electronic Structure Investigation

The starting point of the backbone examination was undertaken with a natural population analysis of NBO 3.1 [48] software, implemented in Gaussian16 [39]. In view of the fact that the backbone is identical for flavones and flavonols, the following statements can be ascribed to both of them, with some exceptions indicated in the text.

Natural bonding orbitals (NBO) analysis revealed that every C–C bond is composed of two sp^2 orbitals, so each carbon atom also has one unoccupied p_y orbital. This can lead to the assumption that free electrons, located on oxygen atoms connected with the aromatic ring, will likely interact with orbitals of carbon atoms, in conjugation and hyperconjugation effects.

Thanks to the p_y orbitals' conjugation, the system's total energy is lowered. This property is highly dependent on the AC- and B-rings' mutual planarity, and as discussed above, the B-ring does not share the same plane as the AC-complex. The dihedral angle varies (Table 2) depending on intramolecular repulsions or hydrogen bonding caused by C3, C2' or C5' residues. Dimitrić Marković et al. [27], explaining the differences in activity between anthocyanidins, delphinidin and pelargonidin against C3-glycosylated anthocyanin, malvin, suggested that the greater activity of the first two is due to the C3 hydroxyl group, which maintains coplanarity of the B- and C-ring, and hence p_y orbitals' conjugation. Nevertheless, in this study something completely different was observed. Flavonols reach exact planar structure when hydrogen from the C3 hydroxyl group is removed. Moreover, considering reorganization enthalpy as a descriptor of the most favorable abstraction site in terms of geometry change, it is indeed the C3 hydroxyl group. It can be concluded that, upon reaction, the torsion caused by this residue does not have an impact on the B-ring anymore, and rotation is thermodynamically favored. When HAE is investigated, C3 residues are generally favored, unless the investigated flavonol has at least two hydroxyl groups nearby. Then, one of their positions is an abstraction site. That way it can be expected that hydrogen bond stabilization energy is more urgent than p_y orbital conjugation. Contrarily, for all flavonols but morin, abstraction from C4' also leads to the planarity of the rings. This can be associated with the formation of radical which, to be transferred onto the C-ring, require double bond formation between the p_y orbitals of C2 and C1'.

The hyperconjugation effect was investigated considering molecular orbitals (MOs) interactions. One can see in Figure S1 that the oxygen atoms' LUMO phases have a different sign than aromatic carbon atoms, indicating possible interaction. Indeed, Milenković et al. [21], in their study on kaempferol structure, found how greatly the interference of oxygen atoms' free electrons with the antibonding orbital of carbon atoms contributes to structure stabilization, decreasing the system's total energy

by up to 34 kcal/mol. However, the structure as a whole is not conjugated. The existence of the carbonyl group in the C-ring, due to the cross-conjugation effect, divides the compound into two electron-separated ring complexes—AC and BC [49]. Therefore, electron density cannot flow freely, in a strict orbital manner, from the A-ring to the B-ring or in reverse, as was stated by Jovanović et al. [50]. To check the other possibility, a hydrogen shift between C5 and the carbonyl residue was elaborated (Appendix A) and its results also go against this hypothesis. Even more, this postulate can be refuted with examination of radicals' spin density distribution—upon forming a radical in the A or B-ring, the density is nearly 0 in B and A-ring atoms, respectively (Figure S2).

The C2–C3 saturation limits electrons' delocalization, indirectly decreasing reduction potential. Evidence confirming this thesis can be found by studying the activity results' comparison between flavonols and flavones against flavanols [51] or flavanones [52] in simple assays, e.g., ferric ion-reducing antioxidant power (FRAP) [53], 2,2'-azino-bis (3-ethylbenothiazoline-6-sulfonic acid) diammonium salt (ABTS) [54], and 2,2-diphenyl-1-picrylhydrazyl (DPPH) [55] or isoflavones in an acrylamide reduction test [56].

Removal of the hydrogen atom by an abstractor creates a radical form, for which Lewis resonance structures are shown in Figure 1. One can see that the biggest resonance effect occurs for the C2', C6' and C4' radicals; it is lower for the C3, C5 and C7 radicals, and the lowest for the C3' and C5' radicals.

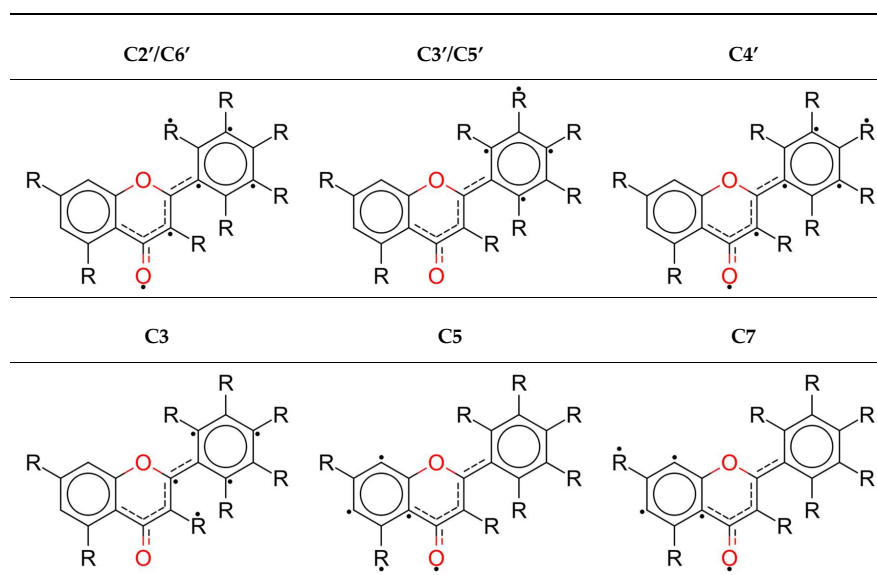


Figure 1. Lewis structures of radicals with the biggest electron densities of atoms marked with a dot.

Formerly presented HAE values (Table 6) are accepted in this study as a main numerical determinant of antioxidative potential, as they are mechanism-independent. In compliance with them, preferred hydrogen abstraction position patterns can be depicted. Just based on HAE values, flavonoids, indeed, can be divided into two groups: (I) compounds with a C3 hydroxyl group (flavonols); (II) compounds lacking a hydroxyl residue at the C3 position (flavones).

For flavones, the C4' position, if present, is the most active one. The reason for that may be attributed to larger delocalization of the electron density upon radical formation, and the possibility of establishing the hydrogen bond with the adjacent hydroxyl residues at C3' or C5'. Similar observations were derived from studies on the activity of phenolic acids [57] or anthocyanidins [27], where C4'

had the most favorable hydrogen abstraction energy. Elaboration of this process was performed and is demonstrated in a latter section (Section 3.3), where the importance of intramolecular hydrogen bonds is confirmed. The A-ring hydroxyl residues have much higher HAE, up to 25 kcal/mol, so their scavenging potential will be lower; thus, these in the B-ring seem to be the main determinants of antioxidant capacity, as was mentioned in the Introduction section.

However, flavonols with an OH group at C3 and a lone hydroxyl moiety at C4' are more likely to convey hydrogen from the first position instead of the latter one, when HAE is compared, e.g., morin and kaempferol. On the other hand, if there are at least two (e.g., quercetin) or even three (e.g., myricetin), the C4' position will be privileged. This indicates that the p_y conjugation is desired only when the radical formed at the B-ring is not stabilized by at least one intramolecular hydrogen bonding.

3.2. Morin

Interesting properties, noted by Amić et al. [25], are exhibited by morin (Figure 2). In this study, it was found that the preferred molecular isomer is not the more planar one (isomer B), but the one able to form a hydrogen bond between C3–C2' residues (isomer A). The difference in enthalpies between these conformers is ~1.8 kcal/mol, and this value seems to be sufficient to break the tendency to planarity. One can name previously noted steric restrictions disabling complete conjugation of p_y orbitals, but the choice of isomer A can also be explained differently—the C3–C2' hydrogen bond is “retained” even after the radical is formed, from either the C2' or C3 hydroxyl group. In the first case, the hydrogen atom from the C3 hydroxyl group rotates from the carbonyl site to the B-ring site, forming a hydrogen bond with the C2' radical, subsequently forcing rotation up to 45° due to the steric effect. In the second case, when the C3 radical is formed, it is not necessary for the hydrogen atom to move, and only C2–C1' bond rotation is performed. This situation is most likely to occur since no energy is used for hydrogen shift, and planarity is achieved.

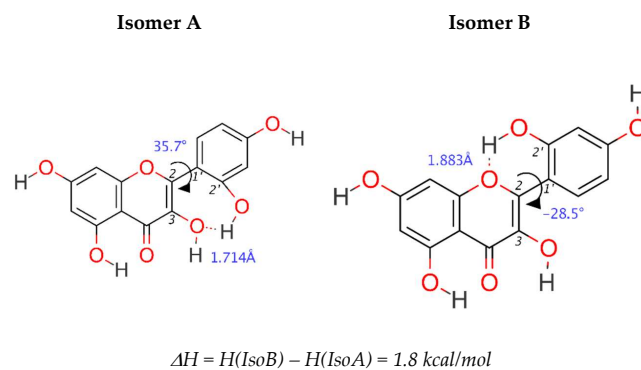


Figure 2. Comparison in geometry between morin's A and B isomer.

3.3. Mechanisms of Action in Terms of the Determinants

The very first step of the mechanism is considered as a thermodynamic determinant of a favored pathway.

3.3.1. Hydrogen Atom Transfer Mechanism

The only investigated mathematical descriptor associated with the HAT mechanism is the bond dissociation enthalpy (Table 3). The lowest is associated with forming the C4' radical, whilst C3' and C3 enthalpies are quite similar. A likely explanation of this could be Mulliken spin density (SD) distribution in the created radicals (Figure S2). The lower the spin density at the radical center, the greater is the delocalization, and the formed radical becomes more stabilized with resonance. For all compounds but morin, the lowest spin density is associated with the C4' radical. However, delocalization cannot be clearly stated as the only determinant of BDE—if it was, the lowest BDE value for fisetin should be at C4' (SD = 0.284), whilst it is C3' (SD = 0.316); for morin, the lowest BDE should be for C2' (SD = 0.303), whilst it is C4' (SD = 0.311). Therefore, it is assumed that some other factors may be crucial to describe the HAT mechanism. One can observe that C4' BDE decreases with the number of adjacent hydroxyl groups—the lowest enthalpy was found for myricetin, where two hydroxyl groups surround C4', while significantly higher values were derived for quercetin, luteolin and fisetin, with only one adjacent hydroxyl group. Conversely, compounds where the C4' hydroxyl group is alone exhibit the highest bond dissociation enthalpies. Thus, it can be stated the HAT definitely depends on intramolecular hydrogen bonding.

3.3.2. Electron Transfer–Proton Transfer Mechanism

The IP values are much bigger than BDE, while PDE is relatively low (Table 4). Since the first step determines the thermodynamically favored reaction pathway, the ETPT mechanism is not likely to be responsible for flavonoid activity. Nevertheless, ionization potential was also examined with frontier molecular orbitals theory (Appendix B).

The lowest energy required for ionization is 108.9 kcal/mol for fisetin and quercetin, while the highest is over 120 kcal/mol for chrysin; these are much greater values than any bond dissociation energies for the same compounds. Even though PDE does not show any regular pattern in the lowest energy centers, it definitely shows the highest—PDE values for the C5 position are the largest. The reason for this may be found in an electronegative repulsion between the carbonyl oxygen and the C5 radical's unpaired electron (the distance between these atoms is about 2.9 Å), as well as breakage of the hydrogen bond between these two residues.

3.3.3. Sequential Proton Loss–Electron Transfer Mechanism

The SPLET mechanism is determined with proton affinity. Calculations showed that PA values are much lower than the corresponding values for the reaction path determinants of the HAT (BDE) or ETPT (IP) mechanisms. Therefore, this one appears to represent the most favored mechanism of action for flavonoids in a water (polar) solvent, as could be expected according to the other studies [27,58], including qualitative structure–activity relationship (QSAR) analysis [59–61]. This is rather surprising as, in general, A-ring hydroxyl groups are considered not to possess scavenging potential [17,62], whilst abstraction takes place at the C7 position for most of the investigated compounds. Gibb's free energies of deprotonation, reported by Álvarez-Diduk et al. [63], are in agreement with the obtained results: the first or second pK is linked with hydrogen dissociation from the C7 hydroxyl group. Interestingly, Lin et al. [24], measuring activity of flavonoids with the DPPH assay, noted that upon glycosylation of C7 in luteolin, its antiradical activity noticeably decreased. They attributed this effect to the decreased availability of the free hydroxyl groups. Whilst the lowest proton affinity enthalpy of luteolin is assigned to C4' (27.4 kcal/mol), the second lowest is assigned to C7 (31.3 kcal/mol). An explanation that could be proposed is the activity of a catechol moiety and a change of polarity within the structure, resulting in overall decreased activity of the compound, instead of a strict change of a favored location. Moreover, since SPLET's ETE determinant is adequate for ETPT's IP, and is lower than this, it can be assumed that an electron transfer is preferred for an ion form instead of a molecule.

Based on the discussion conducted earlier for the ETPT mechanism, similar reasons can explain why the highest PA values are found for C5.

3.3.4. Mechanism-Independent Determinants

The performed elaborations considered unrelaxed forms of intermediate compounds. The proposed reorganization enthalpy is a mathematical explanation of a conformer relaxation, decreasing the total enthalpy. Therefore, one can calculate reorganization enthalpy and, based on derived values, as well as chemical structure, identify significant geometry changes. For example, the lowest RE is for the morin C3 hydroxyl group, which was described earlier in the context of hydrogen bonds and planarity. The low value of RE for C5 can be justified by an electronegative interaction between the C5' radical and carbonyl oxygen atom, which is mediated by a molecule by changing its geometry.

Although three mechanisms and their determinants were investigated, no reaction path can be proposed. It greatly depends on the solvent [34,64] and the abstractor molecule [65]. The lowest enthalpy only indicates where the abstraction is most likely to occur, not how often it will happen. For this reason, a hydrogen abstraction enthalpy can be used, and was used for further elaboration. It points out the most active compound or group, without taking into account how the radical state was reached, rejecting kinetic studies but involving reorganization of geometry. Herein, C4' seems to be the most prominent one, and similar conclusions were stated by Dimitrić Marković et al. [64,66] and Sroka et al. [35]. Furthermore, the second most favored position in a SPLET mechanism is also C4', so the importance of reorganization enthalpy correction may be bigger than one would expect.

3.3.5. Antioxidant Capacity Summary

Assuming an activity is inversely proportional to the enthalpy required for the first step of the mechanism to occur, the investigated compounds have been sorted in the descending order (Table 7). As one can see, flavonols are more active than flavones, and structures with a greater number of hydroxyl groups stand out as the most active ones. The pattern of activity does not change greatly, apart from for flavone luteolin, which is in the top three when HAT and SPLET mechanisms are examined, overtaking most of the flavonols.

Table 7. Relative activity of investigated compounds.

Activity	HAT	ETPT	SPLET
↓	Myricetin		Quercetin
	Quercetin	Fisetin, Quercetin	Luteolin
	Fisetin	Myricetin	Morin
	Luteolin	Kaempferol	Mirycetin
	Morin	Morin	Fisetin
	Kaempferol	Chrysoeriol	Kaempferol
	Galangin	Diosmetin	Galangin
	Chrysoeriol	Galangin	
	Diosmetin	Luteolin	Chrysoeriol, Diosmetin
	Genkanin	Acacetin	Acacetin
	Apigenin	Apigenin	Chrysin
	Accacetin	Genkwanin	Genkwanin
	Chrysin	Chrysin	Apigenin

Flavonoids have been sorted in decreasing order of the enthalpy for the first step of given mechanism.

3.4. Intramolecular Hydrogen Bonding

The polyhydroxy structure of flavonoids provides an opportunity to form an intramolecular hydrogen bond if at least two hydroxyl groups are close to each other. Hydrogen bonds are known for increasing stability of both the molecule and the radical, hence decreasing the energy required to form

the radical [19]. Such a situation can actually be found for every flavonol, where the C3 or C5 hydroxyl group interacts with a carbonyl residue or B-ring hydroxyl groups [21].

Fisetin, luteolin and quercetin do possess two hydroxyl moieties, while myricetin has three at the B-ring. This allows intramolecular hydrogen bonds to be formed when hydrogen is abstracted. Generally, the C4' hydroxyl group can interact with either C5' or C3', whilst C5' and C3' can interact only with C4'. The exception among this group is morin, since its C3 group can interact with C2', leading to a twisted structure. Moreover, a hydrogen bond can be formed between carbonyl group and C3 and C5 residues as well. This study focused only on the hydrogen bonding in B-ring groups, since C4' (or C3' for fisetin) was indicated as a favored position in a thermodynamically preferred SPLET mechanism, as well as a mechanism-independent HAE determinant. In order to measure a hydrogen bonding stabilizing effect on a radical molecule, the difference in the enthalpies between the radical without (ArO_{NHB}^{\bullet}) and with the hydrogen bonds (ArO_{HB}^{\bullet}) was considered, named here as hydrogen bond enthalpy (HBE), and ascribed to the following equation:

$$HBE = H(ArO_{NHB}^{\bullet}) - H(ArO_{HB}^{\bullet}) \quad (11)$$

Since myricetin possesses three hydroxyl groups in the B-ring, in close proximity, two more situations had to be considered. For the C3' radical, the C5' hydroxyl group can be facing the same direction as C4'—named here as a cross hydrogen bond (CHB)—or the opposite one. On the other hand, the C4' radical can be stabilized by two, one or zero hydrogen bonds coming from the C3' and C5' hydroxyl moieties. This leads to the three different situations, as presented in Figure 3, where C4'-radical (DHB) stands for the situation when the hydrogen bond is formed with both C3' and C5' hydroxyl hydrogens. The C3' and C4' radicals assume existence of only one hydrogen bond with a near-situated hydroxyl group.

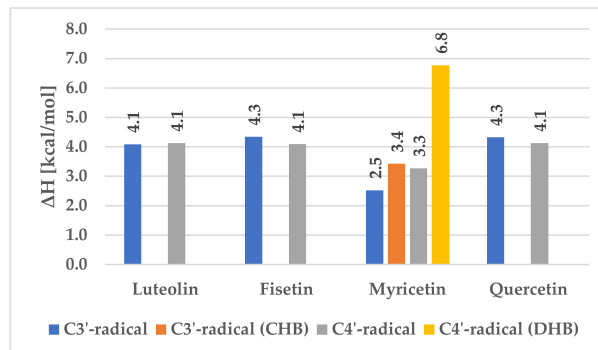


Figure 3. Differences in hydrogen bond enthalpy.

The results are presented below, while the full list of enthalpies is appended to the Supplementary Materials (Figure S3):

For all compounds except myricetin, one can see that the average value of the hydrogen bond stabilization energy is about 4 kcal/mol, regardless of the radical site. For myricetin, C3' stabilization energy without crossed hydrogen bond is lower by 1.5 kcal/mol than any other C3' HBE, because oxygen electronegative repulsion happens over a short distance (2.718 Å), decreasing hydrogen bond stability. However, if all hydrogen bonds are present, this energy difference increases to 3.4 kcal/mol, still being lower than for fisetin, luteolin or quercetin. For the C4' radical, the stabilization energy is lower than the average, because electrons of at least one oxygen interact with the radical at C4' (2.702 Å). If there are two hydrogen bonds, the stabilization energy is much greater, reaching up to 7 kcal/mol.

3.5. Catechol Moiety

Sroka et al. [35] observed an interesting behavior of luteolin, in comparison to structurally similar apigenin. The only difference between them is the existence of a 3,4-diOH catechol moiety in luteolin, and this small dissimilarity resulted in a nearly 100 times greater activity of the compound. Formation of a diradical and its rearrangement to 1,2-benzoquinone is widely stated as an explanation for the antioxidative scavenging potential difference between these already-mentioned structures. Lin et al. [24], in their experimental study, found a large difference of activity between the C3',C4'-dihydroxyl moiety flavonoids and those with a single C4' residue. They have proposed a mechanism explaining this diversity (see Figure 4): (a) a hydrogen abstraction from the most favored position, herein indicated by the HAE value; (b) a hydrogen transfer from the C4' to the C3', if allowed; (c) a second hydrogen abstraction from the C3' hydroxyl group; (d) an intramolecular reorganization and the hydroquinone formation. Within this section, it was investigated in a strict thermochemical scope.

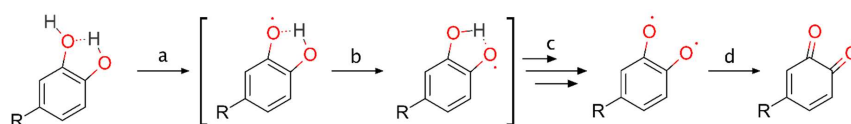


Figure 4. Example of catechol moiety hydrogen swap reaction and reorganization mechanism for C3.

3.5.1. Intramolecular Hydrogen Swap

For all possible B-ring radicals, a synchronous transit-guided quasi-Newton method [67] was conducted to search potential energy surface for imaginary frequencies, corresponding to the presented movement of the hydrogen atom (b). Each compound demonstrated exactly one imaginary value. Next, the optimization to a transition state showed that it is similar to the dioxolane, where the hydrogen atom is suspended between oxygen atoms.

To describe these processes in a thermochemical way, Gibb's free energy was calculated according to the following formula [Equation (12)]:

$$\Delta_r G^0(298\text{K}) = \sum (\varepsilon_0 + G_{\text{corr}})_{\text{products}} - \sum (\varepsilon_0 + G_{\text{corr}})_{\text{reactants}} \quad (12)$$

where:

- $\Delta_r G^0(298\text{K})$ is Gibb's free energy of the reaction, at 298 K (25 °C) and pressure of 1 atmosphere.
- ε_0 is total electronic energy [Hartree].
- G_{corr} is thermal free energy [Hartree].

All values necessary for thermochemical calculations and to plot the reactions profile (Figure 5) are presented in Table S3.

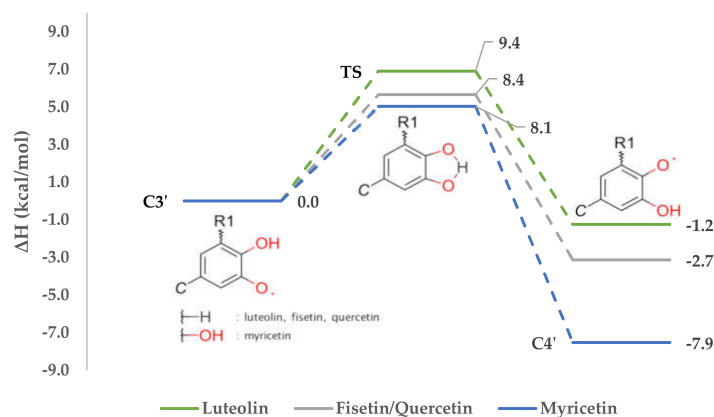


Figure 5. Reactions profile of intramolecular hydrogen swap.

According to Table 6, where HAEs are noted, the hydrogen abstraction from fisetin should take place at C3', while for luteolin, myricetin and quercetin, position C4' is preferred. In consequence, corresponding radicals will be created. The Gibbs free energies calculated for these hydrogen swap reactions are respectively -2.5 kcal/mol, 1.9 kcal/mol, 7.5 kcal/mol and 1.9 kcal/mol. The value obtained for fisetin fits with an assumption that the hydrogen from C4' will likely trade for the free electron at C3'. On the other hand, it can be also stated that the reverse process, the hydrogen swap from C3' to C4', is not going to happen.

If hydrogen abstraction takes place at C3' of luteolin, myricetin or quercetin, an intramolecular swap would happen as well. This allows us to state that despite of investigated compound, if the C4' radical can be formed by the movement of hydrogen from C3' or C5', this will occur, the most stable radical will be formed, and the reaction will be favored thermodynamically. This assumption needs to be tested also on different compounds—e.g., phenolic acids or anthocyanins.

3.5.2. Diradical Formation

To investigate a possible mechanism of the second hydrogen abstraction, the distinctive determinants were calculated for diradical unrelaxed structures, in the same way that radicals were (Table 8).

Table 8. Enthalpies of diradical formation mechanisms [kcal/mol].

Flavonoid	HAT BDE	ETPT		SPLET	
		IP	PDE	PA	ETE
Luteolin	103.6	-282.6	416.1	26.4	107.0
Fisetin	91.6	-287.8	409.2	17.1	104.3
Myricetin	C3'–C4'	90.5	405.3	19.7	100.6
	C4'–C5'	83.7	398.5	15.5	98.1
Quercetin	93.8	-285.7	409.4	18.5	105.2

Bond dissociation enthalpies are usually larger than for the single radical formation, and only luteolin behaves differently. This is correct according to intuition and a knowledge of chemistry—that creating a structure with two unpaired electrons requires more energy. It is not likely that second hydrogen abstraction occurs this way.

Interesting values were achieved for the first step of the ETPT mechanism, because formation of a cation-radical releases nearly 300 kcal/mol. On the other hand, proton dissociation requires nearly 400 kcal/mol; therefore, total average enthalpy required for this process is about 120 kcal/mol. According to the statements made during the investigation into single radicals, the first step shows the thermodynamically preferred pathway. For this reason, the ETPT mechanism is assumed to be responsible for the diradical formation. It is probable that, in studies with explicit water solvent molecules, where hydrogen bonds are involved, the PDE would decrease too.

The first step of the SPLET mechanism has lower enthalpy values than for a single radical, but the second one has higher values. Proton affinities are lower than corresponding values in the single radical formation, and electron transfer energies are quite larger.

3.5.3. o-Hydroquinone Formation

The reorganization of diradicals into o-hydroquinone was determined the same way as the intramolecular hydrogen swap earlier (thermochemical values are presented in Table S4 and shown in Table 9, where o-HFE stands for o-hydroquinone formation enthalpy from diradicals). The results show that the intramolecular reorganization into o-hydroquinone happens since each Gibb's free energy is negative, especially for fisetin, myricetin C3'-C4' and quercetin. O-hydroquinone products were experimentally found by Maini et al. [68].

Table 9. o-Hydroquinone formation parameters [kcal/mol].

Flavonoid	$\Delta_r G^0$	o-HFE	RE	Σ
Luteolin	-5.0	-5.6	-34.4	-40.0
Fisetin	-13.2	-14.4	-15.7	30.1
Myricetin C3'-C4'	-11.9	-11.9	-14.4	-26.3
Myricetin C4'-C5'	-7.5	-8.2	-13.8	-22.0
Quercetin	15.1	-14.4	-15.7	-30.1

The biggest o-hydroquinone formation enthalpy is also denoted for the three stated compounds—all are below -10 kcal/mol. Relaxation of the molecule decreases the system's total enthalpy even more. The reorganization enthalpy of luteolin is nearly -35 kcal/mol. Interestingly, the structure, instead of becoming more planar, increases its dihedral angle to 29.6°.

These values are even greater if o-HFE and RE are summed up. In the end, the whole mechanism of catechol moiety was described.

4. Conclusions

Within this research, flavonols and flavones were analyzed with the B3LYP/6-31+G(d,p) level of computational chemistry theory, and structure-activity relationship dependencies were proposed. First of all, it was noted that free p_y orbitals play a role when the radical is formed. They contribute to the electron delocalization by resonance and hyperconjugation effects, but only in AC- or BC-ring complexes, depending on the hydrogen abstraction site. The reason for this is the cross-conjugation effect of the carbonyl residue. Nevertheless, there is no possibility that hydrogen density would be exchanged between them in any manner—neither directly, nor indirectly via hydrogen atom exchange. Because of this, most flavonols and flavones adapt geometries, for which AC- and B-rings are coplanar, resulting in conjugation enhancement. It was noticed that an intramolecular hydrogen bonding can be even more important, as flavonoids with two or three B-ring hydroxyl groups close together prefer to detach the hydrogen atom from the B-ring instead of the AC-ring, as suggested by the reorganization enthalpy values. Each additional hydrogen bond guarantees greater reduction of the system's total enthalpy due to the stabilization effect. Moreover, if the structure involves a diccatechol moiety, it is likely to form the hydroquinone form via the diradical intermediate state, where ETPT plays a role when the diradical is going to be formed. Thermodynamically, the most favored mechanism of action for

the first hydrogen abstraction in a polar solvent is a C7 SPLET abstraction. On the other hand HAE, by including reorganization enthalpy correction, we see that C3 for flavonols and C4' for flavones (especially if a C3' or C5' hydroxyl group is present) are most favorable.

Supplementary Materials: The following data is available online at <http://www.mdpi.com/2076-3921/9/6/461/s1>, Figure S1: HOMOs (lower) and LUMOs (upper) visualization with isovalue 0.05, Figure S2: Radicals' Mulliken spin densities with hydrogen summed into heavy atoms, Figure S3: Enthalpies of flavonoids' radicals with and without hydrogen bond stabilization (isomer without H-bond is marked *) (a.u.), Table S1: Enthalpies of the flavonoids' lowest energetic isomer at B3LYP/6-31+G(d,p) level of theory (a.u.), Table S2: Enthalpies of unrelaxed and relaxed radicals of investigated compounds (a.u.), Table S3: Radicals thermochemical values (a.u.), Table S4: Diradicals thermochemical values (a.u.). All geometries are deposited as xyz files in the online repository accessible via link <http://dx.doi.org/10.17632/njz3gx3w2d>.

Author Contributions: Conceptualization, M.S.; Formal analysis, M.S.; Funding acquisition, Z.S.; Investigation, M.S.; Methodology, M.S. and T.A.; Supervision, T.A. and Z.S.; Validation, M.S. and T.A.; Visualization, M.S.; Writing—original draft, M.S.; Writing—review & editing, T.A. and Z.S. All authors have read and agreed to the published version of the manuscript.

Funding: This research was funded by Wroclaw Medical University (grant number SUB.D110.19.005) and Wroclaw Medical University Foundation.

Acknowledgments: Calculations have been carried out using resources provided by Wroclaw Centre for Networking and Supercomputing (<http://wcss.pl>), grant No. 12.

Conflicts of Interest: The authors declare no conflict of interest.

Appendix A. Electron Density Swap

As mentioned earlier, AC- and BC-electron complexes are not in a conjugated system. Thus, electron density is locked in one of them, depending on which the hydroxyl group hydrogen was removed. Looking at Lewis structures (Figure 1) and LUMOs (Figure S1) gives an insight into delocalization, indicating that radicals' electron density is concentrated on carbonyl oxygen, especially for the C4' radical. Amić et al. [29] and Heijnen et al. [17] suggested a mechanism of activity, where the hydrogen atom can swap from the C5 position to the carbonyl in exchange for electron density. It was ascertained whether such a transfer from the one complex to another can occur, based on the following mechanism (Figure A1):

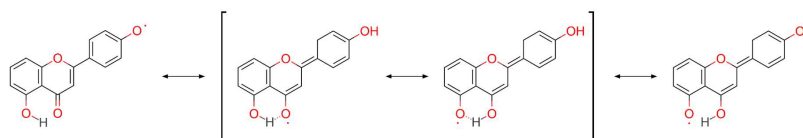


Figure A1. Electron density swap mechanism.

Elaboration of the problem was similar to that presented for a catechol moiety. No imaginary frequency was found. For this reason, a different procedure was used—beside the polarizable continuum model, a water molecule was placed near ($\approx 2.000\text{\AA}$) to the carbonyl oxygen radical and appropriate hydroxyl group. It was thought that it could serve as a hydrogen bridge between carbonyl oxygen. Based on the calculations, the swap mechanism illustrated in Figure A1 cannot be supported. It seems that electron density cannot be moved between A- and C-rings to achieve further stabilization, at least for the model studied here. This finding emphasizes the importance of the B-ring's substitution pattern for flavonoids' antioxidative potential.

Appendix B. Frontier Molecular Orbitals Theory

Appendix B.1. Highest Occupied (HOMO) and Lowest Unoccupied (LUMO) Molecular Orbitals

HOMO and LUMO, relatively, are the fundamentals of electron-donating and electron-accepting characteristics in the frontier molecular orbitals theory. The higher the HOMO energy and the smaller the energy gap between HOMO and LUMO, the better the reducing agent is [69]. Since flavonoids operate via hydrogen particle donation, which is coupled with the bound electron transfer, an electron affinity [EA; Equation (A1)] was calculated, and a chemical hardness [η ; Equation (A2)] [70] was checked and noted (Table A1). Evaluation of this property was performed according to the following statements:

$$\text{ArOH} + e^- \rightarrow \text{ArOH}^-$$

$$\text{EA} = \text{H}(\text{ArOH}^-) - \text{H}(e^-) - \text{H}(\text{ArOH}) \quad (\text{A1})$$

$$\eta = \frac{\text{IP} - \text{EA}}{2} \quad (\text{A2})$$

E_{HOMO} values do not differ significantly, and the largest can be found for fisetin, kaempferol, myricetin and quercetin. Since chemical hardness tends to be a valuable descriptor of hydrogen donating predisposition [71], flavonols were organized into three classes according to their E_{HOMO} values: low active (L), moderate active (M) and highly active (H). With chemical hardness studies, it can be concluded that flavonoids are hard acids, in the hard and soft acids and bases (HSAB) concept, especially flavonols. Results obtained from these calculations indicate the C7 hydroxyl group as a favorable hydrogen abstraction site. This pattern coincides with IP values from Table 4; similar conclusions were made by Mazzone et al. during hydroxycinnamic acid investigations [72].

Table A1. Energies of HOMO, LUMO and chemical hardness of investigated flavonoids [eV].

Flavonoids		E_{HOMO}	E_{LUMO}	C2'	C3'	C4'	$\frac{ \eta }{\text{C5}'}$	C3	C5	C7
Flavones	Acacetin	-6.270 (M)	-2.217						4.572	4.265
	Apigenin	-6.319 (L)	-2.220			4.263			4.512	4.255
	Chrysin	-6.460 (L)	-2.320						4.456	4.170
	Chrysoeriol	-6.135 (M)	-2.221			4.374			4.625	4.319
	Diosmetin	-6.151 (M)	-2.222		4.439				4.624	4.310
	Genkwanin	-6.329 (L)	-2.195			4.245			4.565	
	Luteolin	-6.215 (M)	-2.240		4.393	4.213			4.565	4.297
Flavonols	Fisetin	-5.924 (H)	-2.250		4.413	4.487		4.581		4.398
	Galangin	-6.172 (M)	-2.373					4.394	4.514	4.288
	Kaempferol	-5.982 (H)	-2.283			4.415		4.491	4.631	4.374
	Morin	-6.141 (M)	-2.285	4.505		4.350		4.270	4.534	4.295
	Myricetin	-5.941 (H)	-2.315		4.527	4.377	4.399	4.503	4.638	4.396
	Quercetin	-5.934 (H)	-2.304		4.544	4.340		4.518	4.647	4.400

A visualization of the results (Figure S1) pinpoints the electron density of HOMO on the B-ring, the C2–C3 double bond and the hydroxyl oxygen atoms. Absence of the hydroxyl groups in the B-ring moves density to the A-ring (e.g., chrysin). The C4' hydroxyl group is always occupied with a great amount of electron density, even if the adjacent hydroxyl group is not (e.g., myricetin). This is in agreement with the statement that C4' is the most favored abstraction position. Examination of the LUMO reveals how conjugation between the B-ring and the C2–C3 double bond is formed—one can observe a π -bond swap characteristic for the conjugated system, and creation of C2–C1' and C3–C4 bonds. Apparently, the electron density arises on the chromone and carbonyl group oxygens. Morin is an exception because B- and C-ring p_y orbitals do not overlap, and thus electrons are retained on them.

Appendix B.2. Single Occupied Molecular Orbital (SOMO)

Like HOMOs of molecules, SOMOs can be found when radical structures are described. Being occupied by an unpaired electron, these structures are much more reactive than corresponding neutral particles. Simply, to check whether the particle is nucleophilic or electrophilic, one should compare the radical's E_{SOMO} with the E_{HOMO} and E_{LUMO} of the targeted compound. If the E_{SOMO} is closer to the E_{LUMO} , then the radical will act as nucleophile; otherwise its electrophile properties are demonstrated.

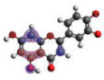
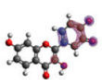
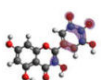
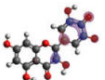
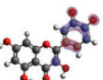
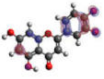
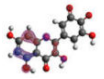
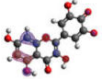
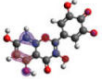
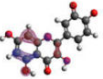
Presented in Table A2, E_{SOMO} is similar to the E_{HOMO} of flavonoids they derive from. Since E_{SOMO} is slightly lower than E_{HOMO} for the corresponding molecule, it may suggest they retain electron-donating properties, and would willingly detach another hydrogen to scavenge another radical. DFT results indicate each SOMO was occupied exactly by one electron.

Table A2. Energies of SOMOs of investigated flavonoids' radicals [eV].

Flavonoids		C2'	C3'	C4'	E_{SOMO} C5'	C3	C5	C7
Flavones	Acacetin						-6.367	-6.502
	Apigenin			-6.570			-6.456	-6.586
	Chrysin						-6.699	-6.925
	Chrysoeriol			-6.470			-6.205	-6.320
	Diosmetin		-6.471				-6.216	-6.319
	Genkwanin			-6.594			-6.429	
	Luteolin		-6.494	-6.557			-6.343	-6.440
Flavonols	Fisetin		-6.329	-6.290		-6.212		-6.195
	Galangin					-6.463	-6.429	-6.573
	Kaempferol			-6.356		-6.230	-6.176	-6.336
	Morin	-6.237		-6.489		-6.400	-6.305	-6.445
	Myricetin	-6.202	-6.246	-6.265	-6.268		-6.102	-6.258
	Quercetin	-6.189	-6.224	-6.292			-6.122	-6.270

According to the obtained results (Table A3), it is clear that luteolin (flavone) SOMO orbitals are quasi-degenerated. The energy gap between them is much lower than for flavonols, where it reaches approximately 0.7–1.2 eV. Moreover, their energies are even lower than for the molecule's HOMO or the radical's SOMO, which the diradical originates from. As a result, SOMO with energy -6.704 eV conforms to other examined diradicals' lowest energetic SOMO.

Table A3. Energies of SOMOs of investigated flavonoids' diradicals [eV].

Luteolin C3'-C4'	Fisetin C3'-C4'	Myricetin		Quercetin C4'-C5'
		C3'-C4'	C4'-C5'	
				
-6.704	-5.989	-6.049	-6.003	-6.032
				
-6.893	-7.184	-6.721	-6.757	-6.866

References

1. Ray, P.D.; Huang, B.W.; Tsuji, Y. Reactive oxygen species (ROS) homeostasis and redox regulation in cellular signaling. *Cell. Signal* **2012**, *24*, 981–990. [[CrossRef](#)] [[PubMed](#)]
2. Hamanaka, R.B.; Chandel, N.S. Mitochondrial reactive oxygen species regulate cellular signaling and dictate biological outcomes. *Trends Biochem. Sci.* **2010**, *35*, 505–513. [[CrossRef](#)] [[PubMed](#)]

3. Adams, L.; Franco, M.C.; Estevez, A.G. Reactive nitrogen species in cellular signaling. *Exp. Biol. Med.* **2015**, *240*, 711–717. [[CrossRef](#)] [[PubMed](#)]
4. Lander, H.M. An essential role for free radicals and derived species in signal transduction. *FASEB J.* **1997**, *11*, 118–124. [[CrossRef](#)]
5. Breen, A.P.; Murphy, J.A. Reactions of oxyl radicals with DNA. *Free Radic. Biol. Med.* **1995**, *18*, 1033–1077. [[CrossRef](#)]
6. Pratt, D.A.; Tallman, K.A.; Porter, N.A. Free radical oxidation of polyunsaturated lipids: New mechanistic insights and the development of peroxy radical clocks. *Acc. Chem. Res.* **2011**, *44*, 458–467. [[CrossRef](#)]
7. Du, J.; Gebicki, J.M. Proteins are major initial cell targets of hydroxyl free radicals. *Int. J. Biochem. Cell Biol.* **2004**, *36*, 2334–2343. [[CrossRef](#)]
8. Hulsmans, M.; Van Dooren, E.; Holvoet, P. Mitochondrial reactive oxygen species and risk of atherosclerosis. *Curr. Atheroscler. Rep.* **2012**, *14*, 264–276. [[CrossRef](#)]
9. Vera-Ramirez, L.; Sanchez-Rovira, P.; Ramirez-Tortosa, M.C.; Ramirez-Tortosa, C.L.; Granados-Principal, S.; Lorente, J.A.; Quiles, J.L. Free radicals in breast carcinogenesis, breast cancer progression and cancer stem cells. Biological bases to develop oxidative-based therapies. *Crit. Rev. Oncol. Hematol.* **2011**, *80*, 347–368. [[CrossRef](#)]
10. Sies, H.; Berndt, C.; Jones, D.P. Oxidative Stress. *Annu. Rev. Biochem.* **2017**, *86*, 715–748. [[CrossRef](#)]
11. Valko, M.; Leibfriz, D.; Moncol, J.; Cronin, M.T.D.; Mazur, M.; Telser, J. Free radicals and antioxidants in normal physiological functions and human disease. *Int. J. Biochem. Cell Biol.* **2007**, *39*, 44–84. [[CrossRef](#)] [[PubMed](#)]
12. Scalbert, A.; Johnson, I.T.; Saltmarsh, M. Polyphenols: Antioxidants and beyond. *Am. J. Clin. Nutr.* **2005**, *81*, 215–217. [[CrossRef](#)] [[PubMed](#)]
13. Martin, D.A.; Bolling, B.W. A review of the efficacy of dietary polyphenols in experimental models of inflammatory bowel diseases. *Food Funct.* **2015**, *6*, 1773–1786. [[CrossRef](#)] [[PubMed](#)]
14. Chen, L.; Teng, H.; Xie, Z.; Cao, H.; Cheang, W.S.; Skalicka-Woniak, K.; Georgiev, M.I.; Xiao, J. Modifications of dietary flavonoids towards improved bioactivity: An update on structure–activity relationship. *Crit. Rev. Food Sci. Nutr.* **2018**, *58*, 513–527. [[CrossRef](#)] [[PubMed](#)]
15. Masek, A.; Chrzescijanska, E.; Latos, M.; Zaborski, M. Influence of hydroxyl substitution on flavanone antioxidants properties. *Food Chem.* **2017**, *215*, 501–507. [[CrossRef](#)] [[PubMed](#)]
16. Musialik, M.; Kuzmicz, R.; Pawlowski, T.S.; Litwinienko, G. Acidity of hydroxyl groups: An overlooked influence on antiradical properties of flavonoids. *J. Org. Chem.* **2009**, *74*, 2699–2709. [[CrossRef](#)]
17. Heijnen, C.G.M.; Haenen, G.R.M.M.; Van Acker, F.A.A.; Van Der Vijgh, W.J.F.; Bast, A. Flavonoids as peroxynitrite scavengers: The role of the hydroxyl groups. *Toxicol. Vitro.* **2001**, *15*, 3–6. [[CrossRef](#)]
18. Amorati, R.; Valgimigli, L. Modulation of the antioxidant activity of phenols by non-covalent interactions. *Org. Biomol. Chem.* **2012**, *10*, 4147–4158. [[CrossRef](#)]
19. Lucarini, M.; Pedulli, G.F.; Guerra, M. A Critical Evaluation of the Factors Determining the Effect of Intramolecular Hydrogen Bonding on the O-H Bond Dissociation Enthalpy of Catechol and of Flavonoid Antioxidants. *Chem. A Eur. J.* **2004**, *10*, 933–939. [[CrossRef](#)]
20. Cano, A.; Williamson, G.; Garcia-Conesa, M.T. Superoxide scavenging by polyphenols: Effect of conjugation and dimerization. *Redox Rep.* **2002**, *7*, 379–383. [[CrossRef](#)]
21. Milenković, D.; Dimitrić Marković, J.M.; Dimić, D.; Jeremić, S.; Amić, D.; Pirković, M.S.; Marković, Z.S. Structural characterization of kaempferol: A spectroscopic and computational study. *Maced. J. Chem. Chem. Eng.* **2019**, *38*, 49–62. [[CrossRef](#)]
22. Lucarini, M.; Pedrielli, P.; Pedulli, G.F.; Cabiddu, S.; Fattuoni, C. Bond dissociation energies of O-H bonds in substituted phenols from equilibration studies. *J. Org. Chem.* **1996**, *61*, 9259–9263. [[CrossRef](#)]
23. Yokozawa, T.; Chen, C.P.; Dong, E.; Tanaka, T.; Nonaka, G.I.; Nishioka, I. Study on the inhibitory effect of tannins and flavonoids against the 1,1-diphenyl-2-picrylhydrazyl radical. *Biochem. Pharmacol.* **1998**, *56*, 213–222. [[CrossRef](#)]
24. Lin, C.; Zhu, C.; Hu, M.; Wu, A.; Zerendawa, B.; Suolangqimei, K. Structure–activity Relationships of Antioxidant Activity in vitro about Flavonoids Isolated from Pyrethrum Tatsienense. *J. Intercult. Ethnopharmacol.* **2014**, *3*, 123. [[CrossRef](#)]

25. Amić, A.; Marković, Z.; Dimitrić Marković, J.M.; Stepanić, V.; Lučić, B.; Amić, D. Towards an improved prediction of the free radical scavenging potency of flavonoids: The significance of double PCET mechanisms. *Food Chem.* **2014**, *152*, 578–585. [[CrossRef](#)]
26. Amić, A.; Marković, Z.; Klein, E.; Dimitrić Marković, J.M.; Milenković, D. Theoretical study of the thermodynamics of the mechanisms underlying antiradical activity of cinnamic acid derivatives. *Food Chem.* **2018**, *246*, 481–489. [[CrossRef](#)]
27. Dimitrić Marković, J.M.; Pejin, B.; Milenković, D.; Amić, D.; Begović, N.; Mojović, M.; Marković, Z.S. Antiradical activity of delphinidin, pelargonidin and malvin towards hydroxyl and nitric oxide radicals: The energy requirements calculations as a prediction of the possible antiradical mechanisms. *Food Chem.* **2017**, *218*, 440–446. [[CrossRef](#)]
28. Rice-Evans, C.A.; Miller, N.J.; Paganga, G. Structure-antioxidant activity relationships of flavonoids and phenolic acids. *Free Radic. Biol. Med.* **1996**, *20*, 933–956. [[CrossRef](#)]
29. Amić, D.; Davidović-Amić, D.; Bešlo, D.; Trinajstić, N. Structure-radical scavenging activity relationships of flavonoids. *Croat. Chem. Acta* **2003**, *76*, 55–61.
30. Rasulev, B.F.; Abdullaev, N.D.; Syrov, V.N.; Leszczynski, J. A Quantitative Structure-Activity Relationship (QSAR) study of the antioxidant activity of flavonoids. *QSAR Comb. Sci.* **2005**, *24*, 1056–1065. [[CrossRef](#)]
31. Van Acker, S.A.B.E.; Van Den Berg, D.J.; Tromp, M.N.J.L.; Griffioen, D.H.; Van Bennekom, W.P.; Van Der Vijgh, W.J.F.; Bast, A. Structural aspects of antioxidant activity of flavonoids. *Free Radic. Biol. Med.* **1996**, *20*, 331–342. [[CrossRef](#)]
32. Bors, W.; Heller, W.; Michel, C.; Saran, M. Flavonoids as antioxidants: Determination of radical-scavenging efficiencies. *Methods Enzymol.* **1990**, *186*, 343–355. [[PubMed](#)]
33. Galano, A.; Raúl Alvarez-Idaboy, J. Computational strategies for predicting free radical scavengers' protection against oxidative stress: Where are we and what might follow? *Int. J. Quantum Chem.* **2019**, *119*, 1–23. [[CrossRef](#)]
34. Marković, Z. Study of the mechanisms of antioxidative action of different antioxidants. *J. Serbian Soc. Comput. Mech.* **2016**, *10*, 135–150. [[CrossRef](#)]
35. Sroka, Z.; Żbikowska, B.; Hładyszowski, J. The antiradical activity of some selected flavones and flavonols. Experimental and quantum mechanical study. *J. Mol. Model.* **2015**, *21*, 307. [[CrossRef](#)]
36. Hanwell, M.D.; Curtis, D.E.; Loni, D.C.; Vandermeersch, T.; Zurek, E.; Hutchison, G.R. Avogadro: An advanced semantic chemical editor, visualization, and analysis platform. *J. Cheminform.* **2012**, *4*, 17. [[CrossRef](#)]
37. Weininger, D. SMILES, a chemical language and information system. 1. Introduction to methodology and encoding rules. *J. Chem. Inf. Model.* **1988**, *28*, 31–36. [[CrossRef](#)]
38. Allouche, A. Software News and Updates Gabedit—A Graphical User Interface for Computational Chemistry Softwares. *J. Comput. Chem.* **2012**, *32*, 174–182. [[CrossRef](#)]
39. Frisch, M.J.; Trucks, G.W.; Schlegel, H.B.; Scuseria, G.E.; Robb, M.A.; Cheeseman, J.R.; Scalmani, G.; Barone, V.; Petersson, G.A.; Nakatsuji, H.; et al. *Gaussian 16*; Gaussian, Inc.: Wallingford, CT, USA, 2016.
40. Becke, A.D. Density-functional thermochemistry. III. The role of exact exchange. *J. Chem. Phys.* **1993**, *98*, 5648–5652. [[CrossRef](#)]
41. Tomasi, J.; Mennucci, B.; Cammi, R. Quantum mechanical continuum solvation models. *Chem. Rev.* **2005**, *105*, 2999–3093. [[CrossRef](#)]
42. Mennucci, B.; Tomasi, J. Continuum solvation models: A new approach to the problem of solute's charge distribution and cavity boundaries. *J. Chem. Phys.* **1997**, *106*, 5151–5158. [[CrossRef](#)]
43. Aparicio, S. A systematic computational study on flavonoids. *Int. J. Mol. Sci.* **2010**, *11*, 2017–2038. [[CrossRef](#)] [[PubMed](#)]
44. Todorova, T.Z.; Traykov, M.G.; Tadjer, A.V.; Velkov, Z.A. Structure of flavones and flavonols. Part I: Role of substituents on the planarity of the system. *Comput. Theor. Chem.* **2013**, *1017*, 85–90. [[CrossRef](#)]
45. Wang, J.; Becke, A.D.; Smith, V.H. Evaluation of $\langle S^2 \rangle$ in restricted, unrestricted Hartree-Fock, and density functional based theories. *J. Chem. Phys.* **1995**, *102*, 3477–3480. [[CrossRef](#)]
46. Tada, K.; Tanaka, S.; Kawakami, T.; Kitagawa, Y.; Okumura, M.; Yamaguchi, K. Spin contamination errors on spin-polarized density functional theory/plane-wave calculations for crystals of one-dimensional materials. *Appl. Phys. Express* **2019**, *12*, 115506. [[CrossRef](#)]

47. Urbaniak, A.; Szelag, M.; Molski, M. Theoretical investigation of stereochemistry and solvent influence on antioxidant activity of ferulic acid. *Comput. Theor. Chem.* **2013**, *1012*, 33–40. [[CrossRef](#)]
48. Glendening, E.D.; Reed, A.E.; Carpenter, J.E.; Weinhold, F. NBO.
49. Limacher, P.A.; Lüthi, H.P. Cross-conjugation. *Wiley Interdiscip. Rev. Comput. Mol. Sci.* **2011**, *1*, 477–486. [[CrossRef](#)]
50. Jovanovic, S.V.; Steenken, S.; Hara, Y.; Simic, M.G. Which Ring in Flavonoids Is Responsible for Antioxidant Activity? *J. Chem. Soc. Perkins Trans.* **1996**, *2*, 2497–2504. [[CrossRef](#)]
51. Hatzidimitriou, E.; Nenadis, N.; Tsimidou, M.Z. Changes in the catechin and epicatechin content of grape seeds on storage under different water activity (aw) conditions. *Food Chem.* **2007**, *105*, 1504–1511. [[CrossRef](#)]
52. Çelik, S.E.; Özyürek, M.; Güçlü, K.; Apak, R. Solvent effects on the antioxidant capacity of lipophilic and hydrophilic antioxidants measured by CUPRAC, ABTS/persulphate and FRAP methods. *Talanta* **2010**, *81*, 1300–1309. [[CrossRef](#)]
53. Benzie, I.F.F.; Strain, J.J. The Ferric Reducing Ability of Plasma (FRAP) as a Measure of “Antioxidant Power”: The FRAP Assay. *Anal. Biochem.* **1996**, *239*, 70–76. [[CrossRef](#)] [[PubMed](#)]
54. Re, R.; Pellegrini, N.; Proteggente, A.; Pannala, A.; Yang, M.; Rice-Evans, C. Antioxidant activity applying an improved ABTS radical cation decolorization assay. *Free Radic. Biol. Med.* **1999**, *26*, 1231–1237. [[CrossRef](#)]
55. Brand-Williams, W.; Cuvelier, M.E.; Berset, C. Use of a free radical method to evaluate antioxidant activity. *LWT Food Sci. Technol.* **1995**, *28*, 25–30. [[CrossRef](#)]
56. Cheng, J.; Chen, X.; Zhao, S.; Zhang, Y. Antioxidant-capacity-based models for the prediction of acrylamide reduction by flavonoids. *Food Chem.* **2015**, *168*, 90–99. [[CrossRef](#)] [[PubMed](#)]
57. Milenković, D.; Dorović, J.; Petrović, V.; Avdović, E.; Marković, Z. Hydrogen atom transfer versus proton coupled electron transfer mechanism of gallic acid with different peroxy radicals. *React. Kinet. Mech. Catal.* **2018**, *123*, 215–230. [[CrossRef](#)]
58. Milenković, D.; Dorović, J.; Jeremić, S.; Dimitrić Marković, J.M.; Avdović, E.H.; Marković, Z. Free Radical Scavenging Potency of Dihydroxybenzoic Acids. *J. Chem.* **2017**, *2017*. [[CrossRef](#)]
59. Jeremić, S.; Radenković, S.; Filipović, M.; Antić, M.; Amić, A.; Marković, Z. Importance of hydrogen bonding and aromaticity indices in QSAR modeling of the antioxidative capacity of selected (poly)phenolic antioxidants. *J. Mol. Graph. Model.* **2017**, *72*, 240–245. [[CrossRef](#)]
60. Filipović, M.; Marković, Z.; Dorović, J.; Marković, J.D.; Lučić, B.; Amić, D. QSAR of the free radical scavenging potency of selected hydroxybenzoic acids and simple phenolics. *Comptes Rendus Chim.* **2015**, *18*, 492–498. [[CrossRef](#)]
61. Chen, Y.; Xiao, H.; Zheng, J.; Liang, G. Structure-thermodynamics-antioxidant activity relationships of selected natural phenolic acids and derivatives: An experimental and theoretical evaluation. *PLoS ONE* **2015**, *10*, 1–20. [[CrossRef](#)]
62. Arora, A.; Nair, M.G.; Strasburg, G.M. Structure-activity relationships for antioxidant activities of a series of flavonoids in a liposomal system. *Free Radic. Biol. Med.* **1998**, *24*, 1355–1363. [[CrossRef](#)]
63. Álvarez-Diduk, R.; Ramírez-Silva, M.T.; Galano, A.; Merkoçi, A. Deprotonation mechanism and acidity constants in aqueous solution of flavonols: A combined experimental and theoretical study. *J. Phys. Chem. B* **2013**, *117*, 12347–12359. [[CrossRef](#)] [[PubMed](#)]
64. Dimitrić Marković, J.M.; Milenković, D.; Amić, D.; Mojović, M.; Pašti, I.; Marković, Z.S. The preferred radical scavenging mechanisms of fisetin and baicalein towards oxygen-centred radicals in polar protic and polar aprotic solvents. *RSC Adv.* **2014**, *4*, 32228–32236. [[CrossRef](#)]
65. Huang, D.; Boxin, O.U.; Prior, R.L. The chemistry behind antioxidant capacity assays. *J. Agric. Food Chem.* **2005**, *53*, 1841–1856. [[CrossRef](#)] [[PubMed](#)]
66. Dimitrić Marković, J.M.; Milenković, D.; Amić, D.; Popović-Bijelić, A.; Mojović, M.; Pašti, I.A.; Marković, Z.S. Energy requirements of the reactions of kaempferol and selected radical species in different media: Towards the prediction of the possible radical scavenging mechanisms. *Struct. Chem.* **2014**, *25*, 1795–1804. [[CrossRef](#)]
67. Peng, C.; Bernhard Schlegel, H. Combining Synchronous Transit and Quasi-Newton Methods to Find Transition States. *Isr. J. Chem.* **1993**, *33*, 449–454. [[CrossRef](#)]
68. Maini, S.; Hodgson, H.L.; Krol, E.S. The UVA and aqueous stability of flavonoids is dependent on B-ring substitution. *J. Agric. Food Chem.* **2012**, *60*, 6966–6976. [[CrossRef](#)]
69. Pearson, R.G. Chemical hardness and density functional theory. *J. Chem. Sci.* **2005**, *117*, 369–377. [[CrossRef](#)]

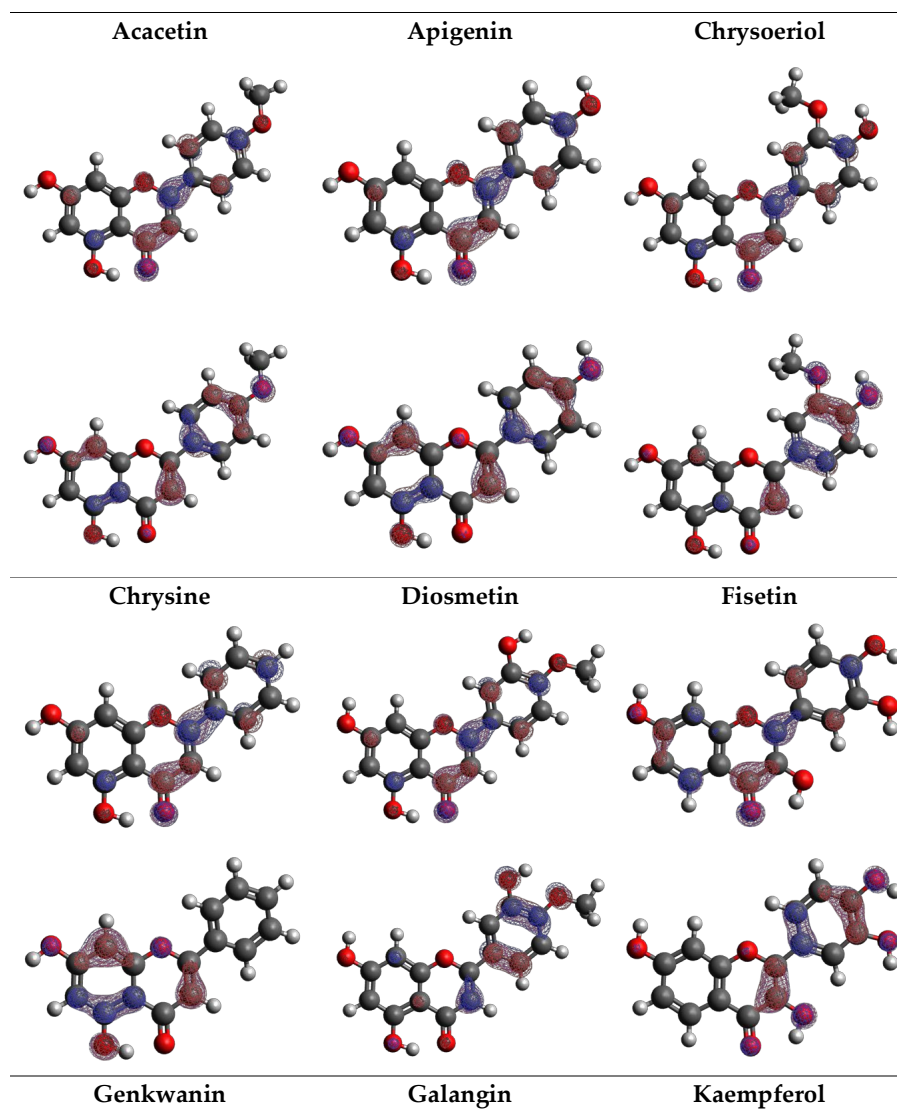
70. Parr, R.G.; Pearson, R.G. Absolute Hardness: Companion Parameter to Absolute Electronegativity. *J. Am. Chem. Soc.* **1983**, *105*, 7512–7516. [[CrossRef](#)]
71. Waki, T.; Nakanishi, I.; Matsumoto, K.I.; Kitajima, J.; Chikuma, T.; Kobayashi, S. Key role of chemical hardness to compare 2,2-diphenyl-1-picrylhydrazyl radical scavenging power of flavone and flavonol O-glycoside and C-glycoside derivatives. *Chem. Pharm. Bull.* **2012**, *60*, 37–44. [[CrossRef](#)]
72. Mazzone, G.; Russo, N.; Toscano, M. Antioxidant properties comparative study of natural hydroxycinnamic acids and structurally modified derivatives: Computational insights. *Comput. Theor. Chem.* **2016**, *1077*, 39–47. [[CrossRef](#)]

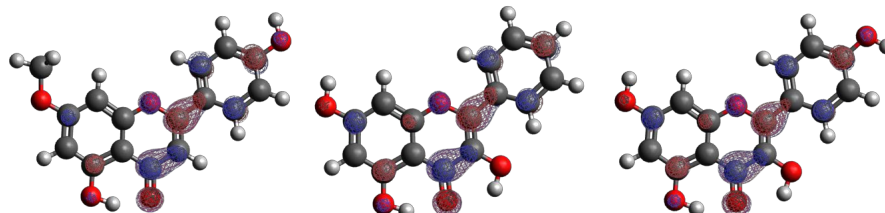


© 2020 by the authors. Licensee MDPI, Basel, Switzerland. This article is an open access article distributed under the terms and conditions of the Creative Commons Attribution (CC BY) license (<http://creativecommons.org/licenses/by/4.0/>).

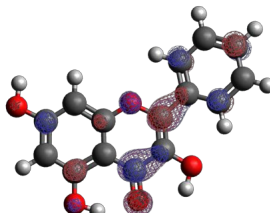
i. Materiały dodatkowe

Supplementary Materials

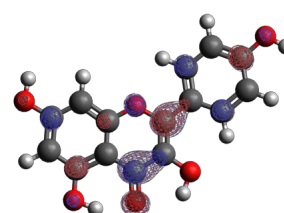
Figures



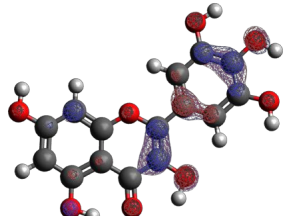
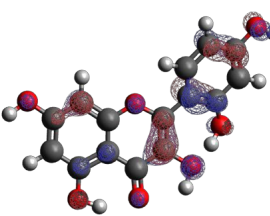
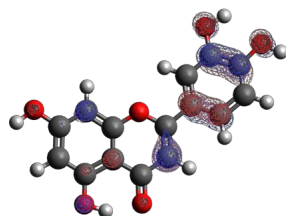
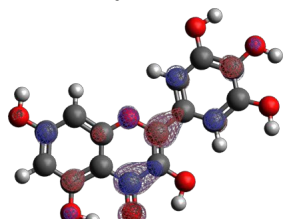
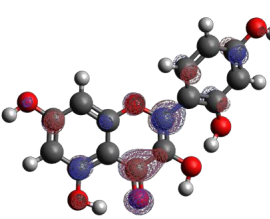
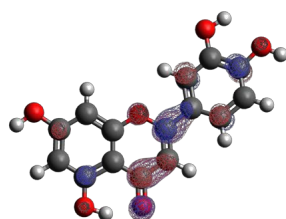
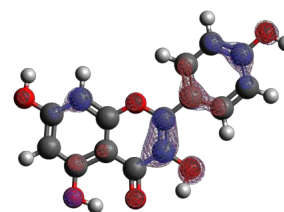
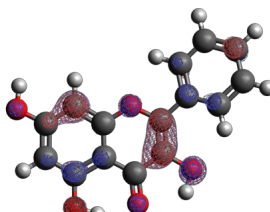
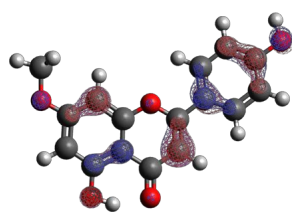
Luteolin



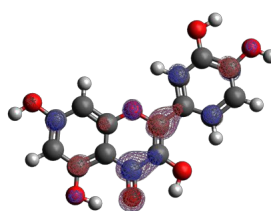
Morin



Myricetin



Quercetin



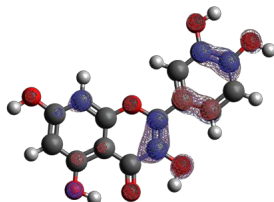
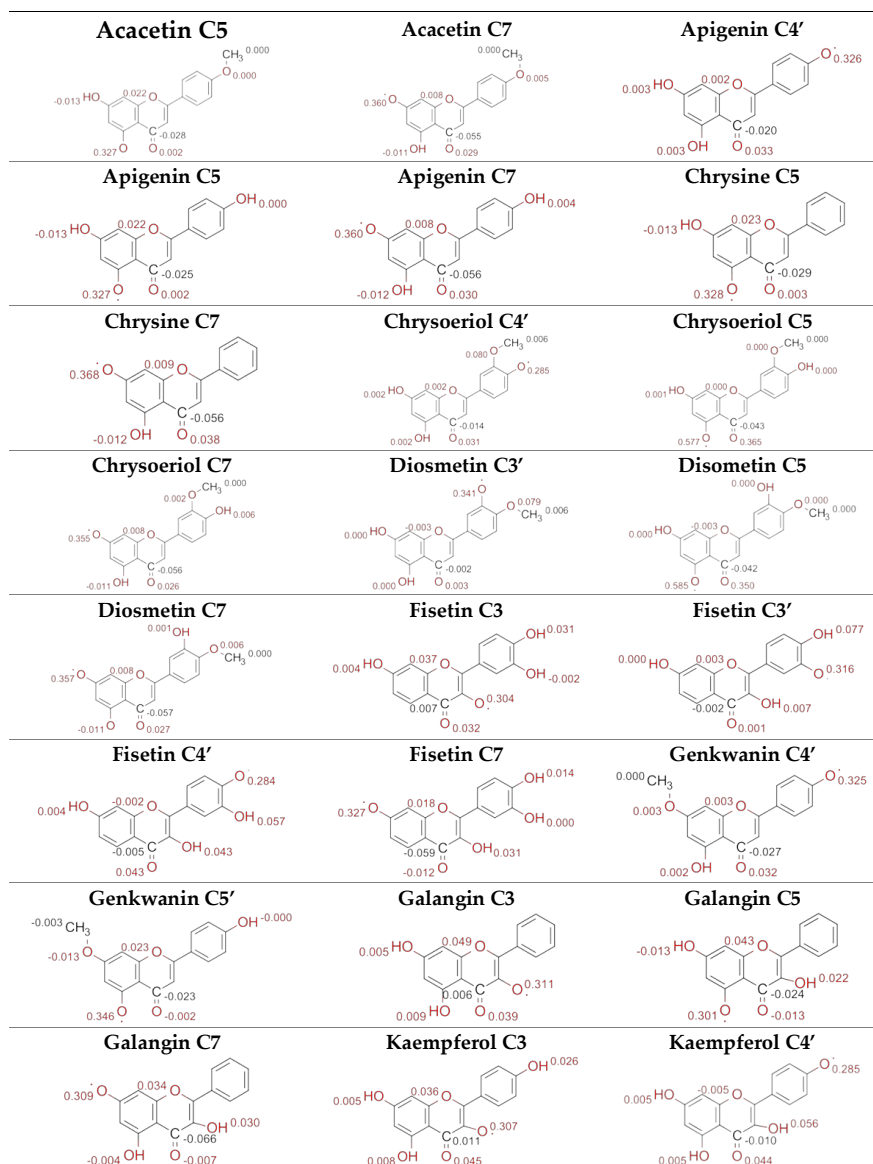


Figure 1. HOMOs (lower) and LUMOs (upper) visualization with isovalue 0.05



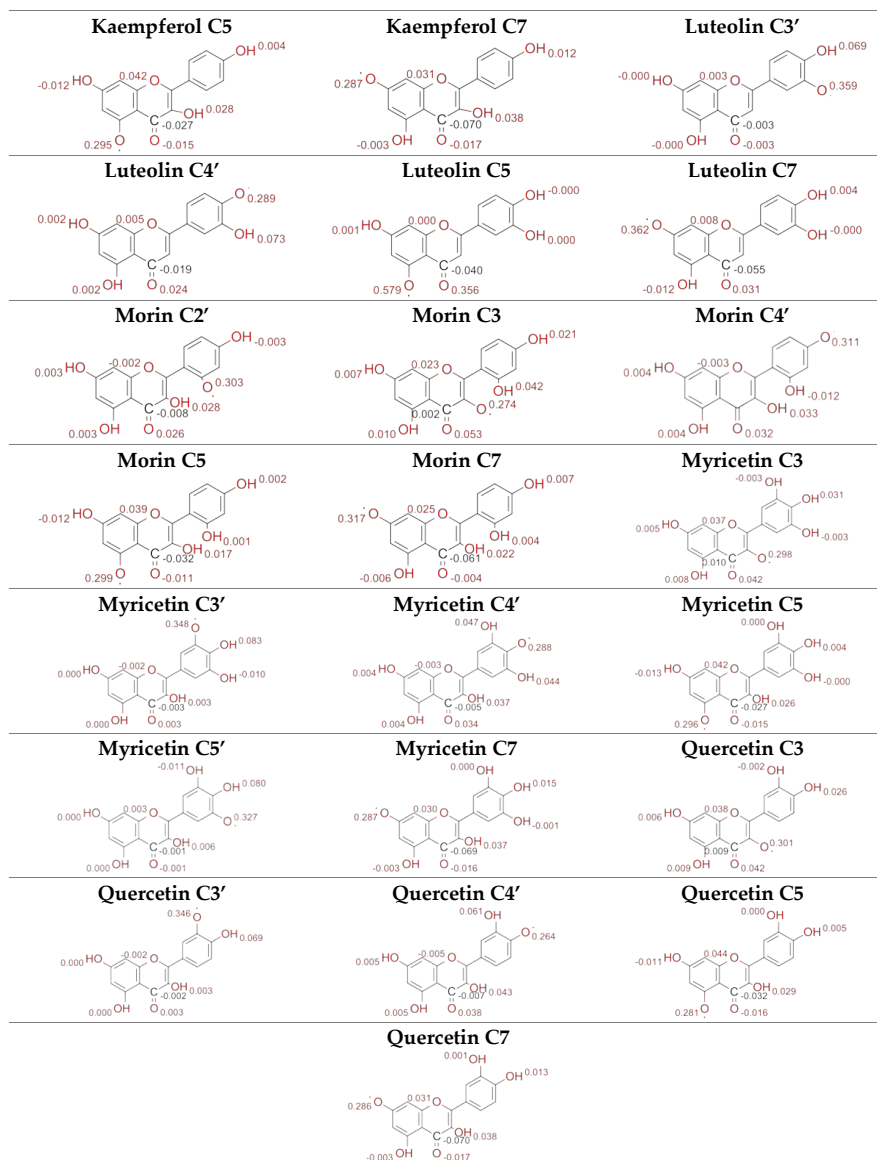


Figure 2. Radicals' Mulliken spin densities with hydrogen summed into heavy atoms

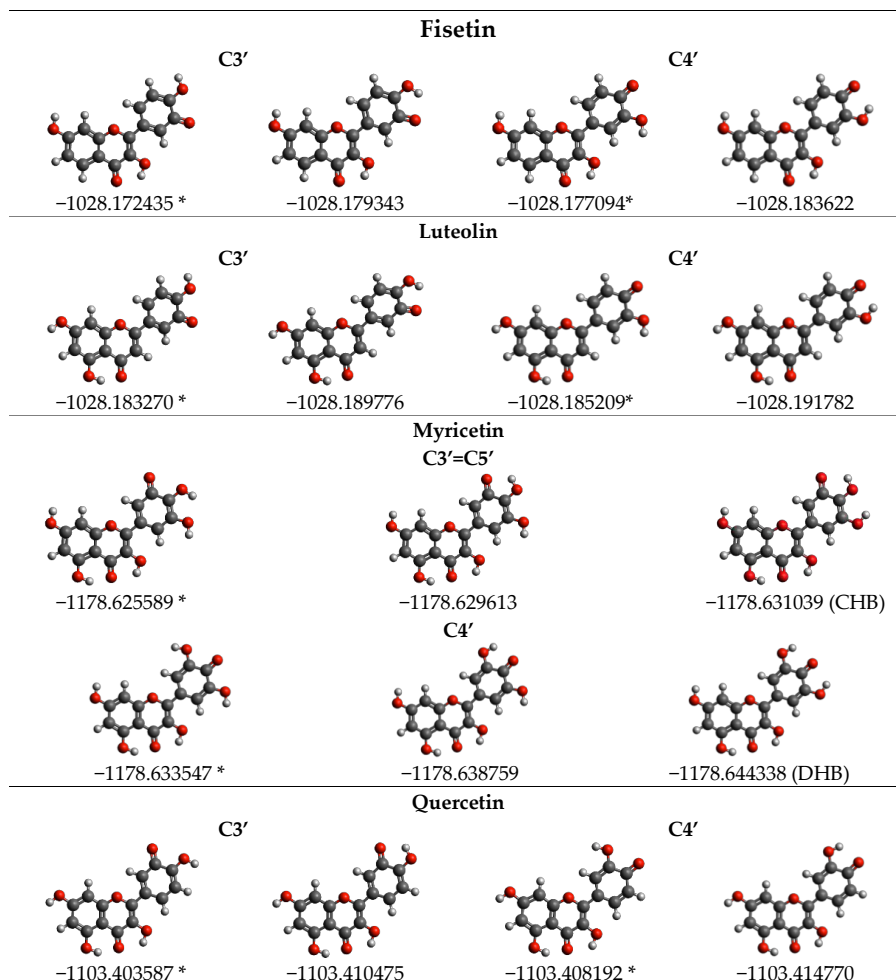
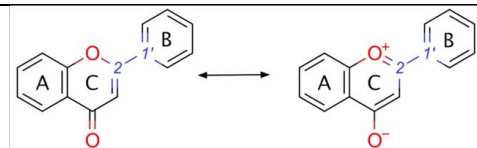


Figure 3. Enthalpies of flavonoids' radicals with and without hydrogen bond stabilization (isomer without H-bond is marked *) [a.u.]

Tables

Table 1. Enthalpies of the flavonoids' lowest energetic isomer at B3LYP/6-31+G(d,p) level of theory [a.u.]



	Flavonoid	Enthalpy
Flavones	Acacetin	-992.861147
	Apigenin	-953.589415
	Chrysin	-878.363148
	Chrysoeriol	-1068.084598
	Diosmetin	-1068.084312
	Genkwanin	-992.861115
	Luteolin	-1028.811831
Flavonols	Fisetin	-1028.799467
	Galangin	-953.582425
	Kaempferol	-1028.808400
	Morin	-1104.033327
	Myricetin	-1179.253341
	Quercetin	-1104.030864

Table 2. Enthalpies of unrelaxed and relaxed radicals of investigated compounds [a.u.]

Flavonoids		Unrelaxed radical	Relaxed radical
Acacetin	C5	-992,199222	-992,213026
	C7	-992,216822	-992,224983
Apigenin	C4'	-952,947947	-952,958621
	C5	-952,930000	-952,941269
	C7	-952,944139	-952,952039
Chrysin	C5	-877,701313	-877,715043
	C7	-877,716141	-877,725026
Chrysoeriol	C4'	-1067,446832	-1067,459122
	C5	-1067,415336	-1067,419226
	C7	-1067,439373	-1067,447632
Diosmetin	C3'	-1067,445198	-1067,456637
	C5	-1067,414907	-1067,418746
Genkwanin	C7	-1067,438585	-1067,447177
	C4'	-992,220493	-992,230596
Luteolin	C5	-992,199106	-992,212595
	C3'	-1028,172077	-1028,183270
Luteolin	C4'	-1028,178156	-1028,191782
	C5	-1028,143630	-1028,146283
	C7	-1028,166412	-1028,174353
Fisetin	C3'	-1028,167323	-1028,179343
	C4'	-1028,164704	-1028,177094
	C3	-1028,162134	-1028,176690
	C7	-1028,156325	-1028,165763
Galangin	C3	-952,944720	-952,958463

	C5	-952,926275	-952,939686
	C7	-952,937061	-952,946355
Kaempferol	C4'	-1028,171031	-1028,182027
	C3	-1028,173008	-1028,186897
	C5	-1028,152508	-1028,166096
	C7	-1028,165319	-1028,174020
		C2'	-1103,385259
Morin	C4'	-1103,392680	-1103,402521
	C3	-1103,399249	-1103,419264
	C5	-1103,376267	-1103,390761
	C7	-1103,388420	-1103,396868
Myricetin	C3'	-1178,614708	-1178,625589
	C4'	-1178,625608	-1178,638759
	C5'	-1178,619670	-1178,631215
	C3	-1178,616992	-1178,631960
	C5	-1178,597496	-1178,611019
	C7	-1178,609123	-1178,618703
Quercetin	C3'	-1103,392412	-1103,403587
	C4'	-1103,401993	-1103,414770
	C3	-1103,395481	-1103,409514
	C5	-1103,375549	-1103,389360
	C7	-1103,387556	-1103,396441

Table 3. Radicals thermochemical values [a.u.]

Flavonoids	Radical	$\epsilon_0 + H_{\text{corr}}$	$\epsilon_0 + G_{\text{corr}}$
Luteolin	C3'	-1028.190	-1028.252
	TS	-1028.179	-1028.240
	C4'	-1028.192	-1028.255
Fisetin	C3'	-1028.179	-1028.243
	TS	-1028.170	-1028.232
	C4'	-1028.184	-1028.247
Myricetin	C3'-C5'	-1178.631	-1178.699
	TS	-1178.623	-1178.691
	C4'	-1178.643	-1178.711
Quercetin	C3'	-1103.410	-1103.477
	TS	-1103.401	-1103.466
	C4'	-1103.415	-1103.480

Table 4. Diradicals thermochemical values [a.u.]ⁱⁱ

Flavonoids	$\epsilon_0 + H_{\text{corr}}^i$	$\epsilon_0 + G_{\text{corr}}$
<i>Luteolin</i>	-1027.514	-1027.574
	<u>-1027.523</u>	<u>-1027.578 (r)</u>
<i>Fisetin</i>	-1027.522	-1027.583
	<u>-1027.545</u>	<u>-1027.570 (r)</u>
<i>Myricetin</i>	-1177.982	-1178.046
	<u>-1178.001</u>	<u>-1178.024 (r)</u>
	-1177.993	-1178.057
	<u>-1178.006</u>	<u>-1178.028 (r)</u>
<i>Quercetin</i>	-1102.753	-1102.815
	<u>-1102.776</u>	<u>-1102.801 (r)</u>

ⁱ (r) marks for the relaxed forms of o-hydroquinone.

ⁱⁱ Underlined numbers stand for o-hydroquinone unrelaxed form.



© 2020 by the authors. Submitted for possible open access publication under the terms and conditions of the Creative Commons Attribution (CC BY) license (<http://creativecommons.org/licenses/by/4.0/>).

ii. Oświadczenia współautorów

Wrocław, 14.04.2023

mgr farm. Maciej Spiegel
Katedra i Zakład Farmakognozji i Leku Roślinnego
Uniwersytet Medyczny im. Piastów Śląskich we Wrocławiu

OŚWIADCZENIE WSPÓŁAUTORA
CO-AUTHORSHIP STATEMENT

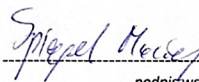
Jako współautor pracy:
As a co-author of the research paper:

Spiegel, M., Andruniów, T., & Sroka, Z. (2020).
Flavones' and flavonols' antiradical structure– activity relationship—a quantum chemical study.
Antioxidants, 9(6), 461.

oświadczam, że mój udział polegał na:

I declare that my contribution consists of:


- sformułowaniu i ewolucji nadrzędnych celów i zadań badawczych
formulation and evolution of overarching research goals and aims
- zastosowaniu technik matematycznych i obliczeniowych do analizy i syntezy danych z badań
application of mathematical and computational techniques to analyze and synthesize study data
- prowadzeniu procesu badawczego i dochodzeniowego oraz gromadzeniu danych
conducting a research and investigation process, and data collection
- rozwoju i zaprojektowaniu metodologii
development and design of methodology
- weryfikacji ogólnej powtarzalności wyników badań
verification of the overall reproducibility of research outputs
- przygotowaniu i stworzeniu opublikowanej pracy, w szczególności wizualizacji i prezentacji danych
preparation and creation of the published work, specifically visualization & data presentation
- przygotowaniu i stworzeniu opublikowanej pracy, w szczególności napisaniu jej wstępnego szkicu
preparation and creation of the published work, specifically writing the initial draft



podpis współautora

Uniwersytet Medyczny we Wrocławiu
KATEDRA I ZAKŁAD FARMAKOGNOZJI
I LEKU ROŚLINNEGO

kierownik



prof. dr hab. Zbigniew Sroka
(2) podpis promotora
(2) supervisor's signature

prof. dr hab. Tadeusz Andruniów
 tytuł, imię i nazwisko
 (title, name and surname)

Wrocław, 12.12.2022

miejsowość, data
 (place, date)

Politechnika Wroclawska
 miejsce zatrudnienia
 (affiliation)

OŚWIADCZENIE WSPÓŁAUTORA CO-AUTHORSHIP STATEMENT

Jako współautor pracy:
 As a co-author of the research paper:

Spiegel, M., Andruniów, T., & Sroka, Z. (2020).
 Flavones' and flavonols' antiradical structure– activity relationship—a quantum chemical study
 Antioxidants, 9(6), 461.

oświadczam, że mój udział polegał na:
 I declare that my contribution consists of:

- opracowaniu i zaprojektowaniu metodologii badań
development and design of the research methodology
- nadzorze i odpowiedzialności kierowniczej za planowanie i realizację działań badawczych
oversight and leadership responsibility for the research activity planning and execution
- weryfikacji ogólnej odtwarzalności wyników
verification of the overall reproducibility of results
- przygotowaniu ostatecznej wersji manuskryptu; w szczególności korekty
preparation of the final version of the manuscript; in particular post-review corrections

T. Andruniów

T. Andruniów

podpis współautora
 (co-author's signature)
 Uniwersytet Medyczny Wrocław
 KATEDRA I ZAKŁAD FARMAKOGNOZJI
 I LEKU ROŚLINNEGO
 Wrocław

prof. dr hab. Zbigniew Sroka
 (2) supervisor's signature

Wrocław, 18.04.2023
miejsowość, data
(place, date)

prof. dr hab. Zbigniew Sroka
tytuł, imię i nazwisko
(title, name and surname)

Katedra i Zakład Farmakognozji i Leku Roślinnego
Uniwersytet Medyczny im. Piastów Śląskich we Wrocławiu
miejsce zatrudnienia
(affiliation)

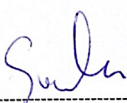
OŚWIADCZENIE WSPÓŁAUTORA CO-AUTHORSHIP STATEMENT

Jako współautor pracy:
As a co-author of the research paper:

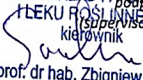
Spiegel, M., Andruniów, T., & Sroka, Z. (2020).
Flavones' and flavonols' antiradical structure– activity relationship—a quantum chemical study
Antioxidants, 9(6), 461.

oświadczam, że mój udział polegał na:
I declare that my contribution consists of:

- uzyskaniu wsparcia finansowego dla projektu prowadzącego do powstania niniejszej publikacji
acquisition of the financial support for the project leading to this publication
- nadzorze i odpowiedzialności kierowniczej za planowanie i realizację działań badawczych
oversight and leadership responsibility for the research activity planning and execution
- przygotowaniu ostatecznej wersji manuskryptu; w szczególności korekty po recenzji
preparation of the final version of the manuscript; in particular post-review corrections



podpis współautora
(co-author's signature)

Uniwersytet Medyczny we Wrocławiu
KATEDRA I ZAKŁAD FARMAKOGNOZJI I LEKU ROŚLINNEGO
Kierownik

prof. dr hab. Zbigniew Sroka
(2)

II. Publikacja [B]



Article

Antioxidant Activity of Selected Phenolic Acids–Ferric Reducing Antioxidant Power Assay and QSAR Analysis of the Structural Features

Maciej Spiegel ¹, Karina Kapusta ^{2,*}, Wojciech Kołodziejczyk ², Julia Saloni ², Beata Żbikowska ¹, Glake A. Hill ² and Zbigniew Sroka ¹

¹ Department of Pharmacognosy, Wrocław Medical University, Borowska 211, 50-556 Wrocław, Poland; maciej.spiegel@student.umed.wroc.pl (M.S.); beata.zbikowska@umed.wroc.pl (B.Ż.); z.g.sroka@gmail.com (Z.S.)

² Interdisciplinary Center for Nanotoxicity, Department of Chemistry, Physics and Atmospheric Sciences, Jackson State University, 1400 J. R. Lynch str., Jackson, MS 39217, USA; dziecial@icnanotox.org (W.K.); julia.m.saloni@jsums.edu (J.S.); glakeh@icnanotox.org (G.A.H.)

* Correspondence: karina.kapusta@icnanotox.org

Academic Editor: Cesar M. Compadre

Received: 29 May 2020; Accepted: 29 June 2020; Published: 7 July 2020



Abstract: Phenolic acids are naturally occurring compounds that are known for their antioxidant and antiradical activity. We present experimental and theoretical studies on the antioxidant potential of the set of 22 phenolic acids with different models of hydroxylation and methoxylation of aromatic rings. Ferric reducing antioxidant power assay was used to evaluate this property. 2,3-dihydroxybenzoic acid was found to be the strongest antioxidant, while mono hydroxylated and methoxylated structures had the lowest activities. A comprehensive structure–activity investigation with density functional theory methods elucidated the influence of compounds topology, resonance stabilization, and intramolecular hydrogen bonding on the exhibited activity. The key factor was found to be a presence of two or more hydroxyl groups being located in *ortho* or *para* position to each other. Finally, the quantitative structure–activity relationship approach was used to build a multiple linear regression model describing the dependence of antioxidant activity on structure of compounds, using features exclusively related to their topology. Coefficients of determination for training set and for the test set equaled 0.9918 and 0.9993 respectively, and Q₂ value for leave-one-out was 0.9716. In addition, the presented model was used to predict activities of phenolic acids that haven't been tested here experimentally.

Keywords: phenolic acids; polyphenols; antioxidants; ferric reducing antioxidant power (FRAP) assay; density functional theory (DFT); quantitative structure–activity relationship (QSAR); multiple linear regression (MLR)

1. Introduction

Nowadays, the popularity of the healthy foods has led to the revival of studies on phytochemicals activity. Plant substances, such as fiber regulate gastrointestinal tract function [1] and unsaturated fatty acids are capable of decreasing risk of atherosclerosis [2], and phenolic compounds can prevent oxidative stress [3]. All these compounds are crucial for the proper function of the human body. A number of important research papers concerning plant antioxidants were published in the last ten years, making an investigation of them an interesting branch of 21st century medical research [4–6].

Phenolic acids are a large group of secondary metabolites, originating from shikimic and benzoic acids [7]. They can be found commonly in plants, especially hydroxybenzoic and hydroxycinnamic

derivatives, which are responsible for organoleptic properties, such as sour and bitter flavor. However, their true medicinal merit is an antioxidant and antiradical activity arising from their chemical structure. It is known that oxidative stress may cause damage to lipid membranes, DNA, and proteins [8], and may further lead to more severe diseases such as diabetes [9], Alzheimer's disease [10], and Parkinson's disease [11] or neoplasms [12]. Each phenolic acid is made of one aromatic ring with hydroxyl residues and carboxyl residue linked to it. Acting as a donor of a hydrogen atom or single electron, they are capable of neutralizing reactive oxygen species (ROS), reducing transition metals responsible for Fenton's reaction, and overall decreasing oxidative stress. Even though terms "antiradical" and "antioxidant" are often referred to the same property, these activities do not necessarily coincide. Thus, antiradical activity must be clearly distinguished from the antioxidant one [13]. While the first characterizes the ability of compounds to scavenge free radicals (for instance cation radical ABTS^{•+} and a stable radical DPPH[•]), the second one represents the ability to inhibit the process of oxidation. Measurement of antiradical activity most commonly is performed using ABTS or DPPH tests. During the ABTS method, proposed by Re et al. [14], pre-generated dark-green cation radical is reduced by a hydrogen-donating compound, such as phenolic acid. In the DPPH test [15], the radical undergoes a reaction with a reducer, becoming a neutral molecule. Both these assays rely on hydrogen exchange mechanism. As for the antioxidant activity, a wide variety of methods may be used, including biological assays, such as cellular antioxidant activity (CAA) [16] and chemical-based methods (FRAP [17], CUPRAC assays [18], etc.). While biological assays are considered to be more appropriate, they also are more expensive and time-consuming compare to chemical-based methods [16]. With all variety of methods results of efficiency measurements for phenolic acids is found to be slightly controversial in the literature [19,20].

Ferric Reducing Antioxidant Power assay (FRAP) [17] is based on reduction of a colorless Fe³⁺-TPTZ complex into intense blue Fe²⁺-TPTZ once it interacts with a potential antioxidant. At low cost, this method showed to be useful for screening of antioxidant capacities and comparing efficiencies of different compounds. Thus, in this study, we used FRAP method for an investigation of antioxidant activity of selected phenolic acids. Interestingly, the exact mechanism of the antioxidant activity for these compounds, and the influence of the compounds' structure on their activity, is still not fully elucidated and controversial in the literature [21–24]. Computational chemistry proved to be a good support for experimental investigations. A great review of strategies in theoretical antioxidants activity research has been recently published by Galano et al. [25]. Not only hydrogen atom transfer (HAT) mechanism, but also sequential proton loss-electron transfer (SPLET) and single electron transfer-proton transfer (SET-PT) are widely studied with density functional theory (DFT) methods to elaborate the most probable mechanism of action of antioxidants [21,26,27]. Obtained results clearly showed that SPLET is the most favorable mechanism of action in a polar solvent, whilst HAT dominates in benzene. Presented computational results complement the experimental studies by explaining rationale used in the experiment. That indicates the importance of computational chemistry methods as a supporting tool in every modern-age research.

Quantitative structure–activity relationship is widely used to find a relationship between structural features of compounds and their activities [28–30]. Finding proper descriptors used to develop a quantitative structure–activity relationship (QSAR) model is the very first step one should consider. For example, to build a model for wine polyphenols, Rastija et al. [31] used lipophilicity, Balaban index, Balaban-type index, and 3D GETAWAY descriptors. Gupta et al. [32] focused on MOLMAP descriptors selected by genetic algorithms. Filipović et al. [33] in their studies on free radical scavenging potency of 21 phenolic acids and simple phenolics proposed three models based on the number of vicinal hydroxyl groups, bond dissociation energy, proton affinity and electron transfer enthalpy. QSAR concept also was used by Chen et al. [21] in their studies on thermodynamic properties as descriptors for prediction of DPPH radical scavenging assay. These models provided a good insight into the nature of antiradical and antioxidant activity, though they require an involvement of quantum chemical calculations or other software for descriptor generation. The aim of this study is to perform

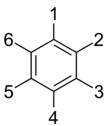
a comprehensive investigation of antioxidants nature for the set of phenolic acids with different models of hydroxylation, and to develop a QSAR model for prediction of these properties based on a topology of tested compounds. FRAP assay has been used to measure antioxidant potential of selected phenolic acids. Purely topological descriptors used in this paper are easy to generate and give an understanding on how structural features of studied compounds influence an activity.

2. Results and Discussion

2.1. Experimental Results

Antioxidant properties of phenolic acids and their structures are presented in Table 1. The strongest activity reducing ion Fe^{3+} to Fe^{2+} was noted for 2,3-dihydroxybenzoic acid. The number of units per μmol of compound ($TAU_{Fe/\mu\text{mol}}$) was equal to 202 ± 10.6 . A slightly lower activity was observed for 3,4-dihydroxyphenylacetic (149 ± 10.0) and 2,5-dihydroxybenzoic acid (128 ± 6.3), while 3-hydroxybenzoic acid possessed the poorest efficiency among tested phenolic acids.

Table 1. Structures of investigated phenolic acids.



Compound ID:	IUPAC Name	C1	C2	C3	C4	C5	C6	$TAU_{Fe/\mu\text{mol}}^*$
1	2,3-dihydroxybenzoic	COOH	OH	OH	H	H	H	202 ± 10.6
2	3,4-dihydroxyphenylacetic	CH_2COOH	H	OH	OH	H	H	149 ± 10.0
3	2,5-dihydroxybenzoic	COOH	OH	H	H	OH	H	128 ± 6.3
4	3,4,5-trihydroxybenzoic	COOH	H	OH	OH	OH	H	119 ± 6.4
5	4-hydroxy-3,5-dimethoxybenzoic	COOH	H	OCH ₃	OH	OCH ₃	H	84.6 ± 3.7
6	4-hydroxy-3,5-dimethoxycinnamic	$\text{CH}=\text{CHCOOH}$	H	OCH ₃	OH	OCH ₃	H	79.2 ± 4.9
7	2,5-dihydroxyphenylacetic	CH_2COOH	OH	H	H	OH	H	72.1 ± 3.3
8	4-hydroxy-3-methoxyphenylacetic	CH_2COOH	H	OCH ₃	OH	H	H	63.9 ± 4.2
9	3,4-dihydroxycinnamic	$\text{CH}=\text{CHCOOH}$	H	OH	OH	H	H	60.9 ± 2.8
10	3,4-dihydroxybenzoic	COOH	H	OH	OH	H	H	52.0 ± 3.2
11	4-hydroxy-3-methoxycinnamic	$\text{CH}=\text{CHCOOH}$	H	OCH ₃	OH	H	H	49.1 ± 3.1
12	4-hydroxy-3-methoxybenzoic	COOH	H	OCH ₃	OH	H	H	2.29 ± 0.07
13	2-hydroxybenzoic	COOH	OH	H	H	H	H	2.01 ± 0.12
14	2,4-dihydroxybenzoic	COOH	OH	H	OH	H	H	1.30 ± 0.08
15	4-hydroxycinnamic	$\text{CH}=\text{CHCOOH}$	H	H	OH	H	H	0.777 ± 0.124
16	2-hydroxycinnamic	$\text{CH}=\text{CHCOOH}$	OH	H	H	H	H	0.556 ± 0.058
17	4-hydroxyphenylacetic	CH_2COOH	H	H	OH	H	H	0.325 ± 0.081
18	3-hydroxycinnamic	$\text{CH}=\text{CHCOOH}$	H	OH	H	H	H	0.141 ± 0.044
19	3,5-dihydroxybenzoic	COOH	H	OH	H	OH	H	0.127 ± 0.044
20	4-hydroxybenzoic	COOH	H	H	OH	H	H	0.126 ± 0.030
21	3,4-dimethoxybenzoic	COOH	H	OCH ₃	OCH ₃	H	H	0.087 ± 0.049
22	3-hydroxybenzoic	COOH	H	OH	H	H	H	0.028 ± 0.032

* Averaged $TAU_{Fe/\mu\text{mol}}$ values with the maximal errors.

The statistical significance of differences between samples was analyzed using HSD Tukey test. Compounds have been divided into more active (1–11) and less active (12–22) set. Statistical significance was tested on level $p < 0.05$. Among the first group for nearly every pair except 8–9 and 10–11 (Table S1, Figure S1) the given criterion was achieved, whereas among the second group pairs 18–19, 18–20, 18–21, 18–22, 19–20, 19–21, 19–22, 20–21, 20–22, 21–22 didn't met it (Table S2, Figure S2).

2.2. SAR Investigation

The results of measured antioxidant activities were used as a subject of structure–activity investigation. In order to explain the structure–activity relationship, three key factors must be investigated separately: mutual position of hydroxyl groups, their methylation, and the distance between phenyl and carboxylic group. These factors have been numerously mentioned in literature [21,22,34], however, the full clarification of their influence has not been reported.

2.3. Mutual Positions of Hydroxyl Groups and Resonance Stabilization

All tested phenolic acids can be clustered into two groups, one including compounds with high activities (1–11), and the other with compounds possessing extremely low activities (12–22) (Figure 1). Clustering of phenolic acids has shown a response dependence on the relative positions of the hydroxyl groups in the ring. Compounds, that contain only one hydroxyl group, (13, 15–18, 20, 22) have exhibited very low efficiency. Phenolic acids with two hydroxyls substituted in the *meta* position in relation to each other, such as 3,5-dihydroxybenzoic acid (19) and 2,4-dihydroxybenzoic acid (14) have also shown a poor activity, compare to ones with two hydroxyls on adjacent carbon atoms.

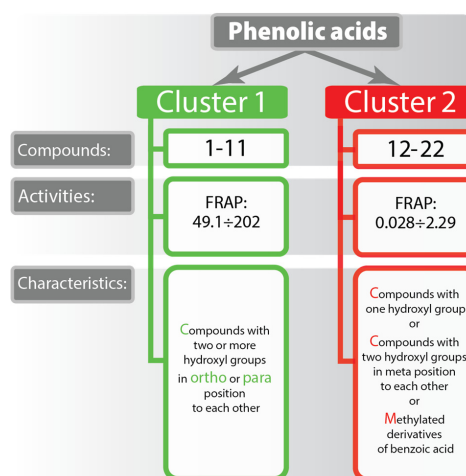
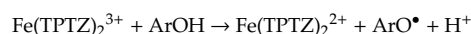


Figure 1. Phenolic acids clustered by their activity.

Since FRAP assay must be performed in low pH values to maintain iron solubility, the ionization potential is also low, which drives hydrogen atom transfer. FRAP assay is based on an electron transfer mechanism with formation of aryloxy radical [35]:



In this case, once aryloxy radical is formed, its stability determines the efficiency of phenolic acid as an antioxidant compound. The fact that 2,4-dihydroxybenzoic acid (14) is much less efficient than 2,3-dihydroxybenzoic acid (1) can be explained by resonance structures of its radicals (Figure 2). In both cases radical is stabilized by delocalization over conjugated aromatic rings system. When the second hydroxyl group present in *ortho*- or *para*- position related to the first one, it allows second oxygen atom to participate in delocalization (Figure 2a). One can see that it leads to the activation of the second hydroxyl group. Hence, the reaction can proceed further reducing one more Fe^{3+} -TPTZ complex with subsequent oxidation to 5,6-dioxo-1,3-cyclohexadiene-1-carboxylic acid. Highly active 2,5-dihydroxybenzoic acid (3) has the same resonance structures with hydroxyl groups being in *para*-position to each other. Meanwhile, the second hydroxyl of compound 14 (Figure 2b) does not participate in a delocalization, thus 2,4-dihydroxybenzoic acid exhibits significantly lower antioxidant activity. To summarize, in order to achieve high antioxidant and antiradical activity it is critical that two or more hydroxyl groups are located either in vicinal positions or on opposite sides of the ring (in *ortho* or *para* position to each other).

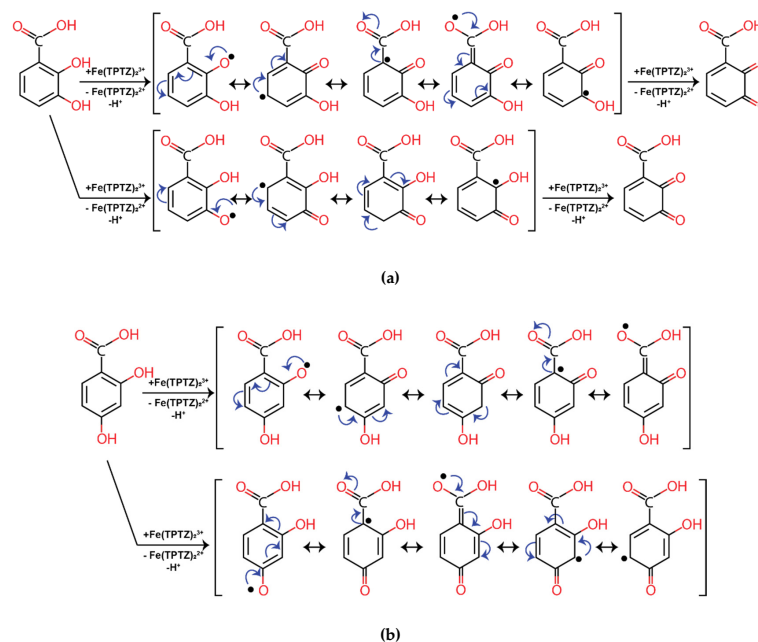


Figure 2. Resonance structures of phenolic acids: (a)—2,3-dihydroxybenzoic acid (1), and (b)—2,4-dihydroxybenzoic acid (14).

Low efficiency of two other compounds from the second cluster (4-hydroxy-3-methoxybenzoic acid (12) and 3,4-dimethoxybenzoic acid (21)) cannot be justified by mutual position of hydroxyl groups as similar in structure 3,4-dihydroxybenzoic acid (10) possesses relatively high efficiency as an antioxidant compound. Thus, methylation of hydroxyl groups must be considered separately.

2.4. The Influence of Methylation

The results of FRAP tests showed a tendency of the methylated compounds to have lower activity than their non-methylated counterparts ($5 < 4$, $21 < 12 < 10$, $11 < 9$, $8 < 2$). Methylation yields a decrease of active electron- and hydrogen-donating groups, which consequently leads to reduced efficiency of the compound as an antioxidant. Interestingly, methylation of the cinnamic acid derivatives has no significant influence on the antioxidant activity, since 4-hydroxy-3-methoxycinnamic acid (11) demonstrates slightly lower activity than 3,4-dihydroxycinnamic one (9). With a decreasing distance between carboxylic group and a ring the influence of methylation is increasing, for example: 3,4-dihydroxyphenylacetic acid (2) is almost two times more efficient than its partially methylated counterpart (8), while the ratio between activities of 3,4-dihydroxybenzoic acid (10), 4-hydroxy-3-methoxybenzoic acid (12), and 3,4-dimethoxybenzoic one (21) amounts 598:26:1. It seems that the farther the carboxylic group is from the methoxylated ring, the more efficient the phenolic acid containing methylated hydroxyl groups. This can be explained by the importance of the inductive effect of carboxylic group. The 4-hydroxy-3,5-dimethoxybenzoic acid (5) is the only exception from the presented trend, it exhibits just slightly lower activity when compared to non-methylated counterparts (4).

2.5. Carboxylic Group Influence and H-Bonding

Antioxidant activity decreases with an increase of the carboxylic group electron-withdrawing effect on a radical delocalization. In most cases, cinnamic acid derivatives have demonstrated improved efficiency over their counterparts derived from benzoic acid. Phenolic acids substituted with hydroxyls in *para-meta* position have their activity decreasing in the following order phenylacetic acid > cinnamic acid > benzoic acid (**2** > **9** > **10**, and **8** > **11** > **12**). This trend suggests that carboxylic group has the biggest influence on the total antioxidant activity. This influence occurs not through inductive effect (-I) (the distance of carboxylic group from the ring), but through the mesomeric effect (-M) (the resonance with the ring). Carboxylic group of phenylacetic acid is not participating in resonance and can influence only through -I effect, while carboxyl group of a benzoic acid shows the strongest -I and -M effects. Interestingly, phenolic acids that are substituted with only one hydroxyl in *para* position have demonstrated a decrease of activity presented in a row cinnamic acid > phenylacetic acid > benzoic acid (**15** > **17** > **20**), that may indicate the importance of inductive effect for low efficient compounds. Though, the difference in their efficiency is negligible. Meanwhile, an antioxidant activity of *ortho*-substituted compounds such as 2,5-dihydroxybenzoic acid (**3**) and 2-hydroxybenzoic acid (**13**) measured by FRAP have shown to be elevated when compared to its phenylacetic counterparts (2,5-dihydroxyphenylacetic (**7**) and 2-hydroxyphenylacetic (**16**) acids). In addition to the resonance stabilization (Figure 2), a radical can be stabilized by intermolecular hydrogen bonds between functional groups and polar protic solvents, as well as intramolecular hydrogen bonds [24]. There are two possible types of intramolecular hydrogen bonding for compounds tested here. One involves only hydroxyl oxygens, and the other is a hydrogen bond between carboxylic and hydroxyl groups.

One of the methods used for approximation of the hydrogen bonding energy is based on the calculation of potential energy density has been implemented in Multiwfn program package [36]. Energies (E_{HB}) for all the studied compounds, where hydrogen bonding is possible, were calculated and collected in Table 2, along with distances between critical point (CP) and hydrogen atom (H_{HB}), the distance between hydrogen (H_{HB}) and acceptor oxygen atom (O_{ac}) as well as the angle ($\angle O_{ac}-CP-H_{HB}$).

Table 2. Hydrogen bonding energies and geometrical parameters calculated using Multiwfn program package.

Compound ID:	IUPAC Name	E_{HB} , (kcal/mol)	CP- H_{HB} Distance, (Å)	O_{ac} - H_{HB} Distance, (Å)	$\angle O_{ac}-CP-H_{HB}$ Angle, (°)
1	2,3-dihydroxybenzoic	-12.91/-5.56	0.572/0.90	1.69/2.13	172.84/160.38
2	3,4-dihydroxyphenylacetic	-5.47	0.890	2.12	163.15
3	2,5-dihydroxybenzoic	-12.45	0.580	1.71	173.16
4	3,4,5-trihydroxybenzoic	-3.61/-3.69	0.882/0.880	2.18/2.18	161.43/162.80
5	4-hydroxy-3,5-dimethoxybenzoic	-6.32	0.836	2.06	167.15
6	4-hydroxy-3,5-dimethoxycinnamic	-6.37	0.833	2.06	167.30
7	2,5-dihydroxyphenylacetic	-11.41	0.601	1.78	176.03
8	4-hydroxy-3-methoxyphenylacetic	-6.16	0.842	2.07	167.46
9	3,4-dihydroxycinnamic	-5.42	0.902	2.13	161.51
10	3,4-dihydroxybenzoic	-5.58	0.882	2.11	163.67
11	4-hydroxy-3-methoxycinnamic	-6.30	0.835	2.06	167.47
12	4-hydroxy-3-methoxybenzoic	-6.26	0.838	2.06	167.31
13	2-hydroxybenzoic	-12.98	0.572	1.69	173.31
14	2,4-dihydroxybenzoic	-15.77	0.542	1.64	173.62

The highest hydrogen bond energy has been found for bonds between hydrogen of hydroxyl group and double-bonded oxygen of benzoic acid's carboxylic group (compound **1**, **3**, **13**, **14**). The lowest hydrogen bond energy is found to be between hydroxyl groups. According to the presented results, the oxygen of hydroxyl group is a less efficient H-bond acceptor when compared to double-bonded oxygen of carboxyl group. Taking into account this difference in H-bond strength, one can explain why for benzoic acid derivatives efficiency is decreasing in the row: *ortho-meta* (2,3-pattern) (**1**) > *ortho-meta* (2,5-pattern) (**3**) > *meta-meta-para* (**4**) > *meta-para* (**10**), while the same tendency does not work for phenylacetic and cinnamic acid derivatives. Similar to

2-hydroxybenzoic acid, 2,5-dihydroxyphenylacetic (7) also can be stabilized by a H-bond between carboxylic group and *ortho*-hydroxyl. However, surprisingly high H-bond energy (-11.41 kcal/mol) in the case of 2,5-dihydroxyphenylacetic one (7) does not justify its low efficiency compare to 3,4-dihydroxyphenylacetic acid (2), where energy of hydrogen bond between two hydroxyl groups is -5.47 kcal/mol. Moreover, due to the steric hindrance in case of the phenylacetic acid derivatives, H-bonding between carboxylic group and *ortho*-hydroxyl should not be that favorable as the one between two hydroxyl groups.

To verify results obtained by the method proposed in Multiwfn, an additional method was employed. Density functional theory was used to calculate enthalpies of H-bond formation. Formation of hydrogen bond in 2-hydroxybenzoic acid (13) results in release of 7.59 kcal/mol of energy (Figure 3a). The energy yield of H-bond formation in case of 3,4-dihydroxybenzoic acid (10) is significantly smaller (1.92 kcal/mol) (Figure 3b). These results are in good agreement with previously obtained data with Multiwfn method. Though, in the case of compound 7 (Figure 3c), H-bonding is not that energetically favorable (1.87 kcal/mol released) due to the steric tension occurring in this molecule. This finding is contrary to results calculated using Multiwfn method.

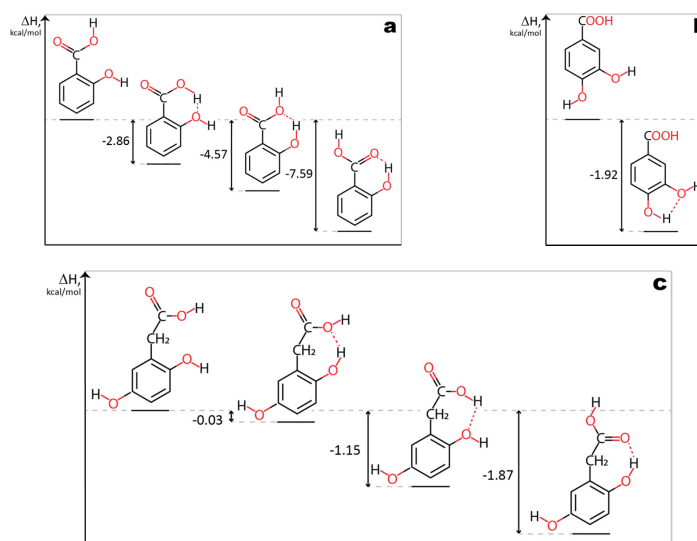


Figure 3. Enthalpies of hydrogen bond formation. (a)—2-hydroxybenzoic acid (13); (b)—3,4-dihydroxybenzoic acid (10); (c)—2,5-dihydroxyphenylacetic acid (7).

The 2,3-dihydroxybenzoic acid (1) (Figure 4a) may form two intramolecular hydrogen bonds: one involving only hydroxyl oxygen atoms and the other involving oxygen of carboxylic group (total of -18.47 kcal/mol, as is shown in Table 2). Similarly, two H-bonds stabilize a 3,4,5-trihydroxybenzoic acid (compound 4, total of -7.30 kcal/mol) (Figure 4b). Though, in this case, the carboxylic group does not participate in H-bonding. The following compounds 2,5-dihydroxybenzoic acid (3) and 3,4-dihydroxybenzoic acid (10) (Figure 4c,d) are stabilized by just one intramolecular H-bond, and only in case of 3 strong interactions with oxygen of carboxylic group takes place (-12.45 kcal/mol, compared to -5.58 kcal/mol for compound 10). It can be seen, that our study explained the trends in effectiveness. Hence, it is assumed that the model of phenolic acids' hydroxylation by two hydroxyl groups, one of each is situated next to carboxyl group (in *ortho* position) may be efficient only for benzoic acid derivatives.

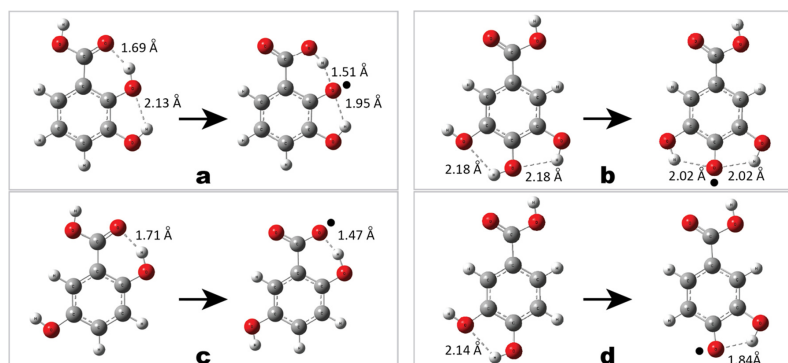


Figure 4. Intramolecular hydrogen bond stabilization of a molecule and its radical: (a)—2,3-dihydroxybenzoic acid (**1**); (b)—3,4,5-trihydroxybenzoic acid (**4**); (c)—2,5-dihydroxybenzoic acid (**3**); (d)—3,4-dihydroxybenzoic acid (**10**).

2.6. QSAR Model

Original model, Multiple linear regression model, for the prediction of the antioxidant $TAU_{Fe/\mu mol}$ activity measured by FRAP assay had one outlier (4-hydroxy-3,5-dimethoxybenzoic acid). As it was earlier discussed this compound did not follow the general trend illustrated in SAR investigation. Thus, this point was excluded from the training set and model was rebuilt. Elimination of the 4-hydroxy-3,5-dimethoxybenzoic acid had no influence on selected descriptors, though it influenced their coefficients and statistical parameters. Finalized model based on four topological descriptors is represented by Equation (1):

$$TAU_{Fe/\mu mol} = -0.507 + 62.03 \cdot HOcOH(count) + 74.83 \cdot Ph_{ortho(para)-meta} + 134.49 \cdot B_{ortho-meta} + 41.804 \cdot C_{methyl}(count) \quad (1)$$

Descriptors used for MLR model have a clear chemical meaning and were in correspondence with the SAR investigation. First and foremost, the presence of HOcOH fragment is crucial. As it was indicated above, two or more hydroxyl groups in *ortho* position to each other positively impact an antioxidant activity due to charge delocalization and OH-OH intramolecular H-bonding. Not only information about mutual position of substituents, but also its methylation is decoded by this descriptor. Only non-methylated groups positively impact on efficiency. The evidence of phenylacetic acid derivatives being more efficient than others is supported by $Ph_{ortho(para)-meta}$ descriptor, that indicates the presence of any *ortho-meta* or *para-meta* substitutes phenylacetic acids (compounds **2**, **7**, **8**). $B_{ortho-meta}$ is a specific descriptor that points out on a presence of *ortho-meta*-substituted benzoic acid derivatives (compounds **1** and **3**). The presence of strong intramolecular H-bonds between *ortho* hydroxyl and carboxylic groups results in significant increase of efficiency. Finally, $C_{methyl}(count)$ descriptor is correcting total activity calculated by the proposed model whilst taking into account the fact that methylation of cinnamic acid derivatives does not critically decrease an efficiency of these compounds.

Finalized model illustrates a good agreement with presented experimental results (Figure 5a) with correlation coefficient for the training set $R = 0.9959$. Interestingly, the mutual position of hydroxyl groups appeared to be an essential descriptor in several models for prediction of antioxidant activity proposed earlier. For instance, the simultaneous presence of the 3',4'-dihydroxy structure at the B-ring or the adjustment of the hydroxyl group at the C-3 atom of selected flavonoid compounds was used among the other descriptors for prediction of inhibitory activity of Lipids peroxidation [37]. Using exclusively this descriptor Rasulev et al. developed a model with correlation coefficient $R = 0.813$. Meanwhile by adding Petjean shape index, dipole moment, and a number of Glycoside-like

fragments as descriptors it was possible to increase a correlation coefficient to $R = 0.938$. The number of vicinal hydroxyl groups was used as a descriptor for MLR models in [33] developed for prediction of antiradical activity measured by ABTS assay and evaluated as vitamin C equivalent (VCEAC) for the set of 21 hydroxybenzoic acids and simple phenolic compounds. Models developed based on only this topological descriptor resulted in correlation coefficient $R = 0.915$. Meanwhile, by combining the number of vicinal hydroxyl groups with a bond dissociation enthalpy proton affinity, or with a proton affinity and an electron-transfer enthalpy as descriptors the accuracy of developed model was improved by $R = 0.957$ and $R = 0.962$, respectively. Model developed by us based purely on the topological descriptors achieved slightly better statistical parameters (Table 3) than earlier models.

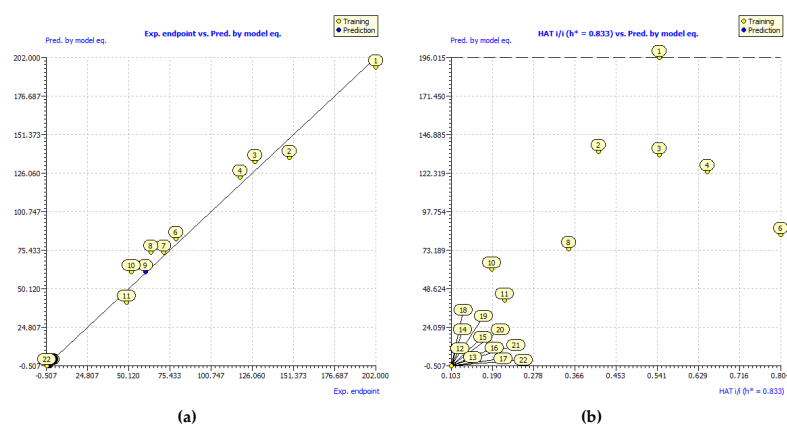


Figure 5. (a)—correlation plot between experimental and predicted values of $TAU_{Fe/\mu mo l}$ antiradical activity; (b)—applicability domain of developed model. Yellow dots represent compounds selected as the training set, while the blue dots represent test set compounds.

Table 3. Statistical parameters for developed model.

	R	R ²	R ² _{adj}	RMSE	MAE	Q ² _{loo}	Q ² _{lmo}
training set	0.9959	0.9918	0.9893	5.5211	4.0678		
cross-validation				10.3056	7.4203	0.9716	0.9592
external validation	0.9996	0.9993	0.9973	1.5429	1.2627		

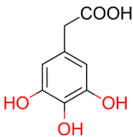
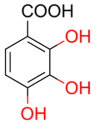
An applicability domain represents the response and chemical structure space in which the model makes predictions with a given reliability. All compounds from the second cluster (12–22) appeared to be on the border of a predicted applicability domain as well as compound 1 (Figure 5b). The location of these compounds close to an outlier region is determined by their extreme response values (extremely low for 12–22, and extremely high for 1). Nevertheless, all 21 phenolic acids were found inside an applicability domain.

The number of statistical parameters that are used to validate developed models increase over years, as described in review by Gramatica et al. [38]. In this study, different validation criteria of robustness and predictivity have been used. The coefficient of determination R^2 (the square of the sample correlation coefficient (R) between the experimental endpoint and predicted one), adjusted coefficient of determination R^2_{adj} (in case when slope is set to zero), root mean square error $RMSE$ (square root of the average of squared differences between predicted and experimental endpoint observation), mean absolute error MAE (the average magnitude of the errors in a set of predictions, without considering their direction) for both training and test sets were calculated. Additionally, specific coefficients of determination Q^2_{LOO} and Q^2_{LMO} (for leave-one-out and leave-many-out cross-validation,

respectively) were calculated and presented in Table 3. Though, it must be noted, that even inadequate models with chance correlation may pass statistical analysis with sufficient values of parameters in case when it is built for data sets that include a small number of samples. When working with small data sets one must rely not only on pure statistics but mostly on a chemical knowledge about mechanism of activity of interest, and structure–activity relationship in order to select an adequate chemically justified model.

With satisfactory statistical parameters and chemically justified descriptors (with p -values for all the descriptors equal to 0), developed here model, presumably, can well reflect the course of the reaction, and potentially be used for efficiency prediction of phenolic acids which activities are unknown. Based on both SAR and QSAR studies one can assume that 3,4,5-trihydroxyphenylacetic and 2,3,4-trihydroxybenzoic acids should be efficient as antioxidant compounds (Table 4), which is found to be in good agreement with the literature [39].

Table 4. Structures of phenolic acids and their antioxidant activities predicted by proposed quantitative structure–activity relationship (QSAR) model.

2D Structure of Tested Compounds	$TAU_{Fe/\mu mol}$ Predicted by MLR QSAR Model
	198.38
	258.05

3. Materials and Methods

3.1. Apparatus

Hitachi U 5100 spectrophotometer (Japan, Tokyo) connected with computer for controlling of measurement and data analyzing, temperature stabilizer, and glass cuvette with 1 cm optical path was used.

3.2. Reagents

3.2.1. Phenolic Acids

Extrasynthese, Genay, France: 3,4-dihydroxyphenylacetic; 4-hydroxyphenylacetic; 4-hydroxy-3-methoxyphenylacetic; 2,5-dihydroxyphenylacetic; 4-hydroxycinnamic; 4-hydroxy-3-methoxycinnamic; 4-hydroxy-3,5-dimethoxycinnamic; 4-hydroxy-3-methoxybenzoic; 3,4,5-trihydroxybenzoic; 2-hydroxycinnamic; 3,4-dihydroxybenzoic.

Koch-Light Laboratories, Haverhill, United Kingdom: 3-hydroxycinnamic; 2,5-dihydroxybenzoic; 2,3-dihydroxybenzoic; 3,5-dihydroxybenzoic; 2,4-dihydroxybenzoic.

Fluka Chemie AG, Buchs, Switzerland: 3-hydroxybenzoic; 3,4-dimethoxybenzoic; 4-hydroxy-3,5-dimethoxybenzoic.

Fluka Chimica, Milano, Italy: 3,4-dihydroxycinnamic.

Sigma-Aldrich, St. Louis, MO, USA: 4-hydroxybenzoic; 2-hydroxybenzoic.

3.2.2. Other Reagents

Merck, Darmstadt, Germany: methanol, gradient grade.

Chempur, Piekary Slaskie, Poland: methanol, pure for analysis; hydrochloric acid 35%, pure for analysis.

Sigma-Aldrich, St. Louis, MO, USA: sodium acetate trihydrate; iron (III) chloride; 2,2-diphenyl-1-picrylhydrazyl radical (*DPPH*[•]); 2,2'-azino-bis(3-ethylbenzothiazoline-6-sulfonic acid) diammonium salt (*ABTS*^{•+}); potassium persulfate (*K₂S₂O₈*).

Fluka, Buchs, Switzerland: 2,4,6-tris(2-pyridyl)-(5)-triazine (*TPTZ*).

3.3. Methods

3.3.1. Measurement of Reducing Activity of Phenolic Acids with FRAP Method

The reducing activity of phenolic acids was measured with the Benzie and Strain method [17]. FRAP reagent was freshly prepared as follows: 12.5 mL of 0.3 mol/L acetate buffer (CH₃COOH:CH₃COONa), pH 3.6 was mixed with the same volume of methanol (Merck, Darmstadt, Germany). 2.5 mL of 10 mmol/L TPTZ in 0.04 mol/L HCl and 2.5 mL of 0.02 mol/L FeCl₃·6H₂O were added to such a solution.

225 μL of 50% solution of methanol in water and 75 μL of investigated phenolic compound solution (concentration chosen individually for each compound) were added to the 2.25 mL of FRAP reagent. The absorbance measurement at 593 nm was made at the beginning of the reaction and after 1 min at 37 °C. Measurements were repeated 5 times, for each phenolic acid. The results of experiments were presented as a reaction rate expressed as number of total antioxidant units per μmol of substance (*TAU_{Fe/μmol}*). One unit is the amount of substance that reduces one μmol of Fe³⁺ to Fe²⁺ at 593 nm during 1 min at 37 °C. Measurements were done in a glass cuvette with 1 cm optical path. The number of units per 1 μmol of phenolic acid was calculated with the following Equation (2):

$$TAU_{Fe/\mu mol} = \frac{1.513 * A_{F0} - A_{F1}}{c} \quad (2)$$

where *TAU_{Fe/μmol}*—is the number of units per μmol of phenolic acid; *A_{F0}*—is the absorbance of the solution at the beginning of the reaction; *A_{F1}*—is the absorbance of the solution after 1 min of the reaction; *c*—is the concentration of phenolic acid in the reaction mixture [mM].

The absolute error was calculated with the total differential method and the statistical significance of differences between samples was estimated using ANOVA with Tukey's test, using Statistica version 13.3.

3.3.2. DFT Calculations

Density functional theory was used to perform thermodynamic calculations in order to support hypothesis proposed in structure–activity relationship (*SAR*) investigations. Molecular structures of the studied compounds have been visualized using GaussView application [40] and optimized using B3LYP/cc-pVDZ level of theory with Gaussian16 [41] in an implicit water solvent, using conductor-like polarizable continuum model (*CPCM*) solvation method. Topology analysis of hydrogen-bonding was performed using Multiwfn 3.7 [36]. Hydrogen bond energy was calculated using Equation (3) [42]:

$$E_{HB} = \frac{V(r_{bcp})}{2} \quad (3)$$

where *V(r_{bcp})*—is a potential energy density *V(r)* at corresponding bond critical point (*BCP*).

Additionally, relative intramolecular hydrogen bond enthalpy (*ΔH*) was calculated by comparing the sum of electronic and thermal enthalpies of the conformer with intramolecular hydrogen bonds

and of the lowest-energy conformer without hydrogen bonds, following the procedure demonstrated by Korth et al. [43].

3.3.3. Topological Descriptors

The choice of descriptors, which might be relevant to the activity of interest, is a problematic task. In this study, our aim was to build a QSAR model that is based exclusively on topology of phenolic acids. Optimized structures of studied compounds were saved in MDL MOL (.mol) format. PaDEL-Descriptor software [44] was used for the calculation of 2D topological descriptors and fingerprints. Calculated 2D descriptors included number of atoms and atoms of a certain element type, aromatic atoms, aromatic bonds, acidic and basic groups, hydrogen bond acceptors and donors, bonds of certain bond order, as well as topological descriptors characterizing the carbon connectivity, topological descriptors combining distance and adjacency information, etc. List of fingerprints calculated included Estate [45], Pubchem, Substructure [46], Klekota-Roth [47] and 2D atom pairs' fingerprints. Additional specific sets of descriptors have been developed manually based on *ortho-para-meta*-substitution pattern of hydroxyl groups, effect of carboxyl group and methylation. A total of 12,355 descriptors were used.

3.3.4. QSAR Model Development and Validation

QSARINS v2.2.4 [48,49] software (QSAR Research Unit in Environmental Chemistry and Ecotoxicology Department of Theoretical and Applied Sciences (DiSTA), University of Insubria, Varese, Italy) was used for data preparation and model development. The entire data set was preprocessed using a filter to eliminate constant (>80%) and codependent (>95%) descriptors. A splitting procedure plays a critical role for small data sets, since assigning an insufficient number of compounds into the validation set may result in the developed model being overtrained, while too many compounds in validation set may lead to loss of information for proper model development. Thus, only three compounds were selected randomly for validation set. Multiple linear regression (MLR) QSAR models were developed using the genetic algorithm (GA) method of variable subset selection. QSARINS software was also used for an applicability domain calculation by the leverage from the diagonal values of the Hat matrix.

4. Conclusions

Antioxidant activity for a set of phenolic acids was measured by FRAP assay. SAR investigation showed that mono hydroxylated compounds and compounds with two hydroxyl groups in *meta* position to each other exhibited the lowest efficiency as antioxidants, while compounds with two or more hydroxyl groups in *ortho* or *para* position to each other illustrated the highest antioxidant properties. Methylated phenolic acids derivatives were shown to be less efficient compare to their nonmethylated counterparts. Two stabilization factors were elucidated: resonance stabilization of radical and intramolecular hydrogen bonding. Due to resonance stabilization, *ortho-meta* and *para-meta* hydroxylated phenolic acids have an improved activity over mono hydroxylated ones and those having two hydroxyl groups in *meta* position to each other. Hydrogen bonding stabilization explained the reason behind the elevated activity of benzoic acid derivatives with substituted *ortho* position. Proposed hypotheses have been validated by quantum chemical calculations.

Multiple Linear Regression model for the prediction of antioxidant activity measured by FRAP assay was built based on four topological descriptors that include the presence of HOcOH fragment, any *ortho-meta* or *para-meta* substitutes phenylacetic acids, *ortho-meta*-substituted benzoic acid derivatives, and the number of methylated fragments of cinnamic acid derivatives. All these descriptors were in correspondence with SAR investigation. Having just one outlier (4-hydroxy-3,5-dimethoxybenzoic acid), the developed model has satisfactory statistical parameters and can be used for activity prediction of new, not yet tested, phenolic acids based on their structural features.

Supplementary Materials: The Supporting Information is available online at Structures of investigated compounds in a .xyz format are accessible at the <http://dx.doi.org/10.17632/77xhdszk3y>.

Author Contributions: Conceptualization: M.S., K.K., and Z.S.; Data curation: K.K. and W.K.; Formal analysis: K.K.; Funding acquisition: G.A.H. and Z.S.; Investigation: M.S., K.K., W.K., and B.Ż.; Methodology: K.K., W.K., and B.Ż.; Project administration: G.A.H. and Z.S.; Resources: W.K., G.A.H., and Z.S.; Supervision: G.A.H. and Z.S.; Validation: M.S. and K.K.; Visualization: M.S., K.K., and J.S.; Writing—original draft: M.S., K.K., W.K., and J.S.; Writing—review & editing: M.S., K.K., J.S., G.A.H., and Z.S. All authors have read and agreed to the published version of the manuscript.

Funding: This research was funded by National Science Foundation (NSF/CREST), grant number HRD-1547754 and Wrocław Medical University Foundation, grant number SUB.D110.19.005.

Acknowledgments: Authors are grateful to Paola Gramatica for providing a free license for QSARINS 2.2.4 and Andrzej Dryś for statistical analysis (ANOVA with post-hoc test). Calculations have been carried out using resources provided Wrocław Centre for Networking and Supercomputing (<http://wcss.pl>), grant No 12.

Conflicts of Interest: The authors declare no conflict of interest.

References

1. Anderson, J.W.; Baird, P.; Davis, R.H.; Ferreri, S.; Knudtson, M.; Koraym, A.; Waters, V.; Williams, C.L. Health benefits of dietary fiber. *Nutr. Rev.* **2009**, *67*, 188–205. [[CrossRef](#)] [[PubMed](#)]
2. Lunn, J.; Theobald, H.E. The health effects of dietary unsaturated fatty acids. *Nutr. Bull.* **2006**, *31*, 178–224. [[CrossRef](#)]
3. Zhang, H.; Tsao, R. Dietary polyphenols, oxidative stress and antioxidant and anti-inflammatory effects. *Curr. Opin. Food Sci.* **2016**, *8*, 33–42. [[CrossRef](#)]
4. Pandey, K.B.; Rizvi, S.I. Plant polyphenols as dietary antioxidants in human health and disease. *Oxid. Med. Cell. Longev.* **2009**, *2*, 270–278. [[CrossRef](#)] [[PubMed](#)]
5. Khan, N.; Afaq, F.; Mukhtar, H. Cancer chemoprevention through dietary antioxidants: Progress and promise. *Antioxid. Redox Signal.* **2008**, *10*, 475–510. [[CrossRef](#)]
6. Kaliora, A.C.; Dedoussis, G.V.Z.; Schmidt, H. Dietary antioxidants in preventing atherogenesis. *Atherosclerosis* **2006**, *187*, 1–17. [[CrossRef](#)]
7. Riechmann, J.L. Transcriptional Regulation: A Genomic Overview. *Arab. B.* **2002**, *1*, e0085. [[CrossRef](#)]
8. Sies, H.; Berndt, C.; Jones, D.P. Oxidative Stress. *Annu. Rev. Biochem.* **2017**, *86*, 715–748. [[CrossRef](#)]
9. Giacco, F.; Brownlee, M. Oxidative stress and diabetic complications. *Circ. Res.* **2010**, *107*, 1058–1070. [[CrossRef](#)]
10. Wang, X.; Wang, W.; Li, L.; Perry, G.; Lee, H.; Zhu, X. Oxidative stress and mitochondrial dysfunction in Alzheimer's disease. *Biochim. Biophys. Acta (BBA)-Molecular Basis Dis.* **2014**, *1842*, 1240–1247. [[CrossRef](#)]
11. Dias, V.; Junn, E.; Mouradian, M.M. The role of oxidative stress in parkinson's disease. *J. Parkinsons. Dis.* **2013**, *3*, 461–491. [[CrossRef](#)] [[PubMed](#)]
12. Reuter, S.; Gupta, S.C.; Chaturvedi, M.M.; Aggarwal, B.B. Oxidative stress, inflammation, and cancer: How are they linked? *Free Radic. Biol. Med.* **2010**, *49*, 1603–1616. [[CrossRef](#)]
13. Tirzitis, G.; Bartosz, G. Determination of antiradical and antioxidant activity: Basic principles and new insights. *Acta Biochim. Pol.* **2010**, *57*, 139–142. [[CrossRef](#)] [[PubMed](#)]
14. Re, R.; Pellegrini, N.; Proteggente, A.; Pannala, A.; Yang, M.; Rice-Evans, C. Antioxidant activity applying an improved ABTS radical cation decolorization assay. *Free Radic. Biol. Med.* **1999**, *26*, 1231–1237. [[CrossRef](#)]
15. Brand-Williams, W.; Cuvelier, M.E.; Berset, C. Use of a free radical method to evaluate antioxidant activity. *LWT Food Sci. Technol.* **1995**, *28*, 25–30. [[CrossRef](#)]
16. López-Alarcón, C.; Denicola, A. Evaluating the antioxidant capacity of natural products: A review on chemical and cellular-based assays. *Anal. Chim. Acta* **2013**, *763*, 1–10. [[CrossRef](#)] [[PubMed](#)]
17. Benzie, I.F.F.; Strain, J.J. The Ferric Reducing Ability of Plasma (FRAP) as a Measure of "Antioxidant Power": The FRAP Assay. *Anal. Biochem.* **1996**, *239*, 70–76. [[CrossRef](#)]
18. Çelik, S.E.; Özyürek, M.; Güçlü, K.; Apak, R. Solvent effects on the antioxidant capacity of lipophilic and hydrophilic antioxidants measured by CUPRAC, ABTS/persulphate and FRAP methods. *Talanta* **2010**, *81*, 1300–1309. [[CrossRef](#)]
19. Rice-Evans, C.A.; Miller, N.J. Antioxidant activities of flavonoids as bioactive components of food. *Biochem. Soc. Trans.* **1996**, *24*, 790–795. [[CrossRef](#)]

20. Yeh, C.T.; Yen, G.C. Effects of phenolic acids on human phenolsulfotransferases in relation to their antioxidant activity. *J. Agric. Food Chem.* **2003**, *51*, 1474–1479. [CrossRef]
21. Chen, Y.; Xiao, H.; Zheng, J.; Liang, G. Structure-thermodynamics-antioxidant activity relationships of selected natural phenolic acids and derivatives: An experimental and theoretical evaluation. *PLoS ONE* **2015**, *10*, 1–20. [CrossRef] [PubMed]
22. Rice-Evans, C.A.; Miller, N.J.; Paganga, G. Structure-antioxidant activity relationships of flavonoids and phenolic acids. *Free Radic. Biol. Med.* **1996**, *20*, 933–956. [CrossRef]
23. Lucarini, M.; Pedrielli, P.; Pedulli, G.F.; Cabiddu, S.; Fattuoni, C. Bond dissociation energies of O-H bonds in substituted phenols from equilibration studies. *J. Org. Chem.* **1996**, *61*, 9259–9263. [CrossRef]
24. Amorati, R.; Valgimigli, L. Modulation of the antioxidant activity of phenols by non-covalent interactions. *Org. Biomol. Chem.* **2012**, *10*, 4147–4158. [CrossRef] [PubMed]
25. Galano, A.; Raúl Alvarez-Idaboy, J. Computational strategies for predicting free radical scavengers' protection against oxidative stress: Where are we and what might follow? *Int. J. Quantum Chem.* **2019**, *119*, e25665. [CrossRef]
26. Milenković, D.; Đorović, J.; Jeremić, S.; Dimitrić Marković, J.M.; Avdović, E.H.; Marković, Z. Free radical scavenging potency of dihydroxybenzoic acids. *J. Chem.* **2017**, *2017*, 1–9. [CrossRef]
27. Markovic, Z.; DJOROVIC, J.; MARKOVIC, J.M.D.; Biocanin, R.; Amic, D. Comparative density functional study of antioxidative activity of the hydroxybenzoic acids and their anions. *Turkish J. Chem.* **2016**, *40*, 499–509. [CrossRef]
28. Kubinyi, H. QSAR and 3D QSAR in drug design. Part 1: Methodology. *Drug Discov. Today* **1997**, *2*, 457–467. [CrossRef]
29. Puzyn, T.; Rasulev, B.; Gajewicz, A.; Hu, X.; Dasari, T.P.; Michalkova, A.; Hwang, H.-M.; Toropov, A.; Leszczynska, D.; Leszczynski, J. Using nano-QSAR to predict the cytotoxicity of metal oxide nanoparticles. *Nat. Nanotechnol.* **2011**, *6*, 175. [CrossRef]
30. Hansch, C.; Hoekman, D.; Leo, A.; Zhang, L.; Li, P. The expanding role of quantitative structure-activity relationships (QSAR) in toxicology. *Toxicol. Lett.* **1995**, *79*, 45–53. [CrossRef]
31. Rastija, V.; Medić-Šarić, M. QSAR study of antioxidant activity of wine polyphenols. *Eur. J. Med. Chem.* **2009**, *44*, 400–408. [CrossRef] [PubMed]
32. Gupta, S.; Matthew, S.; Abreu, P.M.; Aires-De-Sousa, J. QSAR analysis of phenolic antioxidants using MOLMAP descriptors of local properties. *Bioorganic Med. Chem.* **2006**, *14*, 1199–1206. [CrossRef]
33. Filipović, M.; Marković, Z.; Đorović, J.; Marković, J.D.; Lučić, B.; Amić, D. QSAR of the free radical scavenging potency of selected hydroxybenzoic acids and simple phenolics. *Comptes Rendus Chim.* **2015**, *18*, 492–498. [CrossRef]
34. Cai, Y.Z.; Sun, M.; Xing, J.; Luo, Q.; Corke, H. Structure-radical scavenging activity relationships of phenolic compounds from traditional Chinese medicinal plants. *Life Sci.* **2006**, *78*, 2872–2888. [CrossRef] [PubMed]
35. Gupta, D. Methods for determination of antioxidant capacity: A review. *Int. J. Pharm. Sci. Res.* **2015**, *6*, 546.
36. Lu, T.; Chen, F. Multiwfn: A multifunctional wavefunction analyzer. *J. Comput. Chem.* **2012**, *33*, 580–592. [CrossRef]
37. Rasulev, B.F.; Abdullaev, N.D.; Syrov, V.N.; Leszczynski, J. A Quantitative Structure-Activity Relationship (QSAR) Study of the Antioxidant Activity of Flavonoids. *QSAR Comb. Sci.* **2005**, *24*, 1056–1065. [CrossRef]
38. Gramatica, P.; Sangion, A. A historical excursus on the statistical validation parameters for QSAR models: A clarification concerning metrics and terminology. *J. Chem. Inf. Model.* **2016**, *56*, 1127–1131. [CrossRef]
39. Siquet, C.; Paiva-Martins, F.; Lima, J.L.F.C.; Reis, S.; Borges, F. Antioxidant profile of dihydroxy- and trihydroxyphenolic acids—A structure-activity relationship study. *Free Radic. Res.* **2006**, *40*, 433–442. [CrossRef]
40. Dennington, R.; Keith, T.A.; Millam, J.M. *GaussView 2016*; Semichem Inc.: Shawnee Mission, KS, USA, 2016.
41. Frisch, M.J.; Trucks, G.W.; Schlegel, H.B.; Scuseria, G.E.; Robb, M.A.; Cheeseman, J.R.; Scalmani, G.; Barone, V.; Petersson, G.A.; Nakatsuji, H.; et al. Gaussian 16 2016. Available online: <https://gaussian.com/gaussian16/> (accessed on 14 October 2019).
42. Espinosa, E.; Molins, E.; Lecomte, C. Hydrogen bond strengths revealed by topological analyses of experimentally observed electron densities. *Chem. Phys. Lett.* **1998**, *285*, 170–173. [CrossRef]

43. Korth, H.-G.; de Heer, M.I.; Mulder, P. A DFT study on intramolecular hydrogen bonding in 2-substituted phenols: Conformations, enthalpies, and correlation with solute parameters. *J. Phys. Chem. A* **2002**, *106*, 8779–8789. [CrossRef]
44. Yap, C.W. PaDEL-descriptor: An open source software to calculate molecular descriptors and fingerprints. *J. Comput. Chem.* **2011**, *32*, 1466–1474. [CrossRef]
45. Hall, L.H.; Kier, L.B. Electrotopological state indices for atom types: A novel combination of electronic, topological, and valence state information. *J. Chem. Inf. Comput. Sci.* **1995**, *35*, 1039–1045. [CrossRef]
46. Laggner, C. SMARTS Patterns for Functional Group Classification. 2009. Available online: <http://code.google.com/p/semanticchemistry/source/browse/wiki/IntelLigand.wiki?spec=svn41&cr=41> (accessed on 15 May 2010).
47. Klekota, J.; Roth, F.P. Chemical substructures that enrich for biological activity. *Bioinformatics* **2008**, *24*, 2518–2525. [CrossRef] [PubMed]
48. Gramatica, P.; Chirico, N.; Papa, E.; Cassani, S.; Kovarich, S. QSARINS: A new software for the development, analysis, and validation of QSAR MLR models. *J. Comput. Chem.* **2013**, *34*, 2121–2132. [CrossRef]
49. Gramatica, P.; Cassani, S.; Chirico, N. QSARINS-chem: Insubria datasets and new QSAR/QSPR models for environmental pollutants in QSARINS. *J. Comput. Chem.* **2014**, *35*, 1036–1044. [CrossRef]

Sample Availability: Samples of the compounds are not available.



© 2020 by the authors. Licensee MDPI, Basel, Switzerland. This article is an open access article distributed under the terms and conditions of the Creative Commons Attribution (CC BY) license (<http://creativecommons.org/licenses/by/4.0/>).

i. Oświadczenia współautorów

Wrocław, 14.04.2023

mgr farm. Maciej Spiegel
Katedra i Zakład Farmakognozji i Leku Roślinnego
Uniwersytet Medyczny im. Piastów Śląskich we Wrocławiu

OŚWIADCZENIE WSPÓŁAUTORA
CO-AUTHORSHIP STATEMENT

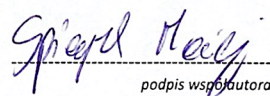
Jako współautor pracy:
As a co-author of the research paper:

Spiegel, M., Kapusta, K., Kołodziejczyk, W., Saloni, J., Żbikowska, B., Hill, G. A., & Sroka, Z. (2020).
Antioxidant activity of selected phenolic acids–ferric reducing antioxidant power assay and QSAR analysis of the structural features.
Molecules, 25(13), 3088.

oświadczam, że mój udział polegał na:

I declare that my own substantial contribution to this publication consists of:

- sformułowaniu i ewolucji nadrzędnych celów i zadań badawczych
formulation or evolution of overarching research goals and aims
- prowadzeniu procesu badawczego i dochodzeniowego oraz gromadzeniu danych
conducting a research and investigation process, and data collection.
- weryfikacji ogólnej powtarzalności wyników badań
verification of the overall reproducibility of research outputs
- przygotowaniu i stworzeniu opublikowanej pracy, w szczególności wizualizacji i prezentacji danych
preparation and creation of the published work, specifically visualization & data presentation.
- przygotowaniu i stworzeniu opublikowanej pracy, w szczególności napisaniu jej wstępnego szkicu
Preparation and creation of the published work, specifically writing the initial draft
- przygotowaniu i stworzeniu opublikowanej pracy, w szczególności wykonaniu krytycznej recenzji, naniesieniu komentarzy oraz korekt
preparation and creation of the published work, specifically critical review, commentary and revision



podpis współautora
(co-author's signature)



Uniwersytet Medyczny we Wrocławiu
KATEDRA I ZAKŁAD FARMAKOGNOZJI
I LEKU ROŚLINNEGO
kierownik
Supervisor's signature

prof. dr hab. Zbigniew Sroka
(2)

Jackson, MS, USA, 09/13/2022
miejsowość, data
(place, date)

Dr. Karina Kapusta, PhD
tytuł, imię i nazwisko
(title, name and surname)

Jackson State University
miejsce zatrudnienia
(affiliation)

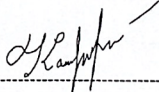
OŚWIADCZENIE WSPÓŁAUTORA CO-AUTHORSHIP STATEMENT

Jako współautor pracy:
As a co-author of the research paper:

Spiegel, M., Kapusta, K., Kołodziejczyk, W., Saloni, J., Żbikowska, B., Hill, G. A., & Sroka, Z. (2020).
Antioxidant activity of selected phenolic acids–ferric reducing antioxidant power assay and QSAR analysis of the structural features.
Molecules, 25(13), 3088.

oświadczam, że mój udział polegał na:
I declare that my contribution consists of:

- formułowaniu i rozwoju nadrzędnych celów i zadań badawczych
formulation and evolution of overarching research goals and aims
- działaniach zarządczych mających na celu tworzenie metadanych, oczyszczaniu danych i utrzymywanie danych badawczych do wstępnego wykorzystania i późniejszego ponownego wykorzystania
management activities to produce metadata, scrub data and maintain research data for initial use and later re-use
- zastosowaniu technik statystycznych, matematycznych i obliczeniowych do analizy i syntezy danych badawczych
application of statistical, mathematical and computational techniques to analyse and synthesize study data.
- prowadzeniu procesu badawczego, w szczególności gromadzeniu danych obliczeniowych
conducting a research, specifically computational data collection
- rozwoju i projektowaniu metodologii; tworzeniu modeli
development or design of methodology; creation of models
- weryfikacji ogólnej odtwarzalności wyników
verification of the overall reproducibility of results
- wizualizacji oraz prezentacji danych
visualization and data presentation
- przygotowaniu wstępnej wersji pracy
preparation of the original draft of the manuscript
- przygotowaniu końcowej wersji pracy, w szczególności korekty
preparation of the final version of the manuscript; in particular post-review corrections



podpis współautora
(co-author's signature)
Uniwersytet Medyczny we Wrocławiu
KATEDRA I ZAKŁAD FARMAKOGNOZJI
I LEKU ROŚLINNEGO
kierownik

podpis promotora
prof. dr hab. Zbigniew Sroka
(supervisor's signature)
(2)

Jackson 14-Wrz-2022
miejsowość, data
(place, date)

Wojciech Kołodziejczyk
tytuł, imię i nazwisko
(title, name and surname)

Jackson State University
miejsce zatrudnienia
(affiliation)

OŚWIADCZENIE WSPÓŁAUTORA CO-AUTHORSHIP STATEMENT

Jako współautor pracy:
As a co-author of the research paper:

Spiegel, M., Kapusta, K., Kołodziejczyk, W., Saloni, J., Żbikowska, B., Hill, G. A., & Sroka, Z. (2020).
Antioxidant activity of selected phenolic acids—ferric reducing antioxidant power assay and QSAR analysis of the structural features.
Molecules, 25(13), 3088.

oświadczam, że mój udział polegał na:
I declare that my contribution consists of:

- działaniach zarządczych mających na celu tworzenie metadanych, oczyszczaniu danych i utrzymywanie danych badawczych do wstępnego wykorzystania i późniejszego ponownego wykorzystania
management activities to produce metadata, scrub data and maintain research data for initial use and later re-use
- prowadzeniu procesu badawczego, w szczególności gromadzeniu danych obliczeniowych
conducting a research, specifically computational data collection
- rozwoju i projektowaniu metodologii
development or design of methodology
- zapewnieniu zasobów obliczeniowych
provision of computing resources
- przygotowaniu końcowej wersji pracy, w szczególności korekty
preparation of the final version of the manuscript; in particular post-review corrections



podpis współautora
Uniwersytet wrocławski
KATEDRA I ZAKŁAD FARMAKOGNOZJI
I LEKU ROŚLINNEGO

podpis promotora
prof. dr hab. Zdzisław Sroka
(2)

Jackson, 15-Wrzesnia-2022

miejsowość, data
(place, date)

Dr Julia Saloni

tytuł, imię i nazwisko
(title, name and surname)


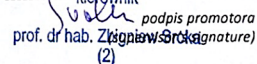
Jackson State University

miejsce zatrudnienia
(affiliation)**OŚWIADCZENIE WSPÓLAUTORA**
CO-AUTHORSHIP STATEMENTJako współautor pracy:
As a co-author of the research paper:

Spiegel, M., Kapusta, K., Kołodziejczyk, W., Saloni, J., Żbikowska, B., Hill, G. A., & Sroka, Z. (2020).
Antioxidant activity of selected phenolic acids–ferric reducing antioxidant power assay and QSAR analysis of the structural features.
Molecules, 25(13), 3088.

oświadczam, że mój udział polegał na:
I declare that my contribution consists of:

- wizualizacji oraz prezentacji danych
visualization and data presentation
- przygotowaniu wstępnej wersji pracy
preparation of the original draft of the manuscript
- przygotowaniu końcowej wersji pracy
preparation of the final version of the manuscript

-----
podpis współautora
(co-author's signature)Uniwersytet Medyczny we Wrocławiu
KATEDRA I ZAKŁAD FARMAKOGNOZJI
I LEKU ROŚLINNEGO-----
kierownik
podpis promotora
prof. dr hab. Zbigniew Sroka
(2)

Wrocław, 17.02.2023
miejsowość, data
(place, date)

mgr Beata Żbikowska
tytuł, imię i nazwisko
(title, name and surname)

Katedra i Zakład Farmakognozji i Leku Roślinnego,
Uniwersytet Medyczny we Wrocławiu
miejsce zatrudnienia
(affiliation)

OŚWIADCZENIE WSPÓŁAUTORA CO-AUTHORSHIP STATEMENT

Jako współautor pracy:
As a co-author of the research paper:

Spiegel, M., Kapusta, K., Kołodziejczyk, W., Saloni, J., Żbikowska, B., Hill, G. A., & Sroka, Z. (2020).
Antioxidant activity of selected phenolic acids–ferric reducing antioxidant power assay and QSAR analysis of the structural features.
Molecules, 25(13), 3088.

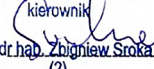
oświadczam, że mój udział polegał na:
I declare that my contribution consists of:

- *przewodzeniu procesu badawczego, w szczególności gromadzeniu danych eksperymentalnych*
conducting a research, specifically experimental data collection
- *rozwoju i projektowaniu metodologii*
development or design of methodology



podpis współautora
(co-author's signature)

Uniwersytet Medyczny we Wrocławiu
KATEDRA I ZAKŁAD FARMAKOGNOZJI
I LEKU ROŚLINNEGO
kierownik


prof. dr hab. Zbigniew Sroka
(2)

podpis promotora
(supervisor's signature)

Jackson, 09/21/2022

miejsowość, data
(place, date)

Glake Hill, Ph. D.

tytuł, imię i nazwisko
(title, name and surname)

Jackson State University

miejsce zatrudnienia
(affiliation)

OŚWIADCZENIE WSPÓŁAUTORA CO-AUTHORSHIP STATEMENT

Jako współautor pracy:


As a co-author of the research paper:

Spiegel, M., Kapusta, K., Kołodziejczyk, W., Saloni, J., Żbikowska, B., Hill, G. A., & Sroka, Z. (2020).
Antioxidant activity of selected phenolic acids–ferric reducing antioxidant power assay and QSAR analysis of the structural features.
Molecules, 25(13), 3088.

oświadczam, że mój udział polegał na:

I declare that my own substantial contribution to this publication consists of:

- pozyskaniu wsparcia finansowego na projekt prowadzący do tej publikacji
acquisition of the financial support for the project leading to this publication
- odpowiedzialności zarządczej i koordynacyjnej za planowanie i realizację działalności badawczej
management and coordination responsibility for the research activity planning and execution
- zapewnieniu zasobów obliczeniowych
provision of computing resources
- odpowiedzialności za nadzór i kierownictwo nad planowaniem i realizacją działań badawczych
oversight and leadership responsibility for the research activity planning and execution
- przygotowaniu końcowej wersji pracy, w szczególności korekty
preparation of the final version of the manuscript; in particular post-review corrections



podpis współautora
(co-author's signature)

Uniwersytet Medyczny we Wrocławiu
KATEDRA I ZAKŁAD FARMAKOGNOZJI
LEKU ROŚLINNEGO

kierownik
podpis promotora
(supervisor's signature)
prof. dr hab. Zbigniew Sroka
(2)

Wrocław, 18.04.2023
miejsowość, data
(place, date)

prof. dr hab. Zbigniew Sroka
tytuł, imię i nazwisko
(title, name and surname)

Katedra i Zakład Farmakognozji i Leku Roślinnego
Uniwersytet Medyczny im. Piastów Śląskich we Wrocławiu
miejsce zatrudnienia
(affiliation)

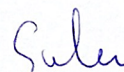
OŚWIADCZENIE WSPÓŁAUTORA CO-AUTHORSHIP STATEMENT

Jako współautor pracy:
As a co-author of the research paper:

Spiegel, M., Kapusta, K., Kołodziejczyk, W., Saloni, J., Żbikowska, B., Hill, G. A., & Sroka, Z. (2020).
Antioxidant activity of selected phenolic acids–ferric reducing antioxidant power assay and QSAR analysis of the structural features
Molecules, 25(13), 3088.

oświadczam, że mój udział polegał na:
I declare that my contribution consists of:

- sformułowaniu i rozwoju nadrzędnych celów i zadań badawczych
formulation and evolution of overarching research goals and aims
- uzyskaniu wsparcia finansowego dla projektu prowadzącego do powstania niniejszej publikacji
acquisition of the financial support for the project leading to this publication
- odpowiedzialności za zarządzanie i koordynację w zakresie planowania i realizacji działań badawczych
management and coordination responsibility for the research activity planning and execution
- dostarczaniu odczynników i innych narzędzi analitycznych
provision of reagents and other analysis tools
- nadzorze i odpowiedzialności kierowniczej za planowanie i realizację działań badawczych
oversight and leadership responsibility for the research activity planning and execution
- przygotowaniu końcowej wersji pracy
preparation of the final version of the manuscript



podpis współautora
(co-author's signature)

Uniwersytet Medyczny we Wrocławiu
KATEDRA I ZAKŁAD FARMAKOGNOZJI
I LEKU ROŚLINNEGO

Kierownik

podpis promotora
prof. dr hab. Zbigniew Sroka
(2)

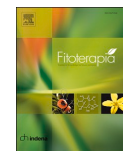
III. Publikacja [C]

Fitoterapia 164 (2023) 105352



Contents lists available at ScienceDirect

Fitoterapia

journal homepage: www.elsevier.com/locate/fitote

Quantum-mechanical characteristics of apigenin: Antiradical, metal chelation and inhibitory properties in physiologically relevant media

Maciej Spiegel^{*}, Zbigniew Sroka

Department of Pharmacognosy and Herbal Medicines, Wrocław Medical University, Borowska 211A, 50-556 Wrocław, Poland

ARTICLE INFO

Keywords:
 Apigenin
 Density Functional Theory
 Antiradical activity
 Complexation
 Molecular docking
 Xanthine oxidase

ABSTRACT

Density functional theory was used to examine the antioxidant activity of apigenin. All protonated species that are present in a non-negligible population at physiological pH were considered in the study. The ability to scavenge the hydroperoxide radical was evaluated in lipid and aqueous environments. The capacity to halt the Fenton reaction by chelating Fe(III) and Cu(II) ions was also investigated, as was the ability to inhibit xanthine oxidase. The results indicate that these activities may be particularly important in describing the beneficial effects of apigenin, especially because of its lower anti- \bullet OOH potential than Trolox or vitamin C. The findings underscore the significant role of dianion in the antiradical and chelating properties, despite its presence in much lower molar fractions than other ions.

1. Introduction

The physiological activity of radicals is a double-edged sword. On the one hand, they are essential for basic organism functions such as the immune response or intracellular signaling, and insufficient amounts may debilitate the body by preventing positive oxidative stress. [1] On the other, when accumulated in quantities far in excess of physiological concentrations, they are recognized triggers of intracellular damage, consequently leading to oxidative stress, which manifests itself in the development of severe disorders such as Alzheimer's or Parkinson's disease, hypercholesterolemia or cancer. [2] While the internal redox system consisting of enzymes and small molecules protects against this situation [3,4], due to external triggers the overall concentration of free radicals in the body is no longer so easy to maintain. For these reasons, scientific efforts are focused on the search for and development of new substances with antiradical activity, and polyphenols seem to be the most appealing in this regard.

These phytochemicals, found in abundance in daily consumed spices [5], fruits and vegetables [6,7], are the first line of support for the internal antioxidant system. In the experiments, polyphenols have been shown to satisfactorily scavenge artificial radicals such as DPPH[•] [8,9], chelate Fe(II) and Fe(III) ions involved in the Fenton reaction [10], or modulate enzymes important in the cellular red-ox system, such xanthine oxidase. [11] The biosynthesis of all phenolic compounds originates from the shikimate pathway and gives rise to three major

classes of polyphenols: flavonoids, phenolic acids and anthocyanidins. The former are built up on a cyclized C6-C3-C6 heterocyclic system, divided into three rings A, B and C, with the AC system representing the fundamental oxygen-containing scaffold. Based on the substitution pattern — the position of the B ring, the number and position of the -OH groups or the presence/absence of the C2=C3 bond — several subclasses of flavonoids can be distinguished. [12] Regardless of the structure, all the mentioned activities are associated with the presence of one or more phenolic hydroxyl groups linked to the aromatic ring or the delocalized electron cloud system itself. Namely, the reaction of a highly active radical with an antioxidant results in a much less reactive radical-antioxidant product whose electron density is distributed throughout the structure, rather than on a single atom, resulting in its stabilization. [13] This structure not only gives them the ability to act as a hydrogen atom/electron donor or form adducts with small radical, but also gives them the ability to form stable complexes with the transition state metals. It has been experimentally proven that antioxidant chelated iron or copper does not participate as actively in the Fenton reaction as free one, thereby reducing the generation of hydroxyl and hydroperoxide radicals through this pathway. [14]

Probably the best recognized dietary polyphenol is apigenin. This flavone is on the top five flavonoids present in the daily diet, found ubiquitously in spices, fruits and vegetables such as parsley, spinach, celery seed, green celery heart, dried oregano, oranges, onions, wheat sprouts, tea and more. Typically presented in glycosylated forms — C-

^{*} Corresponding author.

E-mail address: maciej.spiegel@student.umed.wroc.pl (M. Spiegel).

<https://doi.org/10.1016/j.fitote.2022.105352>

Received 3 October 2022; Received in revised form 11 November 2022; Accepted 11 November 2022

Available online 16 November 2022

0367-326X/© 2022 Elsevier B.V. All rights reserved.

and O-glucosides, glucuronides, O-methyl ethers, and acetylated derivatives — it is easily broken down by the microbiota in the small intestine, followed by absorption and good distribution to tissues. [15] The experimental studies shown the beneficial effects of apigenin intake in preventing the development of diabetes, cancer, Alzheimer's diseases, amnesia, depression or insomnia. [16]

This *another* theoretical study on apigenin may not be considered novel. Over the years, different scientific groups have conducted studies to describe this flavonoid. The impact of solvent and deprotonation on the feasibility of hydrogen atom transfer was studied in the work of Klein et al. [17,18]. This process has also been related to the experimental data elsewhere [19,20], while structure-activity relationships have been combined into the QSAR model by Zuvela et al. [21]. The data on the electronic structure, structural features and intrinsic reactivity indices are also available, whether from the original works [22–25] or the reviews [12,26]. Nevertheless, as can be seen, these works are relatively old. Moreover, they tend to focus on one aspect, such as the bond dissociation process, leaving the other undiscussed. After all, it was not possible for us to find any theoretical investigations on the chelating properties of apigenin or the antiradical activity against specific radicals. This shows that while this may be considered as a trivial topic, it is actually emerging as a still undiscovered field worthy of further exploration, as was partially done by Zheng et al. [27], who studied the effect of varying substituents on the radical scavenging activity.

To fill this unexpected gap, apigenin has been accurately characterized in this article at density functional level of theory on its primary (anti-•OOH) and secondary (Cu²⁺ and Fe³⁺ complexing power and xanthine oxidase inhibition potential) activities, demonstrating the mechanistic properties behind its beneficial activity.

2. Results and discussion

2.1. Acid-base equilibria in water

The chemical structure of apigenin is shown in Fig. 1. The presence of three OH groups indicate that the system may exist simultaneously at three different protonation states.

The acid-base dissociation constants, pK_{a1} , were calculated for the studied system, and were found to be equal to: $pK_{a1} = 7.40$ (C7), $pK_{a2} = 8.41$ (C4'), and $pK_{a3} = 11.61$ (C5). According to other observations [28–30], unless the C3 position is not occupied, the C7 position is most easily deprotonated, while the C5 position is least susceptible to proton detachment. The latter is an expected behavior coming from particularly strong intramolecular hydrogen bond interactions between carbonyl and hydroxyl residues, which indirectly enable density delocalization, as it was demonstrated in previous paper. [23]

Examining a graph plotting the molar fraction as a function of pH (Fig. 2), we find that non-dissociated and single anionic forms are present in equal amounts ($M_{f_{H_3A}} = M_{f_{H_2A^-}} = 48.7\%$) in physiological pH. While di-anion species are also present in a non-negligible population ($M_{f_{HA^{2-}}} = 4.7\%$) and thus remain relevant to the study of apigenin activity, completely dissociated structure not ($M_{f_{A^{3-}}} = 0.0\%$).

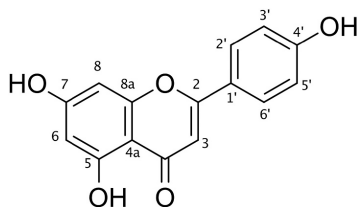


Fig. 1. Chemical structure and atom numbering of apigenin.

2.2. Intrinsic reactivity indices

In order to determine the chemical properties of the isolated species and allow comparison with other substances regardless of the radical scavenged, enthalpies of bond dissociation (a), ionization potential (b), proton affinity (c) and proton dissociation (d) were calculated.

$$BDE = H^\circ(C-O^\bullet) + H^\circ(H^\bullet) - H^\circ(C-OH);$$

$$IP = H^\circ(C-OH^{\bullet+}) + H^\circ(e^-) - H^\circ(C-OH);$$

$$ET = H^\circ(C-O^\bullet) + H^\circ(e^-) - H^\circ(C-O^-);$$

$$PA = H^\circ(C-O) + H^\circ(H^+) - H^\circ(C-OH);$$

$$PDE = H^\circ(C-O^\bullet) + H^\circ(H^+) - H^\circ(C-OH^{\bullet+});$$

The results are shown in Table 1. Ionization appears to be more feasible in aqueous solvent (127.4 kcal/mol — 98.5 kcal/mol) than in pentyl ethanoate (142.4 kcal/mol), which can be linked to the ability to solvate the ultimately antioxidant cation radical. At the same time, it can be seen that successive deprotonations clearly reduce the energetics of the process, confirming the increasing destabilization of the species within each dissociation step. Vaganek et al. [18] reported that IP value for neutral species in water is 117.6 kcal/mol (B3LYP/6-311 + G(d,p)/IEF-PCM), which is about 10 kcal/mol difference with our results. In the work of Zheng et al. [22] with energies estimated at the M06-2X/6-311 + G** level of theory and the SMD solvation model, IP equals 140.1 kcal/mol for species without intramolecular hydrogen bonds and 141.4 kcal/mol for species with them. In their next paper, a value of 139.3 kcal/mol was obtained. Our previous work treating the structure-activity relationships of 13 common flavonoids predicted an IP of 117.0 kcal/mol when B3LYP/6-31 + G(d,p) and PCM water solvent were used. These discrepancies are actually not astonishing — determining IP and EA values appears to be a difficult task and is strongly dependent on functional and basis set used [31].

The of C4' and C7 bond dissociation do not differ between neutral species in water or pentyl ethanoate, but the process is slightly more favored for C5 in the former than the latter (by about 6.0 kcal/mol). Following the results of Chen et al. [22], strong intramolecular hydrogen bonds weaken the antiradical capacity of C5 hydroxyl, to a greater degree in the weakly polarized solvent of pentyl ethanoate, and to a lesser extent in water. After all, dissociation does not seem to affect the values of this index significantly, and the reactivity pattern can be described as C5 < C7 < C4', what goes along with previous studies on flavonoids. [22,32] While only this work provides BDE values for all species present in the physiological environment, there are other data for neutral ones and can be reported for the set (C4', C5, C7) as (82.1, 92.5, 86.4) [17], (88.3, 94.5, 93.7) and (87.8, 89.3, 93.2) [22], (89.3, 100.5, 91.7) [23] and (96.6, 103.3, 102.2) [25], all in kcal/mol.

The pattern of hydrogen atom donating sites obtained in this work also applied to PDE, but not necessarily to PA, whose reactivity trend can be represented as C5 < C4' < C7 in the case of water. Similar one was reported in other papers. [18,22,23] In order to provide complete and systematic data on the intrinsic properties, proton affinity values were also calculated for pentyl ethanoate, although deprotonation should not occur in a solvent devoid of solvation potential. This is evidenced by about 15-20 kcal/mol higher values of the index compared to those obtained in water. Also observable is a shift in the preferred site of deprotonation — it is the C4' position rather than C7. Though the difference is marginal and amounts to 0.6 kcal/mol, so both positions can be considered equivalent.

The electron transfer enthalpy results suggest that this process is less thermochemically demanding in pentyl ethanoate than in water. As the earlier discussion shows, this behavior is perfectly clear — the anionic structure of the antioxidant is less stable than the radical one. While this holds not true for neutral species in water, a similar willingness to detach an electron is already noticeable when the first dissociation (at C5) occurs, and is further amplified in the case of dianion. Like the ionization potential, ETE values also vary in the literature, being in the ranges of 76.3–116.3 (C4'), 67.9–114.4 (C5) and 74.2–119.2 (C7) kcal/mol [17,18,22,23].

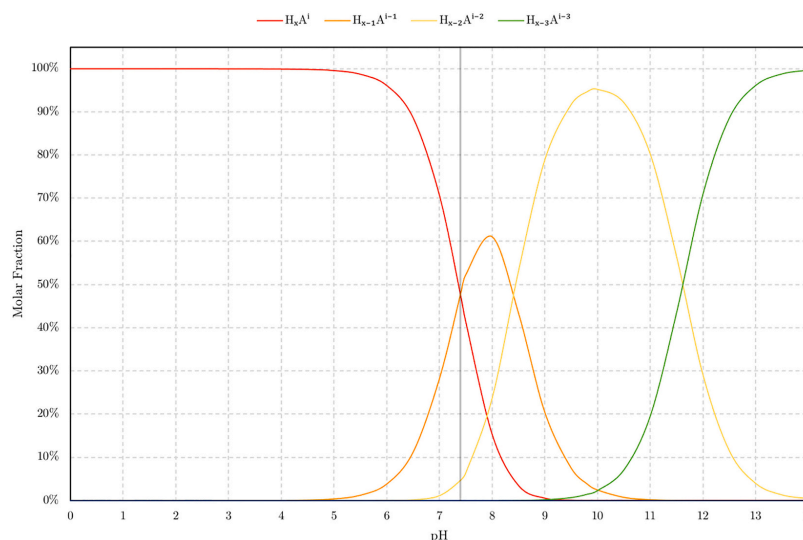


Fig. 2. Molar fractions of apigenin species plotted as a function of pH.

Table 1

IP, BDE, PA, and PDE values calculated for non-negligible apigenin species in pentyl ethanoate and water at 298.15 K. All values are in kcal/mol.

Species	Solvent	Site	IP	BDE	PA	ETE	PDE
H ₃ A	PE	C4'		80.5	46.0	91.8	4.8
		C5	142.4	92.3	59.7	89.8	16.5
		C7		85.6	46.6	96.3	9.8
	water	C4'		80.1	31.0	101.2	4.8
		C5	127.4	86.7	35.4	103.4	11.4
H ₂ A ⁻	water	C7		85.2	29.4	107.9	9.9
		C4'		81.3	32.6	98.5	23.2
	C5	107.9	87.0	41.4	95.4	28.9	
HA ²⁻	water	C5	98.5	85.7	42.6	92.9	37.0

These brief and preliminary outcomes suggest that the *f*-HAT mechanism might be relying primarily on the C4' hydroxyl group. At the same time, the SET mechanism, which is approximated by IP, appears to be much less favored than the former, however the difference between IP and BDE for HA²⁻ is much smaller, suggesting that their two related mechanisms may actually compete in radical scavenging activity. Although the overall results are not exactly the same with those reported elsewhere, it should be recalled that the intrinsic reactivity indices are suggested for comparative purposes only and shall not be taken as determinants of antiradical activity. This can only be achieved by considering the radical being scavenged and examining the kinetic of feasible reactions. Nevertheless, the patterns generally confirm each other, which proves their usefulness for the purpose just stated.

2.3. Thermochemistry and kinetics

The scavenging potential of apigenin and its dissociated forms towards [•]OOH was determined by calculating the Gibbs free energies of the reaction (ΔG°) and the activation energies (ΔG^\ddagger) of the *f*-HAT, RAF and SET mechanisms. For the first two pathways, $\Delta G^\circ < 10.0$ kcal/mol was a prerequisite for the reaction to be considered favorable and studied further. Although this implies the reversibility of the reaction, endergonic pathways may still be important channels if their products

rapidly react further. This would be especially true if these latter steps are sufficiently exergonic to provide the driving force, and if their reaction barriers are low. Given the complexity of biological systems involving many different chemicals, it is likely that this could occur under such conditions. [33–35] Consideration of low endergonic pathways is found also in other works. [36–38] In contrast, such a limitation is not applicable to SET calculations, because the process is described by Marcus theory. All results are summarized in Table 2. It is also important to emphasize that although the pK_a of the [•]OOH/O₂⁻ pair is 4.8, suggesting that the deprotonated form is present in the highest concentration under physiological conditions (0.25% vs. 99.75%), the reaction of superoxide with non-radicals is spin-forbidden, so this species is of little importance, and the oxidative damage comes primarily from the protonated form [39] Hence all calculations presented in the text are for [•]OOH.

The results show that *f*-HAT represents a feasible mechanism of action with ΔG° ranging from between 2.2 kcal/mol (C4' of H₂A⁻) to 9.9 kcal/mol (C5 of H₃A) in all cases except C5 in pentyl ethanoate, for which $\Delta G^\circ = 16.1$ kcal/mol. In contrast, the established Gibbs free energies of SET were found to be significantly higher among neutral species (37.8 kcal/mol) and slightly higher for monoanionic species (18.3 kcal/mol). In the case of HA²⁻, the trend shown is changed, and although this species is present in solution in a small fraction, its kinetic behavior may still be high enough to be considered an important part of the description of the scavenging of hydroperoxide radical by apigenin. Neutral species, regardless of solvent, are completely inactive in electron transfer reactions on [•]OOH. This is to be expected, given the activation energies, which actually drives the kinetics according to conventional transition state theory — so it is anticipated that while non-dissociated species act mainly via *f*-HAT, the antiradical activity of dissociated species might be a combination of both hydrogen atom transfer and electron donation properties. The RAF mechanism was found to be highly endergonic in almost all cases. However, although ΔG° exceeds the imposed threshold of 10.0 kcal/mol, the calculated values of ΔG^\ddagger suggest that the reaction might be competitive with HAT at the C5 and C7 position. The above deliberations are supported by the reaction rates shown in Table 3, for which the transition state structures are depicted

Table 2

Gibbs free energies of reaction (ΔG° , in kcal/mol) and activation (ΔG^\ddagger , in kcal/mol) between the considered apigenin species in water and pentyl ethanoate (mared with ^{PE} apex) at pH = 7.4 and 298.15 K.

Mechanism	Site	H_3A^{PE}		H_3A		H_2A^-		HA^{2-}	
		ΔG°	ΔG^\ddagger	ΔG°	ΔG^\ddagger	ΔG°	ΔG^\ddagger	ΔG°	ΔG^\ddagger
f-HAT	C4'	4.4	22.7	3.3	23.9	2.2	23.1		
	C5	16.1		9.9	29.6	7.9	27.3		
	C7	9.5	25.1	8.4	26.5			6.6	28.0
RAF	C2	18.6		16.2		13.8		15.0	
	C3	14.3		12.2	22.8 ^a	10.0	21.0 ^a	11.7	18.3 ^a
	C4a	33.4		31.9		26.7		26.2	
	C5	21.9		18.9		19.5		19.1	
	C6	22.0		20.3		14.4		14.5	
	C7	25.0		22.9		28.9		27.7	
	C8	21.5		19.2		15.6		15.5	
	C1'	25.5		22.9		22.8		20.0	
	C2'	21.8		19.6		19.4		21.4	
	C3'	21.1		19.6		20.0		13.5	
	C4'	17.5		15.6		15.1		18.8	
	C5'	21.4		20.8		20.8		13.8	
C6'	19.7		17.7		17.6		19.9		
SET				37.8	83.0	18.3	18.8	8.9	12.8

^a See the main text.

Table 3

Rate constants (k , in $M^{-1} s^{-1}$)^a and branching ratios (Γ , in %) of the reactions between $\cdot OOH$ and the considered apigenin species in water and pentyl ethanoate (indicated by ^{PE} apex) at pH = 7.4 and 298.15 K.

Mechanism	H_3A^{PE}		H_3A		H_2A^-		HA^{2-}	
	k	Γ	k	Γ	k	Γ	k	Γ
HAT-C4'	5.75×10^{-1}	99.4	6.11×10^{-1}	98.1	2.99×10^0	93.9		
HAT-C5			1.15×10^{-4}	0.0	6.47×10^{-3}	0.2	1.04×10^{-2}	0.0
HAT-C7	3.72×10^{-3}	0.6	7.58×10^{-3}	1.2				
RAF-C3			3.92×10^{-3}	0.6	7.93×10^{-2}	2.5	7.83×10^0	0.0
SET			8.96×10^{-49}	0.0	1.08×10^{-1}	3.4	1.24×10^2	100.0
k_{total}			6.23×10^{-1}		3.18×10^0		1.25×10^2	
$k_{overall}$	5.79×10^{-1}		2.97×10^{-1}		1.52×10^0		5.78×10^1	
$k_{corrected}$			7.42×10^{-4}		3.79×10^{-3}		1.44×10^1	

^a k_{total} is the sum of all rate constants for a given species; $k_{overall}$ equals k_{total} multiplied by the molar fraction of the species at pH = 7.4; and $k_{corrected}$ equals $k_{overall}$ multiplied by the molar fraction of $\cdot OOH$ under the given conditions.

in Fig. 3.

The overall reaction rate assumes that the hydroperoxide radical is present in significant amounts, much more than the antioxidant, and therefore does not control the reaction kinetics. This is hardly true and can be an error yielding inaccurate results. For this reason, emphasis should be placed on considering the molar fraction of the radical when establishing the reaction rate, particularly if the value is small. Thereby, $k_{corrected}$ was computed to provide a more accurate description of the kinetic process in solution.

The evaluation of kinetic data indicates fairly low reaction rates. In line with previous assumptions, the activity of neutral and monoanionic species is mainly based on hydrogen atom transfer, with the C4' site being the most reactive. Although aqueous solvent and subsequent deprotonations slightly increase the values of the corrected reaction rates, they remain low. However, in accordance with an earlier hypothesis, although present in small amounts, HA^{2-} has a great impact on the proper description of the radical scavenging potential of apigenin. The branching ratio of an individual reaction rate of SET is much higher than any other reported here, and at the same time $k_{corrected}$ is the highest, despite the fact that only 4.66% of this form is present under the conditions studied, corresponding to $1.44 \times 10^1 M^{-1} s^{-1}$.

To determine the relative anti- $\cdot OOH$ potential, the corrected reaction rates were summed ($\Sigma k_{corrected}^{PE} = 5.79 \times 10^{-1} M^{-1} s^{-1}$; $\Sigma k_{corrected} = 2.51 \times 10^1 M^{-1} s^{-1}$) and compared to the reported $k_{overall}$, refined to account for the molar fraction of hydroperoxide in solution, as was done for apigenin. The data indicate that apigenin is a worse radical scavenger than both Trolox ($\Sigma k_{corrected}^{PE} = 8.50 \times 10^2 M^{-1} s^{-1}$; $\Sigma k_{corrected} = 2.24 \times$

$10^4 M^{-1} s^{-1}$) [33] and vitamin C ($\Sigma k_{corrected}^{PE} = 4.05 \times 10^1 M^{-1} s^{-1}$; $\Sigma k_{corrected} = 6.4 \times 10^5 M^{-1} s^{-1}$) [40]. It would be wise to make comparisons to kaempferol (flavonol) and naringenin (flavanone) for the observable effect of the presence of the 3-OH group and the absence of the C2-C3 double bond, respectively, but data are lacking in this context.

2.4. Chelating properties

Complexation of Cu(II) and Fe(III) ions with consequences in intercepting the Fenton reaction is another likely activity exhibited by most dietary antioxidants. Apigenin has only one coordination site, constituting of C4 carbonyl and C5 hydroxyl groups, and this one has been studied for all the species. Thermodynamic and kinetic data are shown in Table 4, while a visualization of the optimized structures is shown in Fig. 4.

The copper ion was found to be coordinated by O—H and C=O groups, with Cu—O distances of the former equal to: 2.138 Å (H_3A), 2.112 Å (H_2A^-) and 2.108 Å (HA^{2-}); the latter: 1.958 Å (H_3A), 1.951 Å (H_2A^-) and 1.946 Å (HA^{2-}). In these complexes, the Jahn–Teller effect causing tetragonal deformation is evident, with the axial water molecules located at distances: [2.461 Å, 2.300 Å] (H_3A), [2.475 Å, 2.313 Å] (H_2A^-) and [2.474 Å, 2.318 Å] (HA^{2-}) from the Cu cation. [41] On the other hand, Fe(III) complexes persists their octahedral structure, and the distance between Fe and the O—H and C=O oxygens was found to be: [1.971, 1.882 Å] (H_3A), [1.963 Å, 1.873 Å] (H_2A^-) and [1.960 Å, 1.863 Å] (HA^{2-}).

The outcomes indicate that the most stable complexes are those with

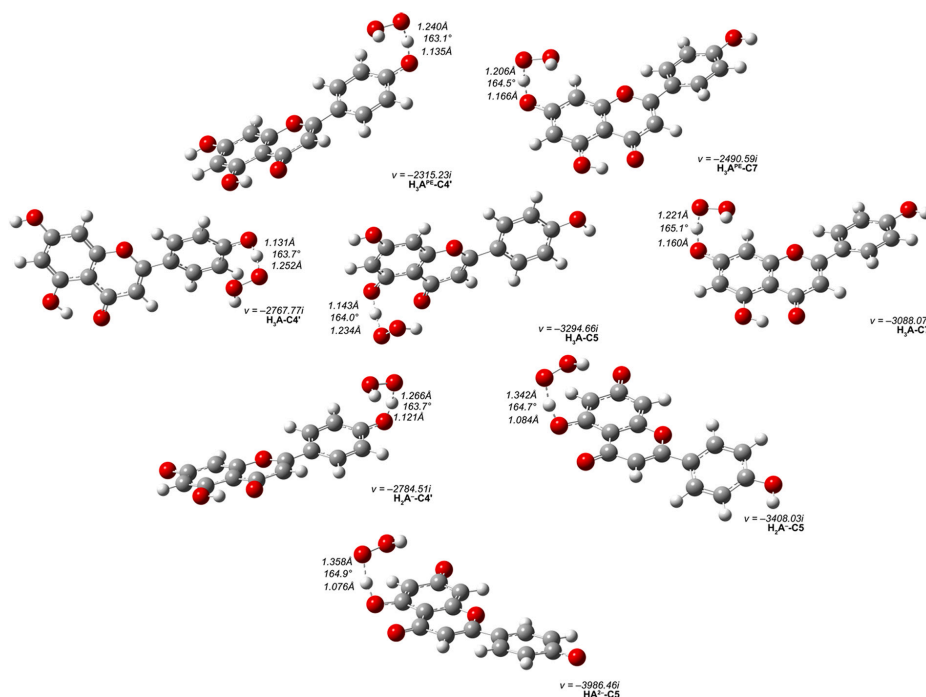


Fig. 3. Transition state structures of viable hydrogen atom transfers. Distances are in Å and angles are in degrees.

Table 4

Gibbs free energies of complexation (ΔG°_f , in kcal/mol) and kinetic constants (K_f , K_f^H and K_f^{pp}) for Cu(II) and Fe(III) ions chelated by C4-C5 coordination site of apigenin species.

Species	ΔG°_f	K_f	K_f^H	K_f^{pp}
Cu(II)				
H ₃ A	-2.2	3.79×10^3	1.81×10^1	
H ₂ A ⁻	-4.6	2.22×10^3	1.06×10^3	6.74×10^3
HA ²⁻	-6.9	1.22×10^3	5.67×10^3	
Fe(III)				
H ₃ A	-7.0	1.39×10^5	6.61×10^4	
H ₂ A ⁻	-12.9	2.91×10^9	1.39×10^9	1.09×10^{12}
HA ²⁻	-18.2	2.34×10^{13}	1.09×10^{12}	

the most dissociated species. This behavior is expected due to the equalization of the metal's positive charge by the successively increasing unpaired electron density. The subsequent deprotonation results in an increase in stability of about 2 kcal/mol and 5 kcal/mol for Cu(II) and Fe(III), respectively. We expect that chelation would be further enhanced if the C5 group also dissociated due to the removal of the steric hindrance at the chelation site, however, such a structure does not occur under the conditions considered. Once equilibrium constants are established, the aforementioned behavior can be further detailed by notable changes in K_f between H₃A (3.79×10^3), H₂A⁻ (2.22×10^3) and HA²⁻ (1.22×10^3). Even larger values occur for Fe(III)-complexes, as would be expected from the much larger ΔG°_f values.

Although the HA²⁻ species accounts for only 4.66% of the total forms in aqueous solution, it seems to prevail when describing Fe(III) complexation, constituting virtually all of apigenin II-type antioxidant

activity ($K_f = K_f^{pp} = 1.09 \times 10^{12}$). To a lesser extent, this is true for Cu(II), since $K_f^{pp} = 6.74 \times 10^3$ is the sum of the contribution of both HA²⁻ (the larger part) and H₂A⁻ (the smaller part). In any case, summarizing the complexation process, the results indicate that apigenin is much better Fe(III) chelator than Cu(II), although being complexed their contribution to the Fenton reaction is naturally smaller.

2.5. Xanthine oxidase inhibition

Preliminary molecular docking studies were carried out to gain insight into how the analyzed species bind to the identified xanthine oxidase active site. The approach was validated by comparing the position of the newly introduced ligand with that of the cocrystallized quercetin (Fig. 5) and the interactions with the surrounding amino acids (Fig. 6).

The data show that apigenin, in any state, has a similar conformation to the original ligand and interacts with the same amino acids. Arg880 and Thr1010 are the common hydrogen bond sites interacting with the ligands. The position of the AC ring in apigenin species differs only slightly from quercetin, while the only difference between the structures in this scaffold is the presence of C3 hydroxyl in the latter. Given that apigenin's conformation results in the formation of a hydrogen bond between Val1010 and Ala1079, albeit not as pronounced as in the case of quercetin, it can be assumed that the absence of 3-OH favors binding, allowing the formation of the two hydrogen bonds mentioned. The process of deprotonation seems to have little effect on the length of the hydrogen bond, and while the distances decrease, the changes are negligible. The binding pocket appears to be strongly hydrophobic, and almost all atoms of the phytochemicals under study are involved in these interactions. Additionally, 3D visualization makes it possible to

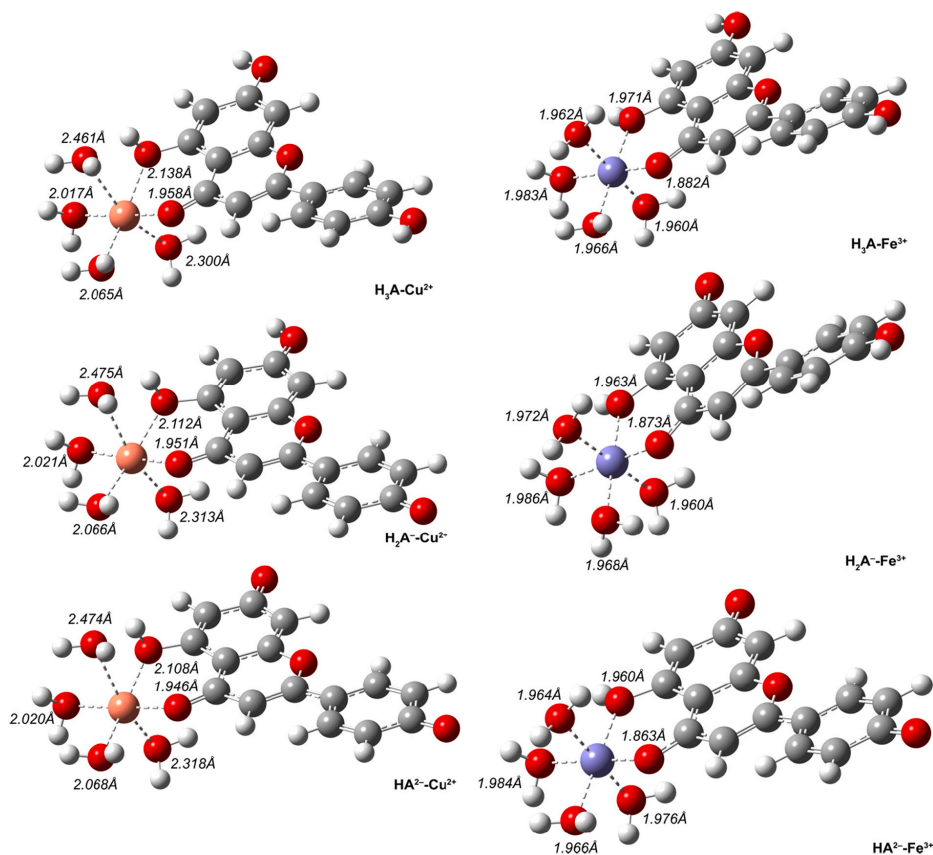


Fig. 4. Structures of Cu(II) and Fe(III) complexes with apigenin species.

prediction π - π interactions with the aromatic rings of Phe914 and Phe1009.

Table 5 shows the established inhibition constants. While the scavenging capacity towards $\cdot\text{OOH}$ and chelating properties depend on the most dissociated species, even though their molar fraction was much lower, the inhibition capacities do not. This is due to the fact that the binding free energies of the studied species are relatively similar, thanks to almost identical orientation in the binding pocket and interactions.

3. Conclusions

DFT experiments revealed the antiradical and antioxidative properties of apigenin and its dissociated forms in biologically relevant solvents. Given these activities, the deprotonation process was shown to be extremely beneficial. Nonetheless, while even a small fraction of dianion species had an effect in the first two, it is much smaller in the case of inhibitory activity. The results of the study are summarized as follows:

- $\cdot\text{OOH}$ is scavenged at a reaction rate constant of $5.79 \times 10^{-1} \text{ M}^{-1} \text{ s}^{-1}$ in the lipid phase and $1.44 \times 10^1 \text{ M}^{-1} \text{ s}^{-1}$ in the aqueous phase. These values are lower than Trolox or vitamin C.

- The Fe(III) cation is much more easily chelated than the Cu(II) cation. The corresponding apparent equilibrium constants were determined to be 1.09×10^{12} and 6.74×10^3 , respectively.
- Xanthine oxidase inhibition is similar to that of quercetin, and similar amino acids are involved in the interactions with ligands. Apigenin, on the other hand, due to its lack of 3-OH is able to rotate and form two more exclusive hydrogen bonds with Val1011 and Ala1079.

4. Computational details

DFT studies were performed in the Gaussian16 software package. [42] The antiradical behavior was studied according to a well-established computational protocol that includes thermochemical and kinetic aspects of the processes undergoing, the QM-ORSA protocol. [43] The meta-hybrid exchange-correlation GGA functional M05-2X [44] combined with the 6-311 + G(d,p) basis set [45,46] was used. The physiologically relevant solvents were modeled by the water and pentyl ethanoate (PE), respectively, within a universal solvation model based on solute electron density (SMD). [47] The same level of theory was used for the frequency computations necessary to ensure the local minimum or transition state character of the geometries found, as well as to account for zero-point energy corrections. The unrestricted procedure was

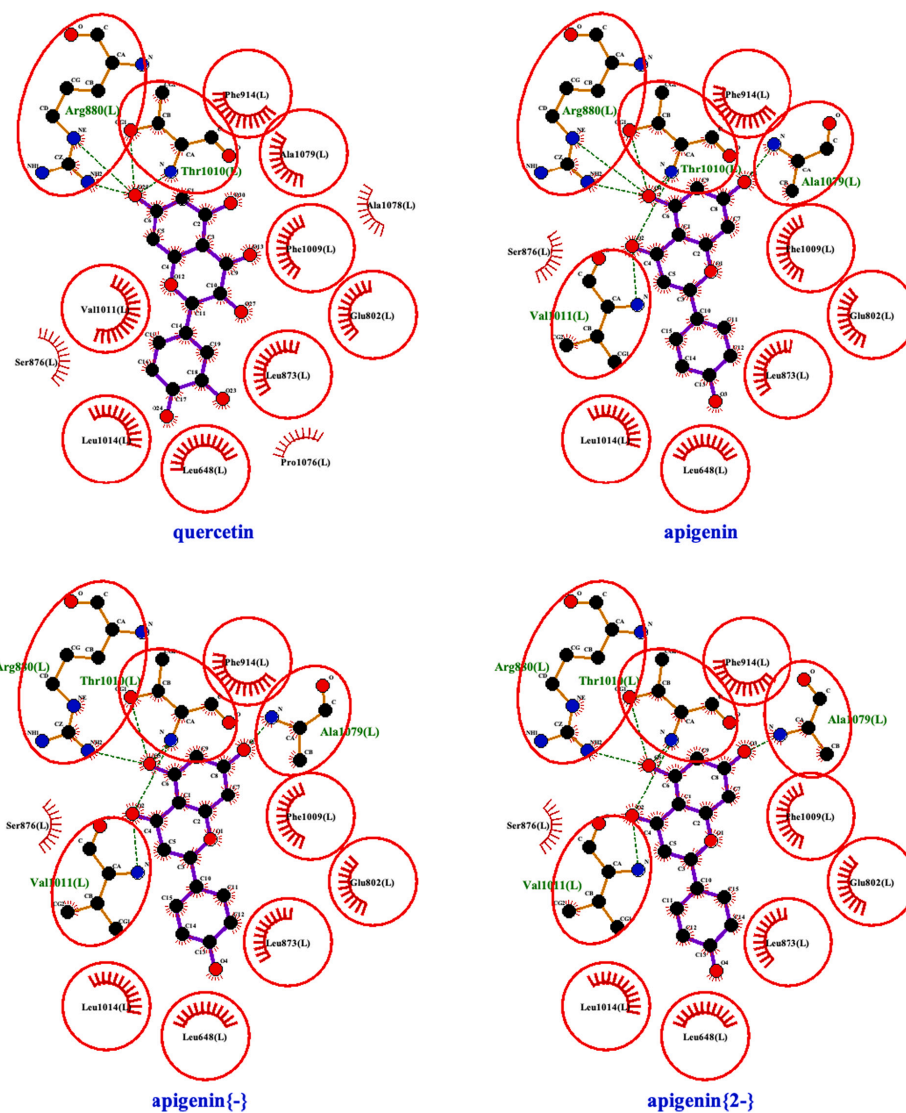


Fig. 6. Intramolecular interactions in the active site of xanthine oxidase. Green dashed lines represent hydrogen bonds, while red circles indicate equivalent residues engaged in hydrophobic interactions. (For interpretation of the references to colour in this figure legend, the reader is referred to the web version of this article.)

Table 5

Bindings free energies ΔG_b^0 , inhibition constants (K_i), molar-fraction weighted inhibition constant (K_b^H) and apparent inhibition constant (K_b^{app}) of apigenin species.

Species	ΔG_b^0	K_b	K_b^H	K_b^{app}
H ₃ A	-9.1	4.76×10^6	2.27×10^6	5.89×10^6
H ₂ A ⁻	-9.3	6.68×10^6	3.18×10^6	
HA ²⁻	-9.5	9.36×10^6	4.36×10^5	

After structure validation, 3NVY was pre-processed by removing quercetin, adding hydrogens and fixing charges. The docking box was centered on the original ligand position, with the dimension and volume covering the amino acids involved in the quercetin docking, and the apigenin species were docked using the AutoDock VINA [58]. The apparent binding constant (K_b^{app}) was obtained from the binding free energy (ΔG_b^0) using the formula:

$$K_b = e^{-\frac{\Delta G_b^0}{RT}}$$

M. Spiegel and Z. Sroka

Fitoterapia 164 (2023) 105352

$$K_b^H = K_b^m f_b$$

$$K_b^{app} = \sum K_b^H$$

where K_b represents the binding constant of a given b species, K_b^H is the individual contribution of a given species determined by accounting for its molar fraction, f_b , in the system at pH = 7.4.

CRedit authorship contribution statement

Maciej Spiegel: Conceptualization, Methodology, Validation, Formal analysis, Investigation, Resources, Data curation, Visualization, Writing – original draft, Writing – review & editing. **Zbigniew Sroka:** Supervision, Project administration.

Declaration of Competing Interest

The authors declare no conflict of interest.

Acknowledgements

This research was supported in part by PLGrid Infrastructure (grant ID: plg antioxidants). MarvinSketch (version 21.15.0, ChemAxon) was used to visualize the structure of apigenin.

References

- L.-J. Yan, Positive oxidative stress in aging and aging-related disease tolerance, *Redox Biol.* 2 (2014) 165–169, <https://doi.org/10.1016/j.redox.2014.01.002>.
- J. Luo, K. Mills, S. le Cessie, R. Noordam, D. van Heemst, Ageing, age-related diseases and oxidative stress: what to do next? *Ageing Res. Rev.* 57 (2020), 100982 <https://doi.org/10.1016/j.arr.2019.100982>.
- I. Mironczuk-Chodakowska, A.M. Witkowska, M.E. Zujko, Endogenous non-enzymatic antioxidants in the human body, *Adv. Med. Sci.* 63 (2018) 68–78, <https://doi.org/10.1016/j.advms.2017.05.005>.
- A.M. Pisoschi, A. Pop, The role of antioxidants in the chemistry of oxidative stress: a review, *Eur. J. Med. Chem.* 97 (2015) 55–74, <https://doi.org/10.1016/j.ejmech.2015.04.040>.
- A. Yashin, Y. Yashin, X. Xia, B. Nemzer, Antioxidant activity of spices and their impact on human health: a review, *Antioxidants*. 6 (2017) 70, <https://doi.org/10.3390/antiox6030070>.
- S. Kamiloglu, G. Toydemir, D. Boyacioglu, J. Beekwilder, R.D. Hall, E. Capanoglu, A review on the effect of drying on antioxidant potential of fruits and vegetables, *Crit. Rev. Food Sci. Nutr.* 56 (2016) S110–S129, <https://doi.org/10.1080/10408398.2015.1045969>.
- M.S. Swallah, H. Sun, R. Affoh, H. Fu, H. Yu, Antioxidant potential overviews of secondary metabolites (polyphenols) in fruits, *Int. J. Food Sci.* 2020 (2020) 1–8, <https://doi.org/10.1155/2020/9081686>.
- R. Hirano, W. Sasamoto, A. Matsumoto, H. Itakura, O. Igarashi, K. Kondo, Antioxidant ability of various flavonoids against DPPH radicals and LDL oxidation, *J. Nutr. Sci. Vitaminol. (Tokyo)* 47 (2001) 357–362, <https://doi.org/10.3177/jnsv.47.357>.
- M. Karamać, A. Kosińska, R.B. Pegg, Comparison of radical-scavenging activities for selected phenolic acids, *Polish J. Food Nutr. Sci.* 55 (2005) 165–170. <http://journal.pan.olsztyn.pl/COMPARISON-OF-RADICAL-SCAVENGING-ACTIVITIES-FOR-SELECTED-PHENOLIC-ACIDS-.97869,0,2.html>.
- Z. Kejík, R. Kaplánek, M. Masářík, P. Babula, A. Matkowski, P. Filipenský, K. Veselá, J. Gburek, D. Šýkora, P. Martásek, M. Jakubek, Iron complexes of flavonoids-antioxidant capacity and beyond, *Int. J. Mol. Sci.* 22 (2021) 646, <https://doi.org/10.3390/ijms22020646>.
- A. Bertelli, M. Biagi, M. Corsini, G. Baini, G. Cappellucci, E. Miraldi, Polyphenols: from theory to practice, *Foods*. 10 (2021) 2595, <https://doi.org/10.3390/foods10112595>.
- M. Parcheta, R. Świsłocka, S. Orzechowska, M. Akimowicz, R. Choińska, W. Lewandowski, Recent developments in effective antioxidants: the structure and antioxidant properties, *Materials (Basel)*. 14 (2021) 1984, <https://doi.org/10.3390/ma14081984>.
- M. Spiegel, Current trends in computational quantum chemistry studies on antioxidant radical scavenging activity, *J. Chem. Inf. Model.* 62 (2022) 2639–2658, <https://doi.org/10.1021/acs.jcim.2c00104>.
- Y. Pan, R. Qin, M. Hou, J. Xue, M. Zhou, L. Xu, Y. Zhang, The interactions of polyphenols with Fe and their application in Fenton/Fenton-like reactions, *Sep. Purif. Technol.* 300 (2022), 121831, <https://doi.org/10.1016/j.seppur.2022.121831>.
- M. Wang, J. Firman, L.S. Liu, K. Yam, A review on flavonoid apigenin: dietary intake, ADME, antimicrobial effects, and interactions with human gut microbiota, *Biomed. Res. Int.* 2019 (2019), <https://doi.org/10.1155/2019/7010467>.
- B. Salehi, A. Venditti, M. Sharifi-Rad, D. Kregiel, J. Sharifi-Rad, A. Durazzo, M. Lucarini, A. Santini, E.B. Souto, E. Novellino, H. Antolak, E. Azzini, W.N. Setzer, N. Martins, The therapeutic potential of Apigenin, *Int. J. Mol. Sci.* 20 (2019) 1305, <https://doi.org/10.3390/ijms20061305>.
- E. Klein, J. Rimarčík, E. Senajová, A. Vagánek, J. Lengyel, Deprotonation of flavonoids severely alters the thermodynamics of the hydrogen atom transfer, *Comput. Theor. Chem.* 1085 (2016) 7–17, <https://doi.org/10.1016/j.comptc.2016.04.004>.
- A. Vagánek, J. Rimarčík, K. Dropková, J. Lengyel, E. Klein, Reaction enthalpies of OH bonds splitting-off in flavonoids: the role of non-polar and polar solvent, *Comput. Theor. Chem.* 1050 (2014) 31–38, <https://doi.org/10.1016/j.comptc.2014.10.020>.
- Z. Sroka, B. Zbikowska, J. Hładyszowski, The antiradical activity of some selected flavones and flavonols. Experimental and quantum mechanical study, *J. Mol. Model.* 21 (2015) 307, <https://doi.org/10.1007/s00894-015-2848-1>.
- H.M. Ali, I.H. Ali, Structure-antioxidant activity relationships, QSAR, DFT calculation, and mechanisms of flavones and flavonols, *Med. Chem. Res.* 28 (2019) 2262–2269, <https://doi.org/10.1007/s00044-019-02452-z>.
- P. Zúvela, J. David, X. Yang, D. Huang, M.W. Wong, Non-linear quantitative structure-activity relationships modelling, mechanistic study and in-silico design of flavonoids as potent antioxidants, *Int. J. Mol. Sci.* 20 (2019) 1–20, <https://doi.org/10.3390/ijms20092328>.
- Y.-Z. Zheng, G. Deng, R. Guo, Z.-M.M. Fu, D.-F.F. Chen, The influence of the H5--O[dbnd]C4 intramolecular hydrogen-bond (IHB) on the antioxidative activity of flavonoid, *Phytochemistry*. 160 (2019) 19–24, <https://doi.org/10.1016/j.phytochem.2019.01.011>.
- M. Spiegel, T. Andrioniów, Z. Sroka, Flavones' and flavonols' antiradical structure-activity relationship—a quantum chemical study, *Antioxidants*. 9 (2020) 461, <https://doi.org/10.3390/antiox9060461>.
- Y.Z. Zheng, G. Deng, D.F. Chen, R. Guo, R.C. Lai, The influence of C2[dbnd]C3 double bond on the antiradical activity of flavonoid: different mechanisms analysis, *Phytochemistry*. 157 (2019) 1–7, <https://doi.org/10.1016/j.phytochem.2018.10.015>.
- Y.-Z. Zheng, Y. Zhou, Q. Liang, D.-F. Chen, R. Guo, C.-L. Xiong, X.-J. Xu, Z.-N. Zhang, Z.-J. Huang, Solvent effects on the intramolecular hydrogen-bond and anti-oxidative properties of apigenin: a DFT approach, *Dyes Pigments* 141 (2017) 179–187, <https://doi.org/10.1016/j.dyepig.2017.02.021>.
- M. Leopoldini, I. Prieto Pitarch, N. Russo, M. Toscano, Structure, conformation, and electronic properties of apigenin, luteolin, and taxifolin antioxidants. A first principle theoretical study, *J. Phys. Chem. A* 108 (2004) 92–96, <https://doi.org/10.1021/jp035901j>.
- Y.-Z. Zheng, D.-F.F. Chen, G. Deng, R. Guo, The substituent effect on the radical scavenging activity of Apigenin, *Molecules*. 23 (2018) 1989, <https://doi.org/10.3390/molecules23081989>.
- A. Vázquez-Espinal, O. Yañez, E. Osorio, C. Areche, O. García-Beltrán, L.M. Ruiz, B. K. Cassels, W. Tiznado, Theoretical study of the antioxidant activity of quercetin oxidation products, *Front. Chem.* 7 (2019) 1–10, <https://doi.org/10.3389/fchem.2019.00818>.
- R. Castañeda-Arriaga, T. Marino, N. Russo, J.R. Alvarez-Idaboy, A. Galano, Chalcogen effects on the primary antioxidant activity of chrysin and quercetin, *New J. Chem.* 44 (2020) 9073–9082, <https://doi.org/10.1039/d0nj01795g>.
- J.M. Dimitrić Marković, D. Milenković, D. Amić, M. Mojović, I. Pašti, Z. S. Marković, The preferred radical scavenging mechanisms of fisetin and baicalein towards oxygen-centred radicals in polar protic and polar aprotic solvents, *RSC Adv.* 4 (2014) 32228–32236, <https://doi.org/10.1039/c4ra02577f>.
- M. Spiegel, A. Gamian, Z. Sroka, A statistically supported antioxidant activity DFT benchmark—the effects of Hartree-Fock exchange and basis set selection on accuracy and resources uptake, *Molecules*. 26 (2021) 5058, <https://doi.org/10.3390/molecules26165058>.
- M. Biela, J. Rimarčík, E. Senajová, A. Kleinová, E. Klein, Antioxidant action of deprotonated flavonoids: thermodynamics of sequential proton-loss electron-transfer, *Phytochemistry*. 180 (2020), <https://doi.org/10.1016/j.phytochem.2020.112528>.
- M.E. Alberto, N. Russo, A. Grand, A. Galano, A physicochemical examination of the free radical scavenging activity of Trolox: mechanism, kinetics and influence of the environment, *Phys. Chem. Chem. Phys.* 15 (2013) 4642, <https://doi.org/10.1039/c3cp43319f>.
- M.E. Medina, C. Iuga, J.R. Álvarez-Idaboy, Antioxidant activity of fraxetin and its regeneration in aqueous media. A density functional theory study, *RSC Adv.* 4 (2014) 52920–52932, <https://doi.org/10.1039/C4RA08394F>.
- A. Galano, D.X. Tan, R.J. Reiter, On the free radical scavenging activities of melatonin's metabolites, AFMK and AMK, *J. Pineal Res.* 54 (2013) 245–257, <https://doi.org/10.1111/jpi.12010>.
- M. Spiegel, T. Marino, M. Prejanó, N. Russo, On the scavenging ability of Scutellarein against the OOH radical in water and lipid-like environments: a theoretical study, *Antioxidants*. 11 (2022) 224, <https://doi.org/10.3390/antiox11020224>.
- M. Spiegel, T. Marino, M. Prejanó, N. Russo, Antioxidant and copper chelating power of new molecules proposed as combined multiple targets agent against Alzheimer's disease. A theoretical insights, *Phys. Chem. Chem. Phys.* 24 (2022) 16353–16359, <https://doi.org/10.1039/d2cp01918c>.
- A. Parise, B.C. De Simone, T. Marino, M. Toscano, N. Russo, Quantum mechanical predictions of the antioxidant capability of moracin C isomers, *Front. Chem.* 9 (2021) 1–9, <https://doi.org/10.3389/fchem.2021.666647>.

- [39] B.H.J. Bielski, D.E. Cabelli, R.L. Arudi, A.B. Ross, Reactivity of HO₂ / O₂ - 2 radicals in aqueous solution, *J. Phys. Chem. Ref. Data* 14 (1985) 1041–1100, <https://doi.org/10.1063/1.555739>.
- [40] T.E.A. Ardjani, J.R. Alvarez-Idaboy, Radical scavenging activity of ascorbic acid analogs: kinetics and mechanisms, *Theor. Chem. Accounts* 137 (2018), <https://doi.org/10.1007/s00214-018-2252-x>.
- [41] I. Persson, P. Persson, M. Sandström, A.-S. Ullström, Structure of Jahn-Teller distorted solvated copper(II) ions in solution, and in solids with apparently regular octahedral coordination geometry, *J. Chem. Soc. Dalton Trans.* (2002) 1256, <https://doi.org/10.1039/b200698g>.
- [42] M.J. Frisch, G.W. Trucks, H.B. Schlegel, G.E. Scuseria, M.A. Robb, J.R. Cheeseman, G. Scalmani, V. Barone, G.A. Petersson, H. Nakatsuji, Gaussian 16, Inc., Wallingford CT 2016, 2016.
- [43] A. Galano, J.R. Alvarez-Idaboy, A computational methodology for accurate predictions of rate constants in solution: application to the assessment of primary antioxidant activity, *J. Comput. Chem.* 34 (2013) 2430–2445, <https://doi.org/10.1002/jcc.23409>.
- [44] Y. Zhao, N.E. Schultz, D.G. Truhlar, Design of density functionals by combining the method of constraint satisfaction with parametrization for thermochemistry, thermochemical kinetics, and noncovalent interactions, *J. Chem. Theory Comput.* 2 (2006) 364–382, <https://doi.org/10.1021/ct0502763>.
- [45] T. Clark, J. Chandrasekhar, G.W. Spitznagel, P.V.R. Schleyer, Efficient diffuse function-augmented basis sets for anion calculations. III. The 3-21+G basis set for first-row elements, Li–F, *J. Comput. Chem.* 4 (1983) 294–301, <https://doi.org/10.1002/jcc.540040303>.
- [46] R. Krishnan, J.S. Binkley, R. Seeger, J.A. Pople, Self-consistent molecular orbital methods. XX. A basis set for correlated wave functions, *J. Chem. Phys.* 72 (1980) 650–654, <https://doi.org/10.1063/1.438955>.
- [47] A.V. Marenich, C.J. Cramer, D.G. Truhlar, Universal solvation model based on solute electron density and on a continuum model of the solvent defined by the bulk dielectric constant and atomic surface tensions, *J. Phys. Chem. B* 113 (2009) 6378–6396, <https://doi.org/10.1021/jp810292n>.
- [48] A. Galano, A. Pérez-González, R. Castañeda-Arriaga, L. Muñoz-Rugeles, G. Mendoza-Sarmiento, A. Romero-Silva, A. Ibarra-Escutia, A.M. Rebollar-Zepeda, J.R. León-Carmona, M.A. Hernández-Olivares, J.R. Alvarez-Idaboy, Empirically fitted parameters for calculating pKa values with small deviations from experiments using a simple computational strategy, *J. Chem. Inf. Model.* 56 (2016) 1714–1724, <https://doi.org/10.1021/acs.jcim.6b00310>.
- [49] J.R. León-Carmona, A. Galano, J.R. Alvarez-Idaboy, Deprotonation routes of anthocyanidins in aqueous solution, pKa values, and speciation under physiological conditions, *RSC Adv.* 6 (2016) 53421–53429, <https://doi.org/10.1039/C6RA10818K>.
- [50] Z. Marković, J. Tošović, D. Milenković, S. Marković, Revisiting the solvation enthalpies and free energies of the proton and electron in various solvents, *Comput. Theor. Chem.* 1077 (2016) 11–17, <https://doi.org/10.1016/j.comptc.2015.09.007>.
- [51] D.G. Truhlar, B.C. Garrett, S.J. Klippenstein, Current status of transition-state theory, *J. Phys. Chem.* 100 (1996) 12771–12800, <https://doi.org/10.1021/jp953748q>.
- [52] R.A. Marcus, On the theory of oxidation-reduction reactions involving Electron transfer. III. Applications to data on the rates of organic redox reactions, *J. Chem. Phys.* 26 (1957) 872–877, <https://doi.org/10.1063/1.1743424>.
- [53] F.C. Collins, G.E. Kimball, Diffusion-controlled reaction rates, *J. Colloid Sci.* 4 (1949) 425–437, [https://doi.org/10.1016/0095-8522\(49\)90023-9](https://doi.org/10.1016/0095-8522(49)90023-9).
- [54] Y. Zhao, N.E. Schultz, D.G. Truhlar, Exchange-correlation functional with broad accuracy for metallic and nonmetallic compounds, kinetics, and noncovalent interactions, *J. Chem. Phys.* 123 (2005), 161103, <https://doi.org/10.1063/1.2126975>.
- [55] M. Dolg, U. Wedig, H. Stoll, H. Preuss, Energy-adjusted a b i n i t i o pseudopotentials for the first row transition elements, *J. Chem. Phys.* 86 (1987) 866–872, <https://doi.org/10.1063/1.452288>.
- [56] J.M.L. Martin, A. Sundermann, Correlation consistent valence basis sets for use with the Stuttgart–Dresden–Bonn relativistic effective core potentials: the atoms Ga–Kr and in–Xe, *J. Chem. Phys.* 114 (2001) 3408–3420, <https://doi.org/10.1063/1.1337864>.
- [57] H. Cao, J.M. Pauff, R. Hille, X-ray crystal structure of a xanthine oxidase complex with the flavonoid inhibitor quercetin, *J. Nat. Prod.* 77 (2014) 1693–1699, <https://doi.org/10.1021/np500320g>.
- [58] O. Trott, A.J. Olson, AutoDock Vina: improving the speed and accuracy of docking with a new scoring function, efficient optimization, and multithreading, *J. Comput. Chem.* (2009), <https://doi.org/10.1002/jcc.21334>. NA-NA.

i. Oświadczenia współautorów

Wrocław, 14.04.2023

mgr farm. Maciej Spiegel
Katedra i Zakład Farmakognozji i Leku Roślinnego
Uniwersytet Medyczny im. Piastów Śląskich we Wrocławiu

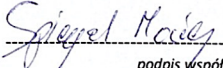
OŚWIADCZENIE WSPÓŁAUTORA
CO-AUTHORSHIP STATEMENT

Jako współautor pracy:
As a co-author of the research paper:


Spiegel, M., & Sroka, Z. (2023).
Quantum-mechanical characteristics of apigenin: Antiradical, metal chelation and inhibitory properties in physiologically relevant media
Fitoterapia, 164(October 2022), 105352.

oświadczam, że mój udział polegał na:
I declare that my contribution consists of:

- sformułowaniu i ewolucji nadrzędnych celów i zadań badawczych
formulation and evolution of overarching research goals and aims
- rozwoju i zaprojektowaniu metodologii
development and design of methodology
- weryfikacji ogólnej odtwarzalności wyników badań
verification of the overall reproducibility of research outputs
- zastosowaniu technik matematycznych i obliczeniowych do analizy oraz syntezy danych z badań
application of mathematical and computational techniques to analyse and synthesize study data
- przeprowadzeniu procesu badawczego i dochodzeniowego oraz zbieraniu danych
conducting a research and investigation process & data collection
- zapewnieniu zasobów obliczeniowych
provision of computing resources
- wykonywaniu działań mających na celu organizację danych badawczych
performing activities to maintain research data
- przygotowaniu i stworzeniu opublikowanej pracy, w szczególności wizualizacji i prezentacji danych
preparation and creation of the published work, specifically visualization & data presentation.
- przygotowaniu i stworzeniu opublikowanej pracy, w szczególności napisanie jej wstępnego szkicu
preparation and creation of the published work, specifically writing the initial draft
- przygotowaniu i stworzeniu opublikowanej, w szczególności naniesieniu korekt
preparation and creation of the published work, specifically revision



podpis współautora
(co-author's signature)

Uniwersytet Medyczny we Wrocławiu
KATEDRA I ZAKŁAD FARMAKOGNOZJI I LEKU ROŚLINNEGO
I LEKU ROŚLINNEGO

prof. dr hab. Zbigniew Sroka
(2)

Wrocław, 18.04.2023
miejsowość, data
(place, date)

prof. dr hab. Zbigniew Sroka
tytuł, imię i nazwisko
(title, name and surname)

Katedra i Zakład Farmakognozji i Leku Roślinnego
Uniwersytet Medyczny im. Piastów Śląskich we Wrocławiu
miejsce zatrudnienia
(affiliation)

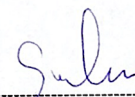
OŚWIADCZENIE WSPÓŁAUTORA CO-AUTHORSHIP STATEMENT

Jako współautor pracy:
As a co-author of the research paper:

Spiegel, M., & Sroka, Z. (2023).
Quantum-mechanical characteristics of apigenin: Antiradical, metal chelation and inhibitory properties in physiologically relevant media
Fitoterapia, 164(October 2022), 105352.

oświadczam, że mój udział polegał na:
I declare that my contribution consists of:

- pozyskaniu wsparcia finansowego na projekt prowadzący do tej publikacji
acquisition of the financial support for the project leading to this publication
- odpowiedzialność za zarządzanie i koordynację w zakresie planowania i realizacji działań badawczych
management and coordination responsibility for the research activity planning and execution



podpis współautora
(co-author's signature)

Uniwersytet Medyczny we Wrocławiu
KATEDRA I ZAKŁAD FARMAKOGNOZJI
I LEKU ROŚLINNEGO

podpis promotora
prof. dr hab. Zbigniew Sroka
(2)

IV. Publikacja [D]

June 13, 2022 Volume 62, Issue 11 pubs.acs.org/jcim

JCIM

JOURNAL OF CHEMICAL INFORMATION AND MODELING

Fukui functions

redox potential

electron and hydrogen donation properties

frontier molecular orbitals

intrinsic reactivity indices

solvation model

antioxidants

2022

molecular dynamics

dissociation constant

TOPOLOGY

QTAIM

NBO

basis set

functional

thermochemistry

kinetics

spin contamination

REACTIVITY

Current Trends in Computational Quantum Chemistry Studies on Antioxidant Radical Scavenging Activity

Maciej Spiegel*

 Cite This: *J. Chem. Inf. Model.* 2022, 62, 2639–2658

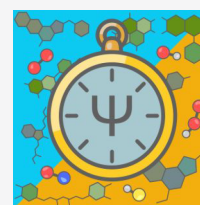
Read Online

ACCESS |

Metrics & More

Article Recommendations

ABSTRACT: The antioxidative nature of chemicals is now routinely studied using computational quantum chemistry. Scientists are constantly proposing new approaches to investigate those methods, and the subject is evolving at a rapid pace. The goal of this review is to collect, consolidate, and present current trends in a clear, methodical, and reference-rich manner. This paper is divided into several sections, each of which corresponds to a different stage of elaborations: preliminary concerns, electronic structure analysis, and general reactivity (thermochemistry and kinetics). The sections are further subdivided based on methodologies used. Concluding remarks and future perspectives are presented based on the remaining elements.



KEYWORDS: Antioxidants, density functional theory, computational chemistry, electronic structure, weak interactions, kinetics, thermochemistry, QM-ORSA

INTRODUCTION

Free radicals play a crucial role in the maintenance of homeostasis by participating in a range of physiologically relevant processes such as immune response and intracellular communication. Nonetheless, whatever the case may be, their uncontrolled accumulation is not favorable. The energy they possess as a due to the unpaired electron on the valence shell or excited state cannot be efficiently neutralized by intracellular antioxidant defense system and is instead transferred to the biologically important targets like lipids, carbohydrates, proteins, and DNA strains. In consequence, these structures degenerate, leading to the development of severe malfunctions resulting in illness such as diabetes, atherosclerosis, Alzheimer's and Parkinson's diseases, or tumor growth.^{1,2}

The expanding awareness of the dual nature of radicals has prompted a surge in interest in compounds that can decrease elevated levels of reactive oxygen, nitrogen, and sulfur species, thereby preventing their harmful activity. These substances, known as *antioxidants*, are a heterogeneous group of molecules able to reduce oxidative stress in different ways. They are classified as follows³

- Type I: chain breakers, which interact directly with radicals by creating species that are more stable and less hazardous to cells than the former ones, thus terminating chain reactions and preventing oxidation of biological targets.
- Type II: preventers, for which, however, a unified mechanism of action is not specified, but it does not include interactions with radicals. Among known activities of that type are metal chelation, particularly iron and copper, which participate in the Fenton reaction,

as well as regulation of enzymes responsible for radical formation or those directly involved in oxidative stress development.^{1,2,4} Compounds capable of regenerating biological antioxidants¹ or absorbing UV radiation⁵ are also included in this category.

- Type III: substances that effectively repair oxidatively damaged biomolecules.¹

However, because most antioxidants exhibit multiple types of activity at the same time, such categorization is often artificial. It is better to do so on the basis of their chemical structure or origin.

Phytochemicals are plant-derived compounds that are plentiful in many herbs and commonly consumed plants such as beetroot, high in betalains;⁶ tea, rich in catechins;⁷ or grapefruit, abundant in flavanols.⁸ This family can be further subdivided into flavonoids,^{9,10,19–28,11,29–37,12–18} phenolic acids,^{38–47} lignans,⁴⁸ aurones,⁴⁹ chalcones,^{49–51} curcuminoids,^{52,53} anthocyanidins,^{54–56} stilbenoids,^{28,57–59} anthraquinones,^{60–63} glucosinolates,^{64,65} alkaloids,^{66,67} coumarins,⁶⁸ terpenes and terpenoids,^{68–72} and others^{41,73,82–86,74–81} (Figure 1), all of them being extensively studied with computational quantum chemistry methods, as evidenced by the number of recent scientific findings. Albeit, plants are not the

Received: January 25, 2022

Published: April 18, 2022



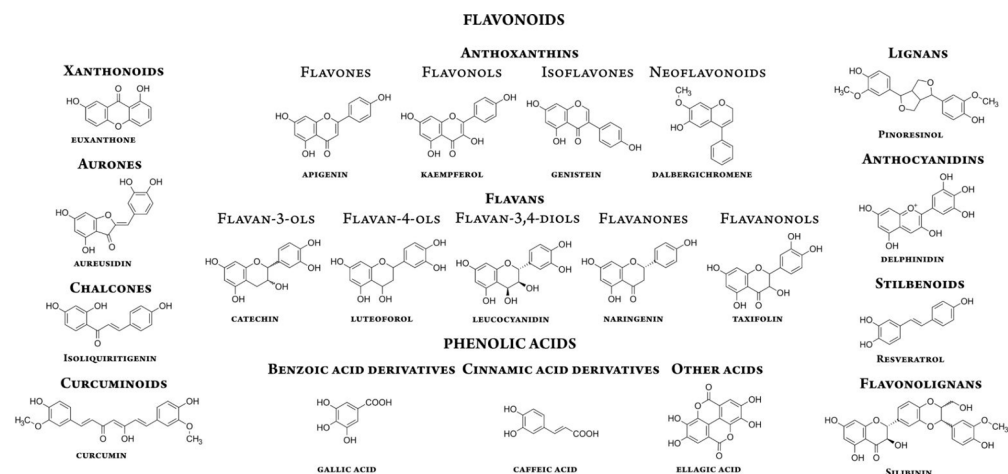


Figure 1. Some of the most commonly distinguished subtypes of dietary antioxidants and their representative examples.

only source of antioxidants —substances with promising antiradical activities have also been found among common drugs,^{87–92} biological substances,^{93–102} and their metabolites.^{59,93,98,100,103–105} All of the listed substances are being heavily modified in an effort to identify derivatives with an improved safety profile and enhanced radical scavenging potential.^{23,36,102,106–114,46,115–124,83,125,86,87,89,94,96,101}

Finally, completely novel structures are proposed and investigated on the basis of recognized pharmacophores: phenolic units,^{126–132} five-heterocyclic rings,^{133–139} quinoline backbones,^{140–142} and other moieties.^{143–146} Importantly, despite their diversity, chain breakers share similar reactivity patterns and mechanisms, allowing common theoretical approaches to be used to study any of them.

This review outlines current trends in “Type I” activity research in a straightforward and methodical manner. The first section deals with preliminary concerns, such as selecting the appropriate level of theory, the solvation model, and the initial structures. Following that, the topic of electronic structure examination is discussed in light of the methodologies documented in the literature. The majority of this work is devoted to thermochemistry and kinetics research, which are the most important for comparing computationally produced results with experimental data. Finally, remaining issues are highlighted and perspectives on the subject provided.

Before proceeding, it is important to note that while this review specifically mentions hydroxyl groups any other residue in which a hydrogen atom is bonded to a highly electronegative atom, such as nitrogen in an amino group or sulfur in a thiol group, can also be considered as the one that may participate in antioxidative activity.⁴⁶

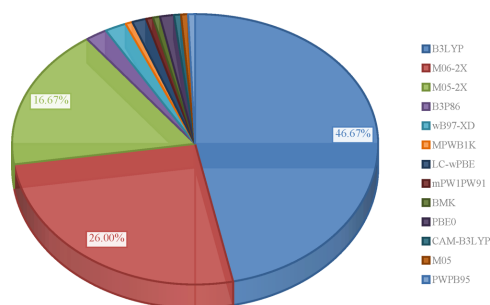
■ PRELIMINARY CONCERNS

The level of theory chosen, which describes the electronic structure of the molecule *as itself*, and the solvation model, which adjusts the system’s electron density cloud to minor perturbations caused by solvent molecules, are two key components influencing chemical behavior that must be taken into account from the beginning of the studies.

Functional and Basis Set. It is frequently advantageous to obtain results that precisely resemble experimental data while needing the least amount of computational time. However, this seemingly easy task is burdened with two fundamental issues: (1) With so many functionals and basis sets available, choosing a level of theory satisfying this condition is difficult. (2) The lack of reference data against which theoretical findings may be compared casts doubt on the latter. Although high-end methods such as CCSD(T)/CBS guarantee quality of the outcomes, this solution is inapplicable for routine computations due to the significant uptake of resources.

As shown in **Chart 1**, there is currently a trend toward the use of density functional theory (DFT) methods, with B3LYP^{147,148}

Chart 1. Share of Functionals in Articles Published in the Last Five Years⁴⁴



⁴⁴Plotted on the basis of refs 9–146.

(~47%), M06-2X¹⁴⁹ (~26%), and M05-2X¹⁵⁰ (~17%) being picked the most commonly. Restricting to any of them is advantageous because it provides researcher a plethora of datapoints the comparison with validate the results in a greater degree than it would happen if it was done against outcomes obtained by completely differently constructed functional.

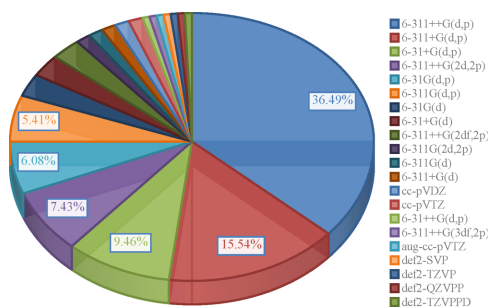
Moreover, other researchers following the given reasoning would more likely cite the paper that use common level of theory since it enables to compare their own theoretical results with those provided by other researchers.

Given their newness, it is visible that these two Minnesota functionals are gradually displacing B3LYP since their release. This could be a result of their superior performance in estimating thermochemistry, kinetic and noncovalent interactions of nonmetal elements, as well as energies of reactions involving free radicals, which they predict extremely close to actual data, as claimed by the developers^{149–151} and continue to be substantiated by independent scientists, either in the course of original research^{39–41,45,77,84,87,129} or in benchmarks.^{152–154} On the other hand, several researchers who used both B3LYP and one of Truhlar's global hybrids noted that while B3LYP tends to underestimate energies there are no substantial differences and the reactivity patterns hold when the same basis set is used.^{60,64,95,123,127}

Although the reasons for selecting certain functional are usually covered in the manuscript with details, the arguments for choosing "this, but not that" basis set are nearly always glossed over. This bad habit have its consequences in the performance of computations. Increasing the number of basis functions is known to increase task processing time, and it has recently been established that those from the Dunning's and Ahlrich's families are particularly vulnerable.¹⁵³ Furthermore, whereas functionals should be kept constant throughout the research, the basis set does not, namely while one can be used for electronic structure investigations, other may be applied for thermochemistry, which allows maneuvering them in order to obtain the best results at the lowest possible cost.

As a result, Chart 2, which depicts the percentage of basis sets used for thermochemistry computations, is much more divided

Chart 2. Share of Basis Sets in Articles Published in the Last Five Years^a



^aPlotted on the basis of refs 9–146.

than the previous one, with Pople's leading the way. A particularly good observation is that combining any of them with one of the three most commonly employed functionals presented in Chart 1, appears to have a little influence on the results as evidenced in the following examples. The findings of Shammera Ahmed et al.⁷⁹ (B3LYP and M062X combined with either 6-31+G(d,p) or 6-311++G(d,p)) and Mendes et al.¹² (B3LYP, LC-wPBE, M062X, and BMK in 6-311G(d,p) and 6-311+G(d,p) bases) show that despite the augmentation of basis set with another diffuse function or inclusion of next function

describing valence shell, the values of reactivity indices found in the gas phase change only slightly, regardless of level of theory used. In their other study,²⁶ the authors demonstrated that shifting from 6-311G(d,p) to 6-311+G(d,p) changed the ionization potential values by less than 4 kcal/mol independently of the environment (gas phase, water, methanol, ethanol, *n*-hexane). Similar results were observed in the investigations of Bakir et al.¹⁴⁶ (B3LYP/6-31G(d,p) and B3LYP/6-311++G(2d,2p)) and Santos et al.⁶⁰ (B3LYP/6-31+G(d,p), B3LYP/6-31++G(d,p) and B3LYP/6-311+G(d,p)), both of which were conducted in gas and water. On the other hand, the differences in ionization potential and electron transfer energy associated with ion formation in water milieu were found to be significantly smaller in the case of B3LYP/6-311++G(d,p) outcomes when compared to those obtained at B3LYP/6-31+G(d,p) level of theory.⁷⁹

Moreover, although the presence of polarization functions is undeniably important for determining the energy of highly polarized bonds, the role diffusion functions, which are widely regarded as necessary for accurately modeling electron clouds in ionic systems and radical involving pathways, must be addressed more thoroughly. Still, the recent research¹⁵³ has shed new light on that issue for it was discovered that using 6-311G(d,p) for overall antioxidant studies produces the best results in terms of both the accuracy between theoretical outcomes and experimental values, as well as computational resource uptake. Further confirmation on that indulging issue and more detailed studies on the role of the basis set are welcome.

It is worth noting that open shell computations are hampered by the possibility of spin contamination.¹⁵⁵ This is because the resulting wave function is an artificial mix of spin states rather than an eigenfunction of total spin, $\langle S^2 \rangle$. In an ideal system, $\langle S^2 \rangle$ equals 0.75 for singlet and 2.0 for triplet

$$\langle S^2 \rangle = s(s + 1) \quad (1)$$

where s denotes the number of unpaired electrons divided by half. Other values are acceptable as long as they deviate by no more than 10%.^{10,109,152} Greater ones indicate the presence of higher spin states, which may alter the energy or geometry, just like the population analysis outcomes, resulting in biased conclusions; such structures should not be considered for future research. Spin-restricted open shell computations may be a solution in those cases, but they consume more resources than unrestricted ones and may still produce incorrect energies of unpaired electrons due to the absence of dynamical correlation caused by the vanishing of spin polarization.

Solvation Model. The physiological media in which antioxidants play fundamental biological roles are body fluids and the lipid bilayer of cells membrane. As a consequence, most experiments are conducted in water or in a nonpolar environment, that computational elaborations must account for. The effect of a polar solvent is a fundamental tenet of theoretical investigations because it distorts a molecule's electron cloud due to electrostatic polarization interactions, affecting the shape of the potential energy surface and chemical activity.^{3,20,28,130,156} Furthermore, if the reaction pathway involves proton or electron detachment, the solvation is a known to be a driving force that eases the process and makes it more feasible than it would be in a nonpolar medium.^{50,116} That is why it is also important for properly modeling dissociation related processes as is stressed later in the text.

For the time being, three methods are employed to incorporate solvent effects: implicit (through a homogeneously

polarizable medium), explicit (by solvent molecules), and a combination of these two. The integral equation formalism variation of the polarizable continuum model (IEFPCM, often referred to as just PCM),¹⁵⁷ conductor-like polarizable continuum model (CPCM),^{158,159} and solvation model based on density (SMD)¹⁶⁰ are examples of continuous solvation models that are implemented in a majority of quantum chemistry software. They are also the most frequently used because they are burdened with a much lower computing cost than implicit or combined approach.

However, the fundamental disadvantage of implicit models is complete negation of intermolecular hydrogen bonds, which are often essential for proper simulation of antiradical activity^{93,103,144} especially when abundant as in the case of capsaicin.⁸⁴ A mutual competition between intramolecular and intermolecular hydrogen bonds is also observed as a relevant factor modulating hydrogen atom transfer proclivity.⁴⁷ The modeling of •OH and •OOH radicals, which are of primary interest in antioxidants research, is an excellent example of how the explicit water molecules can influence the results as well. Accordingly to Pérez-González and Galano,¹²⁵ adding the first water molecule considerably changed the rate constants of the •OH/•OOH path, but adding more or repeating the procedure for the •OOH/•OOH path resulted in no significant change. The fact that their charge is concentrated on a single exposed heteroatom¹⁶¹ is important here.

The application of a homogeneously polarizable medium is a particularly viable method of modeling solvents having large structures. For example, representing the enormous membrane lipid chains would be a time-consuming and inefficient effort. Instead, one of the most common approaches found in the literature is to do that implicitly, by using the largest available aprotic solute, for example, pentyl ethanoate.^{12,100,107,120,132} T_0 account for the cage effect, which manifests as the loss of entropy of any chemical reaction with a molecularity of two or greater, and improve results, the Okuno's corrections¹⁶² and Benson's free volume theory¹⁶³ can be applied (eq 2), as demonstrated.^{40,41,104} The corrected Gibbs free energy, $\Delta G_{\text{sol}}^{\text{FV}}$ is expressed then in a form of

$$\Delta G_{\text{sol}}^{\text{FV}} = \Delta G_{\text{sol}}^0 - RT \{ \ln [n10^{(2n-2)}] - (n-1) \} \quad (2)$$

where n represents the molecularity of the reaction, and ΔG_{sol}^0 is a Gibbs free energy in solvent, R a gaseous constant, and T the temperature.¹⁶⁴

Initial Structure. Let's refer to a thorough conformational studies^{156,165} that were performed on a collection of quercetin structures with variable planarity and intramolecular hydrogen bond counts. These two structural features are known to account for antioxidative activity of flavonoids, and so considerable differences have been found among them. This is not the only case, for similar geometry–activity relationships have been pinpointed also in other studies.^{60,91,107,134} This emphasizes the role of selecting the appropriate conformer for the study as a critical first step in theoretical elaborations.

Molecular dynamics (MD) simulations are most effective for producing excellent starting structures. Different approaches can be undertaken to run MD calculations, such as using software that has implemented molecular mechanic potentials and thus allows for the direct conformational search procedure^{166–168} or dedicated ones designed for more demanding studies, like GROMACS,¹⁶⁹ Amber,¹⁷⁰ or CHARMM,¹⁷¹ for which the molecule under consideration must first be parametrized. This

can be done with either the proposed protocols⁸⁴ or available webservices the most well recognized of which is probably CharmmGUI,¹⁷² although AutomatedTopologyBuilder (ATB)¹⁷³ should also be mentioned.

CharmmGUI has an advantage over ATB in that it has a user-friendly interface and instantly generates a complete set of files that can be submitted for molecular dynamics, whereas ATB only produces force field, structure, and topology data, leaving the user to prepare the remaining files. CharmmGUI, on the other hand, predicts topology using CGenFF,¹⁷⁴ which elucidates it through bond perception and atom typing, while ATB processes input using DFT or semiempirical techniques depending on the size of the system. After all, it is the user's expertise that determines which path to take.

MD frequently generates a large number of molecules, whilst upcoming quantum chemical studies should only consider the most populated states. One of the first filters used to get rid of the undesired structures is the geometric clustering algorithm¹⁷⁵ which, in simple terms, groups conformers based on their structure or kinetics. If there are multiples of them, optimization at the appropriate level of theory followed by Maxwell–Boltzmann distribution analysis may be a viable approach for removing superfluous structures, particularly those with molar fractions less than 0.1%. This threshold is proposed^{46,101,112} because a small energy difference between conformers could indicate an interconversion process: rotatability of OH groups¹⁶⁵ or side chains,⁸⁴ bonds deformation due to keto–enol tautomerism,²¹ shift in E/Z-conformers equilibria,¹³³ and bending of dihedral angles.^{16,20,28,33,50,67,128,165} They can all modulate hydrogen bonds, electrons cloud delocalization, and polarizability, as well as radical accessibility to specific sites of an antioxidant. Furthermore, the molar fraction cannot be too low if the compound is desired to pass biological barriers.⁴⁶

Two equations (eqs 3 and 4) can be used to evaluate the Maxwell–Boltzmann population f of a specific conformer i , in the set of n conformers

$$f_i = \frac{\exp\left(\frac{-G_{i(\text{aq})}}{RT}\right)}{\sum_{i=1}^n \exp\left(\frac{-G_{i(\text{aq})}}{RT}\right)} \text{ for } i = 1, 2, \dots, n \quad (3)$$

and

$$\sum_{i=1}^n f_i = 1 \quad (4)$$

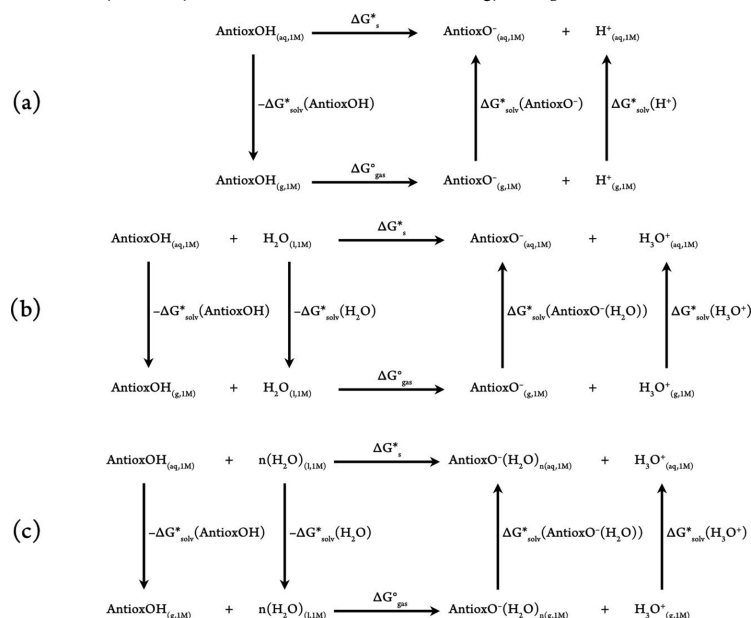
where R is the gas constant, and T is the temperature. $G_{i(\text{aq})}$, the aqueous phase Gibbs free energy of the i th conformer, can be calculated following eq 5

$$G_{i(\text{aq})} = G_i^\circ + \Delta G^{\text{latm} \rightarrow 1\text{M}} + \Delta G_i^* \quad (5)$$

where G_i° denotes a species' gas phase free energy at a given temperature, $\Delta G^{\text{latm} \rightarrow 1\text{M}} = 1.89$ kcal/mol and reflects the shift in standard state from 1 atm (superscripted with °) to 1 M (superscripted with *), and ΔG_i^* denotes a species' aqueous solvation free energy.

Deprotonation and Dissociation Constants. The primary activity of type I antioxidants is based on their reductant capacity, which is frequently, but not always^{64,68,125} linked to the hydrogen-donation capacity from one of their aromatic hydroxyl groups; thus, a simple conclusion can be drawn that the more of them, the greater shall be participation of hydrogen-related channels in overall radical scavenging, and so its viability.¹¹⁶

Scheme 1. Various Thermodynamic Cycles Used to Calculate the Free Energy of Deprotonation



However, because these residues are also weakly acidic, multiple species can coexist in a water environment at the same time. Their molar fraction is governed both internally by their chemical structure⁸² and externally by the pH of an environment.

If radicals are neutralized by mechanisms inaccessible to other forms, a seemingly small amount of one of them may be critical in accurately measuring scavenging activity. At the given pH, for example, it is possible that the antioxidants have already deprotonated all of the hydroxyl groups and thus exhibit only electron-related channels,^{36,85,102,126} whereas the studied radical is efficiently neutralized solely by formal hydrogen atom transfer. Similarly, with each subsequent dissociation, species are less likely to remove another proton, making routes that include its donation, e.g. sequential proton-loss electron transfer or sequential electron transfer-proton transfer, more energetically demanding; on the other hand, electron-donating processes are expected to occur more easily for them.

There are several methods that can be used to estimate dissociation constants and deprotonation pathways. The oldest ones, such as *direct*, *proton exchange*, *hybrid cluster continuum*, and *implicit-explicit*, rely on thermodynamic cycles and have previously been exhaustively discussed in the literature^{176,177} and are thus just briefly mentioned here.

In the *direct* approach, an antioxidant may either (a) adhere to the Arrhenius theory and dissociate directly into anion and proton (Scheme 1a), (b) obey Brønsted–Lowry acid–base theory and react with a water molecule to form conjugated pairs of acid and base (Scheme 1b), or (c) react in the same way as the previous one but in a more sophisticated version in which the formed ion is also solvated by an arbitrary number of water molecules (Scheme 1c).

Regardless of the picked cycle, ΔG_s^* represents the free energy of deprotonation, which is calculated using eq 6

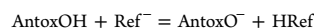
$$\Delta G_s^* = \Delta G_{gas}^* + \sum_{i=1}^{N \text{ products}} n_i \Delta G_{solv}^*(i) - \sum_{j=1}^{N \text{ reactants}} n_j \Delta G_{solv}^*(j) \quad (6)$$

Then, pK_a is determined using a mathematical formula (eq 7)

$$pK_a(\text{AntoxOH}) = \frac{\Delta G_s^*(\text{AntoxOH})}{2.303RT} \quad (7)$$

Despite the fact that one of the major drawbacks for this method is it requires proton or hydronium ion enthalpies, for which theoretical studies do not perfectly match, due to the impact of different solvation models used¹⁷⁸ or methodology,¹⁷⁹ it is still widely used^{27,114,139} owing to its simplicity. The question and recommended values of solvation enthalpies have been extensively elaborated by Marković and coworkers.^{178,180,181}

Another way for determining pH is the *relative method* or *isodesmic method*. It is based on the proton exchange equilibrium between the acid of interest and the conjugated base of the reference acid and is represented by the following general chemical reaction



The acid–base pair of a reference chemical is defined as HRef/Ref[−], and pK_a is computed in the same way as in the direct method but with a modified form of the previously supplied equation, given here as eq 8

$$pK_a(\text{AntoxOH}) = \frac{\Delta G_s^*(\text{AntoxOH})}{RT \ln(10)} + pK_a(\text{HRef}) \quad (8)$$

Although this method has been shown to produce accurate results,^{58,69} it requires HRef to be as structurally close to the HA as possible, and also the knowledge of the experimental value for $pK_a(\text{HRef})$.

Among the newer approaches, the *parameters fitting method*^{182,183} stands out not only due to its much simpler computation protocol but also the accuracy reported in the number of studies that have used it.^{36,41,46,73,85,101,112,126} It employs a linear regression model to determine pK_a values for hydroxyl, carboxylic, amino, and thiol groups in a water solvent. Mathematically, it is expressed by eq 9

$$pK_a(\text{AntoxOH}) = m \Delta G_{\text{AntoxOH}/\text{AntoxO}^-}^* + C \quad (9)$$

where $\Delta G_{\text{AntoxOH}/\text{AntoxO}^-}^*$ denotes the difference in Gibbs free energy between the antioxidant's conjugated base and the corresponding acid, and m and C are empirical parameters available for 20 different functionals, each in one of four Pople's basis sets.

The former, however, is restricted solely to the water solvent. The solution is the *empirical conversion method*¹⁵⁴ presented recently. Although it does not allow for the calculation of pK_a values from scratch, the authors claim that it is useful for converting empirically determined dissociation constants in one solvent to any other with a little error.

Because both, the *parameters fitting method* and the *empirical conversion method*, were developed on strong experimental foundations, combining them in critical situations may not be such a bad idea. However, further testing is required to confirm this.

■ ELECTRONIC STRUCTURE INVESTIGATIONS

Intrinsic Reactivity Indices. A comprehensive study that covers the entire spectrum of antioxidative activity is difficult and time-consuming process. The intrinsic reactivity indices (Table 1) can be evaluated to obtain preliminary data that will guide further steps of the research. Although they do not consider the radical scavenged, the evaluation of preferred reaction paths of isolated species, identification of the most promising ones for a specific goal, and comparisons across antioxidants with similar chemical nature and modes of action is given by them.

Notably, reactivity indices can be calculated vertically or adiabatically, that means with or without orbital relaxation. IP and EA are particularly important in Marcus theory for calculating the activation energy of electron transfer mechanisms and are thus mostly established in this context. The following equations (eq 10 and eq 11) are used to determine their vertical values

$$E_{(N-1)}(g_N) - E_N(g_N) = \text{vertical IP} \quad (10)$$

$$E_{(N)}(g_N) - E_{N+1}(g_N) = \text{vertical EA} \quad (11)$$

The adiabatic ones, on the other hand, are calculated as (eq 12 and eq 13)

$$E_{(N-1)}(g_{N-1}) - E_N(g_N) = \text{adiabatic IP} \quad (12)$$

$$E_{(N)}(g_N) - E_{N+1}(g_{N+1}) = \text{adiabatic EA} \quad (13)$$

Table 1. Names, Associated Reactions, and Explanations of Intrinsic Reactivity Indices

Name (typical acronym)	Related reaction	Brief description
Ionization potential (IP)	$\text{Antox}(\text{OH})_n \rightarrow \text{Antox}(\text{OH})_n^+ + e^-$	The ability to contribute an electron, which is interpreted as a willingness to oxidize itself. The lower the IP, the greater the likelihood of antioxidant protection through electron transfer via electron donation. This is sometimes referred to as ionization energy (IE) in the literature.
Electron affinity (EA)	$\text{Antox}(\text{OH})_n + e^- \rightarrow \text{Antox}(\text{OH})_n^-$	The ability to accept an electron, which can be interpreted as a desire to reduce itself. The lower the EA, the more likely antioxidant protection through electron transfer via electron acceptance.
Bond dissociation enthalpy (BDE)	$\text{Antox}(\text{OH})_n \rightarrow \text{Antox}(\text{OH})_{n-1}\text{O}^\bullet + \text{H}^\bullet$	The amount of energy required to break the O–H bond during homolytic fission, which can be interpreted in the context of the radical's stability. The lower the BDE values, the more active the corresponding –OH residue is in the hydrogen atom transfer mechanism and the more stable the radical formed.
Proton affinity (PA)/Proton dissociation enthalpy (PDE)	$\text{Antox}(\text{OH})_n \rightarrow \text{Antox}(\text{OH})_{n-1}\text{O}^- + \text{H}^+$	The amount of energy required to break the bond during heterolytic fission, which can be interpreted as the anion's stability. The lower the PA/PDE value, the more the corresponding –OH residue will be deprotonated. PA is defined as the inverse of the enthalpy change in a gas phase reaction between an electrically neutral chemical species and a proton to form the conjugated acid of the latter, whereas PDE is the deprotonation of a radical cation in any medium.

Table 2. Names, Mathematical Formulations, and Descriptions of Indices Related to Frontier Molecular Orbitals Theory

Name (typical acronym)	Related formula	Brief description
HOMO–LUMO gap (HLG)	$HLG = IP - EA$	Represents the ease with which the electron in a molecule can be excited from HOMO to LUMO. The lower it is, the easier the electron migrates from one another, and the radical reaction proceeds more quickly because it is more kinetically stable.
Electronegativity (χ)	$\chi = \frac{IP + EA}{2} = -\mu$	The general proclivity to attract electrons.
Chemical potential (μ)	$\mu = -\frac{IP + EA}{2} = -\chi$	Indicates the direction of charge flow as well as the capacity to contribute or accept it. Electrons will migrate from high to low μ locations in a quantity proportional to changes in μ , with a corresponding stabilizing energy μ^2 .
Global hardness (η)	$\eta = \frac{IP - EA}{2}$	Measures the resistance to electron cloud polarization caused by a minor chemical disturbance or a change in electron number.
Global softness (S)	$S = \frac{\eta}{2}$	The ability to accept electrons. It is inversely proportional to chemical hardness.
Electrophilicity (ω)	$\omega = \frac{\mu^2}{2\eta}$	The ability of a system to acquire a partial charge. When two molecules are involved in a chemical reaction, the one with the higher value is considered the acceptor, while the one with the lower value is considered the donor. It is advised to be used to demonstrate the efficacy of electron donation in compounds with extremely low IP values.

Table 3. Names, Mathematical Formulations, and Descriptions of DAM-Related Indices

Name (typical acronym)	Related formula	Brief description
Electrodonating power (ω^-)	$\omega^- = \frac{(3IP + EA)^2}{16(IP - EA)}$	The ability of a chemical system to provide a fractional amount of charge. The lower the ω^- , the more likely it is that the molecule will behave as an electron donor in weak interactions with other species.
Electron-accepting power (ω^+)	$\omega^+ = \frac{(IP + 3EA)^2}{16(IP - EA)}$	The ability of a chemical system to receive a fractional amount of charge. The greater the ω^+ , the more likely it is that the molecule will behave as an electron acceptor in weak interactions with other species.
Donor index (R_d)	$R_d = \frac{\omega_{\text{AntioxOH}}^-}{\omega_{\text{Na}}^-}$	
Acceptor index (R_a)	$R_a = \frac{\omega_{\text{AntioxOH}}^+}{\omega_{\text{F}}^+}$	
Relative value of electron acceptance (REA)	$REA = \frac{EA_{\text{AntioxOH}}}{EA_{\text{F}}}$	
Relative value of electron donation (RIE)	$RIE = \frac{IP_{\text{AntioxOH}}}{IP_{\text{Na}}}$	

where E_N , $E_{(N-1)}$, and E_{N+1} denote the total energies of the N , $N - 1$, and $N + 1$ electron systems, respectively, computed at ground state geometries of (g_N), (g_{N-1}) and (g_{N+1}) systems.

The Hammett sigma constant is one of the tools that draws from reactivity indices. It reflects the electron withdrawing or donating capacities of substituents connected to the aromatic moiety and thus can be applied to assess their impact on the intrinsic reactivity indices in a semiquantitative manner.^{22,23,32,127} They can be also used as a features of quantitative structure–activity relationship (QSAR) models, which numerically relate them and other descriptors to experimental data.^{11,24,43} Recently, an extensive paper on QSAR development and validation was published.¹⁸⁵

Frontier Molecular Orbitals. The energy and distribution of frontier molecular orbitals, specifically the highest-occupied molecular orbital (HOMO), a nucleophilic part of the molecule, and the lowest-unoccupied molecular orbital (LUMO), an electrophilic part of the molecule, can be directly linked to antioxidative activity.¹⁸⁶ This is because Janak's theorem^{187,188} states that the energies (ϵ) of HOMO and LUMO are related to ionization potential (eq 14) and electron affinity (eq 15), respectively, via the following relationship:

$$-\epsilon(\text{HOMO}) = \nu\text{IP} \quad (14)$$

$$-\epsilon(\text{LUMO}) = \nu\text{EA} \quad (15)$$

A molecule with a low HOMO eigenvalue is likely to be a poor electron donor, whereas a molecule with a low LUMO eigenvalue is likely to be a good electron acceptor. Analyzing their values allows for the initial elucidation of the antiradical activity. Although the majority of naturally occurring radicals are electrophilic, and so the interaction between their SOMO and antioxidants' HOMO is of the greatest importance, there also exist nucleophilic ones, typically carbon-centered, which scavenging potential is subjected to the overlap between SOMO of the reactive specie and LUMO of the scavenger. In addition, visualizing HOMO allows for a prediction of which molecular site is more vulnerable to radical attack^{28,50,116}, but presented later Fukui functions are more reliable option.

These approximations of orbitals eigenvalues as ionization potential or electron affinity, however, ignore electron correlation and are highly dependent on the method and basis set employed^{27,52,123,153}. This poses further problems for they serve as the foundation for a slew of global descriptive parameters related to the electrophilic character of the species (Table 2)¹⁸⁹ meaning their improper values may lead to further errors in the study and invalid conclusions. Given the importance of being as precise as possible, direct computations, are strongly advised. On the other hand, M062X/6-311G(d,p) level of theory has been found to approximate energies of frontier molecular orbitals with an error no greater than 0.5eV from the ones calculated in the direct vertical manner.¹⁵³

To ensure the quality of vertical energies obtained, an electron propagator theory (EPT)^{190,191} and a partial third-order quasiparticle theory (P3)¹⁹¹ can be exploited. These theories lay the groundwork for the systematic inclusion of electron correlation in a one-electron model of molecular electronic structure. They have been shown to produce lower mean errors than any other open shell techniques when compared to experimental trial results¹⁹² and are now widely used.^{46,101,112} For the EPT estimations to be valid, the pole strength (PS) values must be greater than 0.80–0.85.^{193,194}

Electron and Hydrogen Donating Properties. To do quick and simultaneous comparisons of the relative electron-donating and electron-accepting properties of a set of species the donor-acceptor map (DAM) is a right choice.¹⁹⁵ It is based on the assumption that in a simple charge-transfer model the response of a molecule submerged in an idealized environment that can either remove or donate charge can be represented by a quadratic interpolation for the energy as a function of the number of electrons.^{196,197} Therefore, DAM exhibits the antioxidant's tendency in charge-related processes in terms of electron-donating (ω^-) and electron-accepting (ω^+) powers (Table 3).

The substance is classified into one of four distinct zones (Figure 2) based on precalculated donor (R_d) and acceptor (R_a)

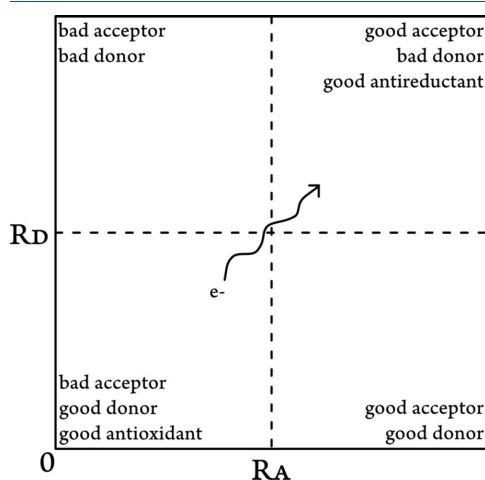


Figure 2. Schematic representation of donor-acceptor map.

indices: (1) the excellent antiradical zone (lower right), where it is both a superior electron donor (small R_d) and acceptor (high R_a), (2) the worst antiradical zone (upper left), where it is both a poor electron donor (high R_d) and a poor electron acceptor (small R_a), (3) the good antireductant zone (upper right), where it is a fine electron acceptor (high R_d and R_a) and thus an effective antiradical, and (4) the strong antioxidant area (lower left), where its good electron donor properties manifest (small R_d and R_a).

R_d and R_a are valued for their electron-donating and electron-accepting powers, respectively, and are defined in relation to the electron-accepting power of fluorine ($\omega_F^+ = 3.40$) and electron-donating power of sodium ($\omega_{Na}^- = 3.46$). F^- and Na^+ are used as references due to their high electron-accepting and electron-

donating capacities. ω_F^+ and ω_{Na}^- can be calculated using experimental data.³² If $R_d < 1$, the substance is a poorer electron acceptor than F, and if $R_d > 1$, it is a poorer electron donor than Na.

Three of the four zones represent the intended antioxidative activity. In the above graph, the electron flow goes from species in the bottom left to species in the top right. When comparing substances, DAM helps to predict which will behave as stronger or weaker oxidizers or reducers,⁸⁵ while also accounting for the effects of the environment.^{62,71} It is good to remember, there is a general trend of increasing electron-donating properties with each subsequent dissociation, so polyanionic species shall generally have lower R_d values than neutral or cationic forms.^{50,91}

Full electron-donor-acceptor map (FEDAM), an improved version of DAM, has been developed to account for the nature of the interacting free radical, which can have such a significant impact that it can even invert the relative importance of the free radical scavenging mechanisms.¹⁹⁸ FEDAM is based on the relative values of electron acceptance (REA) and electron donation (RIE) indices derived from vertical IP and vertical EA, again with Na and F atoms used as references. These are plotted on a map in the same way that DAM is but for both antioxidants and radicals. It has been used to evaluate antioxidant activity of melatonin, as well as its metabolites and derivatives.^{101,105}

The electron- and hydrogen-donating ability map for antioxidants (eH-DAMA)¹⁰¹ is another approach to enhance DAM. It was designed to identify compounds that are good donors in both electron transfer (low ω) and hydrogen atom transfer (low BDE). It is similar to DAM, but the axes change, so the Y axis corresponds to ω , while the X axis refers to BDE. As a result, the species in the left-bottom region are more likely to work in both directions, making them particularly valuable as radical scavengers, such as new sesamol¹¹² or melatonin derivatives¹⁰¹, or modified p-coumaric acid analogs with neuroprotective activity.⁴⁶ In most cases, parent molecules, oxidants, or reference antioxidants, e.g. Trolox, are included for comparison purposes.^{46,112}

Radical Attack Site. Frontier molecular orbital theory introduces a numerical method for investigating the reactivity of individual sites of molecule in three types of reactions. Fukui functions¹⁹⁹ were proposed to represent the difference in electron density at a given point, $\rho(r)$, as a function of the number of electrons, N , at a given external potential, $v(r)$ (eq 16). This is based on the notion that the optimal path for a reagent to approach the other species is the one with the highest initial fluctuation of the electronic chemical potential, μ .

$$f(r) = \left[\frac{\delta\mu}{\delta v(r)} \right]_N = \left[\frac{\partial\rho(r)}{\partial N} \right]_{v(r)} \quad (16)$$

Integrating over that equation for individual atoms in a molecule yields condensed Fukui functions (eqs 17–19), which are a more convenient way of predicting the reaction site than visualization of HOMO or LUMO orbitals. In general, the higher the value, the more reactive this position is to the specific type of attack. For an arbitrary atom A, these functions are defined as

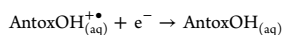
$$f_A^- = q_{N-1}^A - q_N^A \quad \text{for electrophilic attack} \quad (17)$$

$$f_A^+ = q_N^A - q_{N+1}^A \quad \text{for nucleophilic attack} \quad (18)$$

$$f_A^0 = \frac{[f_A^+ + f_A^-]}{2} = \frac{[q_{N-1}^A + q_{N+1}^A]}{2}, \text{ for radical attack} \quad (19)$$

where q_{N-1}^A , q_{N+1}^A represent charges of $(N-1)$ and $(N+1)$ systems obtained vertically from the optimized ground state geometry (N) with charge q_N^A . This ensures that the values are solely determined by the atom's electronegativity and electron density location. At the same time, because of that the atomic charge values used to estimate condensed Fukui functions are heavily reliant on population analysis method.^{124,200,201} Given their varied formulations,²⁰² the condensed Fukui functions may exhibit significant mutual discrepancies—even negative values²⁸—but this has already been explained as a result of the small interatomic distances between atoms.^{203,204} So Atoms-in-Molecule tend to overestimate them;²⁰⁴ Natural Population Analysis is heavily influenced by the functional, and basis set chosen;²⁰⁵ and ESP derived charges, such as ChelpG, have nonsmooth geometry dependence.²⁰⁰ Also a solvent may also affect the final result.¹²⁴ Some studies propose stockholder charge partitioning approaches in this purpose, particularly Hirschfeld analysis,^{15,64,123} since it yields values for which condensed Fukui functions correlate well with the expected data. In fact, a “dual descriptor” better illustrates susceptibility for electrophilic–nucleophilic attack,²⁰⁶ but these types of reactions are beyond the scope of antiradical activity studies.

Redox Potentials. As it was already mentioned, primary activity of antioxidants is related to the direct reduction of radicals. Therefore, the viability of this process can be assessed in terms of electrochemical potentials.²⁰⁷ The Born–Haber thermodynamic cycle is one universal method due to the common pattern of reactivity, and a half-reaction describing that process is always denoted by



for which the standard reduction potential can be calculated using the Nernst equation (eq 20)

$$E_{\text{red}(\text{aq})}^{\circ} = -\frac{\Delta G_{\text{red}}^*}{nF} \quad (20)$$

where ΔG_{red}^* denotes the standard Gibbs free energy of the reduction, and n is the number of electrons transferred and F the Faraday's constant (23.06 kcal/molV). According to the Born–Haber cycle, ΔG_{red}^* equals

$$\Delta G_{\text{red}}^* = G^*(\text{AntoxOH}^{+\bullet}) - G^*(\text{AntoxOH}) - nG^{\circ}(e^-) \quad (21)$$

with $G^{\circ}(e^-)$ being free energy of one electron in the gas phase (−0.876 kcal/mol at 298 K). When comparing results to those obtained experimentally, the computed values must be reduced by an absolute potential of the reference electrode, for example, a standard iron electrode or a standard hydrogen electrode.

Notably, because certain compounds may be partially deprotonated at a given pH, and anions have a lower capacity to donate electrons than neutral forms, they also influence the overall reduction potential. As a result, the average can be calculated accordingly to eq 22

$$E = E^{\text{AntoxOH}^{+\bullet}|\text{AntoxOH}} + \frac{RT}{F} \ln(f_{\text{AntoxOH}^{+\bullet}}) - \frac{RT}{F} \ln(f_{\text{AntoxOH}}) \quad (22)$$

where $E^{\text{AntoxOH}^{+\bullet}|\text{AntoxOH}}$ represents the initial reduction potential, and $f_{\text{AntoxOH}^{+\bullet}}$ denotes the population of the oxidized species that are reduced to produce the species with population f_{AntoxOH} .

Topology Analysis. Hydrogen bonds and weak interactions are important in stabilizing radicals or transition states rendering reactions to be more feasible, for example, by lowering BDE values.⁵⁰ Bader's Quantum Theory of Atoms in Molecules (QTAIM) can be used to quantify their strength^{208,209} and thus has been widely applied in antioxidants research.^{31,58,62,103,122,130} Despite the analysis's complexity, specialized tools such as the Multiwfn software²¹⁰ eases it.

The nature of chemical bonds at bond critical points (BCPs) can be mathematically described by electron densities, ρ , and their associated Laplacian, $\nabla^2\rho$. The theoretical background is explained in detail in Bader's paper;²⁰⁸ here, it will only be mentioned that BCPs of primary importance in such studies correspond to $(3,-1)$ critical points, being the saddle points with a maximum of electron density in two directions of space and a minimum in the third, and that the number of BCPs must obey the Poincaré–Hopf rule.²¹¹

The presence of a bond path between two atoms with a BCP in the middle is the first sign of a bond presence.^{208,215} A second criterion for defining it is that the values of $\rho(\text{BCP})$ and $\nabla^2\rho(\text{BCP})$ are positive, in ranges of 0.002–0.035 and 0.024–0.139, respectively.^{215–217} $\nabla^2\rho(\text{BCP})$ can be expanded as the sum of the eigenvalues $\lambda_1, \lambda_2, \lambda_3$, obtained by diagonalizing the Hessian of the electron density and mutually related as $\lambda_1 < \lambda_2 < \lambda_3$. They can be used to calculate the ellipticity parameter, $\epsilon = \frac{\lambda_1}{\lambda_2} - 1$, which quantifies the amount of charge that accumulates preferentially. A large ϵ indicates topological instability and, as a result, an easily ruptured bond. The λ_3 specifies how easily the BCP can be moved along the bond path,²⁰⁸ and the higher the value is, the stronger the interaction is. A local formulation of the virial theorem²⁰⁸ relates $\nabla^2\rho(\text{BCP})$ to electronic topological parameters by eq 23

$$\frac{\nabla^2\rho(\text{BCP})}{4} = 2G(\text{BCP}) + V(\text{BCP}) \quad (23)$$

where $G(\text{BCP})$ is the Lagrangian kinetic electron density, and $V(\text{BCP})$ represents the potential electron density (also known as the virial field).

Positive $\nabla^2\rho(\text{BCP})$ values indicate that $G(\text{BCP})$ is greater than $V(\text{BCP})$, implying that charge is being depleted along the bond path, as is typical of closed-shell interactions such as hydrogen bonding, ionic bonds, and van der Waals. Its negative values, on the other hand, indicate an excess potential energy at BCP in the form of internuclear charge concentration, which corresponds to covalent interactions; in this case, an electron density is localized in between two nuclei and is mutually accessible to both of them.²¹²

Similarly, the $-G(\text{BCP})/V(\text{BCP})$ ratio can be used for that purpose, because $-G(\text{BCP})/V(\text{BCP}) > 1$ indicates that the intramolecular bond is closed and noncovalent, while $0.5 < -G(\text{BCP})/V(\text{BCP}) < 1$ points out that it is shared—for example partially covalent or ionic.^{208,213,214}

Espinosa and coworkers^{219,220} demonstrated that interatomic interaction energy can be related to potential electron energy density at BCP using the following expression

$$E_{\text{HB}} = \frac{V(\text{BCP})}{2} \quad (24)$$

The above relationship, according to Rozas et al.,²¹⁸ allow hydrogen bonds to be classified as weak ($E_{\text{HB}} < 12.0$ kcal/mol), when $\nabla^2\rho(\text{BCP}) > 0$ and $H(\text{BCP}) > 0$, medium ($12.0 < E_{\text{HB}} < 24.0$ kcal/mol) if $\nabla^2\rho(\text{BCP}) > 0$ and $H(\text{BCP}) < 0$, or strong ($E_{\text{HB}} < 24.0$ kcal/mol) when $\nabla^2\rho(\text{BCP}) < 0$ and $H(\text{BCP}) > 0$, where $H(\text{BCP})$ denotes the density of electrons total energy, $G(\text{BCP}) + V(\text{BCP})$.

This is one of the most useful methods for calculating the energy of hydrogen bond interactions. Furthermore, Korth et al.²²¹ demonstrated how to compute the relative intramolecular hydrogen bond enthalpy by comparing the sum of the conformer's electronic and thermal enthalpies with intramolecular hydrogen bonds.

However, QTAIM analysis must be used with caution in course of the studies. The molecule's wavefunction, which is used to evaluate the aforementioned interactions, is determined by the functional and basis set used. As evidenced from refs 222 and 223, no relevant relationship between climbing Perdew's Jacob's ladder rungs and BCP densities was reported. The basis set, on the other hand, appears to be of primary concern. It has been demonstrated²²⁴ that small, double- ζ basis sets from Pople or Dunning's families are insufficient to accurately assess the properties of BCP related to multiple and polar bonds, as well as weak hydrogen bond interactions. Instead, at least triple- ζ are recommended, which is plausible in the context of the current trend in their choice in the studies on antioxidants.

Natural Bond Orbitals. One of the primary requirements for an antioxidant to effectively scavenge free radicals is that it becomes stable after the reaction. The spin density distribution throughout the molecule, which is often larger for conjugated systems, can be used to examine that property;^{28,33,50,82} however, natural bond orbital analysis^{225–228} represents a much more detailed investigation into the topic.

Refining the wavefunction into a Lewis-like structure corresponding to lone pairs and bonds gives an opportunity to track charge transfer by examining changes in the electron density at bonds, investigate hybridization of the orbitals and bonding interactions, as well as study delocalization and hyperconjugation effects.^{10,34,61,67,85,103,123} During the natural bond orbital analysis, the stabilization energy, $E^{(2)}$, is derived for the electron transfer from filled donor orbital, i , to an empty acceptor orbital, j , and is related by eq 25

$$E^2 = -q^i \frac{(F_{ij})^2}{(E_j - E_i)} \quad (25)$$

where F_{ij} is the off-diagonal Fock matrix element and q^i the orbital occupancy, and E_j and E_i are diagonal elements. The interpretation is clear —, the greater the E^2 energy, the greater degree of interaction.

NBO analysis, just like QTAIM, also requires careful application. Although it is a straightforward and advantageous method, at the same time it is heavily reliant on the geometry of the compound, which stems from the partitioning scheme of the electron density matrix and the localized nature of molecular orbitals. A simple, yet excellent, example of this can be found in the paper of Benassi and Fan²²⁹ where the authors reported on how the delocalization energy and orbital occupancy number differ in pyridine across its seven normal modes and small changes along the displacement coordinates. It has been demonstrated that even minor shift can result in significantly

different $E^{(2)}$ values, which is expected to be amplified in the case of larger antioxidant structures.

REACTIVITY

Thermochemistry. In reality, the antioxidant's ability to scavenge radicals is influenced not only by the antioxidant itself but also by the species with which it interacts. As a result, thermochemical calculations of known pathways (Table 4) produce far more useful data than intrinsic reactivity indices alone; one way to illustrate them is with O'Ferrall–Jencks diagrams^{83,86} (Figure 3). However, before proceeding, a foreword is required: hydroxyl radical, $\cdot\text{OH}$, is so reactive that it quickly reacts with almost any molecule in its vicinity at diffusion-limited rates, before an antioxidant can actually reach it. For this reason, it is skipped from computations and radicals with intermediate to low reactivity are chosen instead for assessing the antiradical potential.^{230–232} Peroxyl radicals, $\text{ROO}\cdot$ (such as $\text{CH}_3\text{OO}\cdot$ or $\text{OOH}\cdot$),^{233,234} are one of these because their half-lives are long enough that they can be intercepted before oxidizing biological targets.^{235,236} Although acid-base equilibrium of hydroperoxide equals 4.8, what means that O_2^- is typically present in physiological conditions, it is not very reactive species and the oxidation damage are primarily stemming from its protonated form.²³⁷ $\text{CCl}_3\text{OO}\cdot$ can also be considered because it is used in experiments to simulate larger radicals.²³⁸ Another possible reduction target might be the $\text{H}_2\text{O}_2/\text{O}_2$ pair, which is more difficult to neutralize than other reactive oxygen species.²³⁹

The polarity of the environment also has an effect on reaction energetics. To begin with, it should come as no surprise that reactions generating neutral species, such as RAF or HAT, perform better in nonpolar solvents than reactions that produces ions. This is due to the fact that nonpolar media do not provide enough solvation to stabilize charged species through the charge separation, thereby propelling the reaction forward. In consequence, such reactions are unlikely to occur in a significant number, and conventional studies in nonpolar media focus solely on RAF and HAT, with the remaining pathways being completely ignored.^{60,63,106,121,139,143}

Furthermore, the first step in a multistep mechanism is thermodynamically significant and so determining its energetics allows for assessing reaction's feasibility, simplifying the analysis by rejecting unfavorable pathways. Because BDE, IP, and PA are the primary indices of the HAT, SET-PT, and SPLET,^{240–243} they can be used for this purpose.

Moreover, because SPLET mechanism is initiated by proton dissociation, which proclivity is controlled by the environment's pH and acid–base equilibrium, the SET and SPLET processes are extremely closely coupled due to the spontaneous. If molar fractions are being considered at the outset, the second step of SPLET actually controls an antioxidant's reactivity, and in this case the entire mechanism becomes equivalent to SET; namely, it is identical to the SET reaction for an acid–base species with $N - 1$ protons. Herein, I will just mention that it is also an electrostatic potential map, which is a useful tool for distinguishing between electrophilic and nucleophilic centers, highlights positively charged hydroxyl hydrogen to be likely involved in proton dissociation mechanisms.^{28,68}

Finally, because IP and EA values govern electron flow between antioxidant and radical, they can be used to estimate the direction of the SET mechanism, providing an early picture of the process. In general, the bare minimum for SET reactions with electrophilic radicals is $\text{IP}(\text{antioxidant}) < \text{EA}(\text{radical})$ and

Table 4. Naming, Associated Reactions, and Descriptions of the Most Commonly Studied Antioxidative Reaction Pathways

Name (typical acronym)	Related reaction	Description
Radical adduct formation (RAF)	$\text{Antox}(\text{OH})_n + \text{X}^\bullet \rightarrow [\text{Antox}(\text{OH})_n\text{X}]^\bullet$	In a single step, the radical forms an adduct with the antioxidant, spreading the spin density across the newly formed molecule. The preferred reaction site is determined by the degree of the unpaired electron delocalization.
Hydrogen atom transfer (HAT)/Proton coupled electron transfer (PCET)	$\text{Antox}(\text{OH})_n + \text{X}^\bullet \rightarrow \text{Antox}(\text{OH})_{n-1}\text{O}^\bullet + \text{HX}$	A one-step mechanism in which an O–H bond is homolytically broken and a hydrogen atom is transferred from antioxidant to free radical, resulting in a more stable antioxidant radical. Low BDE values are common in compounds that promote this path. In the electrochemical sense, it is a reduction process. Although the products of HAT and PCET reactions are identical, the former involves the coordinated transfer of a proton and an electron as a single entity, whereas PCET involves the process of two separated particles, not necessarily from the same sets of orbitals. Formal HAT refers to chemical reactions that have not been defined as HAT or PCET.
Single electron transfer (SET)	$\text{Antox}(\text{OH})_n + \text{X}^\bullet \rightarrow \text{Antox}(\text{OH})_{n-1}^{\bullet/+} + \text{X}^{2-/+}$	Depending on the mutual IP and EA values, a single electron transfer occurs from an antioxidant to a radical or from a radical to an antioxidant. The deprotonation influences the thermochemical viability of the SET process to some extent.
Sequential electron transfer-proton transfer (SET-PT)		It occurs in two steps: first, a radical cation $\text{Antox}(\text{OH})_n^{\bullet/+}$ is formed by electron transfer from an antioxidant to a free radical, and then, it deprotonates to form $\text{Antox}(\text{OH})_{n-1}\text{O}^\bullet$ species. The first step is described by the IP values, while the second step is described by the PDE values.
Electron transfer	1. $\text{Antox}(\text{OH})_n + \text{X}^\bullet \rightarrow \text{Antox}(\text{OH})_n^{\bullet/+} + \text{X}^-$ 2. Proton transfer	The mechanism is divided into two steps: first, an antioxidant is deprotonated (as described by PA) and then, an electron transfer occurs from the deprotonated antioxidant to a free radical (described by IP). Because pK _a values influence the amount of deprotonated species in aqueous solution, knowing their number <i>a priori</i> can assist in determining the relative importance of this process.
Sequential proton loss-electron transfer (SPLET)	1. $\text{Antox}(\text{OH})_n \rightarrow \text{Antox}(\text{OH})_{n-1}\text{O}^- + \text{H}^+$ 2. $\text{Antox}(\text{OH})_{n-1}\text{O}^- + \text{X}^\bullet \rightarrow \text{Antox}(\text{OH})_{n-1}\text{O}^\bullet + \text{X}^-$	The mechanism is identical to SPLET, except that instead of an electron, a hydrogen atom is transferred in the second step. As a result, antioxidants containing at least two hydroxyl groups are particularly appealing. PA describes the first step, and BDE describes the second.
Electron transfer	1. $\text{Antox}(\text{OH})_n \rightarrow \text{Antox}(\text{OH})_{n-1}\text{O}^- + \text{H}^+$ 2. $\text{Antox}(\text{OH})_{n-1}\text{O}^- + \text{X}^\bullet \rightarrow \text{Antox}(\text{OH})_{n-1}\text{O}^\bullet + \text{X}^-$	
Sequential proton loss-hydrogen atom transfer (SPLHAT)	1. Proton loss 2. Electron transfer	
Sequential proton loss-hydrogen atom transfer (SPLHAT)	1. Proton loss 2. Hydrogen atom transfer	

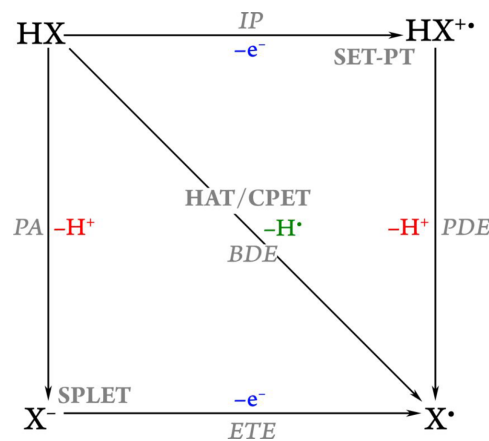


Figure 3. O'Farrell–Jencks diagram of each single step involved in common reaction mechanisms.

opposite holds true for the nucleophilic ones. In case of not so easily recognizable species, a general rule of knowing that electrons flow from the structure of lower IP to the structure of greater EA, makes it possible to predict which molecule will undergo oxidation and which will undergo reduction, and the reverse path can be thereby ignored.

One final point to mention about thermochemical calculations is that they require the Gibbs free energies of electron, proton, and hydrogen. The very last can be estimated directly at the applied level of theory, but the proton and electron cannot, at least not in a straightforward manner, necessitating the use of widely varying reference values.^{178,180,181,244}

Kinetics. An antioxidant is any substance that, even at low concentrations, significantly delays or prevents the oxidation of radical target. Therefore, it must not only react spontaneously with the oxidizing agent, but it must also react faster than the target it is designed to protect.^{245,246} This aspect can only be modeled using kinetic studies, which account for facets skipped by thermochemical studies—tunneling effects, weighted contribution of different mechanisms and different species to total antioxidative potential, or adherence to the Bell–Evans–Polanyi principle³—and is thus critical for accurately assessing antioxidative behavior.

Although spontaneity is an important criterion for chemical reactivity, it is not always enough because an exergonic reaction can occur at either fast or slow rates. When drawing conclusions from thermochemical data without considering kinetics, the Bell–Evans–Polanyi^{247,248} principle, which states that the most exergonic processes have the lowest activation energies and are thus kinetically favored, is implicitly assumed to be followed.³ On the other hand, ignoring a reaction path due to difficulties in locating a transition state may result in a more significant error than accepting the given rule without its confirmation, especially if it was discovered to hold true for a structurally similar compounds.¹¹⁸ It has been recently evidenced that Gibbs free energy is actually proportional to the activation energy of hydrogen atom transfer, and hence reaction rate of this mechanism.^{90,249,250}

Endergonic channels do not need to be included in kinetic calculations in general because even if they occur at high rates,

they are reversible to the point where no products are detected. However, moderately endergonic processes (typically with $\Delta G^\circ < 10.0$ kcal/mol) may still contribute to antioxidant capacity and should be addressed, particularly if their products evolve into other species quickly, providing a driving force, or the reaction barriers are low.¹⁸² This is the case for some RAF reactions,⁸² but it is particularly common for SET, where thermochemical and kinetic data may show opposing trends; in some cases, the mechanism may be associated with positive Gibbs energies and still be relevant, as has been demonstrated in a number of previously reported studies.^{36,46,73,82,154} Highly exergonic SET reactions involving donors with very low IP (such as monoanionic or polyanionic species) may, on the other hand, be found in the inverted region of the Marcus parabola, where that reaction barriers increase as ΔG° decreases what is often to be found for Gibbs free energies much lower than negative of reorganization energy.^{251–253} Despite this is an unexpected behavior, it underlines that particles with extremely low IP are unlikely to be efficient free radical scavengers.^{46,101,125} That is why using ionization potentials may be misleading, and electron-donating power or electrophilicity is far superior because, while it also relies on IP, it does so in a nonlinear fashion, with the shape of this dependency resembling the Marcus parabola.^{46,101,112}

The activation barrier of a reaction is determined by the energy difference between the transition state and the reactants. However, in the case of electron-related processes, assessing it is not so straightforward. The barrier of electron transfer reaction (ΔG_{ET}^\ddagger) is calculated in a different way, using the Marcus theory^{253–255} (eq 26), which defines it in terms of the reaction adiabatic free energy (ΔG_{ET}^0) and nuclear reorganization energy (λ)

$$\Delta G_{ET}^\ddagger = \frac{\lambda}{4} \left(1 + \frac{\Delta G_{ET}^0}{\lambda} \right)^2 \quad (26)$$

The reorganization energy is calculated as the difference between the vertical (ΔE_{ET}) and adiabatic free energies of reaction and accounts for the orbitals relaxation

$$\lambda = \Delta E_{ET} - \Delta G_{ET}^0 \quad (27)$$

The reaction rate constants (k) can be calculated using the conventional transition state theory (TST) which is one of the most robust theoretical methodologies for this purpose, requiring only structural, energy, and vibrational frequency information for reactants and transition states, allowing it to be applied to a wide range of chemical processes.^{256–258} Despite its simplicity, it has been shown to reproduce fine the experimentally measured data on free radicals scavenging kinetics.^{82,84,96,129} It is computed usually in the framework of 1 M standard state²⁵⁸ using the Eyring equation (eq 28)

$$k^{TST} = \frac{k_B T}{h} e^{-\Delta G^\ddagger / RT} \quad (28)$$

where k_B and h are the Boltzmann and Planck constants, respectively. ΔG^\ddagger is the free energy of activation, calculated as the difference in energies between transition state and reactants, while R and T denote the gas constant and temperature, respectively.

The more sophisticated Eckart approach,²⁵⁹ also known as the zero-tunneling method, employs the Boltzmann average of the ratio of quantum and classical probabilities²⁶⁰ and is suggested

for processes in which reactants are transformed into products over energy barriers. Such processes include the HAT reaction, which involves the motion of a light particle (here H^\bullet) that can easily tunnel, as well as some RAF pathways. Tunneling corrections ($\kappa(T)$), also known in the literature as transmission coefficients ($\gamma(T)$), are included, as is reaction path degeneracy (σ). $\kappa(T)$ can significantly modulate reaction rate values between relatively similar reacting species, such as CH_3OO^\bullet or OOH^\bullet .¹¹⁸ It can be estimated using external software, for example Eyringpy.²⁶¹ The number of identical reaction paths, on the other hand, is reflected by σ and can be calculated by labeling all similar atoms and counting the number of different but equivalent configurations that can be formed by rotating, but not reflecting them. They can also be established using the Pollak and Pechukas²⁶² scheme (Table 5). Taking everything into account, eq 29 is obtained

$$k^{TST} = \sigma \kappa(T) \frac{k_B T}{h} e^{-\Delta G^\ddagger / RT} \quad (29)$$

Table 5. Point Groups and the Reaction Path Degeneracy Values That Correspond to Them

Point group	σ	Point group	σ
C_1	1	D_{3h}	6
C_s	1	D_{3d}	10
C_2	2	$D_{\infty h}$	2
C_{2v}	2	D_{3d}	6
C_{3v}	3	T_d	12
$C_{\infty v}$	1	O_h	24
D_{2h}	4		

As previously stated, radicals with high reactivity often react at diffusion-limited rates ($k \geq 10^8$ M⁻¹ s⁻¹) with the vast majority of chemical compounds. For an irreversible bimolecular diffusion-controlled reaction, the Collins–Kimbball theory,²⁶³ in conjunction with the steady-state Smoluchowski rate constant²⁶⁴ and the Stokes–Einstein approaches,²⁶⁵ must be used to calculate rate constants properly (Table 6). They are frequently applied in case of RAF mechanisms, which is not surprising given that these types of radical attacks usually occur in the absence of energy barriers, making it difficult to localize the transition state.

The total reaction rate constant values (k^{TOT}) for all acid–base species (i) present at the specified pH multiplied by the corresponding molar fractions (f) allow the overall reaction rate constant ($k^{overall}$), which corresponds to the empirically observed reaction rate, to be calculated

$$k^{overall} = \sum_{i=\{\text{species}\}} f(i) k^{TOT}(i) \quad (30)$$

The reaction rate constants for each antioxidative mechanism (j) are then added to calculate the k^{TOT} values for all acid–base species

$$k^{TOT} = \sum_{j=\{\text{mechanism}\}} k^{mech}(j) \quad (31)$$

The k^{mech} (eq 32) is defined as the sum of reaction rate constants (k^{TST} or k^{PPP} , depending on the kinetic model used, here simply represented by k) from the same antioxidative mechanism but calculated at different reaction sites (l)

Table 6. Collins–Kimball Theory, Steady-State Smoluchowski, and Stokes–Einstein Equation Mathematical Formulations

Name	Related formula	Variables
Collins–Kimball theory	$k^{\text{app}} = \frac{k^{\text{D}}k^{\text{TST}}}{k^{\text{D}} + k^{\text{TST}}}$	k_{app} : apparent rate constant
Steady-state Smoluchowski	$k^{\text{D}} = 4\pi RD_{\text{AB}}N_{\text{A}}$	k^{D} : steady-state Smoluchowski k^{TST} : thermal rate constant (obtained from TST) R : reaction distance N_{A} : Avogadro number D_{AB} : mutual diffusion coefficient of the reactants A (free radical) and B (antioxidant)
Stokes–Einstein equation	$D_{\text{A or B}} = \frac{k_{\text{B}}T}{6\pi\eta r_{\text{A or B}}}$	k_{B} : Boltzmann constant T : temperature η : viscosity of solvent r : radius of solute

$$k^{\text{mech}} = \sum_{l \in \{\text{pathway}\}} k(l) \quad (32)$$

The branching ratio ($\Gamma(l)$, (eq 33)) can be used to calculate the percentage contribution of an antioxidative pathway (l) to the total reaction rate (l) using the following formula

$$\Gamma(l) = \frac{k(l)}{k^{\text{overall}}} \quad (33)$$

Furthermore, the relative antioxidative activity of the examined molecule can be calculated by dividing its k^{overall} by the k^{overall} of ref 45 (e.g., Trolox, Tx) as presented in eq 34

$$r^T = \frac{k^{\text{overall}}}{k_{\text{Tx}}^{\text{overall}}} \quad (34)$$

A threshold of $k^{\text{overall}} = 1.2 \times 10^3 \text{ M}^{-1} \text{ s}^{-1}$ was proposed for quantifying antioxidant activity as a value close to the rate constant of the interaction between HOO^{\bullet} and polyunsaturated fatty acids^{3,21,126}. Compounds with higher k^{overall} values are thought to be effective antioxidants, while those with lower are thought to be ineffective.

Thermochemistry and Kinetic Ensemble. Galano, Alvarez-Idaboy and coworkers combined the above considerations into the quantum mechanics-based test for overall free radical scavenging activity (QM-ORSA) protocol,^{3,154,266} which is proposed as a feasible tool to assess radical scavenging activity in physiologically relevant solvents. It entails the impact of all existing acid–base forms, identifying RAF, HAT, and SET mechanisms viability, and then subjecting them to kinetic analysis. This method has been already used successfully in numerous papers.^{41,45,58,69,82,88,104,118}

CONCLUDING REMARKS AND ADDITIONAL CONSIDERATIONS

Antioxidants were and are extensively studied using computational quantum chemistry. A number of useful tools are developed to provide insight into their electronic structure and reactivity. Importantly, scientists are not limited in their research to already known procedures but continuously suggest new ones and apply them in their research. Therefore, each paper proposes some novel techniques in this matter, as well as new conclusions that provide greater insight into the chemistry of the antioxidants that have been already studied or projected from the scratch. As previously stated, because all antioxidants

tend to exhibit similar patterns of activity, they can all be examined in the same way, whether we are talking about fullerenes, natural plant products, or entirely newly synthesized structures.

Certain points, however, should be reconsidered or reinterpreted:

- Almost all of the research considered reactive oxygen species, with only a minor focus on radicals containing nitrogen, carbon, and sulfur elements. These are known to be linked to oxidative stress,^{267–269} so research into them would fill the gap.
- When discussing *in vivo* activity, although solvation effects and hence deprotonation are considered, the importance of metabolites should be emphasized. The gut microbiota are the first to alter antioxidant structure, influencing primarily their absorption profile. They are then metabolized in the liver, where they undergo further changes that result in products with vastly different activity. By focusing solely on generic structures the outcomes are indeed limited to *in vitro* results, casting doubt on the physiological activities as free radicals scavengers, capable of halting the development of oxidative stress and resulting diseases.
- The dual nature of free radicals extends to the products derived from the antioxidants. Castañeda-Arriaga et al.¹⁰² discussed possible prooxidant behavior of such, in which the new forms may still be capable of oxidizing biologically relevant structures. The authors also proposed them to be able to self-regenerate, allowing them to work multiple times. This fresh topic appears to be a relevant aspect that needs to be considered when attempting to prove experimental observations.

DATA AND SOFTWARE AVAILABILITY

Multiwfn (current version 3.7) is a free, open-source software developed by Tian Lu for wave function analysis and visualization. It is available for download at <http://sobereva.com/multiwfn/>. Eyring.py (current version 2.0) is a Python-based program developed by the Merino et al. group for computing rate constants of unimolecular or bimolecular reactions in the gas phase and in solution using transition state theory. For that purpose, it takes into account reaction symmetry, tunneling corrections, Collins–Kimball theory, Marcus theory, and species molar fractions. It is available at

<https://www.theochemmerida.org/eyringpy>. GROMACS (current version 2021.5) is a free package, available under a LGPL license, created to perform molecular dynamics of proteins, lipids, nucleic acids as well as nonbiological systems. It is accessible from <http://www.gromacs.org>. Amber (current version 20) is a paid versatile suite of biomolecular simulation programs. It can be found at <https://ambermd.org/index.php>. CHARMM is a molecular simulation program that uses enhanced sampling methods and multiscale techniques to study many-particle systems. For academic users, the version "charm" is free. The software is available for free download at <https://academiccharmm.org>.

AUTHOR INFORMATION

Corresponding Author

Maciej Spiegel – Department of Pharmacognosy and Herbal Medicines, Wrocław Medical University, 50-556 Wrocław, Poland; orcid.org/0000-0002-8012-1026; Email: maciej.spiegel@student.umed.wroc.pl

Complete contact information is available at: <https://pubs.acs.org/10.1021/acs.jcim.2c00104>

Notes

The author declares no competing financial interest.

REFERENCES

- Valko, M.; Leibfritz, D.; Moncol, J.; Cronin, M. T. D.; Mazur, M.; Telsler, J. Free Radicals and Antioxidants in Normal Physiological Functions and Human Disease. *Int. J. Biochem. Cell Biol.* **2007**, *39* (1), 44–84.
- Ames, B. N.; Shigenaga, M. K.; Hagen, T. M. Oxidants, antioxidants, and the degenerative diseases of aging. *Proc. Natl. Acad. Sci. U.S.A.* **1993**, *90* (17), 7915–7922.
- Galano, A.; Alvarez-Idaboy, J. R. Computational Strategies for Predicting Free Radical Scavengers' Protection against Oxidative Stress: Where Are We and What Might Follow? *Int. J. Quantum Chem.* **2019**, *119* (2), No. e25665.
- Kumar, N.; Goel, N. Phenolic Acids: Natural Versatile Molecules with Promising Therapeutic Applications. *Biotechnol. Reports* **2019**, *24*, No. e00370.
- Sisa, M.; Bonnet, S. L.; Ferreira, D.; Van Der Westhuizen, J. H. Photochemistry of Flavonoids. *Molecules* **2010**, *15* (8), 5196–5245.
- Miguel, M. G. Betalains in Some Species of the Amaranthaceae Family: A Review. *Antioxidants* **2018**, *7* (4), 53.
- Reygaert, W. C. Green Tea Catechins: Their Use in Treating and Preventing Infectious Diseases. *Biomed Res. Int.* **2018**, *2018*, 1–9.
- Ross, S. A.; Ziska, D. S.; Zhao, K.; ElSohly, M. A. Variance of Common Flavonoids by Brand of Grapefruit Juice. *Fitoterapia* **2000**, *71* (2), 154–161.
- Ma, Y.; Feng, Y.; Diao, T.; Zeng, W.; Zuo, Y. Experimental and Theoretical Study on Antioxidant Activity of the Four Anthocyanins. *J. Mol. Struct.* **2020**, *1204*, 127509.
- Spiegel, M.; Andruniów, T.; Sroka, Z. Flavones' and Flavonols' Antiradical Structure-Activity Relationship—a Quantum Chemical Study. *Antioxidants* **2020**, *9* (6), 461.
- Ali, H. M.; Ali, I. H. Structure-Antioxidant Activity Relationships, QSAR, DFT Calculation, and Mechanisms of Flavones and Flavonols. *Med. Chem. Res.* **2019**, *28* (12), 2262–2269.
- Mendes, R. A.; Almeida, S. K. C.; Soares, I. N.; Barboza, C. A.; Freitas, R. G.; Brown, A.; de Souza, G. L. C. Evaluation of the Antioxidant Potential of Myricetin 3-O- α -L-Rhamnopyranoside and Myricetin 4'-O- α -L-Rhamnopyranoside through a Computational Study. *J. Mol. Model.* **2019**, *25* (4), 89.
- Maciel, E. N.; Soares, I. N.; da Silva, S. C.; de Souza, G. L. C. A Computational Study on the Reaction between Fisetin and 2,2-Diphenyl-1-Picrylhydrazyl (DPPH). *J. Mol. Model.* **2019**, *25* (4), 103.
- Yi, Y.; Adrijan, B.; Li, J.; Hu, B.; Roszak, S. NMR Studies of Daidzein and Puerarin: Active Anti-Oxidants in Traditional Chinese Medicine. *J. Mol. Model.* **2019**, *25* (7), 202.
- Song, X.; Wang, Y.; Gao, L. Mechanism of Antioxidant Properties of Quercetin and Quercetin-DNA Complex. *J. Mol. Model.* **2020**, *26* (6), 133.
- Son, N. T.; Mai Thanh, D. T.; Van Trang, N. Flavone Norartocarpetin and Isoflavone 2'-Hydroxygenistein: A Spectroscopic Study for Structure, Electronic Property and Antioxidant Potential Using DFT (Density Functional Theory). *J. Mol. Struct.* **2019**, *1193*, 76–88.
- Zheng, Y. Z.; Deng, G.; Guo, R.; Fu, Z. M.; Chen, D. F. Theoretical Insight into the Antioxidative Activity of Isoflavonoid: The Effect of the C2 = C3 Double Bond. *Phytochemistry* **2019**, *166*, 112075.
- Biela, M.; Rimarčík, J.; Senajová, E.; Kleinová, A.; Klein, E. Antioxidant Action of Deprotonated Flavonoids: Thermodynamics of Sequential Proton-Loss Electron-Transfer. *Phytochemistry* **2020**, *180*, 112528.
- Anitha, S.; Krishnan, S.; Senthilkumar, K.; Sasirekha, V. Theoretical Investigation on the Structure and Antioxidant Activity of (+) Catechin and (–) Epicatechin-a Comparative Study. *Mol. Phys.* **2020**, *118* (17), e1745917.
- Ninh The, S.; Do Minh, T.; Nguyen Van, T. Isoflavones and Isoflavone Glycosides: Structural-Electronic Properties and Antioxidant Relations-A Case of DFT Study. *J. Chem.* **2019**, *2019* (d), 1.
- Vásquez-Espinal, A.; Yañez, O.; Osorio, E.; Areche, C.; García-Beltrán, O.; Ruiz, L. M.; Cassels, B. K.; Tiznado, W. Theoretical Study of the Antioxidant Activity of Quercetin Oxidation Products. *Front. Chem.* **2019**, *7*, 1–10.
- Zheng, Y. Z.; Deng, G.; Guo, R.; Chen, D. F.; Fu, Z. M. Substituent Effects on the Radical Scavenging Activity of Isoflavonoid. *Int. J. Mol. Sci.* **2019**, *20* (2), 397.
- Zheng, Y. Z.; Deng, G.; Guo, R.; Chen, D. F.; Fu, Z. M. DFT Studies on the Antioxidant Activity of Naringenin and Its Derivatives: Effects of the Substituents at C3. *Int. J. Mol. Sci.* **2019**, *20* (6), 1450.
- Zúvela, P.; David, J.; Yang, X.; Huang, D.; Wong, M. W. Non-Linear Quantitative Structure-Activity Relationships Modelling, Mechanistic Study and in-Silico Design of Flavonoids as Potent Antioxidants. *Int. J. Mol. Sci.* **2019**, *20* (9), 2328.
- Xu, Y.; Qian, L. L.; Yang, J.; Han, R. M.; Zhang, J. P.; Skibsted, L. H. Kaempferol Binding to Zinc(II), Efficient Radical Scavenging through Increased Phenol Acidity. *J. Phys. Chem. B* **2018**, *122* (44), 10108–10117.
- Mendes, R. A.; Almeida, S. K. C.; Soares, I. N.; Barboza, C. A.; Freitas, R. G.; Brown, A.; de Souza, G. L. C. A Computational Investigation on the Antioxidant Potential of Myricetin 3,4'-Di-O- α -L-Rhamnopyranoside. *J. Mol. Model.* **2018**, *24* (6), 133.
- Rajan, V. K.; Shameera Ahamed, T. K.; Muraleedharan, K. Studies on the UV Filtering and Radical Scavenging Capacity of the Bitter Masking Flavanone Eriodictyol. *J. Photochem. Photobiol. B Biol.* **2018**, *185* (June), 254–261.
- Son, N. T.; Thuy, P. T.; Van Trang, N. Antioxidative Capacities of Stilbenoid Suaveolensone A and Flavonoid Suaveolensone B: A Detailed Analysis of Structural-Electronic Properties and Mechanisms. *J. Mol. Struct.* **2021**, *1224*, 129025.
- Tiwari, M. K.; Mishra, P. C. Scavenging of Hydroxyl, Methoxy, and Nitrogen Dioxide Free Radicals by Some Methylated Isoflavones. *J. Mol. Model.* **2018**, *24* (10), 287.
- Zhou, H.; Li, X.; Shang, Y.; Chen, K. Radical Scavenging Activity of Puerarin: A Theoretical Study. *Antioxidants* **2019**, *8* (12), 590.
- Thong, N. M.; Vo, Q. V.; Huyen, T. L.; Bay, M. V.; Tuan, D.; Nam, P. C. Theoretical Study for Exploring the Diglycoside Substituent Effect on the Antioxidative Capability of Isorhamnetin Extracted from *Anoectochilus Roxburghii*. *ACS Omega* **2019**, *4* (12), 14996–15003.
- Zheng, Y. Z.; Chen, D. F.; Deng, G.; Guo, R. The Substituent Effect on the Radical Scavenging Activity of Apigenin. *Molecules* **2018**, *23* (8), 1989.
- Li, Z.; Moalin, M.; Zhang, M.; Vervoort, L.; Hursel, E.; Mommers, A.; Haenen, G. R. M. M. The Flow of the Redox Energy in

- Quercetin during Its Antioxidant Activity in Water. *Int. J. Mol. Sci.* **2020**, *21* (17), 6015.
- (34) Milenković, D.; Dimitrić Marković, J. M.; Dimić, D.; Jeremić, S.; Amić, D.; Stanojević Pirković, M.; Marković, Z. S. Structural Characterization of Kaempferol: A Spectroscopic and Computational Study. *Maced. J. Chem. Chem. Eng.* **2019**, *38* (1), 49–62.
- (35) Manrique-de-la-Cuba, M. F.; Gamero-Begazo, P.; Valencia, D. E.; Barazorda-Ccahuana, H. L.; Gómez, B. Theoretical Study of the Antioxidant Capacity of the Flavonoids Present in the *Annona muricata* (Soursop) Leaves. *J. Mol. Model.* **2019**, *25* (7), 200.
- (36) Castañeda-Arriaga, R.; Marino, T.; Russo, N.; Alvarez-Idaboy, J. R.; Galano, A. Chalcogen Effects on the Primary Antioxidant Activity of Chrysin and Quercetin. *New J. Chem.* **2020**, *44* (21), 9073–9082.
- (37) Heřmáňková, E.; Zatloukalová, M.; Biler, M.; Sokolová, R.; Bancířová, M.; Tzakos, A. G.; Křen, V.; Kuzma, M.; Trouillas, P.; Vacek, J. Redox Properties of Individual Quercetin Moieties. *Free Radic. Biol. Med.* **2019**, *143*, 240–251.
- (38) Milenković, D.; Đorović, J.; Petrović, V.; Avdović, E.; Marković, Z. Hydrogen Atom Transfer versus Proton Coupled Electron Transfer Mechanism of Gallic Acid with Different Peroxy Radicals. *React. Kinet. Mech. Catal.* **2018**, *123* (1), 215–230.
- (39) Amić, A.; Marković, Z.; Dimitrić Marković, J. M.; Milenković, D.; Štepanić, V. Antioxidative Potential of Ferulic Acid Phenoxy Radical. *Phytochemistry* **2020**, *170*, 112218.
- (40) Vo, Q. V.; Bay, M. V.; Nam, P. C.; Quang, D. T.; Flavel, M.; Hoa, N. T.; Mechler, A. Theoretical and Experimental Studies of the Antioxidant and Antinutrient Activity of Syringic Acid. *J. Org. Chem.* **2020**, *85* (23), 15514–15520.
- (41) Medina, M. E.; Galano, A.; Trigoso, A. Scavenging Ability of Homogentisic Acid and Ergosterol toward Free Radicals Derived from Ethanol Consumption. *J. Phys. Chem. B* **2018**, *122* (30), 7514–7521.
- (42) Kalinowska, M.; Sienkiewicz-Gromiuk, J.; Świdorski, G.; Pietruczuk, A.; Cudowski, A.; Lewandowski, W. Zn(II) Complex of Plant Phenolic Chlorogenic Acid: Antioxidant, Antimicrobial and Structural Studies. *Materials (Basel)* **2020**, *13* (17), 3745.
- (43) Spiegel, M.; Kapusta, K.; Kolodziejczyk, W.; Saloni, J.; Zbikowska, B.; Hill, G. A.; Sroka, Z. Antioxidant Activity of Selected Phenolic Acids-Ferric Reducing Antioxidant Power Assay and QSAR Analysis of the Structural Features. *Molecules* **2020**, *25* (13), 3088.
- (44) Zheng, Y. Z.; Fu, Z. M.; Deng, G.; Guo, R.; Chen, D. F. Free Radical Scavenging Potency of Ellagic Acid and Its Derivatives in Multiple H•/E• Processes. *Phytochemistry* **2020**, *180* (July), 112517.
- (45) Tošović, J.; Bren, U. Antioxidative Action of Ellagic Acid—A Kinetic DFT Study. *Antioxidants* **2020**, *9* (7), 587.
- (46) Reina, M.; Guzmán-López, E. G.; Romeo, I.; Marino, T.; Russo, N.; Galano, A. Computationally Designed: P-Coumaric Acid Analogs: Searching for Neuroprotective Antioxidants. *New J. Chem.* **2021**, *45* (32), 14369–14380.
- (47) Chen, J.; Yang, J.; Ma, L.; Li, J.; Shahzad, N.; Kim, C. K. Structure-Antioxidant Activity Relationship of Methoxy, Phenolic Hydroxyl, and Carboxylic Acid Groups of Phenolic Acids. *Sci. Rep.* **2020**, *10* (1), 2611.
- (48) Vo, Q. V.; Nam, P. C.; Bay, M. V.; Thong, N. M.; Cuong, N. D.; Mechler, A. Density Functional Theory Study of the Role of Benzylic Hydrogen Atoms in the Antioxidant Properties of Lignans. *Sci. Rep.* **2018**, *8* (1), 1–10.
- (49) Xue, Y.; Liu, Y.; Zhang, L.; Wang, H.; Luo, Q.; Chen, R.; Liu, Y.; Li, Y. Antioxidant and Spectral Properties of Chalcones and Analogous Aurones: Theoretical Insights. *Int. J. Quantum Chem.* **2019**, *119* (3), e25808.
- (50) Boulebd, H. The Role of Benzylic-Allylic Hydrogen Atoms on the Antiradical Activity of Prenylated Natural Chalcones: A Thermodynamic and Kinetic Study. *J. Biomol. Struct. Dyn.* **2021**, *39* (6), 1955–1964.
- (51) Xue, Y.; Liu, Y.; Xie, Y.; Cong, C.; Wang, G.; An, L.; Teng, Y.; Chen, M.; Zhang, L. Antioxidant Activity and Mechanism of Dihydrochalcone C-Glycosides: Effects of C-Glycosylation and Hydroxyl Groups. *Phytochemistry* **2020**, *179* (April), 112393.
- (52) Llano, S.; Gómez, S.; Londoño, J.; Restrepo, A. Antioxidant Activity of Curcuminoids. *Phys. Chem. Chem. Phys.* **2019**, *21* (7), 3752–3760.
- (53) Li, Y.; Toscano, M.; Mazzone, G.; Russo, N. Antioxidant Properties and Free Radical Scavenging Mechanisms of Cyclocurcumin. *New J. Chem.* **2018**, *42* (15), 12698–12705.
- (54) Ali, H. M.; Ali, I. H. Energetic and Electronic Computation of the Two-Hydrogen Atom Donation Process in Catecholic and Non-Catecholic Anthocyanidins. *Food Chem.* **2018**, *243*, 145–150.
- (55) Chen, B.; Ma, Y.; Li, H.; Chen, X.; Zhang, C.; Wang, H.; Deng, Z. The Antioxidant Activity and Active Sites of Delphinidin and Petunidin Measured by DFT, in Vitro Chemical-Based and Cell-Based Assays. *J. Food Biochem.* **2019**, *43* (9), 1–11.
- (56) Rajan, V. K.; Hasna, C. K. K.; Muraliedharan, K. The Natural Food Colorant Peonidin from Cranberries as a Potential Radical Scavenger - A DFT Based Mechanistic Analysis. *Food Chem.* **2018**, *262*, 184–190.
- (57) Shang, Y.; Zhou, H.; Li, X.; Zhou, J.; Chen, K. Theoretical Studies on the Antioxidant Activity of Viniferifuran. *New J. Chem.* **2019**, *43* (39), 15736–15742.
- (58) Vo, Q. V.; Cam Nam, P.; Bay, M. V.; Minh Thong, N.; Hieu, L. T.; Mechler, A. A Theoretical Study of the Radical Scavenging Activity of Natural Stilbenes. *RSC Adv.* **2019**, *9* (72), 42020–42028.
- (59) Zheng, Y. Z.; Chen, D. F.; Deng, G.; Guo, R.; Fu, Z. M. The Antioxidative Activity of Piceatannol and Its Different Derivatives: Antioxidative Mechanism Analysis. *Phytochemistry* **2018**, *156* (May), 184–192.
- (60) Santos, J. L. F.; Kauffmann, A. C.; da Silva, S. C.; Silva, V. C. P.; de Souza, G. L. C. Probing Structural Properties and Antioxidant Activity Mechanisms for Eleocarpanthraquinone. *J. Mol. Model.* **2020**, *26* (9), 233.
- (61) Reza Nazifi, S. M.; Asgharshamsi, M. H.; Dehkordi, M. M.; Zborowski, K. K. Antioxidant Properties of Aloe Vera Components: A DFT Theoretical Evaluation. *Free Radic. Res.* **2019**, *53* (8), 922–931.
- (62) Ngo Nyobe, J. C.; Eya Andiga, L. G.; Mama, D. B.; Ateba Amana, B.; Zobo Mfomo, J.; Flavian Aristide Alfred, T.; Ndom, J. C. A DFT Analysis on Antioxidant and Antiradical Activities from Anthraquinones Isolated from the Cameroonian Flora. *J. Chem.* **2019**, *2019*, 1.
- (63) Dorović, J.; Antonijević, M.; Marković, Z. Antioxidative and Inhibition Potency of Cynodontin. *J. Serbian Soc. Comput. Mech.* **2020**, *70*, 59–70.
- (64) Vega-Hissi, E. G.; Andrada, M. F.; Diaz, M. G.; Garro Martinez, J. C. Computational Study of the Hydrogen Peroxide Scavenging Mechanism of Allyl Methyl Disulfide, an Antioxidant Compound from Garlic. *Mol. Divers.* **2019**, *23* (4), 985–995.
- (65) Tiwari, M. K.; Jena, N. R.; Mishra, P. C. Mechanisms of Scavenging Superoxide, Hydroxyl, Nitrogen Dioxide and Methoxy Radicals by Allicin: Catalytic Role of Superoxide Dismutase in Scavenging Superoxide Radical. *J. Chem. Sci.* **2018**, *130* (8), 1–17.
- (66) Cortes, N.; Castañeda, C.; Osorio, E. H.; Cardona-Gomez, G. P.; Osorio, E. Amarylidaceae Alkaloids as Agents with Protective Effects against Oxidative Neural Cell Injury. *Life Sci.* **2018**, *203*, 54–65.
- (67) Dung, N. T.; Thanh, D. M.; Huong, N. T.; Thuy, P. T.; Hoan, N. T.; Thanh, D. T. M.; Van Trang, N.; Son, N. T. Quinolone and Isoquinolone Alkaloids: The Structural-Electronic Effects and the Antioxidant Mechanisms. *Struct. Chem.* **2020**, *31* (6), 2435–2450.
- (68) Boulebd, H. Are Thymol, Rosefuran, Terpinolene and Umbelliferone Good Scavengers of Peroxyl Radicals? *Phytochemistry* **2021**, *184*, 112670.
- (69) Vo, Q. V.; Tam, N. M.; Hieu, L. T.; Van Bay, M.; Thong, N. M.; Le Huyen, T.; Hoa, N. T.; Mechler, A. The Antioxidant Activity of Natural Diterpenes: Theoretical Insights. *RSC Adv.* **2020**, *10* (25), 14937–14943.
- (70) Boulebd, H. DFT Study of the Antiradical Properties of Some Aromatic Compounds Derived from Antioxidant Essential Oils: C-H Bond vs. O-H Bond. *Free Radic. Res.* **2019**, *53* (11–12), 1125–1134.
- (71) Hernandez, D. A.; Tenorio, F. J. Reactivity Indexes of Antioxidant Molecules from *Rosmarinus officinalis*. *Struct. Chem.* **2018**, *29* (3), 741–751.

- (72) Ngo, T. C.; Nguyen, T. H.; Dao, D. Q. Radical Scavenging Activity of Natural-Based Cassaine Diterpenoid Amides and Amines. *J. Chem. Inf. Model.* **2019**, *59* (2), 766–776.
- (73) Romeo, I.; Parise, A.; Galano, A.; Russo, N.; Alvarez-Idaboy, J. R.; Marino, T. The Antioxidant Capability of Higenamine: Insights from Theory. *Antioxidants* **2020**, *9* (5), 358.
- (74) Boulebd, H. Theoretical Insights into the Antioxidant Activity of Moracin T. *Free Radic. Res.* **2020**, *54* (4), 221–230.
- (75) Dao, D. Q.; Phan, T. T. T.; Nguyen, T. L. A.; Trinh, P. T. H.; Tran, T. T. V.; Lee, J. S.; Shin, H. J.; Choi, B.-K. Insight into Antioxidant and Photoprotective Properties of Natural Compounds from Marine Fungus. *J. Chem. Inf. Model.* **2020**, *60* (3), 1329–1351.
- (76) Elshamy, A. I.; Yoneyama, T.; Trang, N. V.; Son, N. T.; Okamoto, Y.; Ban, S.; Noji, M.; Umeyama, A. A New Cerebroside from the Entomopathogenic Fungus *Ophiocordyceps longiissima*: Structural-Electronic and Antioxidant Relations. Experimental and DFT Calculated Studies. *J. Mol. Struct.* **2020**, *1200*, 127061.
- (77) Dávalos, J. Z.; Valderrama-Negrón, A. C.; Barrios, J. R.; Freitas, V. L. S.; Ribeiro Da Silva, M. D. M. C. Energetic and Structural Properties of Two Phenolic Antioxidants: Tyrosol and Hydroxytyrosol. *J. Phys. Chem. A* **2018**, *122* (16), 4130–4137.
- (78) Montero, G.; Arriagada, F.; Günther, G.; Bollo, S.; Mura, F.; Berrios, E.; Morales, J. Phytoestrogen Coumestrol: Antioxidant Capacity and Its Loading in Albumin Nanoparticles. *Int. J. Pharm.* **2019**, *562*, 86–95.
- (79) Shameera Ahamed, T. K.; Rajan, V. K.; Sabira, K.; Muralleedharan, K. DFT and QTAIM Based Investigation on the Structure and Antioxidant Behavior of Lichen Substances Atranorin, Evernic Acid and Diffractaic Acid. *Comput. Biol. Chem.* **2019**, *80*, 66–78.
- (80) Wang, A.; Lu, Y.; Du, X.; Shi, P.; Zhang, H. A Theoretical Study on the Antioxidant Activity of Uralenol and Neouralenol Scavenging Two Radicals. *Struct. Chem.* **2018**, *29* (4), 1067–1075.
- (81) Zhang, D.; Wang, C.; Shen, L.; Shin, H. C.; Lee, K. B.; Ji, B. Comparative Analysis of Oxidative Mechanisms of Phloroglucinol and Dieckol by Electrochemical, Spectroscopic, Cellular and Computational Methods. *RSC Adv.* **2018**, *8* (4), 1963–1972.
- (82) Parise, A.; De Simone, B. C.; Marino, T.; Toscano, M.; Russo, N. Quantum Mechanical Predictions of the Antioxidant Capability of Moracin C Isomers. *Front. Chem.* **2021**, *9* (April), 1–9.
- (83) Gonçalves, L. C. P.; Lopes, N. B.; Augusto, F. A.; Pioli, R. M.; Machado, C. O.; Freitas-Dörr, B. C.; Suffredini, H. B.; Bastos, E. L. Phenolic Betalain as Antioxidants: Meta Means More. *Pure Appl. Chem.* **2020**, *92* (2), 243–253.
- (84) Perez-Gonzalez, A.; Prejano, M.; Russo, N.; Marino, T.; Galano, A. Capsaicin, a Powerful •OH-Inactivating Ligand. *Antioxidants* **2020**, *9* (12), 1247.
- (85) Spiegel, M.; Gamian, A.; Sroka, Z. Antiradical Activity of Beetroot (*Beta Vulgaris* L.) Betalains. *Molecules* **2021**, *26* (9), 2439.
- (86) Nakashima, K. K.; Bastos, E. L. Rationale on the High Radical Scavenging Capacity of Betalains. *Antioxidants* **2019**, *8* (7), 222.
- (87) Tabrizi, L.; Dao, D. Q.; Vu, T. A. Experimental and Theoretical Evaluation on the Antioxidant Activity of a Copper(II) Complex Based on Lidocaine and Ibuprofen Amide-Phenanthroline Agents. *RSC Adv.* **2019**, *9* (6), 3320–3335.
- (88) Boulebd, H.; Tam, N. M.; Mechler, A.; Vo, Q. V. Substitution Effects on the Antiradical Activity of Hydralazine: A DFT Analysis. *New J. Chem.* **2020**, *44* (38), 16577–16583.
- (89) Minelli, C.; Laudadio, E.; Galeazzi, R.; Rusciano, D.; Armeni, T.; Stipa, P.; Cantarini, M.; Mobbili, G. Synthesis, Characterization and Antioxidant Properties of a New Lipophilic Derivative of Edaravone. *Antioxidants* **2019**, *8* (8), 258.
- (90) Bortoli, M.; Dalla Tiezza, M.; Muraro, C.; Pavan, C.; Ribaudo, G.; Rodighiero, A.; Tubaro, C.; Zagotto, G.; Orian, L. Psychiatric Disorders and Oxidative Injury: Antioxidant Effects of Zolpidem Therapy Disclosed In Silico. *Comput. Struct. Biotechnol. J.* **2019**, *17*, 311–318.
- (91) Boulebd, H.; Khodja, I. A.; Bay, M. V.; Hoa, N. T.; Mechler, A.; Vo, Q. V. Thermodynamic and Kinetic Studies of the Radical Scavenging Behavior of Hydralazine and Dihydralazine: Theoretical Insights. *J. Phys. Chem. B* **2020**, *124* (20), 4123–4131.
- (92) Muraro, C.; Dalla Tiezza, M.; Pavan, C.; Ribaudo, G.; Zagotto, G.; Orian, L. Major Depressive Disorder and Oxidative Stress: In Silico Investigation of Fluoxetine Activity against ROS. *Appl. Sci.* **2019**, *9* (17), 3631.
- (93) Purushothaman, A.; Sheeja, A. A.; Janardanan, D. Hydroxyl Radical Scavenging Activity of Melatonin and Its Related Indolamines. *Free Radic. Res.* **2020**, *54* (5), 373–383.
- (94) Baj, A.; Cedrowski, J.; Olchowik-Grabarek, E.; Ratkiewicz, A.; Witkowski, S. Synthesis, DFT Calculations, and in Vitro Antioxidant Study on Novel Carba-Analogs of Vitamin E. *Antioxidants* **2019**, *8* (12), 589.
- (95) Pandithavidana, D. R.; Jayawardana, S. B. Comparative Study of Antioxidant Potential of Selected Dietary Vitamins; Computational Insights. *Molecules* **2019**, *24* (9), 1646.
- (96) Ardjani, T. E. A.; Alvarez-Idaboy, J. R. Radical Scavenging Activity of Ascorbic Acid Analogs: Kinetics and Mechanisms. *Theor. Chem. Acc.* **2018**, *137* (5), na DOI: 10.1007/s00214-018-2252-x.
- (97) Bentz, E. N.; Lobayan, R. M.; Martinez, H.; Redondo, P.; Largo, A. Intrinsic Antioxidant Potential of the Aminoindole Structure: A Computational Kinetics Study of Tryptamine. *J. Phys. Chem. B* **2018**, *122* (24), 6386–6395.
- (98) Dimic, D.; Milenkovic, D.; Markovic, Z.; Dimitric-Markovic, J. The Reactivity of Dopamine Precursors and Metabolites towards ABTS•-: An Experimental and Theoretical Study. *J. Serbian Chem. Soc.* **2019**, *84* (8), 877–889.
- (99) Jabeen, H.; Saleemi, S.; Razzaq, H.; Yaqub, A.; Shakoore, S.; Qureshi, R. Investigating the Scavenging of Reactive Oxygen Species by Antioxidants via Theoretical and Experimental Methods. *J. Photochem. Photobiol. B Biol.* **2018**, *180*, 268–275.
- (100) Dimic, D.; Nakarada, Du.; Mojovic, M.; Dimitric Markovic, J. An Experimental and Theoretical Study of the Reactivity of Selected Catecholamines and Their Precursors towards Ascorbyl Radical. *J. Serbian Soc. Comput. Mech.* **2020**, *12*, 1–12.
- (101) Reina, M.; Castañeda-Arriaga, R.; Perez-Gonzalez, A.; Guzman-Lopez, E. G.; Tan, D.-X.; Reiter, R. J.; Galano, A. A Computer-Assisted Systematic Search for Melatonin Derivatives with High Potential as Antioxidants. *Melatonin Res.* **2018**, *1* (1), 27–58.
- (102) Castañeda-Arriaga, R.; Pérez-González, A.; Reina, M.; Galano, A. Computer-Designed Melatonin Derivatives: Potent Peroxyl Radical Scavengers with No pro-Oxidant Behavior. *Theor. Chem. Acc.* **2020**, *139* (8), 1–12.
- (103) Dimić, D.; Milenković, D.; Ilić, J.; Šmit, B.; Amić, A.; Marković, Z.; Dimitrić Marković, J. Experimental and Theoretical Elucidation of Structural and Antioxidant Properties of Vanillylmandelic Acid and Its Carboxylate Anion. *Spectrochim. Acta - Part A Mol. Biomol. Spectrosc.* **2018**, *198*, 61–70.
- (104) Boulebd, H.; Mechler, A.; Hoa, N. T.; Vo, Q. V. Thermodynamic and Kinetic Studies of the Antiradical Activity of 5-Hydroxymethylfurfural: Computational Insights. *New J. Chem.* **2020**, *44* (23), 9863–9869.
- (105) Reina, M.; Martínez, A. A New Free Radical Scavenging Cascade Involving Melatonin and Three of Its Metabolites (3OHM, AFMK and AMK). *Comput. Theor. Chem.* **2018**, *1123*, 111–118.
- (106) Sykula, A.; Kowalska-Baron, A.; Dzeikala, A.; Bodzioch, A.; Lodyga-Chruscinska, E. An Experimental and DFT Study on Free Radical Scavenging Activity of Hesperetin Schiff Bases. *Chem. Phys.* **2019**, *517*, 91–103.
- (107) Amić, A.; Marković, Z.; Klein, E.; Dimitrić Marković, J. M.; Milenković, D. Theoretical Study of the Thermodynamics of the Mechanisms Underlying Antiradical Activity of Cinnamic Acid Derivatives. *Food Chem.* **2018**, *246*, 481–489.
- (108) Wang, L.; Yang, F.; Zhao, X.; Li, Y. Effects of Nitro- and Amino-Group on the Antioxidant Activity of Genistein: A Theoretical Study. *Food Chem.* **2019**, *275*, 339–345.
- (109) Hernández-García, L.; Sandoval-Lira, J.; Rosete-Luna, S.; Niño-Medina, G.; Sanchez, M. Theoretical Study of Ferulic Acid Dimer

- Derivatives: Bond Dissociation Enthalpy, Spin Density, and HOMO-LUMO Analysis. *Struct. Chem.* **2018**, *29* (5), 1265–1272.
- (110) Zheng, Y. Z.; Zhou, Y.; Guo, R.; Fu, Z. M.; Chen, D. F. Structure-Antioxidant Activity Relationship of Ferulic Acid Derivatives: Effect of Ester Groups at the End of the Carbon Side Chain. *Lwt* **2020**, *120*, 108932.
- (111) Shaikh, S. A. M.; Singh, B. G.; Barik, A.; Balaji, N. V.; Subbaraju, G. V.; Naik, D. B.; Priyadarsini, K. I. Unravelling the Effect of β -Diketo Group Modification on the Antioxidant Mechanism of Curcumin Derivatives: A Combined Experimental and DFT Approach. *J. Mol. Struct.* **2019**, *1193*, 166–176.
- (112) Castro-González, L. M.; Alvarez-Idaboy, J. R.; Galano, A. Computationally Designed Sesamol Derivatives Proposed as Potent Antioxidants. *ACS Omega* **2020**, *5* (16), 9566–9575.
- (113) Liu, Y.; Liu, C.; Li, J. Comparison of Vitamin c and Its Derivative Antioxidant Activity: Evaluated by Using Density Functional Theory. *ACS Omega* **2020**, *5*, 25467–25475.
- (114) Stepanic, V.; Matijasic, M.; Horvat, T.; Verbanac, D.; Kucerova-Chlupacova, M.; Saso, L.; Zarkovic, N. Antioxidant Activities of Alkyl Substituted Pyrazine Derivatives of Chalcones—In Vitro and in Silico Study. *Antioxidants* **2019**, *8* (4), 90.
- (115) Lauberte, L.; Fabre, G.; Ponomarenko, J.; Dizhbite, T.; Evtuguin, D. V.; Telysheva, G.; Trouillas, P. Lignin Modification Supported by DFT-Based Theoretical Study as a Way to Produce Competitive Natural Antioxidants. *Molecules* **2019**, *24* (9), 1794.
- (116) Wang, G.; Liu, Y.; Zhang, L.; An, L.; Chen, R.; Liu, Y.; Luo, Q.; Li, Y.; Wang, H.; Xue, Y. Computational Study on the Antioxidant Property of Coumarin-Fused Coumarins. *Food Chem.* **2020**, *304*, 1–7.
- (117) Xue, Y.; Liu, Y.; Luo, Q.; Wang, H.; Chen, R.; Liu, Y.; Li, Y. Antiradical Activity and Mechanism of Coumarin-Chalcone Hybrids: Theoretical Insights. *J. Phys. Chem. A* **2018**, *122* (43), 8520–8529.
- (118) Castro-González, L. M.; Galano, A.; Alvarez-Idaboy, J. R. Free Radical Scavenging Activity of Newly Designed Sesamol Derivatives. *New J. Chem.* **2021**, *45* (27), 11960–11967.
- (119) Badhani, B.; Kakkar, R. Structural, Electronic, and Reactivity Parameters of Some Triorganotin(IV) Carboxylates: A DFT Analysis. *Struct. Chem.* **2018**, *29* (3), 753–763.
- (120) Tabrizi, L.; Nguyen, T. L. A.; Dao, D. Q. Experimental and Theoretical Investigation of Cyclometalated Phenylpyridine Iridium(III) Complex Based on Flavonol and Ibuprofen Ligands as Potent Antioxidant. *RSC Adv.* **2019**, *9* (30), 17220–17237.
- (121) Hamlaoui, I.; Bencheraiet, R.; Bensegueni, R.; Bencharif, M. Experimental and Theoretical Study on DPPH Radical Scavenging Mechanism of Some Chalcone Quinoline Derivatives. *J. Mol. Struct.* **2018**, *1156*, 385–389.
- (122) Zheng, Y. Z.; Deng, G.; Chen, D. F.; Liang, Q.; Guo, R.; Fu, Z. M. Theoretical Studies on the Antioxidant Activity of Pinobanksin and Its Ester Derivatives: Effects of the Chain Length and Solvent. *Food Chem.* **2018**, *240*, 323–329.
- (123) Almeida-Neto, F. W. Q.; da Silva, L. P.; Ferreira, M. K. A.; Mendes, F. R. S.; de Castro, K. K. A.; Bandeira, P. N.; de Menezes, J. E. S. A.; dos Santos, H. S.; Monteiro, N. K. V.; Marinho, E. S.; de Lima-Neto, P. Characterization of the Structural, Spectroscopic, Nonlinear Optical, Electronic Properties and Antioxidant Activity of the N-{4'-(E)-3-(Fluorophenyl)-1-(Phenyl)-Prop-2-En-1-One}-Acetamide. *J. Mol. Struct.* **2020**, *1220*, 128765.
- (124) Milenković, D.; Avdović, E. H.; Dimić, D.; Bajin, Z.; Ristić, B.; Vuković, N.; Trifunović, S. R.; Marković, Z. S. Reactivity of the Coumarine Derivative towards Cartilage Proteins: Combined NBO, QTAIM, and Molecular Docking Study. *Monatshfte fur Chemie* **2018**, *149* (1), 159–166.
- (125) Pérez-González, A.; Galano, A. On the Outstanding Antioxidant Capacity of Edaravone Derivatives through Single Electron Transfer Reactions. *J. Phys. Chem. B* **2012**, *116* (3), 1180–1188.
- (126) Carreon-Gonzalez, M.; Vivier-Bunge, A.; Alvarez-Idaboy, J. R. Thiophenols, Promising Scavengers of Peroxyl Radicals: Mechanisms and Kinetics. *J. Comput. Chem.* **2019**, *40* (24), 2103–2110.
- (127) Michalík, M.; Poliak, P.; Lukeš, V.; Klein, E. From Phenols to Quinones: Thermodynamics of Radical Scavenging Activity of Para-Substituted Phenols. *Phytochemistry* **2019**, *166* (June), 112077.
- (128) Lee, C. Y.; Sharma, A.; Semanya, J.; Anamoah, C.; Chapman, K. N.; Barone, V. Computational Study of Ortho-Substituent Effects on Antioxidant Activities of Phenolic Dendritic Antioxidants. *Antioxidants* **2020**, *9* (3), 189.
- (129) Marino, T.; Galano, A.; Mazzone, G.; Russo, N.; Alvarez-Idaboy, J. R. Chemical Insights into the Antioxidant Mechanisms of Alkylseleno and Alkyltelluro Phenols: Periodic Relatives Behaving Differently. *Chem. - A Eur. J.* **2018**, *24* (34), 8686–8691.
- (130) Nakarada, Đ.; Petković, M. Mechanistic Insights on How Hydroquinone Disarms OH and OOH Radicals. *Int. J. Quantum Chem.* **2018**, *118* (4), e25496.
- (131) Perin, N.; Roškarić, P.; Sović, I.; Boček, I.; Starčević, K.; Hranjec, M.; Vianello, R. Amino-Substituted Benzamide Derivatives as Promising Antioxidant Agents: A Combined Experimental and Computational Study. *Chem. Res. Toxicol.* **2018**, *31* (9), 974–984.
- (132) Sheng, X. H.; Cui, C. C.; Shan, C.; Li, Y. Z.; Sheng, D. H.; Sun, B.; Chen, D. Z. O-Phenylenediamine: A Privileged Pharmacophore of Ferrostatis for Radical-Trapping Reactivity in Blocking Ferroptosis. *Org. Biomol. Chem.* **2018**, *16* (21), 3952–3960.
- (133) Anastassova, N. O.; Mavrova, A. T.; Yancheva, D. Y.; Kondeva-Burdina, M. S.; Tzankova, V. I.; Stoyanov, S. S.; Shivachev, B. L.; Nikolova, R. P. Hepatotoxicity and Antioxidant Activity of Some New N,N'-Disubstituted Benzimidazole-2-Thiones, Radical Scavenging Mechanism and Structure-Activity Relationship. *Arab. J. Chem.* **2018**, *11* (3), 353–369.
- (134) Orabi, E. A.; Orabi, M. A. A.; Mahross, M. H.; Abdel-Hakim, M. Computational Investigation of the Structure and Antioxidant Activity of Some Pyrazole and Pyrazolone Derivatives. *J. Saudi Chem. Soc.* **2018**, *22* (6), 705–714.
- (135) Cindrić, M.; Sović, I.; Mioč, M.; Hok, L.; Boček, I.; Roškarić, P.; Butković, K.; Martin-Kleiner, I.; Starčević, K.; Vianello, R.; Kralj, M.; Hranjec, M. Experimental and Computational Study of the Antioxidative Potential of Novel Nitro and Amino Substituted Benzimidazole/Benzothiazole-2-Carboxamides with Antiproliferative Activity. *Antioxidants* **2019**, *8* (10), 477.
- (136) Alisi, I. O.; Uzairu, A.; Abechi, S. E. Free Radical Scavenging Mechanism of 1,3,4-Oxadiazole Derivatives: Thermodynamics of O-H and N-H Bond Cleavage. *Heliyon* **2020**, *6* (3), No. e03683.
- (137) Kumar, J.; Kumar, N.; Sati, N.; Hota, P. K. Antioxidant Properties of Ethenyl Indole: DPPH Assay and TDFT Studies. *New J. Chem.* **2020**, *44* (21), 8960–8970.
- (138) Marc, G.; Stana, A.; Oniga, S. D.; Pirnău, A.; Vlase, L.; Oniga, O. New Phenolic Derivatives of Thiazolidine-2,4-Dione with Antioxidant and Antiradical Properties: Synthesis, Characterization, In Vitro Evaluation, and Quantum Studies. *Molecules* **2019**, *24* (11), 2060.
- (139) Sonam; Chahal, V.; Kakkar, R. Theoretical Study of the Structural Features and Antioxidant Potential of 4-Thiazolidinones. *Struct. Chem.* **2020**, *31* (4), 1599–1608.
- (140) Almezia, A. A.; Abuelizz, H. A.; Taie, H. A. A.; ElHassane, A.; Marzouk, M.; Al-Salahi, R. Investigation the Antioxidant Activity of Benzo[g]Triazolozinazoles Correlated with a DFT Study. *Saudi Pharm. J.* **2019**, *27* (1), 133–137.
- (141) Al-Salahi, R.; Anouar, E. H.; Marzouk, M.; Taie, H. A. A.; Abuelizz, H. A. Screening and Evaluation of Antioxidant Activity of Some 1,2,4-Triazololo[1,5-a]Quinazoline Derivatives. *Future Med. Chem.* **2018**, *10* (4), 379–390.
- (142) Bazine, I.; Cheraiet, Z.; Bensegueni, R.; Bensouici, C.; Boukhari, A. Synthesis, Antioxidant and Anticholinesterase Activities of Novel Quinoline-Aminophosphonate Derivatives. *J. Heterocycl. Chem.* **2020**, *57* (5), 2139–2149.
- (143) Çakmak, E.; Özbakır Işın, D. A Theoretical Evaluation on Free Radical Scavenging Activity of 3-Styrylchromone Derivatives: The DFT Study. *J. Mol. Model.* **2020**, *26* (5), 98.
- (144) Wang, Z.; Gao, X.; Zhao, Y. Mechanisms of Antioxidant Activities of Fullerenols from First-Principles Calculation. *J. Phys. Chem. A* **2018**, *122* (41), 8183–8190.

- (145) Orabi, E. A. Tautomerism and Antioxidant Activity of Some 4-Acylpyrazolone-Based Schiff Bases: A Theoretical Study. *RSC Adv.* **2018**, *8* (54), 30842–30850.
- (146) Bakır, T.; Sayiner, H. S.; Kandemirli, F. Experimental and Theoretical Investigation of Antioxidant Activity and Capacity of Thiosemicarbazones Based on Isatin Derivatives. *Phosphorus, Sulfur Silicon Relat. Elem.* **2018**, *193* (8), 493–499.
- (147) Becke, A. D. Density-Functional Thermochemistry. III. The Role of Exact Exchange. *J. Chem. Phys.* **1993**, *98* (7), 5648–5652.
- (148) Lee, C.; Yang, W.; Parr, R. G. Development of the Colle-Salvetti Correlation-Energy Formula into a Functional of the Electron Density. *Phys. Rev. B* **1988**, *37* (2), 785–789.
- (149) Zhao, Y.; Truhlar, D. G. The M06 Suite of Density Functionals for Main Group Thermochemistry, Thermochemical Kinetics, Non-covalent Interactions, Excited States, and Transition Elements: Two New Functionals and Systematic Testing of Four M06-Class Functionals and 12 Other Function. *Theor. Chem. Acc.* **2008**, *120* (1–3), 215–241.
- (150) Zhao, Y.; Schultz, N. E.; Truhlar, D. G. Design of Density Functionals by Combining the Method of Constraint Satisfaction with Parametrization for Thermochemistry, Thermochemical Kinetics, and Noncovalent Interactions. *J. Chem. Theory Comput.* **2006**, *2* (2), 364–382.
- (151) Zhao, Y.; Truhlar, D. G. How Well Can New-Generation Density Functionals Describe the Energetics of Bond-Dissociation Reactions Producing Radicals? *J. Phys. Chem. A* **2008**, *112* (6), 1095–1099.
- (152) De Souza, G. L. C.; Peterson, K. A. Benchmarking Antioxidant-Related Properties for Gallic Acid through the Use of DFT, MP2, CCSD, and CCSD(T) Approaches. *J. Phys. Chem. A* **2021**, *125* (1), 198–208.
- (153) Spiegel, M.; Gamian, A.; Sroka, Z. A Statistically Supported Antioxidant Activity DFT Benchmark—The Effects of Hartree-Fock Exchange and Basis Set Selection on Accuracy and Resources Uptake. *Molecules* **2021**, *26* (16), 5058.
- (154) Galano, A.; Mazzone, G.; Alvarez-Diduk, R.; Marino, T.; Alvarez-Idaboy, J. R.; Russo, N. Food Antioxidants: Chemical Insights at the Molecular Level. *Annu. Rev. Food Sci. Technol.* **2016**, *7* (1), 335–352.
- (155) Wang, J.; Becke, A. D.; Smith, V. H. Evaluation of {S2} in Restricted, Unrestricted Hartree-Fock, and Density Functional Based Theories. *J. Chem. Phys.* **1995**, *102* (8), 3477–3480.
- (156) Brovarets', O. O.; Hovorun, D. M. Conformational Diversity of the Quercetin Molecule: A Quantum-Chemical View. *J. Biomol. Struct. Dyn.* **2020**, *38* (10), 2817–2836.
- (157) Scalmani, G.; Frisch, M. J. Continuous Surface Charge Polarizable Continuum Models of Solvation. I. General Formalism. *J. Chem. Phys.* **2010**, *132* (11), 114110.
- (158) Barone, V.; Cossi, M. Quantum Calculation of Molecular Energies and Energy Gradients in Solution by a Conductor Solvent Model. *J. Phys. Chem. A* **1998**, *102* (11), 1995–2001.
- (159) Cossi, M.; Rega, N.; Scalmani, G.; Barone, V. Energies, Structures, and Electronic Properties of Molecules in Solution with the C-PCM Solvation Model. *J. Comput. Chem.* **2003**, *24* (6), 669–681.
- (160) Marenich, A. V.; Cramer, C. J.; Truhlar, D. G. Universal Solvation Model Based on Solute Electron Density and on a Continuum Model of the Solvent Defined by the Bulk Dielectric Constant and Atomic Surface Tensions. *J. Phys. Chem. B* **2009**, *113* (18), 6378–6396.
- (161) Kelly, C. P.; Cramer, C. J.; Truhlar, D. G. Adding Explicit Solvent Molecules to Continuum Solvent Calculations for the Calculation of Aqueous Acid Dissociation Constants. *J. Phys. Chem. A* **2006**, *110* (7), 2493–2499.
- (162) Okuno, Y. Theoretical Investigation of the Mechanism of the Baeyer-Villiger Reaction in Nonpolar Solvents. *Chem. - A Eur. J.* **1997**, *3* (2), 212–218.
- (163) Benson, S. W. *The Foundation of Chemical Kinetics*; McGraw-Hill, 1960.
- (164) Medina, M. E.; Iuga, C.; Alvarez-Idaboy, J. R. Antioxidant Activity of Propyl Gallate in Aqueous and Lipid Media: A Theoretical Study. *Phys. Chem. Chem. Phys.* **2013**, *15* (31), 13137.
- (165) Brovarets', O. O.; Hovorun, D. M. Conformational Transitions of the Quercetin Molecule via the Rotations of Its Rings: A Comprehensive Theoretical Study. *J. Biomol. Struct. Dyn.* **2020**, *38* (10), 2865–2883.
- (166) Allouche, A. Gabedit — A Graphical User Interface for Computational Chemistry Softwares. *J. Comput. Chem.* **2011**, *32*, 174–182.
- (167) Hanwell, M. D.; Curtis, D. E.; Lonie, D. C.; Vandermeersch, T.; Zurek, E.; Hutchison, G. R. Avogadro: An Advanced Semantic Chemical Editor, Visualization, and Analysis Platform. *J. Cheminform.* **2012**, *4* (8), 17.
- (168) O'Boyle, N. M.; Banck, M.; James, C. A.; Morley, C.; Vandermeersch, T.; Hutchison, G. R. Open Babel: An Open Chemical Toolbox. *J. Cheminform.* **2011**, *3* (1), 33.
- (169) Van Der Spoel, D.; Lindahl, E.; Hess, B.; Groenhof, G.; Mark, A. E.; Berendsen, H. J. C. GROMACS: Fast, Flexible, and Free. *J. Comput. Chem.* **2005**, *26* (16), 1701–1718.
- (170) Salomon-Ferrer, R.; Case, D. A.; Walker, R. C. An Overview of the Amber Biomolecular Simulation Package. *Wiley Interdiscip. Rev. Comput. Mol. Sci.* **2013**, *3* (2), 198–210.
- (171) Brooks, B. R.; Brooks, C. L.; Mackerell, A. D.; Nilsson, L.; Petrella, R. J.; Roux, B.; Won, Y.; Archontis, G.; Bartels, C.; Boresch, S.; Caflich, A.; Caves, L.; Cui, Q.; Dinner, A. R.; Feig, M.; Fischer, S.; Gao, J.; Hodoscek, M.; Im, W.; Kuczera, K.; Lazaridis, T.; Ma, J.; Ovchinnikov, V.; Paci, E.; Pastor, R. W.; Post, C. B.; Pu, J. Z.; Schaefer, M.; Tidor, B.; Venable, R. M.; Woodcock, H. L.; Wu, X.; Yang, W.; York, D. M.; Karplus, M. CHARMM: The Biomolecular Simulation Program. *J. Comput. Chem.* **2009**, *30* (10), 1545–1614.
- (172) Jo, S.; Kim, T.; Iyer, V. G.; Im, W. CHARMM-GUI: A Web-Based Graphical User Interface for CHARMM. *J. Comput. Chem.* **2008**, *29* (11), 1859–1865.
- (173) Malde, A. K.; Zuo, L.; Breeze, M.; Stroet, M.; Poger, D.; Nair, P. C.; Oostenbrink, C.; Mark, A. E. An Automated Force Field Topology Builder (ATB) and Repository: Version 1.0. *J. Chem. Theory Comput.* **2011**, *7* (12), 4026–4037.
- (174) Vanommeslaeghe, K.; MacKerell, A. D. Automation of the CHARMM General Force Field (CGenFF) I: Bond Perception and Atom Typing. *J. Chem. Inf. Model.* **2012**, *52* (12), 3144–3154.
- (175) Daura, X.; Gademann, K.; Jaun, B.; Seebach, D.; van Gunsteren, W. F.; Mark, A. E. Peptide Folding: When Simulation Meets Experiment. *Angew. Chemie Int. Ed.* **1999**, *38* (1–2), 236–240.
- (176) Ho, J.; Coote, M. L. A Universal Approach for Continuum Solvent PK a Calculations: Are We There Yet? *Theor. Chem. Acc.* **2010**, *125* (1–2), 3–21.
- (177) Casasnovas, R.; Ortega-Castro, J.; Frau, J.; Donoso, J.; Muñoz, F. Theoretical PKa Calculations with Continuum Model Solvents, Alternative Protocols to Thermodynamic Cycles. *Int. J. Quantum Chem.* **2014**, *114* (20), 1350–1363.
- (178) Tošović, J.; Marković, S.; Milenković, D.; Marković, Z. Solvation Enthalpies and Gibbs Energies of the Proton and Electron - Influence of Solvation Models. *J. Serbian Soc. Comput. Mech.* **2016**, *10* (2), 66–76.
- (179) Malloum, A.; Fifen, J. J.; Conradie, J. Determination of the Absolute Solvation Free Energy and Enthalpy of the Proton in Solutions. *J. Mol. Liq.* **2021**, *322*, 114919.
- (180) Marković, Z.; Milenković, D.; Dorović, J.; Jeremić, S. Solvation Enthalpies of the Proton and Electron in Polar and Non-Polar Solvents. *J. Serbian Soc. Comput. Mech.* **2013**, *7* (2), 1–9.
- (181) Marković, Z.; Tošović, J.; Milenković, D.; Marković, S. Revisiting the Solvation Enthalpies and Free Energies of the Proton and Electron in Various Solvents. *Comput. Theor. Chem.* **2016**, *1077*, 11–17.
- (182) Galano, A.; Pérez-González, A.; Castañeda-Arriaga, R.; Muñoz-Rugeles, L.; Mendoza-Sarmiento, G.; Romero-Silva, A.; Ibarra-Escutia, A.; Rebollar-Zepeda, A. M.; León-Carmona, J. R.; Hernández-Olivares, M. A.; Alvarez-Idaboy, J. R. Empirically Fitted Parameters for

Calculating PKa Values with Small Deviations from Experiments Using a Simple Computational Strategy. *J. Chem. Inf. Model.* **2016**, *56* (9), 1714–1724.

(183) Pérez-González, A.; Castañeda-Arriaga, R.; Verastegui, B.; Carreón-González, M.; Alvarez-Idaboy, J. R.; Galano, A. Estimation of Empirically Fitted Parameters for Calculating PK a Values of Thiols in a Fast and Reliable Way. *Theor. Chem. Acc.* **2018**, *137* (1), 5.

(184) Rossini, E.; Bochevarov, A. D.; Knapp, E. W. Empirical Conversion of p K a Values between Different Solvents and Interpretation of the Parameters: Application to Water, Acetonitrile, Dimethyl Sulfoxide, and Methanol. *ACS Omega* **2018**, *3* (2), 1653–1662.

(185) Gramatica, P. Principles of QSAR Modeling. *Int. J. Quant. Struct. Relationships* **2020**, *5* (3), 61–97.

(186) Fukui, K.; Yonezawa, T.; Shingu, H. A Molecular Orbital Theory of Reactivity in Aromatic Hydrocarbons. *J. Chem. Phys.* **1952**, *20* (4), 722–725.

(187) Janak, J. F. Proof That $\delta E_{\text{HOMO}} = \epsilon$ in Density-Functional Theory. *Phys. Rev. B* **1978**, *18* (12), 7165–7168.

(188) Koopmans, T. Über Die Zuordnung von Wellenfunktionen Und Eigenwerten Zu Den Einzelnen Elektronen Eines Atoms. *Physica* **1934**, *1* (1–6), 104–113.

(189) Parr, R. G.; Szentpály, L. v.; Liu, S. Electrophilicity Index. *J. Am. Chem. Soc.* **1999**, *121* (9), 1922–1924.

(190) Ortiz, J. V. Electron Propagator Theory: An Approach to Prediction and Interpretation in Quantum Chemistry. *Wiley Interdiscip. Rev. Comput. Mol. Sci.* **2013**, *3* (2), 123–142.

(191) Ortiz, J. V. Partial Third-order Quasiparticle Theory: Comparisons for Closed-shell Ionization Energies and an Application to the Borazine Photoelectron Spectrum. *J. Chem. Phys.* **1996**, *104* (19), 7599–7605.

(192) Pérez-González, A.; Galano, A.; Ortiz, J. V. Vertical Ionization Energies of Free Radicals and Electron Detachment Energies of Their Anions: A Comparison of Direct and Indirect Methods Versus Experiment. *J. Phys. Chem. A* **2014**, *118* (31), 6125–6131.

(193) Ortiz, J. V. Quasiparticle Approximations and Electron Propagator Theory. *Int. J. Quantum Chem.* **2003**, *95* (4–5), 593–599.

(194) Singh, R. K.; Ortiz, J. V.; Mishra, M. K. Tautomeric Forms of Adenine: Vertical Ionization Energies and Dyson Orbitals. *Int. J. Quantum Chem.* **2009**, na.

(195) Martínez, A.; Rodríguez-Girones, M. A.; Barbosa, A.; Costas, M. Donator Acceptor Map for Carotenoids, Melatonin and Vitamins. *J. Phys. Chem. A* **2008**, *112* (38), 9037–9042.

(196) Gázquez, J. L.; Cedillo, A.; Vela, A. Electrodonating and Electroaccepting Powers. *J. Phys. Chem. A* **2007**, *111* (10), 1966–1970.

(197) Gázquez, J. L. Perspectives on the Density Functional Theory of Chemical Reactivity. *J. Mex. Chem. Soc.* **2008**, *52* (1), 3–10.

(198) Martínez, A.; Vargas, R.; Galano, A. What Is Important to Prevent Oxidative Stress? A Theoretical Study on Electron-Transfer Reactions between Carotenoids and Free Radicals. *J. Phys. Chem. B* **2009**, *113* (35), 12113–12120.

(199) Parr, R. G.; Yang, W. Density Functional Approach to the Frontier-Electron Theory of Chemical Reactivity. *J. Am. Chem. Soc.* **1984**, *106* (14), 4049–4050.

(200) Mei, Y.; Simmonett, A. C.; Pickard, F. C.; Distasio, R. A.; Brooks, B. R.; Shao, Y. Numerical Study on the Partitioning of the Molecular Polarizability into Fluctuating Charge and Induced Atomic Dipole Contributions. *J. Phys. Chem. A* **2015**, *119* (22), 5865–5882.

(201) Martin, F.; Zipse, H. Charge Distribution in the Water Molecule - A Comparison of Methods. *J. Comput. Chem.* **2005**, *26* (1), 97–105.

(202) Mao, J. X. Atomic Charges in Molecules: A Classical Concept in Modern Computational Chemistry. *Postdoc J.* **2014**, *2* (2), na DOI: 10.14304/SURYAJPR.V2N2.2.

(203) Bultinck, P.; Carbó-Dorca, R.; Langenaeker, W. Negative Fukui Functions: New Insights Based on Electronegativity Equalization. *J. Chem. Phys.* **2003**, *118* (10), 4349–4356.

(204) Senthilkumar, L.; Kolandaivel, P. Study of Effective Hardness and Condensed Fukui Functions Using AIM, Ab Initio, and DFT Methods. *Mol. Phys.* **2005**, *103* (4), 547–556.

(205) De Proft, F.; Martin, J. M. L.; Geerlings, P. Calculation of Molecular Electrostatic Potentials and Fukui Functions Using Density Functional Methods. *Chem. Phys. Lett.* **1996**, *256* (4–5), 400–408.

(206) Martínez-Araya, J. I. Why Is the Dual Descriptor a More Accurate Local Reactivity Descriptor than Fukui Functions? *J. Math. Chem.* **2015**, *53* (2), 451–465.

(207) Kohen, R.; Gati, I. Skin Low Molecular Weight Antioxidants and Their Role in Aging and in Oxidative Stress. *Toxicology* **2000**, *148* (2–3), 149–157.

(208) Bader, R. F. W. Atoms in Molecules. *Acc. Chem. Res.* **1985**, *18* (1), 9–15.

(209) Bader, R. F. W. A Quantum Theory of Molecular Structure and Its Applications. *Chem. Rev.* **1991**, *91* (5), 893–928.

(210) Lu, T.; Chen, F. Multiwfn: A Multifunctional Wavefunction Analyzer. *J. Comput. Chem.* **2012**, *33* (5), 580–592.

(211) Jenkins, S.; Liu, Z.; Kirk, S. R. A Bond, Ring and Cage Resolved Poincaré-Hopf Relationship for Isomerisation Reaction Pathways. *Mol. Phys.* **2013**, *111* (20), 3104–3116.

(212) Pakiari, A. H.; Eskandari, K. The Chemical Nature of Very Strong Hydrogen Bonds in Some Categories of Compounds. *J. Mol. Struct. THEOCHEM* **2006**, *759* (1–3), 51–60.

(213) Shainyan, B. A.; Chiparina, N. N.; Aksamentova, T. N.; Oznobikhina, L. P.; Rosentsveig, G. N.; Rosentsveig, I. B. Intramolecular Hydrogen Bonds in the Sulfonamide Derivatives of Oxamide, Dithiooxamide, and Biuret. FT-IR and DFT Study, AIM and NBO Analysis. *Tetrahedron* **2010**, *66* (44), 8551–8556.

(214) Hibbs, D. E.; Overgaard, J.; Piltz, R. O. X-N Charge Density Analysis of the Hydrogen Bonding Motif in 1-(2-Hydroxy-5-Nitrophenyl)Ethanone. Electronic Supplementary Information (ESI) Available: Multipole Population Coefficients and Pseudoatom Parameterization. See <http://www.rsc.org/Suppdata/Ob/B2/>. *Org. Biomol. Chem.* **2003**, *1* (7), 1191–1198.

(215) Popelier, P. L. A. Characterization of a Dihydrogen Bond on the Basis of the Electron Density. *J. Phys. Chem. A* **1998**, *102* (10), 1873–1878.

(216) Koch, U.; Popelier, P. L. A. Characterization of C-H-O Hydrogen Bonds on the Basis of the Charge Density. *J. Phys. Chem.* **1995**, *99* (24), 9747–9754.

(217) Ebrahimi, A.; Roohi, H.; Habibi, M.; Mohammadi, M.; Vaziri, R. Characterization of Conformers of Non-Ionized Proline on the Basis of Topological and NBO Analyses: Can Nitrogen Be a Donor of Hydrogen Bond? *Chem. Phys.* **2006**, *322* (3), 289–297.

(218) Rozas, I.; Alkorta, I.; Elguero, J. Behavior of Ylides Containing N, O, and C Atoms as Hydrogen Bond Acceptors. *J. Am. Chem. Soc.* **2000**, *122* (45), 11154–11161.

(219) Espinosa, E.; Molins, E.; Lecomte, C. Hydrogen Bond Strengths Revealed by Topological Analyses of Experimentally Observed Electron Densities. *Chem. Phys. Lett.* **1998**, *285* (3–4), 170–173.

(220) Mata, I.; Alkorta, I.; Espinosa, E.; Molins, E. Relationships between Interaction Energy, Intermolecular Distance and Electron Density Properties in Hydrogen Bonded Complexes under External Electric Fields. *Chem. Phys. Lett.* **2011**, *507* (1–3), 185–189.

(221) Korth, H. G.; De Heer, M. I.; Mulder, P. A. DFT Study on Intramolecular Hydrogen Bonding in 2-Substituted Phenols: Conformations, Enthalpies, and Correlation with Solute Parameters. *J. Phys. Chem. A* **2002**, *106* (37), 8779–8789.

(222) Tognetti, V.; Joubert, L. On the Influence of Density Functional Approximations on Some Local Baders Atoms-in-Molecules Properties. *J. Phys. Chem. A* **2011**, *115* (21), 5505–5515.

(223) Jabłoński, M. QTAIM-Based Comparison of Agostic Bonds and Intramolecular Charge-Inverted Hydrogen Bonds. *J. Phys. Chem. A* **2015**, *119* (20), 4993–5008.

(224) Jabłoński, M.; Palusiak, M. Basis Set and Method Dependence in Quantum Theory of Atoms in Molecules Calculations for Covalent Bonds. *J. Phys. Chem. A* **2010**, *114* (47), 12498–12505.

(225) Foster, J. P.; Weinhold, F. Natural Hybrid Orbitals. *J. Am. Chem. Soc.* **1980**, *102* (24), 7211–7218.

- (226) Reed, A. E.; Curtiss, L. A.; Weinhold, F. Intermolecular Interactions from a Natural Bond Orbital, Donor–Acceptor Viewpoint. *Chem. Rev.* **1988**, *88* (6), 899–926.
- (227) Reed, A. E.; Weinstock, R. B.; Weinhold, F. Natural Population Analysis. *J. Chem. Phys.* **1985**, *83* (2), 735–746.
- (228) Carpenter, J. E.; Weinhold, F. Analysis of the Geometry of the Hydroxymethyl Radical by the “Different Hybrids for Different Spins” Natural Bond Orbital Procedure. *J. Mol. Struct. THEOCHEM* **1988**, *169* (C), 41–62.
- (229) Benassi, E.; Fan, H. Quantitative Characterisation of the Ring Normal Modes. Pyridine as a Study Case. *Spectrochim. Acta - Part A Mol. Biomol. Spectrosc.* **2021**, *246*, 119026.
- (230) Rose, R. C.; Bode, A. M. Biology of Free Radical Scavengers: An Evaluation of Ascorbate. *FASEB J.* **1993**, *7* (12), 1135–1142.
- (231) Galano, A.; Tan, D. X.; Reiter, R. J. Melatonin as a Natural Ally against Oxidative Stress: A Physicochemical Examination. *J. Pineal Res.* **2011**, *51* (1), 1–16.
- (232) Márquez, L.; García-Bueno, B.; Madrigal, J. L. M.; Leza, J. C. Mangiferin Decreases Inflammation and Oxidative Damage in Rat Brain after Stress. *Eur. J. Nutr.* **2012**, *51* (6), 729–739.
- (233) Masuda, T.; Yamada, K.; Maekawa, T.; Takeda, Y.; Yamaguchi, H. Antioxidant Mechanism Studies on Ferulic Acid: Identification of Oxidative Coupling Products from Methyl Ferulate and Linoleate. *J. Agric. Food Chem.* **2006**, *54* (16), 6069–6074.
- (234) MASUDA, T.; YAMADA, K.; MAEKAWA, T.; TAKEDA, Y.; YAMAGUCHI, H. Antioxidant Mechanism Studies on Ferulic Acid: Isolation and Structure Identification of the Main Antioxidation Product from Methyl Ferulate. *Food Sci. Technol. Res.* **2006**, *12* (3), 173–177.
- (235) Sies, H. Oxidative Stress: Oxidants and Antioxidants. *Exp. Physiol.* **1997**, *82* (2), 291–295.
- (236) Terpin, P.; Abramović, H. A Kinetic Approach for Evaluation of the Antioxidant Activity of Selected Phenolic Acids. *Food Chem.* **2010**, *121* (2), 366–371.
- (237) Land, E. J.; Ebert, M. *Trans. Faraday Soc.* **1967**, *63*, 1181.
- (238) Aruoma, O. I.; Murcia, A.; Butler, J.; Halliwell, B. Evaluation of the Antioxidant and Prooxidant Actions of Gallic Acid and Its Derivatives. *J. Agric. Food Chem.* **1993**, *41* (11), 1880–1885.
- (239) Galano, A. On the Direct Scavenging Activity of Melatonin towards Hydroxyl and a Series of Peroxyl Radicals. *Phys. Chem. Chem. Phys.* **2011**, *13* (15), 7178.
- (240) Litwinienko, G.; Ingold, K. U. Abnormal Solvent Effects on Hydrogen Atom Abstractions. 1. The Reactions of Phenols with 2,2-Diphenyl-1-Picrylhydrazyl (Dpph •) in Alcohols. *J. Org. Chem.* **2003**, *68* (9), 3433–3438.
- (241) Litwinienko, G.; Ingold, K. U. Abnormal Solvent Effects on Hydrogen Atom Abstraction. 2. Resolution of the Curcumin Antioxidant Controversy: The Role of Sequential Proton Loss Electron Transfer. *J. Org. Chem.* **2004**, *69* (18), 5888–5896.
- (242) Litwinienko, G.; Ingold, K. U. Abnormal Solvent Effects on Hydrogen Atom Abstraction. 3. Novel Kinetics in Sequential Proton Loss Electron Transfer Chemistry. *J. Org. Chem.* **2005**, *70* (22), 8982–8990.
- (243) Litwinienko, G.; Ingold, K. U. Solvent Effects on the Rates and Mechanisms of Reaction of Phenols with Free Radicals. *Acc. Chem. Res.* **2007**, *40* (3), 222–230.
- (244) Bartmess, J. E. Thermodynamics of the Electron and the Proton. *J. Phys. Chem.* **1994**, *98* (25), 6420–6424.
- (245) Halliwell, B.; Murcia, M. A.; Chirico, S.; Aruoma, O. I. Free Radicals and Antioxidants in Food and in Vivo: What They Do and How They Work. *Crit. Rev. Food Sci. Nutr.* **1995**, *35* (1–2), 7–20.
- (246) Halliwell, B.; Whiteman, M. Measuring Reactive Species and Oxidative Damage in Vivo and in Cell Culture: How Should You Do It and What Do the Results Mean? *Br. J. Pharmacol.* **2004**, *142* (2), 231–255.
- (247) Bell, R. P. The Theory of Reactions Involving Proton Transfers. *Proc. R. Soc. London. Ser. A - Math. Phys. Sci.* **1936**, *154* (882), 414–429.
- (248) Evans, M. G.; Polanyi, M. Further Considerations on the Thermodynamics of Chemical Equilibria and Reaction Rates. *Trans. Faraday Soc.* **1936**, *32*, 1333.
- (249) Muraro, C.; Polato, M.; Bortoli, M.; Aiolfi, F.; Orian, L. Radical scavenging activity of natural antioxidants and drugs: Development of a combined machine learning and quantum chemistry protocol. *J. Chem. Phys.* **2020**, *153*, 114117.
- (250) Ribaud, G.; Bortoli, M.; Witt, C. E.; Parke, B.; Mena, S.; Oselladore, E.; Zagotto, G.; Hashemi, P.; Orian, L. ROS-Scavenging Selenofluoxetine Derivatives Inhibit In Vivo Serotonin Reuptake. *ACS Omega* **2022**, *7*, 8314–8322.
- (251) Ulstrup, J.; Jortner, J. The Effect of Intramolecular Quantum Modes on Free Energy Relationships for Electron Transfer Reactions. *J. Chem. Phys.* **1975**, *63* (10), 4358–4368.
- (252) Marcus, R. A.; Sutin, N. Electron Transfers in Chemistry and Biology. *Biochim. Biophys. Acta - Rev. Bioenerg.* **1985**, *811* (3), 265–322.
- (253) Marcus, R. A. Electron Transfer Reactions in Chemistry. Theory and Experiment. *Rev. Mod. Phys.* **1993**, *65* (3), 599–610.
- (254) Marcus, R. A. Chemical and Electrochemical Electron-Transfer Theory. *Annu. Rev. Phys. Chem.* **1964**, *15* (1), 155–196.
- (255) Marcus, R. A. On the Theory of Oxidation-Reduction Reactions Involving Electron Transfer. III. Applications to Data on the Rates of Organic Redox Reactions. *J. Chem. Phys.* **1957**, *26* (4), 872–877.
- (256) Eyring, H. The Activated Complex in Chemical Reactions. *J. Chem. Phys.* **1935**, *3* (2), 107–115.
- (257) Evans, M. G.; Polanyi, M. Some Applications of the Transition State Method to the Calculation of Reaction Velocities, Especially in Solution. *Trans. Faraday Soc.* **1935**, *31*, 875.
- (258) Truhlar, D. G.; Garrett, B. C.; Klippenstein, S. J. Current Status of Transition-State Theory. *J. Phys. Chem.* **1996**, *100* (31), 12771–12800.
- (259) Eckart, C. The Penetration of a Potential Barrier by Electrons. *Phys. Rev.* **1930**, *35* (11), 1303–1309.
- (260) Kuppermann, A.; Truhlar, D. G. Exact Tunneling Calculations. *J. Am. Chem. Soc.* **1971**, *93* (8), 1840–1851.
- (261) Dzib, E.; Cabellos, J. L.; Ortiz-Chi, F.; Pan, S.; Galano, A.; Merino, G. Eyringpy: A Program for Computing Rate Constants in the Gas Phase and in Solution. *Int. J. Quantum Chem.* **2019**, *119* (2), No. e25686.
- (262) Pollak, E.; Pechukas, P. Symmetry Numbers, Not Statistical Factors, Should Be Used in Absolute Rate Theory and in Bronsted Relations. *J. Am. Chem. Soc.* **1978**, *100* (10), 2984–2991.
- (263) Collins, F. C.; Kimball, G. E. Diffusion-Controlled Reaction Rates. *J. Colloid Sci.* **1949**, *4* (4), 425–437.
- (264) Smolouchowski, M. v. Versuch Einer Mathematischen Theorie Der Koagulationskinetik Kolloider Lösungen. *Zeitschrift für Phys. Chemie* **1918**, *92U* (1), 129–168.
- (265) Einstein, A. Über Die von Der Molekularkinetischen Theorie Der Wärme Geforderte Bewegung von in Ruhenden Flüssigkeiten Suspendierten Teilchen. *Ann. Phys.* **1905**, *322* (8), 549–560.
- (266) Galano, A.; Alvarez-Idaboy, J. R. A Computational Methodology for Accurate Predictions of Rate Constants in Solution: Application to the Assessment of Primary Antioxidant Activity. *J. Comput. Chem.* **2013**, *34* (28), 2430–2445.
- (267) Olson, K. R. Reactive Oxygen Species or Reactive Sulfur Species: Why We Should Consider the Latter. *J. Exp. Biol.* **2020**, *223* (4), jeb196352.
- (268) Dedon, P. C.; Tannenbaum, S. R. Reactive Nitrogen Species in the Chemical Biology of Inflammation. *Arch. Biochem. Biophys.* **2004**, *423* (1), 12–22.
- (269) Reinke, L. A. Spin Trapping Evidence for Alcohol-Associated Oxidative Stress^{1,2} This Article Is Part of a Series of Reviews on “Alcohol, Oxidative Stress, and Cell Injury.” The Full List of Papers May Be Found on the Homepage of the Journal. *Free Radic. Biol. Med.* **2002**, *32* (10), 953–957.

V. Wykaz publikacji potwierdzony przez Bibliotekę UMW

Wrocław, 12.04.2023 r.

Maciej Spiegel

Wykaz publikacji

1. Publikacje w czasopismach naukowych

1.1 Publikacje w czasopiśmie z IF

Lp.	Opis bibliograficzny	IF	Punkty ministerialne
1	Spiegel Maciej , Andruniów Tadeusz, Sroka Zbigniew: Flavones' and flavonols' antiradical structure-activity relationship - a quantum chemical study, <i>Antioxidants</i> , 2020, vol. 9, nr 6, art.461 [21 s.], DOI:10.3390/antiox9060461	6,313	100
2	Spiegel Maciej , Kapusta Karina, Kołodziejczyk Wojciech, Saloni Julia, Żbikowska Beata, Hill Glake A., Sroka Zbigniew: Antioxidant activity of selected phenolic acids - ferric reducing antioxidant power assay and QSAR analysis of the structural features, <i>Molecules</i> , 2020, vol. 25, nr 13, art.3088 [15 s.], DOI:10.3390/molecules25133088	4,412	140
3	Machalska Ewa, Zając Grzegorz, Wierzbę Aleksandra J., Kapitan Josef, Andruniów Tadeusz, Spiegel Maciej , Gryko Dorota, Bour Petr, Barańska Małgorzata: Recognition of the true and false resonance Raman optical activity, <i>Angewandte Chemie-International Edition</i> , 2021, vol. 60, nr 39, s. 21205-21210, DOI:10.1002/anie.202107600	16,823	200
4	Malchrzak Wojciech, Mastalerz-Migas Agnieszka, Sroka Zbigniew, Spiegel Maciej : One year of the COVID-19 pandemic. What do we know and what is yet to come? - the summarising review, <i>International Journal of Public Health</i> , 2021, vol. 66, art.1603975 [10 s.], DOI:10.3389/ijph.2021.1603975	5,1	100
5	Spiegel Maciej , Gamian Andrzej, Sroka Zbigniew: Antiradical activity of beetroot (<i>Beta vulgaris</i> L.) betalains, <i>Molecules</i> , 2021, vol. 26, nr 9, art.2439 [20 s.], DOI:10.3390/molecules26092439	4,927	140
6	Spiegel Maciej , Gamian Andrzej, Sroka Zbigniew: A statistically supported antioxidant activity DFT benchmark - the effects of Hartree-Fock exchange and basis set selection on accuracy and resources uptake, <i>Molecules</i> , 2021, vol. 26, nr 16, art.5058 [22 s.], DOI:10.3390/molecules26165058	4,927	140
7	Spiegel Maciej , Marino Tiziana, Prejanò Mario, Russo Nino: On the scavenging ability of scutellarein against the OOH radical in water and lipid-like environments: a theoretical study, <i>Antioxidants</i> , 2022, vol. 11, nr 2, art.224 [9 s.], DOI:10.3390/antiox11020224	7,675*	100

Lp.	Opis bibliograficzny	IF	Punkty ministerialne
8	Dudek Anita, Spiegel Maciej , Strugała-Danak Paulina, Gabrielska Janina: Analytical and theoretical studies of antioxidant properties of chosen anthocyanins; a structure-dependent relationships, <i>International Journal of Molecular Sciences</i> , 2022, vol. 23, nr 10, art.5432 [18 s.], DOI:10.3390/ijms23105432	6,208*	140
9	Spiegel Maciej : Current trends in computational quantum chemistry studies on antioxidant radical scavenging activity, <i>Journal of Chemical Information and Modeling</i> , 2022, vol. 62, nr 11, s. 2639-2658, DOI:10.1021/acs.jcim.2c00104	6,162*	100
10	Strugała-Danak Paulina, Spiegel Maciej , Hurynowicz Kacper, Gabrielska Janina: Interference of malvidin and its mono- and diglucosides on the membrane - combined in vitro and computational chemistry study, <i>Journal of Functional Foods</i> , 2022, vol. 99, art.105340 [13 s.], DOI:10.1016/j.jff.2022.105340	5,223*	100
11	Spiegel Maciej , Marino Tiziana, Prejanò Mario, Russo Nino: Primary and secondary antioxidant properties of scutellarin and scutellarein in water and lipid-like environments: a theoretical investigation, <i>Journal of Molecular Liquids</i> , 2022, vol. 366, art.120343 [9 s.], DOI:10.1016/j.molliq.2022.120343	6,633*	100
12	Spiegel Maciej , Krzyżek Paweł, Dworniczek Ewa, Adamski Ryszard, Sroka Zbigniew: In silico screening and in vitro assessment of natural products with anti-virulence activity against <i>Helicobacter pylori</i> , <i>Molecules</i> , 2022, vol. 27, nr 1, art.20 [20 s.], DOI:10.3390/molecules27010020	4,927*	140
13	Spiegel Maciej , Marino Tiziana, Prejanò Mario, Russo Nino: Antioxidant and copper-chelating power of new molecules suggested as multiple target agents against Alzheimer's disease. A theoretical comparative study, <i>Physical Chemistry Chemical Physics</i> , 2022, vol. 24, nr 26, s. 16353-16359, DOI:10.1039/d2cp01918c	3,945*	100
14	Spiegel Maciej , Sroka Zbigniew: Natural dihydroisobenzofuran derivatives as a template for promising radical scavengers: theoretical insights into structure - activity relationships, thermochemistry and kinetics, <i>Theoretical Chemistry Accounts</i> , 2022, vol. 141, nr 11, art.61 [14 s.], DOI:10.1007/s00214-022-02922-5	2,154*	70
15	Selahi Daniel, Spiegel Maciej , Hadzik Jakub, Piłutaj Artur, Michalak Filip, Kubasiewicz-Ross Paweł, Dominiak Marzena: The appliance of A-PRF and CGF in the treatment of impacted mandibular third molar extraction sockets - narrative review, <i>Applied Sciences-Basel</i> , 2023, vol. 13, nr 1, art.165 [12 s.], DOI:10.3390/app13010165	2,838*	100
16	Spiegel Maciej , Sroka Zbigniew: Quantum-mechanical characteristics of apigenin: Antiradical, metal chelation and inhibitory properties in physiologically relevant media, <i>Fitoterapia</i> , 2023, vol. 164, art.105352, DOI:10.1016/j.fitote.2022.105352	3,204*	100

Lp.	Opis bibliograficzny	IF	Punkty ministerialne
17	Spiegel Maciej , Cel Katarzyna, Sroka Zbigniew: The mechanistic insights into the role of pH and solvent on antiradical and prooxidant properties of polyphenols — Nine compounds case study, Food Chemistry, 2023, vol. 407, art.134677 [10 s.], DOI:10.1016/j.foodchem.2022.134677	9,231*	200
18	Spiegel Maciej , Ciardullo Giada, Marino Tiziana, Russo Nino: Computational investigation on the antioxidant activities and on the Mpro SARS-CoV-2 non-covalent inhibition of isorhamnetin, Frontiers in Chemistry, 2023, vol. 11, art.1122880 [13 s.], DOI:10.3389/fchem.2023.1122880	5,545*	100
19	Maciej Spiegel , Carlo Adamo : Tuning the Photophysical Properties of Ru(II) Photosensitizers for PDT by Protonation and Metallation: A DFT Study, Journal of Physical Chemistry A, 2023, [11 s.] https://doi.org/10.1021/acs.jpca.3c00839 [Ahead of Print]	2,944*	100

*IF 2021

2. Abstrakty

Lp.	Opis bibliograficzny
1	Spiegel Maciej , Żbikowska Beata, Sroka Zbigniew, Hładyszowski Jerzy: Quantum chemistry aided examination of antioxidative potential of phenolic acids, W: 4th International Wrocław Scientific Meetings. Wrocław, 09-10 October 2020, (red.) Julita Kulbacka, Nina Rembiałkowska, Joanna Weźgowiec, Wrocław 2020, Wydawnictwo Naukowe TYGIEL sp. z o.o., s. 220-222, ISBN 978-83-66489-37-0
2	Spiegel Maciej , Andruniów Tadeusz, Sroka Zbigniew: Influence of structural features on the antiradical Activity of flavones and flavonols - a quantum chemical study, W: 4th International Wrocław Scientific Meetings. Wrocław, 09-10 October 2020, (red.) Julita Kulbacka, Nina Rembiałkowska, Joanna Weźgowiec, Wrocław 2020, Wydawnictwo Naukowe TYGIEL sp. z o.o., s. 222-223, ISBN 978-83-66489-37-0

Impact Factor : 109,191 (liczba prac : 19)

Punkty ministerialne : 2270

Uniwersytet Medyczny we Wrocławiu
 FILIA NR 1 BIBLIOTEKI GŁÓWNEJ
 ul. Borowska 211, 50-556 Wrocław
 tel. 71 784 03 51, faks: 71 784 03 55

12.04.2023r.

Alina Zapodzień

VI. Osiągnięcia naukowo-badawcze

i. Analiza bibliometryczna całkowitego dorobku naukowego

Publikacji w czasopismach naukowych:	19
h–indeks (<i>Web of Science Core Collection</i>):	6
Sumaryczna ilość cytowań (<i>Web of Science Core Collection</i>):	169
Sumaryczny współczynnik wpływu (Impact Factor):	109.191
Sumaryczna punktacja Ministerstwa Edukacji i Nauki:	2270

ii. Konferencje naukowe

- “4th International Wrocław Scientific Meetings”, Wrocław, Polska, 09–10.10.2020:
 - “Quantum Chemistry Aided Examination of Antioxidative Potential of Phenolic Acids”, poster. [współautorzy: Beata Żbikowska, Zbigniew Sroka i Jerzy Hładyszowski]
 - “Influence of Structural Features on the Antiradical Activity of Flavones and Flavonols – A Quantum Chemical Study”, poster. [współautorzy: Tadeusz Andruniów i Zbigniew Sroka]

iii. Projekty krajowe

- Grant PRELUDIUM21 (kierownik projektu), „Zastosowanie sztucznej inteligencji w poszukiwaniu nowych substancji leczniczych pochodzenia naturalnego o mechanizmach działania ukierunkowanych na zmniejszanie stężenia wolnych rodników w organizmie” (na mocy decyzji nr DEC–2022/45/N/NZ7/02264), Narodowe Centrum Nauki, Kraków, 2022

iv. Wyróżnienia i nagrody

- Laureat „Studenckiego Programu Stypendialnego” organizowanego przez Urząd Miejski we Wrocławiu, Edycja 2022 [online: <https://www.wroclaw.pl/akademicki-wroclaw/znamy-nazwiska-doktorantow-z-przyznanymi-stypendiami-w-studenckim-programie-stypendialnym>]
- Wybranie artykułu [D] na okładkę wydania (*Journal of Chemical Information and Modeling*; June 13, 2022; Volume 62, Issue 11; Pages 2631–2900) [online: <https://pubs.acs.org/toc/jcisd8/62/11>]
- Zaproszenie do przedstawienia tematyki badań w postaci artykułu opublikowanego w Raporcie Rocznym 2022 Poznańskiego Centrum Superkomputerowo–Sieciowego [online: https://www.pcss.pl/files/2022/12/PCSS_Raport_2022.pdf]

v. Aktywność recenzencka

- Członek łoży recenzentów w czasopismach:
 - *Frontiers in Bioscience–Landmark (BRI)*
[online: https://www.imrpess.com/journal/FBL/about/reviewer_board]
 - *Symmetry (MDPI)*
[online: https://www.mdpi.com/journal/symmetry/submission_reviewers]
- Wykonano 8 recenzji dla: *Theoretical Chemistry Accounts (1)*, *Phytochemistry (1)*, *Free Radicals Research (2)*, *Frontiers in Bioscience–Landmark (1)*, *Journal of Molecular Modeling (1)*, *Molecules (1)*, *Journal of Molecular Liquids (1)*

vi. Warsztaty, kursy, seminaria

- „What is a Chemical? Part IV: Innovation in Chemical Descriptions”, webinar. IUPAC, 17 lutego 2023.
- „Berlin Digital Science for Drug Discovery Meeting”, webinar. DigiDrug.NET, 15 lutego 2023.
- “Cambridge Cheminformatics Meeting”, webinar. University of Cambridge, 8 lutego 2023.
- “Quantum Computing: What are the Pharma Use Cases?”, webinar. Pistoia Alliance, 7 lutego 2023.

- “5th International Mini-Symposium on Molecular Machine Learning”, webinar. University of Münster, 19 stycznia 2023.
- „Protein structure prediction – What’s next after AlphaFold?”, webinar. Discngine Labs, 12 stycznia 2023.
- "Computation in Drug Discovery – An Insider's View", webinar. CDD, 1 grudnia 2022.
- "ELLIS Machine Learning for Molecule Discovery Workshop", webinar. ELLIS Cambridge, 28 listopada 2022.
- "3rd European Symposium on Chemical Bonding (CBOND2022)", webinar. Vrije Universiteit Amsterdam, 20–22 września 2022.
- "DFT calculations (Abinit, Siesta) within an HPC environment", webinar. Interdyscyplinarne Centrum Modelowania Matematycznego i Komputerowego, Uniwersytet Warszawski, 26 maja 2022.
- "Obliczenia metodami chemii kwantowej: programy Gamess i Gaussian – przykłady zastosowań w projektowaniu nowych materiałów funkcjonalnych", webinar. Centrum Informatyczne Trójmiejskiej Akademickiej Sieci Komputerowej, 16 maja 2022.
- "Exploring the Chemical Bonding in Main Group Chemistry", wykład. Institute of Chemistry for Life and Health Sciences, Chimie ParisTech, Paryż, Francja, kwiecień 2022.
- "Studying Potential Energies with Machine Learning", wykład. Institute of Chemistry for Life and Health Sciences, Chimie ParisTech, Paryż, Francja, kwiecień 2022.
- " Od teorii do eksperymentu - czyli wpływ reorganizacji wewnątrz- i międzycząsteczkowej na właściwości cząsteczek w mikro- i makroskali", webinar. Wydział Chemiczny, Uniwersytet Wrocławski. 18 lutego 2021.
- "Applied Pharmaceutical Bioinformatics", kurs zdalny. Uppsala University, Uppsala, Szwecja, listopad–grudzień 2019.
- "Pharmaceutical Bioinformatics", kurs zdalny. Uppsala University, Uppsala, Sweden, wrzesień–listopad 2019.
- "Visiting Professors – Denis Jacquemin", wykłady i warsztaty. Politechnika Wrocławska, 22–24 października 2019.
- "Mapping Polypharmacy Chemical Reactions in At-Risk Populations", zdalny projekt. Hackseq19 – genomics hackathon collective, October 2019. [online: <https://github.com/hackseq/hs19-pop>.]
- "Applied Pharmaceutical Structural Bioinformatics", kurs zdalny. Uppsala University, Uppsala, Sweden, wrzesień–październik 2019.
- "Electronic Structure Theory Workshop: Advanced Quantum Chemistry in Python", warsztaty. Politechnika Wrocławska, 23-25 września 2019.

vii. Stáže zagraniczne

- „Introduction to and Application of Novel Approaches in Computational Chemistry” (2023–02 — 2023–04) Weizmann Institute of Science, Rehovot, Izrael; mentor: **profesor Jan M.L. Martin**;
- „Modeling Optical Properties of Metal Complexes for Photodynamic Therapy Using Quantum Chemical Approaches” (2022–03 — 2022–06) Institute of Chemistry for Life and Health Sciences (I-CLeHS), Chimie ParisTech, Paris Cedex 05, Paryż, Francja; mentor: **profesor Carlo Adamo**;
- „Theoretical Study About the Reaction Mechanisms of Antioxidants” (2021–07 — 2021–09) Department of Chemistry and Chemical Technology, University of Calabria, Arcavacata di Rende, Cosenza, Włochy; mentor: **profesor Nino Russo**.

viii. Pozostałe aktywności

- Opiekun naukowy pracy magisterskiej mgr farm. Katarzyny Cel, wykonywanej w Katedrze i Zakładzie Farmakognozji i Leku Roślinnego, zatytułowanej „Wpływ czynników środowiskowych na dwojaką aktywność polifenoli – antyoksydanty i potencjalne prooksydanty – badania *in silico*”.